CHARACTERIZATION OF INTERLEUKIN-1 BETA 2, A NOVEL INTERLEUKIN-1 EXPRESSED BY THE EARLY PIG CONCEPTUS DURING ESTABLISHMENT OF PREGNANCY

A Dissertation presented to the Faculty of the Graduate School

University of Missouri-Columbia

In Partial Fulfillment

Of the Requirements for the Degree

Doctor of Philosophy

by

DANIEL J. MATHEW

Drs. Matthew C. Lucy and Rodney D. Geisert, Dissertation Advisors

DECEMBER 2014

The undersigned, appointed by the Dean of the Graduate School, have examined the Dissertation entitled

CHARACTERIZATION OF INTERLEUKIN-1 BETA 2, A NOVEL INTERLEUKIN-1 EXPRESSED BY THE EARLY PIG CONCEPTUS DURING ESTABLISHMENT OF PREGNANCY

presented by Daniel J. Mathew,

a candidate for the degree Doctor of Philosophy,

and we hereby certify that, in our opinion, it is worthy of acceptance.

Dr. Matthew Lucy – Dissertation Advisor

Dr. Rodney Geisert – Dissertation Advisor

Dr. Jason Ross

Dr. Jonathan Green

Dr. Emma Teixeiro-Pernas

DEDICATIONS

This Dissertation is dedicated to my family and friends. It was their love, understanding and humor that gave me the endurance to achieve my goal.

ACKNOWLEDGEMENTS

I have made many friends during my time at the University of Missouri. Firstly, I'd like to thank the University of Missouri faculty and graduate students (past and present) for their enduring support and friendship. I would also like to thank my teammates and coaches from the Columbia Rugby Football Club. Their humor and support, both on and off the pitch, are unmatched. I will never forget you or the great times we've shared.

I would also like to thank Dr. Cliff Murphy, Dr. Yuksel Agca, Dr. Rocio Rivera, Emily Newsom, Lee Spate, Lonnie and Jason Dowell for their help and hard work during the Lentiviral study. I could not have completed this project without their dedication. I'd also like to thank my Ph.D. committee members Dr. Lucy, Dr. Geisert, Dr. Ross, Dr. Green and Dr. Teixeiro for their scientific guidance and willingness to believe in me during my Ph.D. studies. Specifically, I would like to thank my advisors Dr. Lucy and Dr. Geisert. They helped develop me into the scientist that I am today and for that, I am forever grateful.

Lastly, I would like to thank my family. I could not have achieved this goal without their love and understanding. Most importantly, I'd like to thank my Mom and Dad. They have always supported my passion for science and provided me with opportunities to experience life independently and to the fullest.

TABLE OF CONTENTS

LIST OF TABLES

LIST OF FIGURES

LIST OF APPENDICES

LIST OF ABBREVIATIONS

ACTβ	Beta actin
AI	Artificial insemination
ANK	Ankyrin
APC	antigen presenting cells
BGal	Beta galactosidase
bp	Base pair
C	Celsius
c-Src	Cellular sarcoma kinase
CASP1	Caspase-1
cDNA	Cloned deoxyribonucleic acid
CL	Corpus luteum/Corpora lutea
cm	Centimeter
d	Day/Days
dGE	Deep glandular epithelium
DNA	Deoxyribonucleic acid
E2	Estradiol-17beta
EDTA	Ethylenediaminetetraacetic acid
ESR1	Estradiol receptor alpha
ET	Embryo transfer
FGF 7	Fibroblast growth factor 7
FSH	Follicle stimulating hormone

GAF	Gamma-activation factor
GAS	Interferon-gamma activated sequence
GE	Glandular epithelium/Glandular epithelia
GFP	Green fluorescent protein
GLM	General linear model
GnRH	Gonadotropin releasing hormone
h	Hour
H/E	Hematoxylin/Eosin-Y
ICM	Inner cell mass
IFN	Interferon
IFNαR	Interferon-alpha receptor
IFNγ	Interferon-gamma
IFNγR	Interferon-gamma receptor
IFNδ	Interferon-delta
IFNτ	Interferon-tau
IHC	Immunohistochemistry
IKK	IκB kinase
IL-1	Interleukin-1
IL-18	Interleukin-18
IL-1RA	Interleukin-1 receptor antagonist
IL-1RAP	Interleukin-1 receptor accessory protein
IL-1RI	Interleukin-1 receptor type I
IL-1RII	Interleukin-1 receptor type II

IL-1α	Interleukin-1 alpha
IL-1β	Interleukin-1 beta
IL-1β1	Interleukin-1 beta 1
IL-1β2	Interleukin-1 beta 2
IL-6	Interleukin-6
IP3K	Inositol 1, 4,5-triphosphate 3-kinase
IRAK4	IL-1R-associated kinase 4
IRF1	Interferon regulatory factor 1
IRF2	Interferon regulatory factor 2
IRF9	Interferon regulatory factor 9
ISG	Interferon stimulated gene
ISGF3	Interferon-stimulated gene factor 3
ISRE	Interferon stimulated response element
IκB	Inhibitor of NF-κB
Jak	Janus associated kinase
kDa	Kilodalton
L	Liter
LE	Luminal epithelium/Luminal epithelia
LE/sGE	Luminal epithelium/surface glandular epithelium
LH	Luteinizing hormone
LIF	Leukemia inhibitory factor
LPS	Lipopolysaccharide
LSM	Least squares means

MAPK	Mitogen-activated protein kinase
mat-IL-1β1	Mature IL-1β1
mat-IL-1β2	Mature IL-1β1
mg	Milligram
MHC	Major histocompatibility complex
min	Minute
mL	Milliliter
mm	Millimeter
MMP-9	Matrix matealloproteinase-9
mRNA	Messenger ribonucleic acid
MUC-1	Mucin-1
MyD88	Myeloid differentiation primary response protein 88
NF-κB	Nuclear factor-kappa B
ng	Nanogram
NTC	No template control
OXT	Oxytocin
OXTR	Oxytocin receptor
P	Page
P4	Progesterone
PAT	PBS/Sodium azide/Tween-20 solution
PBS	Phosphate buffering solution
PCR	Polymerase chain reaction
pg	Picogram

PG	Prostaglandin
$PGF_{2\alpha}$	Prostaglandin $F_{2\alpha}$
PGH_2	Progstaglandin H_2
PGR(s)	Progesterone receptor(s)
PTGS1	Prostaglandin-endoperoxidase synthase 1
PTGS2	Prostaglandin-endoperoxidase synthase 2
RHD	Rel homology domain
RT-PCR	Real time polymerase chain reaction
SAL1	Salivary lipocalin 1
SAS	Statistical analysis system
SEM	Standard error of the lsmean
SLA	Swine leukocyte Ag
SPP1	Phosphoprotein 1/osteopontin
STAT	Signal transducers and activation of transcription
TAD	Transactivation domain
TCR	T cell receptors
TRAF6	Tumor necrosis factor receptor-associated factor 6
TXA	Thromboxane A
uNK	Uterine natural killer cell
US	United States
USP	Ubiquitin-specific protease
ZO1	Zonula occluden 1
αV	Alpha V integrin

β_2m	Beta 2 microglobulin
β3	Beta 3 integrin
μg	Microgram
μL	Microliter
μm	Micrometer
μmol	Micromole

CHARACTERIZATION OF INTERLEUKIN-1 BETA 2, A NOVEL INTERLEUKIN-1 EXPRESSED BY THE EARLY PIG CONCEPTUS DURING ESTABLISHMENT OF PREGNANCY

Daniel Joseph Mathew

Drs. Matthew C. Lucy and Rodney D. Geisert, Dissertation Advisors

Abstract

Conceptus mortality is greatest in mammals during the peri-implantation period, a time when conceptuses appose and attach to the uterine surface epithelium while releasing pro-inflammatory molecules. Interleukin-1 beta (*IL-1β*), a pro-inflammatory cytokine, is released by the primate, rodent and pig blastocyst during the peri-implantation period and is believed to be essential for establishment of pregnancy. The gene encoding *IL-1β* has duplicated in the pig, resulting in a novel gene. Preliminary observations indicate that the novel *IL-1β* is specifically expressed by pig conceptuses during the peri-implantation period and during rapid elongation, a morphological change made by the conceptus that increases the placenta surface area. Interleukin-1 signaling factors, IL-1 receptor type 1 (*IL-1RI*) and IL-1 receptor accessory protein (*IL-1RAP*), transiently increase in the conceptus and uterine luminal epithelium at that time suggesting that the novel *IL-1β* may influence elongation and implantation through

autocrine and paracrine activities, respectively. To verify that pig conceptuses express a novel IL-1, *IL-1β* was cloned from mRNA isolated from d 12 pig conceptuses and compared with *IL-1β* cloned from mRNA isolated from pig peripheral blood leukocytes (PBL). The pig conceptuses but not PBL expressed a novel *IL-1β*, referred to as interleukin-1 beta 2 (*IL-1β2*). To test the paracrine activity IL-1β2, porcine endometrium was treated with recombinant porcine IL-1β1, the prototypical cytokine, and IL-1β2 proteins. Immunohistochemistry (IHC) and real-time reverse transcriptase-polymerase chain reaction (RT-PCR) were used to measure activation of nuclear factor-kappa B (NF-κB) and NF-κB-regulated transcripts within the endometrium, respectively. Both IL-1β1 and IL-1β2 activated NF-κB in the uterine luminal epithelium within 4 h. The NF-κB activation and related gene expression, however, were reduced in endometrium treated with IL-1β2 suggesting that the conceptus-derived cytokine may have decreased activity within the uterus.

To test the autocrine activity IL-1β2 and its involvement in conceptus elongation, we developed a lentiviral mediated RNAi (knockdown) system targeting *IL-1β2* in early pig conceptuses. Multiple knockdown (KdV) and scrambled control knockdown (SV) viruses were developed and microinjected under the zona pellucida of in vitro produced pig zygotes. Conceptuses were then allowed to develop in culture (d 6 or 8) or were transferred to the oviduct of recipient gilts on d 4 of the estrous cycle. Transferred conceptuses were flushed from the uterus on d 13 of development. Microinjections of pig zygotes with V (KdV and SV combined) reduced the number conceptuses that became blastocyst by d 6 compared with conceptuses that were not microinjected. Expression of beta actin (*ACTβ*), a developmental control gene, in individual pig blastocyst treated with

SV tended to be less when compared with NV (no virus control) conceptuses. Expression of *IL-1β2* was detected in individual d 6 pig blastocysts and although expression was numerically lower in KdV when compared with NV and SV treated conceptuses, the expression level was not significantly different. With respect to the embryo transfer experiments, NV conceptuses were elongated on d 13. Out of three gilts that received KdV conceptuses, one gilt produced two elongated conceptuses (GFP positive) and two gilts produced abnormally small spherical conceptuses on d 13. Gilts that received SV conceptuses produced fragments of conceptus tissue or no conceptus tissue. A lentiviral mediated RNAi system-targeting *IL-1β2*, therefore, could not be used to effectively test the function of this cytokine during elongation of the early pig conceptus. Expression of *IL-1β2* in the d 6-pig blastocyst suggests that this cytokine may play an important role in development of the pig conceptus prior to elongation.

To investigate differences in protein structure between IL-1β1 and IL-1β2, we predicted and aligned the atomic structures of the cytokines using DNASTAR's Novafold program. In order for IL-1β to bind the IL-1RI, caspase-1 (CASP1) must process pro-IL-1β into a mature functional cytokine. Alignment of predicted pro and mature protein structures resulted in an RMSD of (3.47 Å) and (0.70 Å), respectively, indicating that IL-1β1 and IL-1β2 are highly similar in the absence of the pro-domains. Viewing the solvent accessible surface area of the pro-proteins suggested that there is a possible steric hindrance of the first caspase-1 (CASP1) site in IL-1β2 compared with that of IL-1β1. For the mature proteins, Novafold predicted that IL-1β1 and IL-1β2 bind the IL-1RI with 35 and 32 binding sites, respectively. Thirty-two binding sites were shared between the two proteins. Of these binding sites, IL-1β2 had three non-conserved amino acid

substitutions that resulted in a complete change of charge and solvent accessible surface areas compared with IL-1β1. Overall, differences in protein structure, the number of IL-1RI binding sites and amino acid side chain charges could affect the availability and activity of IL-1β2 compared with IL-1β1. In conclusion, the peri-implantation pig conceptus expresses a novel *IL-1β* that can activate NF-κB within the uterine surface epithelium, likely creating a pro-inflammatory microenvironment during establishment of pregnancy in the pig.

CHAPTER ONE

INTRODUCTION

Swine are an important resource for economic growth in the United States (US). Pork is consumed more than any other meat protein in the world and the US is projected to produce a record 10.9 million metric tons of pork (carcass weigh equivalent) in 2015 (www.usda.gov). The US is the third largest producer of pork worldwide (China and the European Union are first and second, respectively) and the world's largest exporter (www.usda.gov). Pigs are also important for biomedical research. Transgenic rodents have greatly contributed to the study of human diseases, however, pigs are more genetically and anatomically similar to humans and recent advances in production of transgenic pigs has lead to the development of more suitable human disease models. Transgenic pigs are now being used to study human cardiovascular disease, diabetes, cancer, retinitis pigmentosa, cystic fibrosis and organ xenotransplantation (Prather et al., 2008). Undoubtedly, pigs will continue to be an important resource for the production of food and scientific discovery.

Pigs are also important for the study of early embryo implantation and embryonic mortality. Pigs and other mammals, including humans, lose 25 and 60% of their embryos or pregnancies, respectively, within the first month of gestation (Wilmut et al., 1986;

Macklon et al., 2002). This phenomenon is commonly referred to as early embryonic mortality. Complications during development and implantation of the early conceptus (embryo and extra-embryonic membranes) are believed to be responsible. Early embryonic mortality may reflect inadequate "uterine receptivity", a transient endometrial state that favors attachment of the conceptus to the uterine surface epithelium and in some species, invasion into the endometrium (implantation) (Dekel et al., 2010; Cakmak and Taylor, 2011; Cha et al., 2012;). Uterine receptivity is achieved for a limited time each reproductive cycle and is influenced by maternal hormones such as progesterone. Further, hormones released by the conceptus can initiate communication or "crosstalk" with the endometrium, enhancing uterine receptivity (Simón et al., 1995; 2008; Cha et al., 2012). If development of the conceptus is delayed or if uterine receptivity is disrupted, this can result in communication breakdown and implantation failure. There are many ethical and technical limitations when studying conceptus-endometrial crosstalk and attachment in primates. However, research of early pregnancy in pigs can overcome these limitations as pig conceptuses are loosely associated with the uterine surface epithelium until d 14 of pregnancy and have a prolonged phase of attachment. In comparison, the mouse and primate conceptus initiates attachment and implantation on d 4 and 7 of development, respectively.

Research dedicated to unraveling the molecular control of early pregnancy in mammals has revealed that pro-inflammatory cytokines, small signaling proteins commonly released by immune cells, are secreted by the conceptus and endometrium during early pregnancy and are essential for proper embryo development, uterine receptivity and implantation (Simón et al., 1995; 2008; van Mourik et al., 2009). This

may not be surprising as historic and recent observations suggest that decidualization and implantation can be enhanced by injury induced inflammatory reactions within the endometrium (Granot et al., 2012; Dekel et al., 2014). For instance, during recent clinical studies, it was shown that scraping or nicking the endometrium before embryo transfer more than doubled the rate of implantation, clinical pregnancy and live birth in women who repeatedly experienced pregnancy failure (Granot et al., 2012; Dekel et al., 2014). Pro-inflammatory cytokines, released by the damaged endometrium, are believed to enhance the implantation process.

Recently it was found that *IL-1β*, a gene that encodes a master proinflammatory cytokine, has duplicated in the pig resulting in a novel IL-1 (Groenen et al., 2012). IL-1β is commonly released by leukocytes during innate and adaptive immune responses and can initiate the acute phase response, recruit leukocytes into infected tissues and act as an endogenous pyrogen. Released by the human and rodent conceptus during implantation, IL-1β is believed to be essential for establishment of pregnancy by acting on both the conceptus and endometrium (Simón et al., 1995; 2008). The newly discovered IL-1 in the pig is referred to as interleukin-1 beta 2 (*IL-1β2*) because of its cDNA and protein sequence similarity to the prototypical *IL-1β* (IL-1β1 in the pig).

Similar to the primate and rodent conceptus, pig conceptuses abundantly release an IL-1, the novel IL-1β2, into the uterine lumen during early pregnancy. Pig conceptuses maximally up regulate and secrete IL-1β2 during elongation, a critical morphological transformation of the conceptus, and just prior to their attachment to the uterine surface (Ross et al., 2003a). IL-1β2 is hypothesized to promote elongation and prepare the endometrium for implantation as both the conceptus and uterine surface epithelium

increase expression IL-1 signaling factors, the functional IL-1 receptor type I (*IL-1RI*) and the IL-1 receptor accessory protein (*IL-1RAP*), during its secretion (Ross et al., 2003a; Seo et al., 2012). In the endometrium, IL-1β2 is hypothesized to activate nuclear factor-kappa B (NF-κB), a transcription factor that controls expression of over a hundred genes, many of which modulate the inflammatory response and could promote implantation (Ross et al., 2010; Mathew et al., 2011). These events occur within the uterus at a time when embryonic mortality is believed to be at its greatest (Bazer and Johnson, 2014).

In Chapter Two, we review the cellular and molecular events that are believed to occur within the uterus during elongation, maternal recognition of pregnancy and implantation in the pig with specific emphasis on the hypothesized actions of proinflammatory cytokines IL-1 and interferons (IFN) during these processes.

CHAPTER TWO

LITERATURE REVIEW

INTRODUCTION

The first three weeks of pregnancy are the most critical for survival of the mammalian conceptus. Following early cleavage and passage from the oviduct into the uterus, formation of the morula will initiate pathways for cellular differentiation to establish the lineages of epiblast and trophoectoderm during blastocyst development. Hatching from the zona pellucida exposes the conceptus to a variety of maternal uterine secretory factors that include various proteins and micro molecules. Implantation (extent of uterine invasion varies among mammals) allows the trophectoderm to intimately associate with the endometrium and initiate communication through the uterine luminal (LE) and glandular (GE) epithelium, stromal fibroblasts and immune cells that patrol the maternal endometrium. There is a defined “window” of uterine receptivity, which allows the trophoblast to attach and in some species, invade beyond the LE until pregnancy is established. Throughout the entire process, 25-60% of conceptuses are lost, some of which may result of asynchrony between the developing conceptus and the receptive

uterus and inadequate communication or “cross-talk” between the trophectoderm and endometrium at the time of implantation (Wilmut et al., 1986; Macklon et al., 2002).

During early pregnancy, a cytokine network exists within the uterus that serves as a communication link or “conduit” between the foreign conceptus and cells within the endometrium. This network, which includes pro-inflammatory cytokines, is necessary for proper development of the conceptus and creates a uterine environment that favors implantation and establishment of pregnancy.

Evidence suggests that a moderate pro-inflammatory environment within the endometrium at the time of implantation enhances uterine receptivity and pregnancy success. For instance, it has been shown that scrapping or nicking the uterine surface prior to embryo transfer, slightly damaging the endometrium, can more than double the rate implantation, clinical pregnancy and live birth in women who repeatedly fail to maintain pregnancy (Raziel et al., 2007; Dekel et al., 2010; Granot et al., 2012). It’s believed that the damaged tissue releases pro-inflammatory cytokines, manifesting a pro-inflammatory environment that enhances uterine receptivity and implantation (Granot et al., 2012).

Pro-inflammatory cytokines are small signaling proteins (< 100 kDa) commonly released by leukocytes during innate and adaptive immune responses. These cytokines are believed to be essential mediators of communication between the conceptus and endometrium, enhancing uterine receptivity and implantation (Simón et al., 2007a; Dekel et al., 2010; Mor et al., 2011; Granot et al., 2012). Interleukins (IL) and interferons (IFN) are some of the most well studied factors proposed to influence mammalian reproduction. Studies indicate that primate and rodent blastocysts initiate communication with the

endometrium by releasing interleukin-1 beta (IL-1β), which enhances uterine surface receptivity and increases invasive characteristics of the cytotrophoblast (Librach et al., 1994; Simón et al., 1995). Furthermore, IL-1β is also expressed within the reproductive tissues of placental reptiles, leading some to believe IL-1β may have contributed to the evolution of placental viviparity (Paulesu et al., 2005). The pig is unique in that the IL-1β gene has duplicated, resulting in a novel gene and conceptus form of IL-1β (Tuo et al., 1996; Ross et al., 2003a; Mathew et al., 2011b; Groenen et al., 2012; Tuggle et al., 2012). Up-regulation of the novel IL-1β is directly followed by abundant production of interferon gamma (IFNγ) by pig conceptuses and in lesser concentrations, a pregnancy specific type I IFN, interferon delta (IFNδ) (Cross and Roberts, 1989; La Bonnardière et al., 1991; Cencič and La Bonnardière, 2002). In pigs, these cytokines are released in concert with conceptus estrogens, the maternal recognition of pregnancy signal (Bazer and Thatcher, 1977).

Based on studies investigating implantation in pigs, the combined spacio-temporal activities of these molecules on specific cell types within the adjacent endometrium set in motion a series of coordinated events that promote implantation and establishment of pregnancy (Bazer et al., 2012; Bazer and Johnson, 2014).

Porcine Estrous Cycle

A healthy female pig will become reproductively mature and initiate her first estrous cycle at approximately 6 months of age. After which she will express signs of estrus and ovulate from both ovaries every 21 days (d) until conception occurs.

During estrus, the female pig will remain receptive to the boar for 48 to 72 h during which peak concentrations of estradiol (E2) within the blood cause a surge release of luteinizing hormone (LH) from the anterior pituitary resulting in ovulation (rupture of Graffian follicles and release of oocytes), luteinization of follicular cells (granulasa and theca interna) and resumption oocyte meiosis. As concentrations of E2 decline within the blood, luteinization of the follicular cells results in formation of corpora hemorragica.

Between d 3 and 4 of the estrous cycle (beginning of the luteal phase), the corpora hemorragica mature into functional corpora lutea (CL), synthesizing and releasing increasing concentrations of progesterone (P4) into the blood. By d 5 of the estrous cycle and until d 16, the uterine environment is completely dominated by P4. In response, the uterine myometrium is quiescent and uterine luminal epithelial and surface glandular epithelial cells (LE/sGE) secrete histotroph, a large collection of micro molecules and proteins that can nourish conceptuses (Bazer et al., 2011).

The length of the pig estrous cycle is controlled by P4 and is uterine-dependent. Stimulation of the uterus with P4 for 10 to 12 days leads to endometrial production of luteolytic prostaglandin $F_{2\alpha}$ ($PGF_{2\alpha}$) and its secretion into the blood, causing luteolysis (McCracken et al., 1999). If multiple pig conceptuses are not present to release the maternal recognition of pregnancy signal and disrupt this process, the CL will regress, blood P4 will decrease and the sow will initiate another follicular phase, again, expressing signs of estrus (Spencer et al., 2004). The cyclic pattern of the estrous cycle, controlled by P4, allows the pig to recycle and return to estrus for another attempt at conception in the absence of fertilization.

Early Pregnancy in the Pig

On average, the typical US production sow will ovulate between 20 and 30 oocytes during estrus. The rate of fertilization by natural mating or using standard artificial insemination (AI) methods is suggested to be greater than 95% (Polge, 1978; Caárdenas and Pope, 2002; Geisert and Schmitt, 2002; Foxcroft et al., 2006). Because the rate of embryonic loss is very low during the first week of gestation, as many as thirty conceptuses can enter the uterine lumen (approximately three days after the onset of estrus and insemination). Pig blastocysts hatch from the zona pellucida on day 6 to 7 of gestation, which then exposes the conceptus to the uterine milieu; a collection of ions, nutrient transport proteins, proteases, growth factors as well as cytokines and other substances collectively referred to as histotroph. Histotroph is secreted by surface epithelial and glandular epithelial cells in response to ovarian progesterone. After hatching, the spherical pig blastocyst continues to grow and expand within the uterine lumen until near d 11 of gestation. Between d 11 and 12, the conceptus rapidly transforms morphologically and elongates in shape. Elongation is a critical stage of development for the pig conceptus, defining the surface area for its individual placental attachment (Bazer et al., 2012; Bazer and Johnson, 2014). The process is not unique to early ungulate development as cattle and sheep conceptuses also elongate, however, the rate at which this process is achieved in the pig is extraordinary. At this time, cellular mitosis decreases and cellular hypertrophy and migration of the surrounding trophoblast cells results in extensive remodeling (Geisert et al., 1982; Bazer et al., 2012; Bazer and Johnson, 2014). The pig conceptus becomes ovoid, tubular (15 mm by 50 mm) and then a 1 mm by 200 mm filamentous like structure in 2-3 h, extending along the mesometrial

interface through a complex landscape of endometrial crypts and folds at a rate of 30 to 45 mm/h (Geisert et al., 1982; Bazer and Johnson, 2014). This is referred to as rapid elongation (Fig. 2.1).

After d 12, the conceptus will more slowly elongate and expand in the uterine lumen reaching over a meter in length while attaching to the LE between d 13 to 18 of gestation (Bazer at al., 2012; Bazer and Johnson, 2014) (Fig. 2.1). Attachment of the trophoblast begins nearest to the developing embryo body and extends outward. Within attachment sites, surface area is enhanced by the presence of endometrial tuffs, surface epithelial folds and microvilli between the trophoblast and domed shaped LE cells for which are coated by a thick glycocalyx (Dantzer, 1985; Keys and King, 1990). Although pig trophoblast cells are invasive and send long projections between adjacent uterine LE cells, they do not penetrate beyond LE tight junctions (Dantzer, 1985; Keys and King, 1990).

The window of receptivity for conceptus attachment is programmed through ovarian P4 secretion, which down-regulates P4 receptors (PGR) within the uterine LE and surface GE (LE/sGE) cells in mammals (Bazer and Johnson, 2014). In pigs, loss of PGR in the epithelium reduces expression of mucin-1 (MUC-1), a large glycoprotein regulated by P4, along the uterine surface epithelium (Bowen et al., 1996; Bazer et al., 2012). Furthermore, the loss of PGR in the epithelium allows for expression of estrogen receptor alpha (ESR1) within the uterine LE/sGE, which is activated by conceptus estrogens (maternal recognition pregnancy signal) secretion between d 10 to 18 of pregnancy (Geisert et al., 1993; Bazer et al., 2014). In response, surface epithelial ESR1 stimulate production of “estramedins” such as secreted phosphoprotein 1 (SPP1; also

known as osteopontin) and fibroblast growth factor 7 (FGF7), which aid in adhesion, proliferation and implantation of the pig conceptus (Fig. 2.2) (Bazer and Johnson, 2014). Although PGRs are down regulated in the LE/sGE, they are expressed within stromal fibroblast cells, deep glandular epithelium (dGE) and myometrium, stimulating the release of "progestamedins" that may act on the LE and conceptus (Bazer and Johnson, 2014).

Maternal Recognition of Pregnancy

The term "maternal recognition of pregnancy" was coined by Short in 1969 and today refers to the requirement of the conceptus to produce factors that can act on the uterus and/or CL to ensure continued production of ovarian P4; a steroid hormone produced by CL that is required to maintain pregnancy in most mammals (Bazer, 2013).

Interferon tau (IFNτ) is a type I IFN released by the ovine conceptus mononuclear trophoblast cells between d 12 and 15 of gestation and serves as the maternal recognition of pregnancy signal by disrupting a series of coordinated events within the uterine surface epithelium that would ultimately lead to luteolysis (structural and functional regression of the CL) (Bazer et al., 1997; Roberts et al., 1999; Roberts, 2007). Disruption of luteolysis extends the life span of the CL and maintains elevated levels of P4 that aid in retention and development of the conceptus (Roberts, 2007).

The actions of IFNτ during maternal recognition of pregnancy in the ewe is summarized in a working model proposed by Spencer and others (2004) in accordance with the McCracken model of luteolysis (McCracken et al., 1999). During the ovine estrous cycle and formation of the CL following ovulation, the subsequent increase in P4

results in down regulation of PGR within the uterine LE/sGE as described above. If the ovine conceptus is not present to release the maternal recognition of pregnancy signal, ESR1 reestablishes and increases expression of oxytocin receptors (OXTR) within these cells. After which, oxytocin (OXT) released from the pituitary and ovary set in motion pulsatile synthesis of luteolytic prostaglandin F 2 alpha ($PGF_{2\alpha}$) within the uterine LE/sGE. The $PGF_{2\alpha}$ can then enter the endometrial vasculature, where by countercurrent exchange between the uterine vein and ovarian artery, reach the ovary causing degradation of the CL. In the absence of disease and if the animal has reached puberty, this process will repeat each estrous cycle (approximately every 17 days in sheep) during the breeding season until conception occurs and the maternal recognition of pregnancy signal is released. According to the model proposed by Spencer and others (2004), the ovine conceptus releases INFτ, blocking luteolysis by signaling through LE/sGE-interferon alpha-receptor complex (IFNαR). Described in greater detail below, down steam intra cytoplasmic signaling through the janus associated kinase-signal transducer and activator of transcription (Jak-STAT) signaling pathway results in repression of ESR1 and ultimately OXTR expression within the LE/sGE. This disrupts endometrial synthesis of $PGF_{2\alpha}$.

Although elongating pig conceptuses trophoblast cells express both type 1 and II IFNs (IFNδ and IFNγ, respectively), estrogens (catecholestrogens, estrone and estradiol), synthesized by the conceptus between d 10 and 18 of gestation, are the maternal recognition of pregnancy signal in pigs (Bazer and Thatcher, 1977; Lefèvre et al., 1998; Bazer et al., 2013). Unlike sheep and cattle, IFN are not antiluteolytic in this species, as intrauterine infusion of IFNγ and IFNδ in pigs does not extend the interestrus interval or

the functional lifespan of CL (Lefèvre et al., 1998b). Also, unlike sheep, pig conceptuses do not block LE/sGE OXTR expression and synthesis of luteolytic $PGF_{2\alpha}$ (Ludwig et al., 1998; Hu et al., 2001). Rather, to maintain progesterone synthesis by the CL, pig conceptuses release estrogens, that, through an unknown mechanism, redirect endometrial $PGF_{2\alpha}$ from the uterine venues system to the uterine lumen possibly by influencing LE/sGE cell polarity (Bazer et al., 1982; Spencer et al., 2004; Sukjumlong et al., 2005). Developed by Bazer and Thatcher (1977), the sequestration of $PGF_{2\alpha}$ in the uterine lumen by conceptus estrogens, rather than release into the vasculature, is referred to the "exocrine-endocrine" model of maternal recognition of pregnancy in pigs. Aside from the effects that conceptus estrogens, early pig conceptuses release a novel IL-1, IFNγ and IFNδ that are hypothesized to stimulate luteo-protective factors within the endometrium, such as PGE_2, that may contribute to CL maintenance during gestation (Harney and Bazer, 1989; Johnson et al., 2009; Waclawik, 2011). The actions of conceptus IL-1 and IFN are also believed to have functions related to development of the conceptus and implantation during establishment of pregnancy in the pig (Fig. 2.2 and 2.3). The following provides the current knowledge of the IL-1 superfamily of cytokines and their role in establishment of pregnancy.

Interleukin-1

Interleukin-1 beta is a master pro-inflammatory cytokine, serving as a central mediator of inflammation and innate immunity in mammals (Dinarello, 2011; Garlanda et al., 2013). Commonly released by hematopoietic cells such as blood monocytes, macrophages, skin dendritic cells as well as brain microglia, IL-1β is an endogenous

pyrogen, likely promoting leukocyte proliferation and migration during infection by inducing fever (Sims and Smith, 2010; Garlanda et al., 2013). IL-1β and interleukin-1 alpha (IL-1α), which bind the same receptor, stimulate the effector function of neutrophils and macrophages while orchestrating the differentiation and function of innate and adaptive lymphoid cells (Garlanda et al., 2013). Like other cytokines, IL-1 is pleiotropic and can influence the biology of virtually all cells and tissues including those involved in mammalian reproduction (Simón et al., 1997a; Garlanda et al., 2013).

Unregulated, IL-1 production and signaling can lead to auto-inflammatory, autoimmune, infectious and degenerative diseases that include malignant cancers and type II diabetes (Dinarello, 2009; Sims and Smith, 2010; Dinarello, 2011; Garlanda et al., 2013). Therefore, IL-1 transcription, translation, processing, secretion and signaling are highly regulated (Dinarello, 2009; Sims and Smith, 2010; Garlanda et al., 2013). Combined, the IL-1 and IL-1 receptor family consists of twenty-two molecules which include pro-inflammatory cytokines IL-1β and IL-1α, an IL-1 receptor antagonist (IL-1RA), an IL-1 receptor accessory protein (IL-1RAP), a functional IL-1 receptor (IL-1RI) and a decoy receptor, the IL-1 receptor type II (IL-1RII) (Sims and Smith, 2010; Dinarello, 2011; Garlanda et al., 2013). Release of active pro-inflammatory IL-1β occurs following formation of the inflammasome for which is associated with a cysteine protease, caspase 1 (CASP1). Active CASP1 cleaves Pro-IL-1β and Pro-IL-18, another member of the IL-1 family, resulting in formation of mature, functional, pro-inflammatory cytokines that are then secreted into the extracellular space and can circulate within the blood (Sims and Smith, 2010; Garlanda et al., 2013).

Both IL-1β and IL-1RA competitively bind the extra cellular immunoglobulin domains of IL-1RI, however; only the IL-1β-IL-1RI complex recruits the IL-1RAP which is necessary to trigger a biological response (Dunne and O'Neill, 2003). Juxtapositioning of the toll interleukin-1 receptor (TIR) domains within the cytoplasmic region of IL-1RI and IL-1RAP effectively recruit myeloid differentiation primary response protein 88 (MyD88), IL-1R-associated kinase 4 (IRAK4), tumor necrosis factor receptor-associated factor 6 (TRAF6) and other downstream intermediates that activate nuclear factor-kappa B (NF-κB) and mitogen-activated protein kinase (MAPK) signaling pathways (Sims and Smith, 2010). Unlike IL-1β, IL-1α is commonly released as a precursor that acts locally rather than in circulation, however, this cytokine can also bind the IL-1RI resulting in a similar biological response. Interestingly, the IL-1α precursor can rapidly enter the cell nucleus and act as transcriptional trans activator, binding DNA and influencing transcription (Sims and Smith, 2010; Garlanda et al., 2013). Signaling between IL-1 and the IL-1RI is highly controlled by the IL-1RA and IL-1RII, the IL-1 decoy receptor. Compared to IL-1, the IL-1RA has a higher affinity for IL-1RI and less affinity for IL-1RII. Further, IL-1RII may be soluble or insoluble and can bind the IL-1RAP, which may also be soluble or membrane bound, minimizing activation of IL-1RI (Dunne and O'Neill, 2003; Sims and Smith, 2010). Human IL-1RA and IL-1α, with amino acid sequences that are 26% and 25% homologous with mature IL-1β, respectively, bind the IL-1RI (Dinarello, 1991; Veerapandian, 1992).

Nuclear factor-kappa B

IL-1 signaling activates NF-κB; a family of transcription factors composed of evolutionarily conserved subunits that are critical modulators of innate and adaptive immune responses (Caamaño and Hunter, 2002). Sen and Baltimore discovered NF-κB in 1986 as a DNA binding factor in B-lymphocytes that recognized the immunoglobulin-kappa light chain enhancer, hints the name, nuclear factor-kappa B (Sen and Baltimore, 1986). Present in nearly every mammalian cell, NF-κB transcription factors can reside as homo or hetero dimers consisting of a combination of five subunits that belong to the Rel protein family [c-Rel, RelA (p65), RelB, NF-κB1-(p105/p50) and NF-κB2-(p100/p52)]. These subunits share a conserved N-terminal domain, referred to as the Rel homology domain (RHD). The RHD is responsible for nuclear translocation, DNA binding, subunit dimerization and interaction of NF-κB with IκB (inhibitor of NF-κB) proteins (Caamaño and Hunter, 2002). The RHD domain shares homology with the N-terminal domain of relish (Rel), a transcription factor that modulates the immune responses against bacteria in Drosophila (Dushay et al., 1996). In mammals, the c-Rel, RelA and RelB subunits contain C-terminal transactivation domains (TAD) that promote transcription (Hayden and Ghosh, 2012). Therefore, NF-κB dimers without a TAD (p50:p52) can repress transcription by reducing availably of NF-κB binding sites (κB-sites) within the promoter and enhancer regions of DNA (Hayden and Ghosh, 2012). Although NF-κB2, RelB and c-Rel are expressed specifically in mammalian lymphoid tissues, the NF-κB1 and p65 subunits, the latter containing a TAD, are ubiquitously expressed in most tissues resulting in the more common NF-κB dimer, p65:p50 (Caamaño and Hunter, 2002).

Inactive and awaiting signal, most NF-κB dimers are sequestered in the cytoplasm by IκB proteins (Oeckinghaus et al., 2011). The IκB proteins, characterized as having multiple ankyrin repeat (ANK) domains, interfere with NF-κB's RHD nuclear translocation and DNA binding sequences. In mammals, there are multiple IκB proteins [IκBα, IκBβ, IκBε, IκBζ, B-cell lymphoma 3 (BCL-3) and IκBns] (Hayden and Ghosh, 2012). Like Drosophila's Rel factor, NF-κB1 and NF-κB2 precursor subunits [NF-κB1-(p105) and NF-κB2-(p100), respectively] contain a self-inhibiting IκB like domain (with ANK) that in mammals must be processed or degraded before nuclear translocation of NF-κB1-p50 and NF-κB2-p52 subunits can occur (Hayden and Ghosh, 2012; Dushay et al., 1996).

Within the cytoplasm, the p65:p50 transcription factor is commonly held inactive by IκBα. When IL-1 binds its receptor, triggering of the second messenger cascade ultimately activates the IKK complex (Oeckinghaus et al., 2011; Hayden and Ghosh, 2012). Comprised of IKK-beta (IKK-β), IKK-alpha (IKK-α) and the regulatory subunit IKK-gamma (IKK-γ; also known as NEMO), the activated IKK complex (specifically IKK-β) phosphorylates IκBα (Oeckinghaus et al., 2011; Hayden and Ghosh, 2012). This is referred to as the canconical pathway of NF-κB activation and phosphorylation of IκBα destines the inhibitor protein for degradation by the 26S proteasome (Oeckinghaus et al., 2011; Hayden and Ghosh, 2012). Release p65:p50 exposes the transcription factor's nuclear localization signal, allowing it to quickly enter the nucleus, bind the DNA, and promote transcription of over a hundred genes including those encoding cytokines, chemokines, growth factors, adhesion molecules, immunoreceptors, antigen presentation molecules, and other transcription factors (Hayden and Ghosh, 2012).

IL-1 signaling and activation of NF-κB can have a dramatic effect on a cell's biology and for this reason their activities are highly regulated by various feedback mechanisms. NF-κB can increase expression of IκB proteins, including *IκBα,* NF-κB subunits, and members of the IL-1 family such as *IL-1β*, *IL-1α,* and *IL-1RA* (Hiscott et al., 1993; Smith et al., 1994; Mori and Prager, 1996; Hayden and Ghosh, 2012). Uncontrolled, IL-1 signaling and NF-κB activation leads to radical cell proliferation and malignant cancer growth, making the various components of the IL-1-NF-κB signaling pathway an attractive target for anti-cancer therapies.

IL-1 and Reproduction

IL-1 is believed to be an ancient modulator of vertebrate reproduction, detected within the reproductive tissues of animals using very different reproductive strategies including oviparous, ovuliparous and aplacental viviparous species (Bird et al., 2002; Jantra et al., 2007). Furthermore, IL-1β is expressed by the placenta of mammalian and non-mammalian vertebrates such as squamite reptiles and elasmobranch fishes, leading some investigators to suggest that IL-1β is a fundamental mediator of placental viviparity, influencing conceptus attachment, invasion and fetal-maternal immune tolerance (Simón et al., 1995; Paulesu et al., 2005). In respect to placental mammals, IL-1 crosstalk occurs between the conceptus and endometrium during implantation in primates, rodents and pigs (Simón et al., 1994a; 1997a; 1998; Tuo et al., 1996; Ross et al., 2003a).

IL-1β and *IL-1RI* are expressed in the early primate blastocyst and elevated production of IL-1β by the conceptus is correlated with successful implantation. These

conclusions are based on embryo transfer (ET) studies where greater concentrations of IL-1β in conceptus-conditioned culture medium were positively correlated with improved rates of implantation (Barañao et al., 1997). Further, human conceptuses produced from blastomeres with increased *IL1RA* are more likely to arrest during early development (Krüssel et al., 1998). Within the uterus, IL-1 is believed to have a direct effect on the LE for implantation. The IL-1RI increases within the endometrium and is greatest within the uterine surface epithelium during the receptive phase of implantation (Simón et al., 1993). Further, IL-1β has a direct effect on uterine receptivity through modulation of adhesion molecules alpha V (αV) and beta 3 (β3) integrin subunits in the uterine epithelium (Simón et al., 1993; Simón 1997b; Barañao et al., 1997; Krüssel et al., 1998).

Aside from its effects on uterine receptivity, IL-1 may promote invasive implantation in primates. During invasion into the maternal decidua, IL-1β can be detected within conceptus villous cytotrophoblast, extravillous intermediate trophoblast, syncytotrophoblast as well as maternal stromal decidua cells (Simón et al., 1994a; Barañao et al., 1997). The IL-1RI can be detected within the first trimester cytotrophoblast, syncytotrophoblast and endometrial glands (Simón et al., 1994a; Librach et al., 1994; Barañao et al., 1997;). During *in vitro* experiments, IL-1β increased production of matrix metalloproteinase-9 (MMP-9) and invasive characteristics in human cytotrophoblast cells (Steele et al., 1992; Librach et al., 1994). In similar studies, IL-1β increased estrogen synthesis and human chorionic gonadotropin (hCG) expression in human cytotrophoblast cells (Steele et al., 1992; Nester et al., 1993).

Mouse conceptuses express *IL-1β*, *IL-1RI* and *IL-1RA* until implantation and induction of decidualization in pseudopregnant mice increases *IL-1β* and *IL-1α* mRNA

within the endometrium that is temporally associated with implantation (Choudhuri and Wood, 1993; Takacs and Kauma, 1996; Krüssel et al., 1997). Similar to primates, IL-1β directly influences uterine receptivity for implantation in mice, up-regulating αV and β3 integrins and promoting alterations in surface epithelial cell morphology (Simón et al., 1994b; Simón et al., 1998). However, the importance of IL-1β during early pregnancy in rodents is unclear. Intraperitonial infusion of IL-1RA between d 3 and 6 of pregnancy in mice results in complete implantation failure, yet, knockout mice lacking *IL-1RI* are fertile, having only slightly reduced litter sizes (Simón et al., 1994b; Abbondanzo et al., 1996; Simón et al., 1998). Similarly, conceptuses lacking *IL-1β*, *IL-1α* or *IL-1β/IL-1α* develop normally suggesting that other factors may compensate for the lack of IL-1 signaling within the endometrium during implantation in mice (Horai et al., 1998).

Tuo and others (1996) were the first to report that pig conceptuses up-regulate expression of an *IL-1β* during early development and at the time of conceptus elongation. Expression of conceptus *IL-1β* rapidly increases during the short period of elongation and then dramatically decreases (2000 fold) as the conceptus attaches to the uterine surface, becoming nearly undetectable by d 14 (Ross et al., 2003a; Tuggle et al., 2003). During peak expression (d 12 of development), *IL-1β* is one of the most abundant transcripts expressed by pig conceptus, leading to intrauterine proteins concentrations approaching 4000 ng per uterine horn (Ross et al., 2003a, 2003b). This exceeds the concentration commonly released during IL-1 signaling (Pinteaux et al., 2009). Although expression rapidly declines following elongation, IL-1β protein can be detected within the uterine lumen between days 12 to 15 of gestation (Ross et al., 2003a).

Novel Pig Interleukin-1 Beta

Over 20 years ago, Vandenbroeck and others suggest that an alternate *IL-1β* genomic sequence existed within the pig (Vandenbroeck et al., 1993). Using southern blot hybridization to probe for *IL-1β* within the wild and domesticated pig genomic DNA, they detected the presence of multiple bands within the blot suggesting a gene duplication. In 1996, Tou and others detected expression of an *IL-1β* in the d 12 pig conceptus, however, it wasn't until Ross and others (2003a) attempted to characterize the IL-1 system during early pregnancy when their data suggested that the pig conceptus expressed an alternate transcript. Using RT-PCR to measure *IL-1β* in reproductive tissues, they found that primers used to amplify *IL-1β* in pig endometrium could not be used to amplify *IL-1β* in the conceptus. Recent assembly and analysis of pig genomic sequences revealed the presence of a novel *IL-1β* within the long arm of pig chromosome three (Groenen et al., 2012; Dawson et al., 2013). Therefore, two *IL-1β* genes reside within the pig, interleukin-1 beta 1 (*IL-1β1*) and interleukin-1 beta 2 (*IL-1β2*). Despite advances in genome sequencing technology, the pig genomic region containing *IL-1β1* and *IL-1β2* has not been completely sequenced, consisting of many homologous sequences and repetitive elements that make accurate assembly of the region challenging. Based on PCR data and expressed sequence tags published within GenBank, investigators have concluded that early pig conceptuses abundantly express *IL-1β2* prior to implantation. However, the function of this novel IL-1 during early pregnancy in the pig has not been characterized.

Before *IL-1β2* was discovered, a number of experiments were conducted to elucidate the role of IL-1β during establishment of pregnancy in pigs. These studies often

involved treating cyclic pig endometrium with recombinant human IL-1β or IL-1β1, the pig prototypical cytokine, measuring changes in endometrial gene expression. Although these experiments did not involve *IL-1β2*, they have greatly contributed to our understanding of how IL-1 might influence reproduction in the pig and are described in detail below.

IL-1 and the Pig Endometrium

In pigs, IL-1β (rather IL-1β2), is suggested to promote early development, rapid conceptus elongation, enhance uterine receptivity for implantation and increase endometrial blood vessel permeability to promote fetal-maternal hemotrophic exchange (Keys and King, 1988; Ross et al., 2003a; Blomberg et al., 2008; Degrelle et al., 2009; Waclawik et al., 2009; Waclawik et al., 2011). Using RT-PCR, *IL-1β1* can be detected within the endometrium during early pregnancy, however, transcript abundance is minimum compared with conceptus *IL-1β2* and is not effected by day or pregnancy status (Ross et al., 2003a). Conceptus expression of *IL-1β2* is temporally associated with up regulation of *IL-1RI* and *IL-1RAP* within the adjacent uterine LE, both of which are predominately expressed in endometrium adjacent to elongating rather than spherical conceptuses (Seo et al., 2012). The IL-1 receptor antagonist, *IL-1RA*, decreases within the endometrium at this time (Ross et al., 2003a). IL-1RI and IL-1RAP are likely modulated by IL-1β2 alone or in combination with conceptus estrogens, acting as a positive feed back loop for IL-1 signaling at the time of conceptus elongation. IL-1 has been shown to enhance signaling within target tissues by increasing transcription of *IL1B*, *IL1RI* and *IL1RAP* (Bellehumeur et al., 2009; Dinarello, 2011).

To examine the affect of IL-1 and IFNs on endometrial IL-1 signaling components in pigs, Seo and others (2012) treated d 12 cyclic endometrium with increasing concentrations of recombinant human IL-1β or IFNγ for 24 h in the presence of reproductive steroids, E2 and P4. After which, they measured total endometrial *IL-1RI* and *IL-1RAP* mRNA. They found that IFNγ had no effect on endometrial *IL1RI* or *IL1RAP*; however, treating endometrium with IL-1β caused a dose wise increase in expression of *IL-1RI*. Transcript levels for *IL1RAP* also increased but were greater in response to the lowest dose of IL-1β (1 ng/mL) and were influenced by E2 (Seo et al., 2012). During a similar study, treatment of d 12 cyclic pig endometrial explants *in vitro* with human IL-1β in the presence of E2 increased expression of calbindin-D9K (S100G), a calcium transport protein (Choi et al., 2012).

The combined effects of conceptus estrogens and IL-1β within the endometrium, particularly within the uterine surface epithelium, may be complex. Estrogens are known to have anti-inflammatory properties. Both *in vitro* and *in vivo* studies suggest that ESR and NF-κB signaling pathways partake in reciprocal inhibitory crosstalk; suggesting that conceptus estrogens could lessen IL-1β2 induced pro-inflammatory activities within the endometrium that could be detrimental to establishment of pregnancy (Evans et al., 2001; Quaedackers et al., 2007; King et al., 2010). However, positive interactions between ESR and IL-1β signaling pathways have been reported within reproductive tissues, particularly, in human endometrial epithelial cell lines suggesting that conceptus estrogens and IL-1β2 may collaborate to promote implantation in the pig (King et al., 2010).

Alpha V and Beta 3 Integrins in Pigs

Pig conceptus IL-1β2 may not promote uterine attachment through up regulation of integrin subunits, as does IL-1 in primates and rodents. Bowen and others (1996) did not detect a significant increase in integrin expression in response to the conceptus, including αV and β3 subunits. Alpha V and β3 were constitutively expressed and remained high during both the estrous cycle and early pregnancy. Integrin subunits α4, α5 and β1 did increase between d 11 and 15 of the estrous cycle and pregnancy but appear to be controlled by P4 alone or in combination with E2 (Bowen et al., 1996). Pig conceptus IL-1β2 may promote endometrial blood vessel permeability, preparing the maternal environment for fetal maternal hemotrophic exchange (Martin et al., 1988; Puhlmann et al., 2005; Waclawik et al., 2011). IL-1β has been shown to increase blood vessel permeability which is enhanced in uterine sub-epithelial capillaries by d 13 of pregnancy in pigs, temporally associated with elevated concentrations of IL-1β2 within the pig uterine lumen (Keys and King, 1988; Laforest and King, 1992; Ross et al., 2003a).

Salivary Lipocalin 1 (SAL1)

Lipocalins belongs to a group of small extracellular proteins that bind hydrophobic molecules, such as lipids, transporting them within aqueous environments (Seo et al., 2011). *SAL1* is expressed within the boar submaxillary gland and has been shown to bind pheromones; contributing to the late theory that *SAL1* expression is male and tissue specific (Loebel et al., 2000). However, SAL1 protein was recently identified within pig uterine flushings and believed to be a component of uterine histotroph (Ka et al., 2009). Seo and others (2011) characterized SAL1 within pig reproductive tissues

during the estrous cycle and early pregnancy. They found that endometrial *SAL1* could be detected on d 12 and 15 of the estrous cycle with the greatest expression on d 12 of gestation. Conceptus factors released during elongation are believed to be responsible for up regulation of *SAL1* as endometrium adjacent to elongating (d 12) rather than d 11 spherical conceptuses had greater total *SAL1 mRNA*. In situ hybridization (ISH) and immunohistochemistry (IHC) experiments localized *SAL1* mRNA and protein, respectively, to the deep GE. Within the conceptus, only SAL1 protein could be detected. These observations prompted Seo and others (2011) to investigate SAL1 regulation within d 12 cyclic endometrium in response to reproductive steroids P4 and E2 as well as cytokines IL-1β (human) and IFNγ. Elaborate explant culture experiments revealed that dose dependent increases in IL-1β, in the presence of P4 and E2, could increase total endometrial *SAL1* mRNA within 24 h. The function of this protein during early pregnancy in the pig has not been determined. However, the authors suggest that like other lipocalins, SAL1 may bind lipids, transporting them to the developing conceptus. Alternatively, the authors suggest that SAL1 could acts as a scavenger of toxic lipid byproducts produced by the conceptus as it synthesizes large concentrations of estrogens for maternal recognition of pregnancy.

Activation of NF-κB in the Endometrium

The autocrine and paracrine effects of IL-1β2 during pregnancy, although not well characterized, involve activation of NF-κB and NF-κB regulated genes, which include prostaglandin-endoperoxide synthase 2 (*PTGS2*), leukemia inhibitory factor (*LIF*) and interleukin-6 (*IL-6*) (Ashworth et al., 2006; Ross et al., 2010; Franczak et al., 2010;

Mathew et al., 2011a; Blitek et al., 2012; Seo et al., 2012). In primates and rodents, conceptus IL-1 enhances uterine receptivity and promotes implantation by activating NF-κB, particularly, within the uterine surface epithelium (Laird et al., 2000; King et al., 2010). Protein for NF-κB subunits, NF-κB1 and p65, increase in the uterine epithelium during the "window" of uterine receptivity in humans (Laird et al., 2000; Page et al., 2002; King et al., 2010). In mice, NF-κB1 and p65 increase within the uterine GE on d 1.5 post-coitum and continues throughout implantation (Nakamura et al., 2004).

Similar to implantation in primates and rodents, pig conceptus IL-1β2 likely modulates uterine surface epithelial gene expression for uterine receptivity and implantation by activating NF-κB (Ross et al., 2010; Mathew et al., 2011a). During early pregnancy and peak production of IL-1β2, p65 is activated (localized to nuclei) within uterine LE cells directly adjacent to elongating pig conceptuses (Mathew et al., 2011a). Within the rodent and primate uterine epithelium, NF-κB increases expression of prostaglandin synthases and inflammatory cytokines considered essential for establishment of pregnancy such as *PTGS2*, *IL-6*, colony stimulating factor 1 (*CSF1*) and *LIF* (Pollard et al., 1991; Stewert et al., 1992; Laird et al., 2000; Nakamura et al., 2004).

Prostaglandins

Prostaglandins (PG) are fatty acid derived lipid mediators that modulate reproductive processes in mammals that include ovulation, blastocyst transport, hatching, implantation, decidualization and parturition (Lim et al., 1997; Ni et al., 2002; Kennedy et al., 2007; St-Louis et al., 2010). Prostaglandin-endoperoxide synthase 1 (PTGS1) and prostaglandin-endoperoxide synthase 2 (PTGS2) are rate limiting enzymes during PG

synthesis by converting arachidonic acid, cleaved by phospholipase A2, to prostaglandin H2 (PGH2). The PGH2 may be further metabolized to PGE_2, $PGF_{2\alpha}$, PGI_2, PGD_2 or thromboxane A (TXA) by other synthases (Ni et al., 2002; Simmons et al., 2004; St-Louis et al., 2010). Although *PTGS1* is constitutively expressed in most tissues, *PTGS2* transcription is triggered by inflammatory stimuli and commonly found within reproductive tissues. Partly in response to conceptus IL-1β, *PTGS2* is expressed within the endometrium of primates and rodents and knockout studies in mice indicate that PTGS2 is essential for implantation and decidualization (Lim et al., 1997; Marions et al., 1999; St-Louis et al., 2010). Regulation of endometrial *PTGS2* is less clear in the pig, however, similar to primates and rodents, pig conceptuses may promote endometrial *PTGS2* activity by releasing IL-1β2 and activating NF-κB. In respect to PG, these molecules are immune modulatory and have both anti-inflammatory and pro-inflammatory properties. Their synthesis is essential for establishment of pregnancy in pigs (Kraeling et al., 1985; Waclawik, 2011). Prostaglandins, specifically PGE_2, are hypothesized to enhance endometrial vascular remodeling in support hemotrophic exchange between the mother and the fetus but may also contribute to luteal maintenance during pregnancy in pigs (Kraeling et al., 1985; Waclawik et al., 2011).

During both the estrous cycle and pregnancy, total endometrial mRNA and protein for PTGS1 and PTGS2 increases after d 10 and d 5, respectively, and remains elevated until d 18 (Ashworth et al., 2006). In situ hybridization experiments indicate an increase in uterine surface epithelial *PTGS2* by d 12 of pregnancy and d 15 of the estrous cycle (Ashworth et al., 2006). However, there is no detectable increase in total endometrial *PTGS2* between d 10 and 14 of pregnancy or between d 12 cyclic or

pregnant pig endometrium; a time when conceptuses release peak concentrations of IL-1β2 (Ashworth et al., 2006; Blitek et al., 2006; Franczak et al., 2010). Previously, it was reported that recombinant IL-1β [human or pig (IL-1β1)] increased transcripts for *PTGS1* and *PTGS2* as well as PG transport molecules within the pig endometrium at the time of implantation (White et al., 2009; Franczak et al., 2010; Seo et al., 2012). Further research is needed to determine if IL-1β2 can increase *PTGS2* within the pig uterine surface epithelium. NF-κB, a stimulator of PTGS2 transcription, is highly activated within this tissue during early pregnancy (Ross et al., 2010; Mathew et al., 2011).

Aside from *PTGS2*, IL-1β can increase expression of phospholipase A2, an enzyme for which may enhance cell membrane fluidity by cleaving arachodonic acid from membrane associated lipid rafts (Kol et al., 2002; Ross et al., 2003a). It has been hypothesized that conceptus IL-1β2 may increase this enzyme within the LE and/or the conceptus, thereby stimulating architectural changes along the fetal-maternal interface that are necessary for implantation (Ross et al., 2003a; Waclawik et al., 2009).

IL-6 and LIF

Inhibition of NF-κB blocks IL-1β/IL-1α induced *IL-6* and *LIF* expression within cultured human endometrial epithelial cells (Laird et al., 2000). A decrease in *IL-6* and *LIF* mRNA during early pregnancy is correlated with infertility in humans and implantation does not occur in *LIF* knockout mice (Stewert et al., 1992; Laird et al., 2000). Furthermore, suppression of NF-κB activity blocks implantation in mice but implantation can be partially rescued by uterine viral transfection of *LIF* cDNA (Nakamura et al., 2004). Activation of NF-κB by conceptus release of IL-1β2 may be

partly responsible for up-regulation of these cytokines within the endometrium of pigs (Sparacio et al., 1992; Bamberger et al., 1997; Laird et al., 2000; Nakamura et al., 2004).

Blitek and others (2012) characterized endometrial IL-6 and LIF between d 10 and 18 of the estrous cycle and pregnancy in pigs. Transcript expression for *IL-6* and *LIF* increase within the pig endometrium between d 10 and 12 of gestation. More over, peak concentrations of LIF proteins were detected in uterine luminal flushings on d 12 of pregnancy; temporally associated with conceptus expression of *IL-1β2* and activation of the p65 subunit of NF-κB with the uterine surface epithelium (Ross et al., 2003a; Ross et al., 2010; Mathew et al., 2011a; Seo et al., 2012; Blitek et al., 2012). Furthermore, d 12 conceptus-conditioned culture medium, which would contain peak concentrations of IL-1β2, increased *IL-6* and *LIF* mRNAs in d 12 cyclic pig endometrium within 6 h of culture (Blitek et al., 2012). A similar mechanism may exist in the conceptus as expression of *IL-6* transiently increases during elongation (Blitek et al., 2012; Modrić et al., 2000). During implantation in pigs, endometrial *LIF* expression maybe intensified by the combined effects of conceptus estrogens and IL-1β2. In mice, ovarian estrogen increases endometrial *LIF* expression during implantation and LIF protein can replace nidatory estrogen by inducing implantation and decidualization in ovariectomized mice (Chen et al., 2000). This may not be true for endometrial IL-6 as ESR have been shown to have a negative effect on *IL-6* expression by inhibiting NF-κB-DNA binding within the IL-6 promoter (Galien and Garcia, 1997). Although the activities of IL-6 and LIF have been well studied in both humans and mice in regards to implantation and embryonic survival, little is known about the effects of these cytokines during establishment of pregnancy in pigs. However, receptors for IL6 and LIF are expressed by both the conceptus and

endometrium between d 10 and 14 of pregnancy, specifically within the uterine surface epithelium, indicating that these molecules have an important role during implantation in this species (Modrić et al., 2000; Østrup et al., 2010; Blitek et al., 2012). Over all, NF-κB may enhance uterine receptivity, implantation and/or conceptus development by modulating uterine surface epithelial gene expression at the time of elongation. Crosstalk between NF-κB and other signaling pathways including those that activate MAPK and inositol 1, 4,5-triphosphate 3-kinase (IP3K) are not uncommon and likely optimize the endometrial environment for establishment of pregnancy at the fetal-maternal interface (Oeckinghaus et al., 2011).

IL-1β2 and Immune Modulation

Conceptus release of IL-1β2 into the pig uterine lumen may modulate endometrial immune cell trafficking and function during implantation. During pig uterine infusion studies, an increase in the number of stromal leukocytes near the uterine epithelial layer in response recombinant pig IL-1β1 was observed, suggesting that in pigs, this cytokine and possibly IL-1β2, has to capacity to modulate endometrial leukocyte activity (Geisert, Ross, Roberts and White; data not published). The major leukocyte populations within the pig endometrium are lymphocytes, macrophages, neutrophils and dendritic-like cells with T cell and/or uNK lymphocytes the most abundant during pregnancy (Engelhardt et al., 2002). Although there is an increase in the number of intraepithelial lymphocytes between d 10 and 19 of the estrous cycle, these cells decrease during early pregnancy, apparently in response to unknown factors released by the conceptus (King, 1988). Interesting, Engelhardt and others, (2002), detected a 3 fold increase in the number of

stromal leukocytes with phenotypes similar to T, B and/or uNK cells adjacent to the d 15 conceptus attachment vs. non-attachment sites. The number of intraepithelial leukocytes was independent of conceptus location on d 15 and remained low. Following release of IL-1β2, pig conceptuses express a type I and type II IFN, of which may also modulate endometrial immune cell activity (Joyce et al., 2008; Kim et al., 2012).

IL-1 and the Conceptus

It's hypothesized that IL-1β2 promotes steroidogenesis in the early pig conceptus and developmental changes associated with elongation (Blomberg et al., 2008; Degrelle et al., 2009). These conclusions are based on the finding that pig conceptuses temporally and abundantly express *IL-1RI* and *IL-1β2* during the height of these processes. Peak intrauterine protein concentrations of pig conceptus IL-1β2, between d 10 and 15 of pregnancy, are temporally associated with elevated expression of aromatase and acute release of estrogens by pig conceptus into the uterine lumen for maternal recognition of pregnancy (Yelich et al., 1997; Ross et al., 2003a; 2003b). IL-1β has been shown to increase aromatase expression and estrogens synthesis in human cytotrophoblast cells in culture (Nester, 1993). In addition, global proteomic analysis of pig conceptuses revealed that IL-1β (rather IL-1β2 as this study was conducted prior to its discovery) exists as focal protein between the three primary protein networks during elongation (Degrelle, 2009). These networks included proteins involved in cellular assembly and organization, embryonic development as well as cell growth and proliferation which suggests that intracellular signaling triggered by the IL-1β2 might control a large number of genes involved in distinct biological processes during rapid elongation. The autocrine and

paracrine effects of pig conceptus IL-1 during pregnancy, although not well characterized, likely involve activation of NF-κB and NF-κB regulated genes (Ross et al., 2010; Mathew et al., 2011a).

Interferons

Over the last 30 years, research dedicated to unraveling the molecular control of establishment of pregnancy in mammals has expanded the role of IFN cytokines well beyond their antiviral and immune-modulatory properties (Platanias, 2005; González-Navajas et al., 2012; Bazer, 2013). IFNs are expressed by the peri-implantation primate, rodent and ungulate trophectoderm and are believed coordinate essential interactions at the fetal-maternal interface (Bazer, 2013). Aside from indirectly extending the life span of the CL in ruminants, which is essential in maintaining pregnancy beyond the length of the normal estrous cycle, conceptus INFs stimulate expression of classical (antiviral) and non-classical IFN stimulated genes (ISGs) that are under spacio-temporal regulation within the mammalian endometrium (Spencer et al., 2008). Although the functions of endometrial ISGs remain unclear, studies investigating IFN signaling within the uterus of livestock species suggest they modulate fetal-maternal immune tolerance, endometrial architecture changes for uterine receptivity and vascular remodeling for maternal-fetal hemotrophic support of pregnancy.

Mammalian IFNs are classified under two main types: type I and type II. Thus far, type I IFNs include interferon-alpha (IFNα), beta (IFNβ), kappa (IFNκ), omega (IFNω), epsilon (IFNε), tau (IFNτ) and IFNδ, some of which consist of more than one subtype but all of which bind the same receptor complex, the interferon-alpha receptor (IFNαR), to

signal a biological response. The type II interferon consists of one member, IFNγ, which does not share structural homology with type I IFNs and has it's own receptor complex, the interferon gamma receptor (IFNγR) (Platanias, 2005).

Type I and type II IFNs trigger expression of classical ISGs through activation of the Jak-STAT signaling pathways and therefore stimulate similar genes. However, the IFNs can promote distinct expression profiles and can have dissimilar immunological properties (Platanias, 2005). Cells release type I IFNs during viral infection, up regulating and activating enzymes that interfere with viral replication, such 2', 5' oligoadenylate synthase (OAS) and RNase L (Abbas et al., 2007; Ivashkiv and Donlin, 2014). Type I IFNs also promote innate immune responses by enhancing recognition of infection through up-regulation of MHC class I molecules on the cell surface and augmenting NK cell responses (Ivashkiv and Donlin, 2014).

The type II IFN, IFNγ, functions mostly to trigger innate immune responses and adaptive cell-mediated immunity against viruses and intracellular bacteria (Abbas et al., 2007). During the innate immune response, antigen presenting cells (APCs), most notably macrophages, will recruit NK cells via IL-18 and promote NK cell production of IFNγ. In turn, IFNγ stimulates APC killing of the phagocytosed pathogens. Activated $CD8^+$ cytotoxic and $CD4^+$ helper T lymphocytes also produce IFNγ which can further promote cell mediated immunity by up-regulating MHC class I and II molecules in target cells (Schroder et al., 2004; Abbas et al., 2007).

Interferon signaling is complex and at minimum includes binding of type I IFNs to IFNαR, resulting in phosphorylation and activation of STAT1 and STAT2 (Platanias, 2005; González-Navajas et al., 2012). Similarly, binding of IFNγ to IFNγR results in

phosphorylation and activation of STAT1 (Platanias, 2005; González-Navajas et al., 2012; Bazer, 2013). During type I IFN signaling, phosphorylated STAT1 and STAT2 can dimerize and associate with interferon regulatory factor 9 (IRF9), forming a complex referred to as interferon-stimulated gene factor 3 (ISGF3). The ISGF3 can bind IFN stimulated response elements (ISRE) within the promoter regions of DNA, up-regulating ISGs (Platanias, 2005; González-Navajas et al., 2012; Bazer, 2013). Both type I and type II IFN signaling provoke formation of STAT1 dimers, also known as gamma-activation factor (GAF), that bind IFNγ-activated sequences (GAS) within the promoter of some ISGs (Platanias, 2005; González-Navajas et al., 2012; Bazer, 2013). Importantly, a GAS sequence can be found in the promoter region of interferon regulatory factor 1 (IRF1), a protein that can also bind and activate ISREs. Although, type I IFNs can activate GAF, the ISGF3 complex dominates during IFNαR signaling, as STAT2 and IRF9 are ISGs and favor assembly of ISGF3 rather than GAF (Platanias, 2005; González-Navajas et al., 2012; Bazer, 2013). In summary, both Type I and II IFNs activate classical Jak-STAT signaling pathways to up-regulate ISGs, however, activation of several other downstream cascades have been reported and are represented by the pleiotropic effects of type I and II IFNs, particularly within the endometrium during early pregnancy in mammals (Bazer, 2013).

IFNγ/IFNδ and Reproduction

The discovery that a type I IFN, IFNτ, could serve as the maternal recognition of pregnancy signal in ruminants, prompted investigations of IFN signaling within the reproductive tissues of other mammals, including pigs. By 1990, it had been confirmed

that antiviral activity could be detected in pig uterine flushings and conceptus-conditioned culture medium between d 12 and 17 of gestation, indicating that pig conceptuses express and release IFNs (Cross and Roberts, 1989; Mirando et al., 1990). Later, it was determined that pig conceptuses express a type II IFN, *IFNγ*, and a novel type I IFN, *IFNδ* (Lefèvre et al., 1990; La Bonnardière et al., 1991; Lefèvre and Boulay, 1993).

Interferon gamma is the most abundant pig conceptus IFN and transcripts are easily detectable in conceptus RNAs between d 13 to d 20 of development (Joyce et al., 2007a). Peak concentrations of IFNγ protein (250 μg per uterine horn) are detected in uterine flushings between d 15 and 16 of pregnancy (Cencič and La Bonnardière, 2002). Although it is not known what initially stimulates pig conceptuses to express *IFNγ*, it's hypothesized that the pro-inflammatory cytokine IL-18, released by the pig endometrium between d 15 and 18 of gestation, may be involved (Ashworth et al., 2010). Only transcripts for *IFNδ* have been detected within conceptus tissues. Expression of *IFNδ* can be detected between d 14 to d 20 with the greatest expression near d 15 (Lefèvre and Boulay, 1993; Joyce et al., 2007a). IFNγ protein has been localized within cytoplasmic vesicles at the apical surface of the extra embryonic trophectoderm but not the embryo proper or endoderm (Lefèvre et al., 1990; Joyce et al., 2007a). INFγ is the dominate pig conceptus IFN, accounting for 75% of antiviral activity in uterine flushings as compared to 25% by IFNδ.

Transcripts for *IFNγR* have been detected by RT-PCR in d 10 spherical pig conceptuses and are present within the trophoblast and ICM from d 11 to 15. However, conceptus IFNγR protein was undetectable on d 12 and weakly detected on 15, leading

some to believe that the endometrium is the initial and primary target (D'Andréa and La Bonnardière, 1998). Furthermore, pig trophoblast vesicles, which express IFNG and IFND, have little antiviral qualities even after treatment with the recombinant IFNG and IFND (D'Andréa et al., 1994). Indeed, endometrial *IFNγR* expression is detected on d 15 of pregnancy in pigs, temporally associated with peak production of IFNγ by conceptuses (D'Andréa and La Bonnardière, 1998).

IFNγ has been shown to reduce zonula occluden 1 (ZO1), a tight junction protein, that when modified, can enhance tissue remodeling including blood vessels (Youakim and Ahdieh, 1999; Cencič et al., 2003; Bian et al., 2009). Cencič and others (2003) hypothesized that pig conceptus IFNγ changes the endometrial architecture for implantation by altering uterine surface epithelial ZO1 and therefore, localized these proteins along the fetal maternal interface (Youakim and Ahdieh, 1999). IFNγ protein was unevenly localized to individual LE cells or clusters of LE cells that were adjacent to the IFNγ positive trophoblast on d 15 of pregnancy. Within the LE cells, IFNγ protein was greatest at the apex, yet extended through the cell to the basil region. Interestingly, in some areas of close apposition between the trophoblast and LE, IFNγ was not detected within the endometrium. Furthermore, the authors found that ZO1 had been redistributed from the apical to the basal region of LE cells, suggesting that conceptus proteins, namely IFNγ, likely alter uterine LE cell polarity in preparation of attachment (Cencič et al., 2003). The redistribution of ZO1 within the LE of pregnant animals was accompanied by an increase in MHC class II molecule protein that was localized specifically to endometrial endothelial cells, suggesting that conceptus IFNs penetrate through the LE

and into the stroma, providing a pathogen free environment during implantation and/or modulation of maternal blood vessels.

Classical and Non-Classical Endometrial ISGs

Alongside its role as the maternal recognition of pregnancy signal in sheep, conceptus IFNτ is hypothesized to stimulate classical and non-classical ISGs within the endometrial stroma/dGE and LE/sGE, respectively, regardless of conceptus location within the uterus. Within the stroma/dGE, IRF1 and ISGF3 respond to IFNτ by modulating expression of classical ISGs that are believed to be essential for establishment of pregnancy (Bazer et al., 2009). Within the LE/sGE, IFNτ stimulates IRF2, a potent inhibitor of IRF1 and ISGF3 activity, blocking expression of classical ISGs including ISGF3 assembly factors *STAT1*, *STAT2* and *IRF9* as well as interferon stimulated gene 15 (*ISG15*), MHC class 1 polypeptide (*MIC*), beta 2 microglobulin ($\beta_2 m$), *OAS* and *ESR1*; down-regulation of the latter ultimately prevents luteolysis (Choi et al., 2001; Joyce et al., 2007b; Spencer et al., 2007). The IRF2 blockade of classical ISGs within the uterine surface epithelium may be essential for maternal-fetal immune tolerance as MIC and β_2m are well known to modulate immune rejection processes (Choi et al., 2003; Bazer et al., 2010). Conceptus IFNτ and progesterone, *via* stroma and dGE derived progestamedins, are hypothesized to stimulate and induce, respectively, non-classical ISG expression within the LE/sGE. This may be achieved through a non-canonical second messenger pathway (independent of the STAT) that includes activation of PI3K and MAPK; the latter pathway can lead to nuclear localization (activation) of NF-κB (Bazer et al., 2010). Non-classical ISGs, up regulated in the LE/sGE, are suggested to influence conceptus

development, glucose and amino acid transport into the lumen, uterine receptivity and attachment of the trophoblast during implantation (Bazer et al., 2009).

As in sheep, classical and non-classical ISGs, in a cell specific manor, may be differentially regulated within the pig uterus during early pregnancy, yet, the mechanism by which this is achieved, although similar to sheep, is novel to the pig and under the control of ovarian progesterone, and paracrine activities of conceptus estrogens and IFNγ and IFNδ, the latter two possibly acting synergistically within the endometrium.

The similarities in endometrial *IRF1* and *IRF2* expression between pigs and sheep supports the theory that in general pig conceptuses activate IRF1 within the stroma and glandular epithelium (GE) and IRF2 within the surface epithelium, stimulating and inhibiting expression of classical ISGs, respectively, within the endometrium during implantation (Johnson et al., 2009). This may be true with the exception of STAT1, a classical ISG expressed within the pig uterine surface epithelium during this time (Joyce et al., 2007a; Stewart et al., 2003). After d 12 of pregnancy, *IRF1* is up regulated within the stroma/GE and *IRF2* increases in the uterine surface epithelium, which is temporally associated with conceptus release of IFNs and estrogens (Joyce et al., 2007b). Conceptus estrogens and IFNs or conceptus IFNs alone may up-regulate *IRF1* within the stroma/GE as administration of E2 to cyclic pigs does not increase stromal *IRF1*, however, administration of E2 in combination with osmotic pump release CSP (containing IFNδ and IFNγ) into the uterine lumen will increase *IRF1* in this tissue. The increase in *IRF1* during early pregnancy is temporally associated with up regulation of classical ISGs that were localized within the stroma and/or GE such as *STAT1*, *STAT2*, myxovirus resistance 1 (*MX1*), and $\beta_2 m$ (Hicks et al., 2003; Joyce et al., 2007a; 2007b; 2008). Unlike sheep,

conceptus estrogens (rather than IFNs) likely stimulate IRF2 within the LE/sGE as treatment of cyclic gilts with estrogen at a time when conceptuses normally release estrogens for the maternal recognition of pregnancy, increased *IRF2* within uterine surface epithelium (Joyce et al., 2007b).

Activation of endometrial STAT1 by pig conceptuses is hypothesized to influence conceptus development and endometrial remodeling for uterine receptivity and implantation (van Boxel-Dezaire et al., 2006; Spencer et al., 2007; Johnson et al., 2009). Regulation of endometrial STAT1 during pregnancy in pigs is different when compared to sheep in two ways; 1) *STAT1*, a classical ISG, increases within the LE during early pregnancy, apparently, in response to conceptus estrogens and 2) *STAT1* increases only in endometrium directly adjacent to the elongated pig conceptuses (Stewart et al., 2003; Joyce et al., 2007a; Johnson et al., 2009). In the pig, endometrial transcripts for *STAT1* increase between d 9 and 12 in the LE followed by a second increase between d 12 and 15 in the stroma/GE. *STAT1* remains high in all three-cell types until d 20. Similarly, STAT1 protein is highest on d 12 in the LE and d 15 in the stroma/GE. Conceptuses estrogens and IFNs are likely responsible for up regulation of STAT1 within the LE and later, within the stroma/GE, respectively. Treating cyclic pigs with E2 alone increases *STAT1* mRNA and protein within the LE but not stroma. Furthermore, STAT1 increases in the endometrial stroma with the addition of intrauterine infusion of CSPs containing IFNG and IFND (Joyce et al., 2007a).

Pig conceptuses produce IFNγ at concentrations comparable to IFNτ produced by sheep conceptuses, however, *STAT1* increases only within endometrial stromal/GE cells that are directly adjacent to the trophoblast, rather than universally throughout the uterus

as in sheep (Joyce et al., 2007a; Spencer et al., 2007; Johnson et al., 2009). Therefore, it's suggested that IFNγ in combination with lesser-produced IFNδ, act synergistically within the local stroma/GE to stimulate endometrial expression of classical ISGs during early pregnancy (Joyce et al., 2007a; Johnson et al., 2009).

INFγ/INFδ and Immune Modulation

Cell major histocompatibility complex (MHC) displays self or non-self peptide antigens to surveying T lymphocytes or bind inhibitory and activating molecules on NK cells and other leukocytes to eliminate foreign or abnormal/infected host cells. The MHC class I consist of a classical or non-classical trans-membrane alpha chain, encoded within the MHC loci, non-covalently linked to an extracellular beta-chain, B_2m, on the cell surface. In pigs, a B_2m in combination with one of three classical MHC class I alpha chains, encoded by the swine leukocyte Ag (*SLA*) genes *SLA1*, *SLA2* and *SLA3*, display peptide antigens to T cell receptors (TCR) on T lymphocytes (Joyce et al., 2008; Tanaka-Matsuda et al., 2009). The most common non-classical molecules are encoded by *SLA6*, *SLA7*, *SLA8* genes in the pig and they too, with a few exceptions, associate with B_2m during antigen presentation (Chardon et al., 2001; Blumberg et al., 2001; Joyce et al., 2008; Tanaka-Matsuda et al., 2009).

Classical MHC class I molecules are highly polymorphic, are expressed on almost all somatic cells and can present peptides derived from self-proteins or from proteins derived from intracellular pathogens, such as viral proteins, to $CD8^+$ cytotoxic T lymphocytes (CTL). The non-classical MHC class I molecules are less polymorphic, are expressed by specific cell types, and have different antigen presentation features as

compared to the classical molecules, which include presentation of lipids and bacterial cell wall components (Allen, 2001; Joyce et al., 2008). Both classical and non-classical MHC class I can interact with NK cells; however, these interactions appear to be more dynamic (Allen, 2001; Blumberg et al., 2001).

The MHC class II molecules consist of heterodimers of alpha and beta-chains that are predominantly expressed within antigen presenting cells such as macrophages, dendritic cells and B cells. These molecules display peptides derived from phagocytosed extracellular pathogens to TCRs on $CD4^+$ helper T lymphocytes. In the pig, the alpha and beta-chains are encoded by *SLA-DRA, SLA-DRB1, SLA-DQA, SLA-DQB, SLA-DOA, SLA-DOB1, SLA-DMA* and *SLA-DMB.* In addition, *SLA-DR* and *SLA-DQ* are also expressed in endothelial cells and T lymphocytes (Kim et al., 2012).

The MHC is responsible for the majority of immune responses during tissue graft rejection and spacio-temporal modulation of these molecules within reproductive tissues is necessary to avoid rejection of the fetal semi-allograft. MHC class II molecules are not expressed in mammalian trophoblast and down-regulation of classical MHC class I molecules within the trophoblast appears to be a common feature within mammalian reproduction, “camouflaging” the conceptus from maternal immune responses that would be detrimental to survival (Huddleston and Schust, 2004; Joyce et al., 2008). Evidence suggests that expression of non-classical MHC class I molecules in placental tissues of some mammals, such as human trophoblast, may protect the conceptus from negative T and NK cell responses (Blumberg et al., 2001; Joyce et al., 2008; Chen et al., 2012). This is not true for the trophoblast of non-invasive placental mammals, such as the pig, which

does not express classical or non-classical MHC class I molecules during the first trimester of pregnancy (Joyce et al., 2008).

Joyce and others (2008) characterized endometrial β_2m and classical (SLA1, SLA2 and SLA3) and non-classical (SLA6, SLA7 and SLA8) MHC class I molecule expression during the estrous cycle and early pregnancy in pigs. Overall, they found that β_2m and MHC class I molecules increase in the uterine LE during the early estrous cycle and pregnancy (before implantation), increase in the stroma around the time of implantation (d 10 to 25), and then decrease in the uterine LE immediately after initial attachment of the trophectoderm, becoming undetectable after d 20 of pregnancy. The spacio-temporal down regulation of MHC molecules that occurred within the uterine surface epithelium after attachment, tightly mimicked up regulation of ubiquitin-specific protease (USP), a protein that represses type I IFN signaling, within these cells. Observations made during experiments by Joyce and others (2008) suggests that pig conceptus IFNs likely up-regulate classical and non-classical MHC class I molecules within the stroma during implantation and yet, conceptus estrogens decrease their expression in the LE through up-regulation of IRF2 which may act in conjunction with the signaling repressor USP. Additionally, unlike sheep, MHC class I molecules are expressed within the uterine epithelium during the early estrous cycle in pigs and appear to increase in response to ovarian progesterone, possibly as a means of defense against intrauterine pathogens (Joyce et al., 2008).

Previously, SLA-DQA, a pig MHC class II molecule, was detected as a differential expressed gene in d 12 cyclic and pregnant pig endometrium (Ka et al., 2009). This prompted Kim and others (2012) to characterize endometrial SLA-DQ

molecules (SLA-DQA and SLA-DQB) during the estrous cycle and pregnancy. Expression of the MHC class II molecules was similar between cyclic and pregnant pigs on d 12, however, by d 15, expression had increased in pregnant endometrium. In situ hybridization and IHC assays localized *SLA-DQA* mRNA and SLA-DQ (A and B) proteins, respectively, to the endometrial sub-epithelial stromal cells and blood vessels. Treating cyclic endometrium with recombinant IFNγ, the authors detected a dose wise increase in endometrial *SLA-DQ* expression (Kim et al., 2012).

Collectively, it's hypothesized that pig conceptus IFNs increase classical ISGs β_2m and MHC class I molecules within in the adjacent stroma, facilitating endometrial vascular changes in support of pregnancy (Joyce et al., 2008). These conclusions are based on studies of pregnancy in humans and rodents, where uterine NK cells release IFNγ promoting uterine vascular modification (Ashkar et al., 2000; Joyce et al., 2008). In addition, the non-classical MHC class I molecule, HLA-G, is suspected of regulating angiogenesis during trophoblast invasion in humans (Le Bouteiller et al., 2007; Joyce et al., 2008). The complete lack MHC molecules in the pig trophoblast undoubtedly contributes to immune tolerance, however, down-regulation of β_2m and MHC class I molecules within the uterine surface epithelium could further minimize negative immune responses toward the fetal semi-allograft (Ramsoondar, 1999; Joyce et al., 2008). MHC class II molecules present exogenous derived peptides on antigen presenting cells, such as macrophages, to $CD4^+$ helper T cells. Therefore, it's logical to suggest that MHC class II molecules are expressed by cells within the endometrium as a means of protecting the mother and/or conceptus from uterine pathogens. However, Kim and others (2012) speculate that up-regulation of endometrial MHC class II molecules by pig conceptus

IFNγ, specifically, within the sub-epithelial stroma, could modulate $CD4^+$ T lymphocyte function near the fetal-maternal interface promoting immune tolerance during establishment of pregnancy in pigs.

Summary and Conclusion

The cellular and molecular interactions that control early pregnancy in mammals are multifaceted and complex, yet, trends exist across species and investigations of early pregnancy in primates, rodents and agricultural animals can help delineate elusive pathways. During early pregnancy in mammals, pro-inflammatory cytokines are commonly released by the conceptus and endometrium and when controlled, are believed to promote establishment of pregnancy and embryonic survival (Fig. 2.2 and Fig. 2.3). In pigs, these cytokines likely create a balanced pro-inflammatory microenvironment within the endometrium by spacio-temporally triggering activation of NF-κB, MAPK and IP3K signaling pathways within the uterine surface epithelium and at minimum, Jak-STAT pathways within the uterine stroma and glandular epithelium during the extended implantation phase. IL-1β2 may have the capacity to trigger similar pathways in the conceptus, influencing development and promoting rapid elongation. Collectively, these cytokines, which may be complimented by up-regulation of pro-inflammatory LIF, IL-6 and IL-18 as well as synthesis of PG within the endometrium likely promote establishment of pregnancy in pigs by modulating endometrial gene expression for uterine receptivity, endometrial architectural changes, angiogenesis, blood vessel permeability, and leukocyte function during immune tolerance of the fetal semi-allograft.

Concluding Remarks

Despite the discovery that pig conceptuses express a novel IL-1, very little data has been published in respect to IL-1β2 or the cytokine's influence on early pregnancy in the pig. Interestingly, Katebi et al. (2010), who used a computer program to predict pro and mature (mat) IL-1β1 and IL-1β2 protein structures, concluded that CASP1 might have a lesser capacity to proteolytically cleave pro-IL-1β2. Further, they concluded that mat-IL-1β2 might have an altered or reduced activity compared to mat-IL-1β1. The experiments described in the following Chapters were designed verify that elongating pig conceptuses express *IL-1β2* rather than *IL-1β1*. Further, we attempted to test hypotheses that IL-1β2 can activate NF-κB in the pig uterine LE, that IL-1β2 has a reduced activity compared with IL-1β1 and finally, that IL-1β2 is essential for elongation of the early pig conceptus.

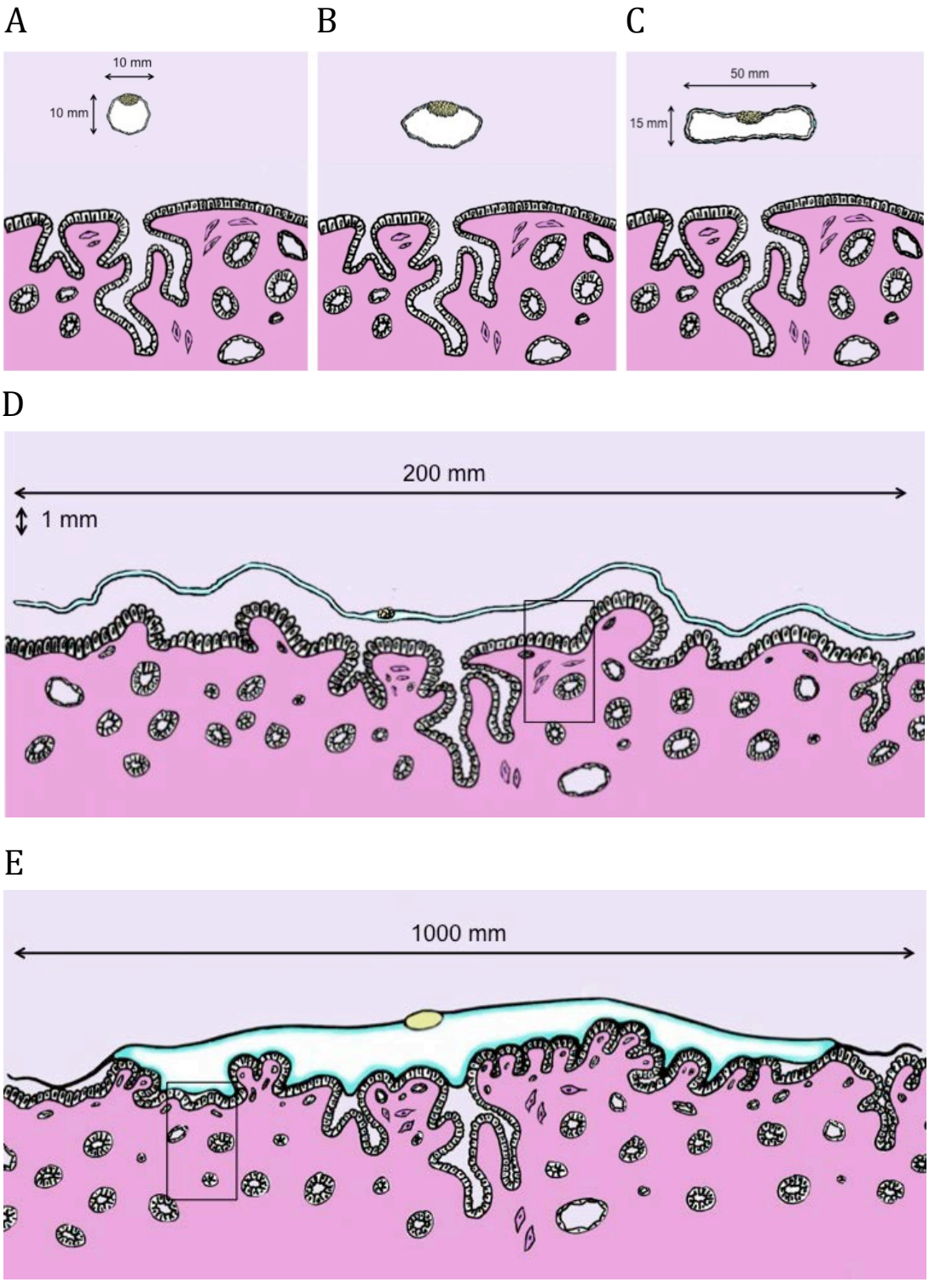
A
B
C
10 mm
10 mm
50 mm
15 mm
D
200 mm
1 mm
E
1000 mm

FIGURE 2.1 Elongation and implantation of a pig conceptus between days (d) 11 and 15 of gestation. (A) The spherical pig conceptus expands within the uterine lumen until it reaches approximately 10 mm in diameter (near d 11 of pregnancy). At this point, the conceptus becomes (B) ovoid and then (C) tubular before (D) rapidly elongating 150 mm in less than 3 h due to cellular hypertrophy and migration of the surrounding trophoblast cells. (D) Elongation occurs adjacent to the mesometrium which consists of stroma fibroblast cells, endothelial cells, leukocytes, glandular epithelium and luminal epithelial cells, the latter have a domed shape appearance as they proliferate and form epithelial "tuffs" that extend from the uterine surface. Implantation is initiated near d 13 of pregnancy as the trophoblast and luminal epithelial cell microvilli intimately associate within exaggerated folds of the endometrium. (E) By d 15, the conceptus may be over a meter in length but occupies less than a third of this distance (approximately 10-20 cm) within the uterus due to the elaborate architecture of the uterine surface.

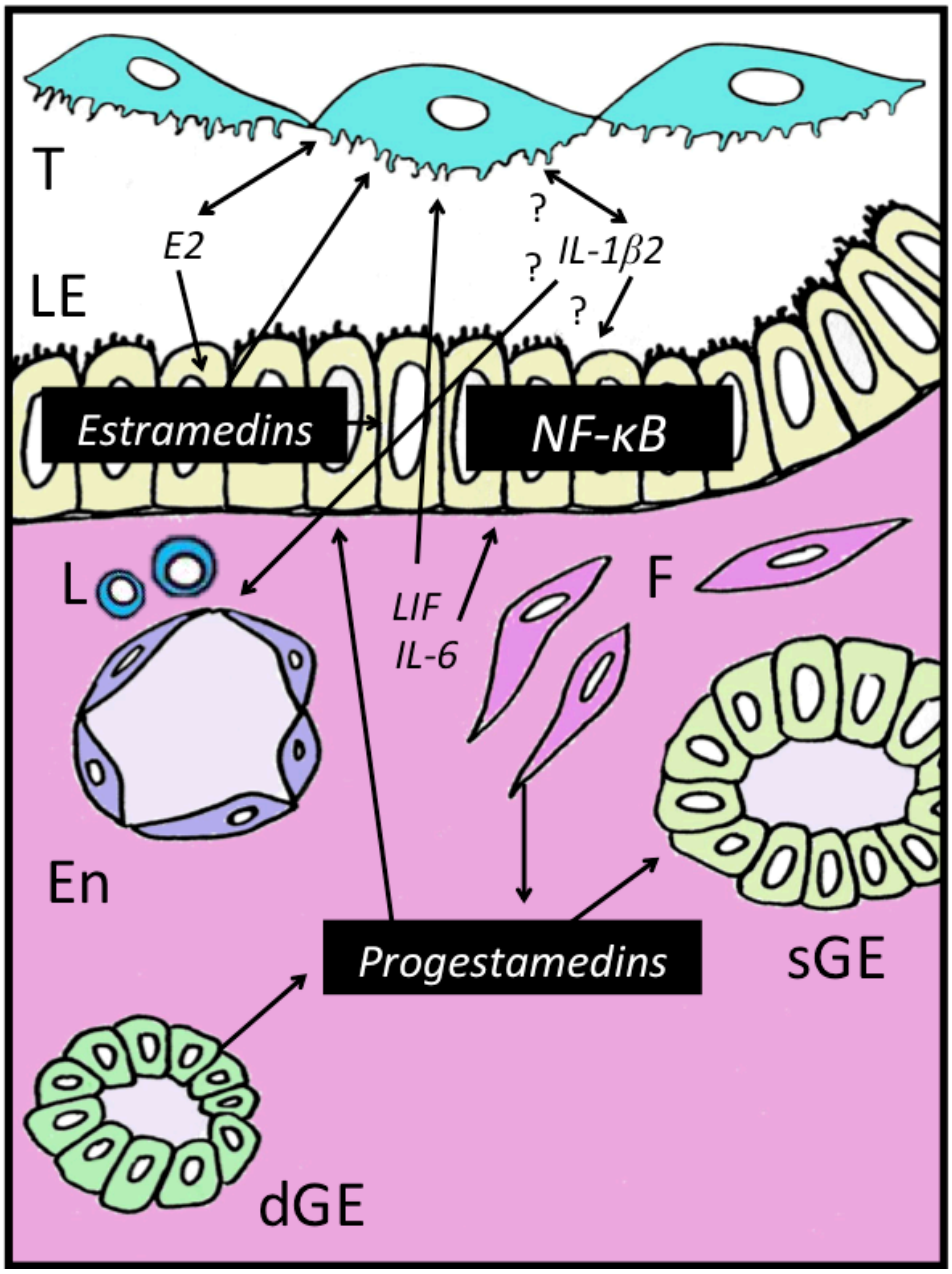
T
LE
E2
?
?
IL-1β2
?
Estramedins
NF-κB
L
LIF
IL-6
F
En
Progestamedins
sGE
dGE

FIGURE 2.2 A working model representing the uterine environment during conceptus elongation and hypothesized actions of interleukin-1 beta 2 (IL-1β2) (See box in Figure 2.1-D). By Day 12 of pregnancy, ovarian progesterone has auto down regulated progesterone receptors (PGRs) within the uterine luminal (LE) and surface glandular epithelium (sGE), decreasing expression of mucin-1, a large glycoprotein, and enhancing uterine receptivity. However, similar to sheep, PGRs remain in pig stroma fibroblast (F) cells, deep glandular epithelium (dGE) and myometrium and may produce progestamedins that act on PGR negative surface epithelial cells to promote establishment of pregnancy. As the pig conceptus elongates over the LE, the trophoblast (T) cells release estradiol (E2) and other estrogens as the maternal recognition of pregnancy signal. In response to E2, estrogen receptors within the LE can increase production of estramedins such as fibroblast growth factor 7 or secreted phosphoprotein 1, enhancing conceptus development, LE-T adhesion and implantation. Elongating pig conceptuses express *IL-1β2*, a novel IL-1 that are hypothesized to act on the conceptus and the adjacent LE through the interleukin-1 receptor type I, activating the transcription factor nuclear factor-kappa B (NF-κB) and possibly, the mitogen-activated protein kinase (MAPK) and inositol 1, 4,5-triphosphate 3-kinase (IP3K) signaling pathways. Activation of NF-κB may increase NF-κB responsive genes such prostaglandin-endoperoxide synthase 2 for production of prostaglandins as well as leukemia inhibitory factor (LIF) or interleukin-6 (IL-6) that likely bind receptors within the conceptus and LE, promoting implantation. Further, by stimulating the release of factors from LE or by passing through the LE barrier into the underling stroma, IL-1β2 may influence endometrial leukocytes (L) and endothelial (En) cells, altering immune cell function/motility and increasing blood vessel permeability, respectively.

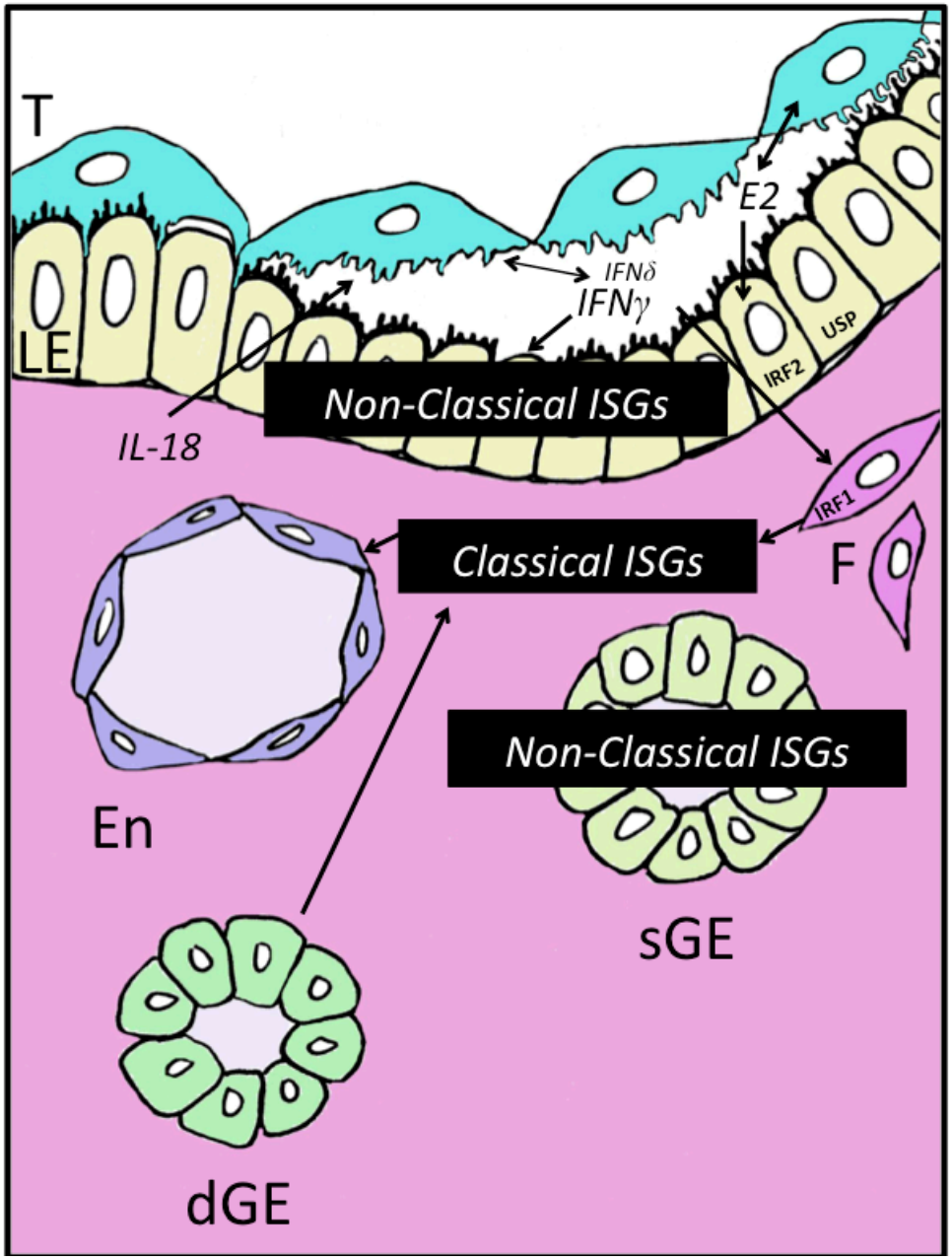
T
LE
E2
IFNδ
IFNγ
USP
IRF2
Non-Classical ISGs
IL-18
IRF1
F
Classical ISGs
En
Non-Classical ISGs
sGE
dGE

FIGURE 2.3 An evolving model representing the uterine environment during pig conceptus implantation and expression of interferon gamma (IFNγ) and interferon delta (IFNδ) (See insert box in Figure 2.1-E). Near d 15 of gestation, pig conceptuses release peak concentrations of IFNγ and in lesser amounts, IFNδ, which are proposed to synergistically stimulate janus associated kinases and signal transducers and activators of transcription (Jak-STAT) signaling pathways and expression of interferon regulatory factor 1 (IRF1), a transcriptional activator of classical interferon stimulated genes (ISGs), within the adjacent stroma fibroblast cells (F) and deep glandular epithelium (dGE). Classical ISGs, up-regulated within the endometrium, are suggested to modulate endometrial leukocyte function and endothelial (En) cell activity, thereby, promoting immune tolerance to the conceptus and endometrial angiogenesis, respectively. Within the luminal epithelium (LE) and probably the surface glandular epithelium (sGE) adjacent to the trophoblast, conceptus estrogens up-regulate expression of interferon regulatory factor 2 (IRF2), an inhibitor of classical ISGs that can block classical ISGs beta 2 microglobulin and MHC class I molecules along the uterine surface, also contributing to immune tolerance. Expression of classical ISGs may further be inhibited by the presence of surface epithelial ubiquitin-specific protease (USP). Endometrial derived progestamedins and conceptus IFNs are proposed to induce and stimulate, respectively, non-classical ISGs within the LE/sGE through activation of NF-κB, MAPK and IP3K signaling pathways that likely modulate conceptus development, glucose and amino acid transport into the lumen, uterine receptivity and attachment of the trophoblast (T) during implantation. Between d 15 and 18 of gestation, endometrial interleukin-18 (IL-18) is released into the uterine lumen and is hypothesized to further stimulate IFNγ production by the pig conceptus.

CHAPTER THREE

ACTIVATION OF THE TRANSCRIPTION FACTOR NUCLEAR FACTOR-KAPPA B IN UTERINE LUMINAL EPITHELIAL CELLS BY INTERLEUKIN-1 BETA 2: A NOVEL INTERLEUKIN-1 EXPRESSED BY THE ELONGATING PIG CONCEPTUS

Abstract

Conceptus mortality is greatest in mammals during the peri-implantation period, a time when conceptuses appose and attach to the uterine surface epithelium while releasing proinflammatory molecules. Interleukin-1 beta (*IL-1β*), a master proinflammatory cytokine, is released by the primate, rodent and pig blastocyst during the peri-implantation period and is believed to be essential for establishment of pregnancy. The gene encoding *IL-1β* has duplicated in the pig, resulting in a novel gene. Preliminary observations indicate that the novel *IL-1β* is specifically expressed by pig conceptuses during the peri-implantation period. To verify this, *IL-1β* was cloned from mRNA isolated from d 12 pig conceptuses and compared with *IL-1β* cloned from mRNA isolated from pig peripheral blood leukocytes (PBL). The pig conceptuses but not PBL expressed a novel *IL-1β*, referred to in this manuscript as interleukin-1 beta 2 (*IL-1β2*).

Porcine endometrium was treated with recombinant porcine IL-1β1, the prototypical cytokine, and IL-1β2 proteins. Immunohistochemistry (IHC) and real-time reverse transcriptase-polymerase chain reaction (RT-PCR) were used to measure activation of nuclear factor-kappa B (NF-κB) and NF-κB-regulated transcripts within the endometrium, respectively. Both IL-1β1 and IL-1β2 activated NF-κB in the uterine luminal epithelium within 4 h. The NF-κB activation and related gene expression, however, were lesser in endometrium treated with IL-1β2 suggesting that the conceptus-derived cytokine may have reduced activity within the uterus. In conclusion, the peri-implantation pig conceptus expresses a novel *IL-1β* that can activate NF-κB within the uterine surface epithelium, likely creating a pro-inflammatory microenvironment during establishment of pregnancy in the pig.

INTRODUCTION

Implantation is the most-critical stage of pregnancy, during which 25 to 60% of conceptuses or pregnancies do not survive (Wilmut et al., 1986; Macklon et al., 2002). Inadequate or asynchronous molecular crosstalk between the conceptus and endometrium, that includes pro-inflammatory cytokines, is suspected to be a major contributor of implantation failure and conceptus mortality that occurs during early pregnancy (Simón et al., 1997; Mor et al., 2011; Dekel et al., 2010; Granot et al., 2012).

Interleukin-1 beta (IL-1β) is a master proinflammatory cytokine. It is released by the primate, rodent and pig blastocyst and enhances establishment of pregnancy by promoting conceptus attachment to the endometrium and implantation (Choudhuri and

Wood, 1993; Tuo et al., 1996; Simón et al., 1998). The interleukin-1 (IL-1) signaling system is complex. Together, the IL-1 and IL-1 receptor families consist of twenty-two molecules including proinflammatory cytokines [IL-1β and interleukin-1 alpha (IL-1α) (collectively referred to as IL-1)], a functional receptor [the IL-1 receptor type I (IL-1RI)], a decoy receptor [the IL-1 receptor type II (IL-1RII)], an antagonist [the IL-1 receptor antagonist (IL-1RA)] and an IL-1 receptor accessory protein (IL-1RAP) involved in transmembrane signaling (Dinarello, 2011, 2012; Garlanda et al., 2013). Both IL-1β and IL-1RA can bind the IL-1RI but only the IL-1β-IL-1RI complex can recruit the IL-1RAP (Garlanda et al., 2013). Juxtapositioning of the IL-1RI and IL-1RAP toll/interleukin-1 receptor (TIR) domains within the cytoplasm is necessary to initiate a cascade of second messenger protein interactions. These interactions activate nuclear factor-kappa B (NF-κB), a transcription factor comprised of conserved subunits that control innate and adaptive immune responses (Caamaño and Hunter, 2002; Garlanda et al., 2013). Upon activation, NF-κB can enter the nucleus and regulate expression of over a hundred genes by binding kappa-B sites within the gene promoter (Hayden and Ghosh, 2012). Endometrial activation of NF-κB at the time of implantation, especially the uterine epithelium, may be necessary for establishment of pregnancy in mammals (Laird et al., 2000; Nakamura et al., 2004; King et al., 2010; Mathew et al., 2011; Geisert et al., 2012).

The pig conceptus up-regulates expression of *IL-1β* during the peri-implantation period (Tuo et al., 1996; Smith et al., 2001; Ross et al., 2003a, 2003b; Tuggle et al., 2003) but the function of this cytokine is unknown. At approximately d 11 of pregnancy, the pig blastocyst becomes ovoid and then tubular before rapidly elongating into a filamentous shape. The change in morphology is believed to maximize contact between

the embryo and the uterine surface for fetal-maternal nutrient exchange (Geisert et al., 1982; Dziuk, 1985; Dantzer et al., 1985; Degrelle et al., 2009). The trophoblasts increase expression of *IL-1β* during elongation so that *IL-1β* becomes one of the most abundant transcripts in the pig conceptus (Smith et al., 2001; Ross et al., 2003b). Once trophoblast elongation is complete, expression of the *IL-1β* decreases 2000-fold (Ross et al., 2003a).

Pig conceptus IL-1β likely plays a critical role in conceptus elongation and during establishment of pregnancy through its effects on the uterine surface epithelium. Production of IL-1β by pig conceptuses is temporally associated with increased expression of *IL-1RI* and *IL-1RAP* within the endometrium as well as activation of NF-κB in the uterine epithelium adjacent to the conceptus (Ross et al., 2003a; Mathew et al., 2011). Porcine genomes (wild and domesticated) contain two copies of the *IL-1β* gene on chromosome 3, referred to in this manuscript as pig interleukin-1 beta 1 (IL-1β1) and interleukin-1 beta 2 (IL-1β2) (Groenen et al., 2012). The second *IL-1β* is likely the result of a gene duplication and is believed to be unique to the pig (Groenen et al., 2012). Based on published cDNA sequences, the original *IL-1β* sequence (IL-1β1) transcribes the prototypical cytokine expressed in immune cells and the novel *IL-1β* (*IL-1β2*) is transcribed by the pig conceptus during the peri-implantation period.

In this study, we investigated the *IL-1β1*/*IL-1β2* genomic region, compared pig *IL-1β1* and *IL-1β2* transcripts and expressed both proteins *in vitro*. We then tested their biological activity on pig alveolar immune cells and endometrium to assess activation of the transcription factor NF-κB. Activation of target genes in endometrium in response to each cytokine was also measured.

MATERIALS AND METHODS

General Procedures

Animals. All procedures used in the present study were approved by the University of Missouri-Columbia Institutional Animal Care and Use Committee and in accordance with specific SSR guidelines and standards. Pigs were either Large White-Landrace crossbred or Large White-Chester crossbred. Both gilts and sows were used. When artificial insemination (AI) was performed, the pigs were checked for estrus and inseminated on the first day of estrus (Day 0) and 1 day later with fresh semen collected from a single Large White-Landrace boar. Pigs were sacrificed with either Euthasol (Virbac Animal Health) or by electric stunning followed by exsanguination (University of Missouri abattoir). To collect elongated pig conceptuses, gilts were sacrificed 12 days after AI and the uteri were removed and placed on ice before being flushed with 20 mL of ice cold PBS (Gibco, Life Technologies).

RNA isolation. Conceptus and adult tissues were collected, snap frozen in liquid nitrogen and stored at -80°C until RNA extraction. One mL of TRIzol reagent (Invitrogen; Life Technologies) was added to the tissue (< 100 mg) and total cellular RNA was isolated following the manufacture's recommendations. Peripheral blood leukocyte (PBL) RNA was extracted using the QIAamp RNA Blood Mini extraction kit (Qiagen). The integrity of RNA was determined by calculating the ratio of absorbance at 260 nm and 280 nm (NanoDrop ND-1000, NanoDrop Technologies), followed by gel

electrophoresis (0.8% agarose gel in 0.09 M Tris-borate and 0.002 M EDTA buffer with 0.5 μg/mL ethidium bromide). The RNA was stored at -80°C.

Real-time PCR. The real-time RT-PCR were prepared with 1 μM concentrations of both forward and reverse primers (Table 1), sample cDNA, (see individual experiments for cDNA synthesis) and Power SYBR® Green (Applied Biosystems). All samples were run in triplicate and within a single plate. High, medium and low control samples (sequential 1:4 dilutions) of pooled cDNA were run in triplicate and used as a standard. Each PCR 96-well plate contained a "no template control" (water substituted for cDNA in the reaction) to ensure that there was no amplification in samples without cDNA. The PCR were performed and fluorescence quantified by using the ABI Prism 7500 Sequence Detector (Applied Biosystems). Unless specified, standard thermocycler settings consisted of an initial temperature of 50°C of 2 min, a polymerase activation temperature of 95°C for 10 min followed by 40 PCR cycles consisting of 2 stages: 1) melting at 95°C for 15 sec and 2) annealing and extension at 60°C for 1 min. Analyses of amplification plots were performed by the Sequence Detection Software (Applied Biosystems). Data from the serial dilutions of the control sample were used to calculate the amplification efficiencies for the PCR targets (Table 1). The equation used for the efficiency calculation was efficiency = $10^{(-1/\text{slope})}$. The slope refers to the slope of a linear plot of C_T values achieved by the high, medium and low-pooled cDNA standards versus the log of the dilution. Fold change differences for the respective samples were calculated using the equation: fold change = efficiency $^{(\text{mean medium control } C_T - \text{mean sample } C_T)}$ where the medium control was the same sample in each plate (i.e., an internal control standard for between

plate normalization). DNA sequencing was done at the University of Missouri DNA Core facility.

Experiments

Cloning IL-1β1 and IL-1β2 cDNA

RNA was isolated from Day 12 conceptuses (see general procedures). For PBL RNA, 10 mL of blood was collected from the jugular vein and into vacutainer blood collection tubes containing acid citrate dextrose (ACD) solution A (Becton, Dickinson and Company) (n=4 sows). Blood was placed on ice and within 30 min RNA was isolated from PBL (see general procedures). For cDNA, 1 to 3 μg of RNA was reverse transcribed using the High Capacity cDNA Reverse Transcription kit (Applied Biosystems).

Forward and reverse primers were designed to amplify full protein-coding length *IL-1β1* and *IL-1β2* transcript sequences from PBL and conceptus cDNA, respectively (Fig. 3.1). The primer sequences were derived from pig genomic sequences and expressed sequence tags (EST) within GenBank of NCBI (National Center for Biotechnology Information; Bethesda, MD). The forward primer sequences were 5′-CAGCCAGTCTTCATTGTTCAGGTT-3′ for *IL-1β1* and 5′-AGGACGGCATTCTGAAGGAA-3′ for *IL-1β2*. A common reverse primer was used 5′-ATCTAGGGAAGACAGCTGGGCAT-3′. The PCR reactions (20 μL) were performed using the Jumpstart REDtaq DNA polymerase (Sigma-Aldrich). The thermocycler settings for PCR consisted of 34 cycles of 30 sec melting and annealing at 94°C and 60°C, respectively, followed by 1 min extension at 72°C (Eppendorf Mastercycler®).

The PCR products for *IL-1β1* and *IL-1β2* were ligated into the pCR 2.1-TOPO cloning vector using the TOPO TA cloning Kit (Invitrogen, Life Technologies). DH5α *E. coli* cells were transformed with the ligated vectors following the manufacture's instructions. Three and four cDNA clones for *IL-1β1* and *IL-1β2*, respectively, were DNA sequenced and aligned by using the BLAST program of NCBI against pig genomic sequences and EST. The *IL-1β1* and *IL-1β2* cDNA and corresponding amino acid sequences were aligned against one another using NCBI's blastn and blastp programs to determine percent homology (Fig. 3.1 and 3.2). The percentage of identical amino acids within the pro-region was compared with the percentage of amino acids in the mature-region of IL-1β1 and IL-1β2 using the Chi-square test. Significance was declared at $P < 0.05$.

Ribonuclease Protection Assays (RPA)

A ribonuclease protection assay (RPA) was used to differentially detect *IL-1β1* and *IL-1β2* transcripts in PBL and conceptus RNA. Two RPA probes were designed to specifically anneal to either *IL-1β1* or *IL-1β2* within the 5' region of the mRNA (Fig. 3.1). Forward and reverse primers were designed to PCR amplify 196 and 205 bp of the 5' region of *IL-1β1* and *IL-1β2*, respectively. Forward primer sequences were 5′-CAGCCAGTCTTCATTGTTCAGGTT-3′ for *IL-1β1* and 5′-AGGACGGCATTCTGAAGGAA-3′ for *IL-1β2*. A common reverse primer was used 5′-AGATTTGCAGCTGGATGCTC-3′. The PCR reactions were identical to the reactions described previously. The PCR products were ligated into the pCR 4-TOPO vector by using the TOPO TA cloning kit (Invitrogen, Life Technologies). The ligated vectors were cloned into TOP10 *E. coli* cells following the manufactures instructions. The *IL-1β1* and

IL-1β2 plasmids were amplified, isolated, and then DNA sequenced to verify the respective sequences. Plasmids were linearized and the ^{32}P labeled-antisense RNA probes were synthesized from the cloned sequences using the *in vitro* Transcription MAXIscript kit (Ambion, Life Technologies) following the manufacture's recommendations. The radiolabelled RNA probes were used for the RPA by using the RPA III kit (Ambion; Life Technologies) and following the manufacturer's instructions. Twenty μg of total Torula yeast (hybridization negative control) as well as RNA isolated from PBL and elongating conceptuses were tested. A ^{32}P labeled RNA Century Marker (100-500 bp; Life Technologies), undigested probe and samples were electrophoresed for 1 h at 250V through a 6% polyacrylamide gel. The gel was dried and then exposed to autoradiography film (Eastern Kodak Company) for short or extended periods of time to visualize intense as well as faint signals. Composite images from a single experiment were created using the Microsoft Office computer program.

To measure expression for *IL-1β1* and *IL-1β2* in pig conceptuses and across a variety of adult tissues, RNA was extracted and cDNA synthesized (see general procedures) from d 12 elongated pig conceptuses, esophageal smooth muscle, central nervous system [brain (frontal lobe) and spinal cord], whole ovary, endometrium, adipose tissue, skin, thyroid gland, hypothalamus, liver, lung, heart, spleen, kidney and small intestine. Transcripts for *IL-1β1* and *IL-1β2* were measured by real time RT-PCR using the same primer sequences used to clone peripheral blood leukocyte *IL-1β1* and pig conceptus *IL-1β2* cDNA (see above).

Preparation of Protein Expression Plasmids

Forward and reverse primers were designed to amplify cDNA sequences corresponding to pro-IL-1β1 and pro-IL-1β2 proteins from sequences previously cloned in the pCR 2.1-TOPO plasmid (above) (Fig. 3.1). The forward primers were designed with a four-bp extension at the 5' end to allow for ligation into the expression plasmid (Champion pET Directional TOPO Expression Kit; Invitrogen, Life Technologies). The forward primer sequences were 5′- CACCATGGCCATAGTACCTGAACCC-3′ and 5′-CACCATGGCCACGGTACCTGAACCT-3′ for *pro-IL-1β1* and *pro-IL-1β2*, respectively. A common reverse primer was used (5′-TTAGGGAGAGAGGACTTCCATGGT-3′). To amplify the pro-sequences, 1 ng of the pCR 2.1-TOPO plasmid DNA and Jumpstart REDtaq DNA polymerase (Sigma-Aldrich) was used in a 20 μL reaction. For both *pro-IL-1β1* and *pro-IL-1β2*, the thermocycler settings consisted of 40 cycles of 30 sec melting and annealing at 98°C and 60°C, respectively, followed by a 1 min extension at 72°C. The PCR products were DNA sequenced to verify the correct sequences. Products were then ligated into the pET100/D-TOPO expression plasmid supplied in the Champion Kit following the manufacturer's recommendations.

The previously isolated pro-IL-1β1 and pro-IL-1β2 pET100/D-TOPO expression plasmids were used as templates to create the mat-IL-1β1 and mat-IL-1β2 expression plasmids. The forward primer sequences were 5′-GCCAACGTGCAGTCTATGGAGTGC-3′ and 5′-GCCACCCCCGTGCAGTCCGTGGAC -3′ for the mat-IL-1β1 and mat-IL-1β2 expression plasmid, respectively. A common reverse primer, corresponding to base pairs (bp) 381-404 of the pET100/D-TOPO expression plasmid, was used (5′-

GGTGAAGGGATGATCCTTATCGTC-3′). The PCR products were purified using the QIAquick PCR Purification Kit (Qiagen) and the blunt ends were phosphorylated and ligated together. TOP10 *E. coli* cells were transformed with the four (*pro-IL-1β1*, *pro-IL-1β2*, *mat-IL-1β1* and *mat-IL-1β2*) expression vectors and plated on LB agar plates containing ampicillin (100 μg/mL). The cells were incubated overnight at 37°C before single colonies were picked and grown overnight in 4 mL of LB containing ampicillin (100 μg/mL), while shaking at 35°C. The plasmid DNA was then isolated, phenol-chloroform extracted and DNA sequenced to verify correct plasmid sequence.

Expression of IL-1β1 and IL-1β2 Recombinant Proteins

Recombinant proteins were expressed and purified according to instructions provided by the Champion pET Directional TOPO (Invitrogen, Life Technologies) and Qiagen Ni-NTA Fast Start (Qiagen) kits. A 50 μL aliquot of BL21 Star *E. coli* cells was transformed with 5 to 10 ng of expression plasmid DNA. An expression control supplied by the Champion kit was used to express beta galactosidase (BGal). After transformation, 250 μL SOC medium was added to each *E. coli* aliquot and cells were incubated, while shaking, for 30 min at 37°C. The entire culture was then added to 10 mL of LB (100 μg/mL of ampicillin) and cells were incubated overnight, while shaking, at 37°C. The next day, 250 mL of LB (ampicillin; 100μg/mL) was inoculated with the 10 mL culture and incubated, while shaking, for 60 min at 37°C. To induce expression, IPTG was added to each culture at a final concentration of 1 mM and cells were allowed to incubate, while shaking, for 5 h at 37°C. After induction, cells were harvested by centrifugation at 4000 x g for 10 min and pellets were frozen at -20°C. Cell pellets were thawed and lysed and the

soluble proteins captured using the Ni-NTA column (Qiagen). To verify protein expression, the eluted proteins were electrophoresed through a NuPAGE 4-12% Bis-Tris-Gel (Invitrogen; Life Technologies) at 200V and 125mA for 60 min and stained with coomassie blue. Western blots, using the advanced western blotting detection Kit (GE Healthcare Life Sciences) and antibodies against porcine IL-1β (PP425; Thermo Scientific) and His Tag (A00174; GenScript), were performed to verify expression of IL-1β proteins. Dialysis of the eluted protein solution was used to remove small contaminants (Pierce; Thermo Scientific) and proteins were electrophoresed and stained with coomassie blue for visualization. A BCA assay (Pierce; Thermo Scientific) was conducted to measure the concentration of BGal (control protein) and IL-1β proteins. Glycerol (Sigma-Aldrich) was then added to the protein at a 1:2 ratio before freezing at -20°C.

Treating Alveolar Cells with Recombinant IL-1β1 and IL-1β2

Alveolar cells were collected by lung lavage with ice cold PBS (Gibco, Life Technologies) from a crossbred gilt immediately after euthanasia. The trachea was exposed after a ventral incision through the neck. Approximately 5 cm of rubber tubing with an outside diameter of 20 mm and an inner diameter of 10 mm was fed caudally between two tracheal rings into the trachea. The trachea was fastened to the tubing before approximately 1.5 L of PBS was forced into the lungs using a syringe attached to a stopcock. The PBS backflow containing alveolar cells was collected into a sterile container and placed on ice. Cells were filtered through a Falcon 100 μm cell strainer (DB Falcon) and centrifuged at 2000 x g for 10 min. The cells were re-suspended in PBS

and seeded onto sterile covers slips within six well plates. The alveolar cells where allowed to adhere to the coverslips for 2 h at 37°C in an atmosphere of 5 % CO_2 in air. Afterwards, cells were washed with PBS and incubated for an additional 6 h in DMEM (Gibco, Life Technologies) with 1% FBS before new medium was added containing recombinant proteins. Cells were either left untreated (DMEM/FBS alone; Non-treated; negative control), or treated with LPS (1 μg/mL; positive control), recombinant beta galactosidase (BGal; expression/protein negative control), human mature IL-1β (human mat-IL-1β; rhil-1b 10319-mm; InvivoGen), pig pro-IL-1β1 (pro-IL-1β1), pig pro-IL-1β2 (pro-IL-1β2), pig mature IL-1β1 (mat-IL-1β1) or pig mature IL-1β2 (mat-IL-1β2) cytokines (50 ng/mL) in 3 mL of DMEM/FBS for 4 h at 37°C and 5% carbon dioxide in air. Experiments were done in duplicate.

Alveolar cells were washed with PBS and fixed in 10% buffered formalin phosphate for 10 min following treatment. The cells were then permeated with 0.1% Triton X-100 (Sigma) in PBS for 10 min and blocked with 5% goat serum in PBS for 1 h at 37°C. After blocking, a rabbit anti-human primary antibody, directed against the RelA/p65 subunit of NF-κB (sc-372, Santa Cruz Biotechnology), was added to the cells at a 1:500 dilution (0.4 μg/mL) in PBS containing 1.5% goat serum. The cells were incubated overnight in the antibody solution at 4°C. The next day, cells were washed with PBS before a fluorescently labeled (Alexa Flour 488), goat anti-rabbit secondary antibody (Life Technologies) was added to the cells at a 1:400 dilution (5 μg/mL) in PBS (1.5% goat serum) for 45 min at room temperature. Negative control slides were prepared using pre-immune rabbit serum in place of the primary antibody or in the absence of the secondary antibody. To localize alveolar cell nuclei, DNA was stained with DAPI (300

nM; Molecular Probes) in PBS for 5 min. The coverslips, containing alveolar cells, were then washed with PBS before they were mounted onto frosted white microscope slides with Mowiol. Treatments applied to specific cover slips were blinded and pictures of the cells were taken in nine random locations on the slide at 200 and 400 X magnification by using a microscope equipped with fluorescence illumination.

Treating Porcine Endometrium with Recombinant IL-1β Cytokines

Endometrium was collected from three gilts on day 12 after estrus. The endometrium was dissected away from the myometrium and washed with ice cold PBS containing 2% Antibiotic-Antimycotic (ABAM; Gibco, Life Technologies). Approximately 250 mg of endometrial tissue was then incubated in six well plates at 37°C for 4 h in a modified MEM [1% MEM Vitamin Solution (Gibco, Life Technologies), 1% ABAM, 1% Non-Essential Amino Acids (NEAA; Gibco, Life Technologies) and 16.6 mM of D-(+)-Glucose (Sigma) in MEM-L-Glutamine (Gibco; Life Technologies)] while on a rocking device in an atmosphere consisting of 47.5% nitrogen, 5% carbon dioxide, 21% oxygen and balanced air (Basha et al., 1980; Green et al., 1998). After incubation, spent medium was removed and the tissue was left untreated in three wells (modified MEM, Non-treated; negative control; well one, two and three) or treated with a low, medium or high dose of LPS (1, 10 or 100 μg/mL; positive control), BGal (expression negative control), human mat-IL-1β, pro-IL-1β1, pro-IL-1β2, mat-IL-1β1, or mat-IL-1β2 at either 10, 100 or 1000 ng/mL in 3 mL of modified MEM at 37°C for 4 h. The experiment was done in duplicate for each gilt. The tissue remained on a rocking device while under positive gas pressure during treatment (see above). After

treatment, tissues from each well were fixed in 10% buffered formalin phosphate for IHC or snap frozen in liquid nitrogen before storage -80°C for RNA extraction.

Immunohistochemistry (IHC) for Uterine Epithelial NF-κB

The following protocol was previously described by our laboratory (Mathew et al., 2011). Formalin-fixed endometrium was sectioned (5 µm) and mounted onto frosted white microscope slides before the tissue was deparaffinized and rehydrated. Epitope retrieval was achieved by boiling slides for 6 min in 0.01 M sodium citrate buffer. Slides were allowed to cool for 45 min before they were incubated overnight at room temperature in 500 µL of a rabbit anti-human polyclonal antibody, directed against the p65 subunit of NF-κB (sc-372, Santa Cruz Biotechnology), diluted 1:100 in PAT [0.001% Tween-20 and 0.001% sodium azide in 1.0% PBS] solution (2 µg/mL). The next day, slides were placed in PBS for 30 min before adding 500 µL of a fluorescent labeled (Alexa Flour 488), goat anti-rabbit secondary antibody (A11034, Life Technologies) at a 1:400 dilution in PAT solution (5 µg/mL). Slides were incubated at room temperature with the secondary antibody for 70 min before re-submerging them in PBS. The secondary antibody/PAT solution was incubated with a washed bovine liver powder for 1 h at 37°C to reduce background fluorescence. Cover slips were then mounted over the uterine tissue with Mowiol and the slides were then refrigerated at 4°C overnight in the dark. Two negative control slides were made using pre-immune rabbit serum in place of the primary antibody or PBS in place of the second antibody. Cell DNA was stained with DAPI (D-1306, Life Technologies; Molecular Probes) in PBS for 15 min to localize

uterine LE cell nuclei. Treatments on the slide were blinded and images were taken at a 200 and 400 X magnification.

Evaluation of NF-κB Activation

Immunofluorescence was used to localize NF-κB in porcine alveolar and uterine LE cells treated with LPS or recombinant cytokines. NF-κB was considered activated when the cell nuclear fluorescence was equal to or greater than that of the cytoplasm. For slides containing alveolar cells, nine, 200 X images were taken at random locations in the slide and the NIH Image J computer program was used to count the number of activated cells within the total number of cells in the image (percent of activated cells). For 400 X images of alveolar and uterine LE cells, the intensity of fluorescence within the nucleus and cytoplasm for individual cells was measured using Image J. Therefore; a nuclear vs. cytoplasmic fluorescent ratio (intensity of activation, IOA) was calculated.

Endometrial RNA Isolation, Reverse Transcription and Real Time RT-PCR

A 100 mg sample of endometrium was used for total cellular RNA isolation (see general procedures). The RNA was stored at -80°C before reverse transcription of 5 μg of total cellular RNA to cDNA using the High Capacity cDNA Reverse Transcription kit (Applied Biosystems). Primer sets for prostaglandin-endoperoxidase synthase 2 (*PTGS2*), salivary lipocalin 1 *(SAL1)*, integrin beta 3 *(β3)*, integrin alpha v *(AV)*, *IL-1β1*, *IL-1RI*, inhibitor of nuclear factor-kappa B alpha *(IκBα)*, ribosomal protein L7 *(RPL7)* and beta actin (*ACTβ*) were designed based on porcine nucleotide sequences (Table 3.1). The cDNA was diluted 1:10 and a PCR gradient was developed for each primer set. The real-

time RT-PCR were prepared with 1 µL (10 ng RNA equivalent) of the diluted cDNA sample. Thermocycler settings were the same as described in the general procedures for all amplifications with the exception of *IκBα* and *PTGS2*. For *IκBα*, annealing was modified to 67°C and for *PTGS2*, annealing and extension was modified to 67°C for 40 sec, respectively. The products were DNA sequenced to verify amplification of the target sequence. The analysis of gene expression by RT-PCR was performed as described in the general methods section. Fold changes in gene expression were normalized to the geometric mean of control genes *RPL7* and *ACTβ.*

Statistical Analysis of NF-κB Activation and Endometrial Gene Expression

A general linear model (GLM) procedure within the Statistical Analysis System (SAS; SAS Institute, Inc.) was used to analyze the alveolar cell NF-κB activation data. For the "intensity of activation (IOA)" and "percent of activated cells" the model statement included an effect of treatment. The "percent of activated cells" data were rank-transformed to control for inherent variation. Significance was declared at $P < 0.05$. A Duncan's multiple range test was used ($P = 0.05$) to test for differences between treatment means for both non-transformed and transformed data. A mixed models procedure (PROC MIXED) within SAS was used to analyze the IOA in uterine LE cells and normalized fold changes in total endometrial gene expression. For the IOA and gene expression data, the model statement included an effect of treatment, concentration and the treatment by concentration interaction. A Bartlett's test was used within SAS to test for homogeneity of the variance for the expression data. When heterogeneous variance was encountered, the data were log 10 transformed. Data are presented as the non-

transformed least squares means (LSM) ± standard error of the least square means (SEM). A significant difference was declared at $P < 0.05$.

RESULTS

Porcine Peripheral Blood Leukocyte IL-1β1 and *Conceptus IL-1β2 Homology*

Porcine PBL *IL-1β1* and conceptus *IL-1β2* cDNAs were 984 and 977 bp in length, respectively. The sequences were 93% identical at the nucleic acid level (Fig. 3.1). The predicted amino acid sequences for *IL-1β1* and *IL-1β2* were similar in length (267 amino acids; Fig. 3.2) and 85% identical. Within the pro-region, the amino acid sequences were 78% identical and less homologous ($P < 0.01$) when compared with the mature region of the peptide (92% identical). Homology was 100% from amino acid 204 to the end of the sequences (amino acid 267; Fig. 3.2).

Expression of IL-1β1 and IL-1β2

Ribonuclease protection assays detected *IL-1β1* in PBL but not in elongated pig conceptus RNA (Fig. 3.3A). The opposite was true for *IL-1β2,* where transcripts for *IL-1β2* could be detected in pig conceptus but not in PBL RNA (Fig. 3.3B). RT-PCR analysis for *IL-1β1* and *IL-1β2* in the central nervous system, ovary, endometrium, adipose tissue, thyroid, hypothalamus, liver, small intestine, spleen, kidney, lung, smooth muscle and heart confirmed that *IL-1β1* was expressed in all adult tissues but *IL-1β2* was only expressed in the conceptus (data not shown).

Activation of NF-κB in alveolar cells

Treating alveolar cells with LPS and recombinant IL-1 cytokines increased the percentage of activated cells (transformed data; Treatment; $P < 0.05$) and their intensity of NF-κB activation (IOA; Treatment; $P < 0.001$; Fig. 3.4 and Fig. 3.5A and B). Alveolar cells treated with mat-IL-1β2 and LPS had the greatest percentage of activated cells and greatest IOA when compared with all other treatments ($P < 0.05$). In terms of percent of cells activated, all other treatments were similar.

Activation of NF-κB in uterine luminal epithelial cells

Treating porcine endometrium with increasing doses of LPS and recombinant IL-1 cytokines for 4 h increased the uterine LE cell intensity of NF-κB activation (IOA) and the effect depended on treatment and dose concentration (Treatment x Concentration interaction, $P < 0.01$; Fig. 3.6A and B). Across all doses, endometrium treated with pig mat-IL-1β1, LPS, human mat-IL-1β, and mat-IL-1β2 had a greater IOA in LE cells compared with Non-treated and BGal-treated endometrium ($P < 0.05$, Fig. 3.6A and B). Tissue treated with pig mat-IL-1β1 had the greatest uterine LE-IOA ($P < 0.05$, Fig. 3.6A and B).

Endometrial transcripts in response to recombinant IL-1 cytokines

IL-1β1 and IL-1RI. The endometrial *IL-1β1* expression data were highly variable; therefore the data were log 10 transformed to eliminate heterogeneous variance. There was an effect of treatment ($P < 0.001$) and concentration ($P < 0.001$) on endometrial *IL-1β1* expression (Table 3.2). Expression of *IL-1β1* increased with concentration (data not

shown). Treating endometrium with LPS for 4 h had the greatest affect on *IL-1β1*, resulting in 3-fold greater expression over all other treatments ($P < 0.001$; Table 3.2). Treating endometrium with increasing concentrations of LPS or mat-IL-1β2 affected total endometrial expression of *IL-1β1*. Expression of *IL-1βI* was greater in endometrium treated with a high concentration when compared to endometrium treated with a medium concentration of mat-IL-1β2 ($P < 0.05$; data not shown). A similar but a less significant effect was observed for LPS ($P = 0.0901$; data not shown). Treating endometrium with LPS or recombinant IL-1 cytokines for 4 h had no affect on endometrial *IL-1RI*.

PTGS2 and IκBα. Treating endometrium with LPS and recombinant IL-1 cytokines affected total endometrial *PTGS2* and *IκBα* expression within 4 h. The *PTGS2* expression data were highly variable and therefore, the data was log 10 transformed. For endometrial *PTGS2*, there was an effect of treatment ($P < 0.001$; Table 3.2). Endometrium treated with LPS and pig mat-IL-1β1 had a greater abundance of *PTGS2* transcripts when compared with all other treatments ($P < 0.05$; all comparisons; Table 3.2). There was no difference in BGal control and mat-IL-1β2 treated endometrium for *PTGS2* expression. However, treating endometrium with increasing concentrations of mat-IL-1β2 affected total endometrial expression of *PTGS2*. Expression of *PTGS2* was greater in endometrium treated with a high concentration when compared with endometrium treated with a low or medium concentration of mat-IL-1β2 ($P < 0.05$; Figure 3.7D).

There was an effect of treatment ($P < 0.001$) and concentration ($P < 0.001$) on endometrial *IκBα* (Table 3.2). The *IκBα* increased with concentration (data not shown). Endometrium treated with LPS had greater *IκBα* expression when compared with all

other treatments ($P < 0.001$). Endometrium treated with pig mat-IL-1β1 had greater *IκBα* expression compared with control (BGal) treated endometrium ($P < 0.001$; Table 3.2). Similar to *PTGS2*, there was not a significant difference in *IκBα* expression between BGal and mat-IL-1β2 treated endometrium. However, treating endometrium with increasing concentrations of LPS or mat-IL-1β2 affected total endometrial expression of *IκBα*. In endometrium treated with LPS, expression of *IκBα* increased with concentration (1 μg/mL compared to 100 μg/mL, $P < 0.05$; Fig. 3.7E). Similar to *PTGS2*, transcripts for *IκBα* were greater in endometrium treated with a high concentration when compared with endometrium treated with a low or medium concentration of mat-IL-1β2 ($P = 0.0591$ and $P < 0.05$, respectively; Fig. 3.7H).

β3, αV and SAL1. Treating endometrium with LPS and recombinant IL-1 cytokines affected total endometrial *β3* but not *αV* integrin expression within 4 h of treatment. There was an effect of treatment ($P < 0.001$) and concentration ($P < 0.01$) on endometrial *β3* (Table 3.2). The *β3* increased with concentration (data not shown). Compared with all other treatments, endometrium treated with pig mat-IL-1β1 had the greatest *β3* expression ($P < 0.01$; Table 3.2). Neither pro nor mature IL-1β2 had an effect on endometrial *β3*. Treating endometrium with increasing concentrations of mat-IL-1β1 affected total endometrial expression of *β3*. Expression of *β3* was greater in endometrium treated with a medium concentration when compared to endometrium treated with a low or a high concentration of mat-IL-1β1 ($P < 0.01$ and $P = 0.0598$, respectively; Fig. 3.7K). There was no effect of treatment or concentration on endometrial *SAL1*.

DISCUSSION

We tested the capacity of IL-1β2, a novel pig conceptus IL-1, to activate NF-κB within the uterine LE. Major findings were that 1) *IL-1β2*, rather than *IL-1β1*, is expressed by the elongating pig conceptus on d 12 of development; 2) *IL-1β2* is not expressed by pig blood leukocytes or other adult tissues 3) recombinant IL-1β2 can activate NF-κB in pig alveolar macrophages and uterine surface epithelium, in what would be adjacent to the elongating pig conceptus, and 4) within pig endometrium, IL-1β2 may have reduced activity compared with blood leukocyte IL-1β1. Similar to the primate and rodent conceptus, we report that elongating pig conceptuses express an IL-1β that can directly affect the endometrium by activating NF-κB within the uterine surface epithelium (Simón et al., 1998; King et al., 2010). Activation of NF-κB within the uterine epithelium may enhance uterine receptivity and development of the early pig conceptus during establishment of pregnancy.

Interleukin-1 beta is a master proinflammatory cytokine released by blood monocytes, macrophages, skin dendritic cells, and brain microglia that can modulate innate and adaptive immune processes (Sims and Smith, 2010; Garlanda et al., 2013). During infection, IL-1β acts as an endogenous pyrogen, inducing fever that likely stimulates leukocyte proliferation and migration (Boron and Boulpaep, 2009; Sims and Smith, 2010; Garlanda et al., 2013). When released by macrophages onto blood vessels,

IL-1β increases endothelial cell adhesion molecule expression and permeability, thus allowing peripheral blood leukocytes to bind, extravasate and migrate into infected tissues (Dinarello, 1996; 2005; Dunne, 2003). IL-1β, however, is pleotropic when bound to the IL-1RI and can influence the biology of many different cell types including those involved in mammalian reproduction. For instance, IL-1β is secreted by the primate, rodent and pig blastocyst, and is believed to initiate communication between the conceptus and endometrium for implantation. Interleukin-1 beta is thought to promote conceptus development through an up-regulation of uterine epithelial adhesion molecules, trophoblast invasion, vascular permeability and endometrial leukocyte activity (Librach et al., 1994; Barañao et al., 1997; Simón et al., 1998; Marions and Danielsson, 1999; Ross et al., 2003a;).

Vandenbroeck et al. (1993) were the first to suggest that an alternate *IL-1β* sequence existed within the pig genome. Later, Tuo et al. (1996) detected expression of an *IL-1β* in elongating pig conceptus, a study that was followed up by Ross et al. (2003a) who suggested that the pig conceptus expressed an alternate *IL-1β* transcript. Sequencing and assembly of the porcine genome has confirmed the presence of a second *IL-1β* gene, unique to pig (Groenen et al., 2012). The RPA (Fig. 3) and RT-PCR data support the conclusion that pig conceptuses express this unique form of *IL-1β*, a gene that we call embryonic *IL-1β* or *IL-1β2*. During these experiments, we could not detect expression of *IL-1β2* in blood leukocytes or adult tissues suggesting that expression of *IL-1β2* may be exclusive to the pig conceptus.

The *IL-1β1/IL-1β2* genomic region in pigs has not been completely sequenced perhaps because the two highly homologous sequences make sequencing assembly

difficult. The gene encoding *IL-1β2* appears to be a duplication of *IL-1β1*. Both genes consist of seven exons and transcribe nucleic acid sequences that are 93% similar (Fig. 3.1). Compared with *IL-1β1*, a gene that spans nearly 7kb, *IL-1β2* has an insertion and two deletions of genomic sequence within in its original proximal promoter region (Fig. 3.8). As a result, the *IL-1β2* gene spans approximately 16.5 kb; transcribing an alternate exon one that is further up-stream of exon two when compared with *IL-1β1*. Reconfiguration of the *IL-1β2* promoter region may have changed its transcriptional regulation. This could partially explain why *IL-1β2* is expressed by pig conceptuses but not by leukocytes or other adult tissues that commonly express *IL-1β1*. Comparison of full length *IL-1β1* and *IL-1β2* cDNA revealed that the 5' region is the least homologous, particularly within exon one (Fig. 3.1), making it relatively easy to discriminate between the two genes during RNA or DNA analysis (Fig. 3.3).

Interleukin-1 beta mRNA are first translated into pro-proteins that are later cleaved by caspase-1 (CASP1), a protease, into mature functional cytokines. Like pro-IL-1β1 cloned from pig blood leukocytes, the pig conceptus *IL-1β2* cDNA sequence encodes a 267 amino acid protein with a predicted molecular weight (MW) of ~30 kDa. When we compared the pro-IL-1β1 and pro-IL-1β2 protein sequences, they were 85% identical (Fig. 3.2). Based on human IL-1β protein sequences and published pig sequences within GenBank, CASP1 cleaves the pro-region of pig IL-1β1 in two sequential locations (Asp^{27} and Gly^{28} followed by Asp^{114} and Ala^{115}), forming a mature, functional, cytokine with a MW of ~17.5 kDa (Hailey et al., 2009; Fig. 3.2). These amino acids are conserved within pro-IL-1β2 and translation of the "mature" IL-1β2 sequence corresponds to a similar MW (17.5 kDa). However, a number of amino acids differed between pig pro-IL-1β1 and pro-

IL-1β2 immediately upstream of the second protease cleavage site. A proline has also been inserted two amino acids downstream of this location in IL-1β2. Based on these differences, classical CASP1 activity may not be the same for these two cytokines and/or other proteases may be involved in the processing of pro-IL-1β2 (Katebi et al., 2010). Indeed, human pro-IL-1β can be cleaved by proteases other than CASP1 (Dinarello, 1996; Coeshott et al., 1999; Netea et al., 2010; Dinarello, 2011). When we compared the pro and mature regions of IL-1β1 and IL-1β2 based on classic CASP1 activity, the cytokines were less homologous within the pro (78%) and more homologous within mature (92%) region of the proteins (Fig. 3.2). This was not surprising as all amino acids involved in binding and activation of the IL-1RI are located within the mature region of IL-1β. Interestingly, compared with mature IL-1β1, there were two non-conserved amino acid substitutions in IL-1β2 (amino acids 129 and 139) that are believed to be involved in IL-1RI binding based on human IL-1β sequences. These substitutions include exchanges of a histidine and methionine residues (positively charged and hydrophobic side chains, respectively) with negatively charged glutamate residues (Fig. 3.2). When Katebi et al. (2010) compared the computationally predicted protein structure of IL-1β2 with IL-1β1 they concluded that amino acid substitutions within this region could affect the activity of IL-1β2.

Maximal expression of *IL-1RI* and *IL-1RAP* in pig endometrium is temporally associated with conceptus elongation and expression of *IL-1β2* (Tuo et al., 1996; Ross et al., 2003a, 2003b). Similar to IL-1β in humans and mice, binding of IL-1β2 to endometrial IL-1R1 may prepare the uterus for implantation by activating NF-κB and modulating endometrial gene expression. Within the endometrium, Ross et al. (2010)

detected an increase in mRNA for *NF-κB1* and *p65* subunits of NF-κB between d 5 and 15 of the estrous cycle and pregnancy that was temporally associated with implantation. Using IHC, they detected greater nuclear localization (activation) of the p65 subunit of NF-κB within the LE on d 12 and 13 of pregnancy compared with the estrous cycle. The activation of NF-κB was temporally associated with conceptus expression of *IL-1β2* (Ross et al., 2010). In the present study, treating pig endometrium with increasing concentrations of mat-IL-1β1 or mat-IL-1β2 activated the p65 subunit of NF-κB in the uterine epithelium within 4 h (Fig. 3.6A and B). Activation of NF-κB within the uterine LE was greatest in response to mat-IL-1β1, indicating that this cytokine has greater proinflammatory activity within the endometrium. Although we did not specifically measure activation within the glandular epithelium, the number of cells with nuclear NF-κB appeared to decrease from the surface epithelium to the deeper glandular epithelium in response to the mature cytokines (data not shown). A similar response was observed by Mathew et al. (2011) who detected activation of NF-κB in d 12 pregnant pig uterine epithelium specifically adjacent to elongating pig conceptuses.

We measured transcripts that are regulated by IL-1β or NF-κB in the mammalian endometrium. Of these, *PTGS2* (also known as *COX2*; a rate-limiting enzyme involved the synthesis of prostaglandins) is known to increase within the mammalian endometrium during implantation and is believed to be essential for successful pregnancy (Kraeling et al., 1985; Lim et al., 1997; St-Louis et al., 2010). As part of a negative feed back loop, NF-κB also regulates expression of *IκBα*, an inhibitor protein that sequesters NF-κB in the cell cytoplasm until activation is signaled (Hiscott et al., 1993; Hayden and Ghosh, 2012). Interestingly, on d 12 of pregnancy in the pig, a time when elongating pig

conceptuses release peak concentrations of *IL-1β2* and locally activate NF-κB within the uterine surface epithelium, there is no detectable increase in total endometrial *PTGS2* or *IκBα* expression (Ashworth et al., 2006; Blitek et al., 2006; Franczak et al., 2010; Ross et al., 2010; Mathew et al., 2011).

When we treated non-pregnant pig endometrium collected during the luteal phase for 4 h with LPS or recombinant mat-IL-1β1, we detected an increase in total endometrial transcripts for *PTGS2* and *IκBα* (Table 3.2). For endometrium treated with mat-IL-1β2, the expression of *PTGS2* and *IκBα* increased in response to the highest dose (1000 ng/mL) of this protein (Fig. 3.7D and Fig. 3.7H). We suggest that IL-1β2 has a lesser capacity to activate NF-κB within the endometrium as compared with IL-1β1 (Fig. 3.6) and, therefore, lower doses of IL-1β2 are unable to increase total endometrial expression of NF-κB responsive genes (*PTGS2* and *IκBα*) within 4 h of treatment (Table 3.2). This may explain why up-regulation of some NF-κB responsive transcripts has not been detected at the time of elongation in total endometrium of pregnant pigs. Endometrium proximal to the elongating pig blastocyst may have NF-κB responsive genes up-regulated in response to a local paracrine mechanism involving IL-1β2. Nuclear factor-kappa B was strongly activated within the luminal and surface glandular epithelial cells directly adjacent to conceptus tissues during elongation (Mathew et al., 2011). Other factors released by the pig conceptus are hypothesized to have local rather than global effects within the endometrium. For example, conceptus estrogens and cytokines interferon gamma (IFNγ) and interferon delta (IFNδ) fall into this category (White et al., 2005; Joyce et al., 2007; Joyce et al., 2008; Johnson et al., 2009)

Similar to pigs, the primate and rodent conceptus releases IL-1β during implantation. The IL-1β up-regulates *αV* and *β3* integrin subunits within the uterine epithelium and enhances endometrial affinity for the blastocyst (Simón et al., 1998). In pig endometrium, αV and β3 integrins are highly expressed during implantation and their expression is believed to be important for placental attachment and development (Bowen et al., 1996; Lin et al., 2007; Bazer et al., 2012). Although total endometrial transcripts for *αV* did not change in this study, we detected up-regulation of *β3* in response to LPS and mat-IL-1β1. The up-regulation of β3 may be a conserved mechanism that persists within the endometrium of primates, rodents and the domesticated pig in response to IL-1β (Table 3.2). We did not detect an increase in total endometrial β3 in response to mat-IL-1β2, again, indicating that this cytokine has less activity within the pig endometrium compared with IL-1β1.

We tested the capacity of mat-IL-1β1 and mat-IL-1β2 to activate NF-κB using pig alveolar leukocytes before we performed our studies of the pig endometrium. Surprisingly, we did not detect activation of NF-κB in alveolar cells treated with mat-IL-1β1; however, at the same concentration, mat-IL-1β2 increased nuclear translocation of NF-κB in these cells (Fig. 3.4; Fig. 3.5A and Fig. 3.5B). We have not investigated the mode of IL-1β2 signal transduction within the endometrium or in alveolar macrophages (Zeidler and Kim, 1985). The unique interaction of IL-1β2 with various components of the IL-1 system, such as IL-1RI, IL-1RII (an IL-1 mock receptor) or IL-1R accessory proteins or the interaction of IL-1β2 with factors outside the IL-1 system could provide an explanation for the tissue dependent responses we observed during our investigation.

SUMMARY AND CONCLUSION

The mammalian conceptus creates a proinflammatory uterine environment within the endometrium during the peri-implantation period. This environment is believed to enhance uterine receptivity and implantation, thereby, promoting survival of the conceptus in utero. The pig genome contains a novel IL-1β gene (IL-1β2) that does not exist in other mammals. Based on our findings and evidence provided by other laboratories, IL-1β2 (rather than IL-1β1) is expressed by the pig conceptus before implantation. We found that IL-1β1 has greater activity within the endometrium compared with IL-1β2 but, nonetheless, IL-1β2 has the capacity to activate NF-κB within the uterine LE. We propose that as the pig conceptus expands its trophoblast and elongates over the uterine surface, it releases IL-1β2 onto the adjacent uterine LE. The release of IL-1β2 likely initiates a controlled proinflammatory microenvironment within the maternal tissues to promote establishment of pregnancy. Expression of IL-1 receptors within the elongating conceptus, and the synchronous pattern for which IL-1β2 is expressed during elongation, suggests that IL-1β2 may have a role in elongation and development of the early pig embryo. Future *in vivo* studies investigating the autocrine and paracrine effects of IL-1β2 on the pig conceptus and the maternal tissues, respectively, could reveal how endogenous proinflammatory molecules function in a pro-survival manner during the peri-implantation period.

TABLE 3.1 GenBank accession number, gene name, primer sequence, size of the amplicon and amplification efficiency for the individual genes whose expression was measured using real-time reverse transcription polymerase chain reaction (RT-PCR).

GenBank	*Gene name*	*Primer*	*Primer sequence (5′-3′)*	*Product size (bp)*	*Efficiency*
U07786.1	*ACTβ*	Forward Reverse	ACATCAAGGAGAAGCTCTGCTACG GAGGGGCGATGATCTTGATCTTCA	366	2.07
NM_001113217.1	*RPL7*	Forward Reverse	AAGCCAAGCACTATCACAAGGAATACA TGCAACACCTTTCTGACCTTTGG	172	1.99
NM_214321.1	*PTGS2*	Forward Reverse	TCGACCAGAGCAGAGAGATGAGAT ACCATAGAGCGCTTCTAACTCTGC	133	2.05
NM_001005150.1	*IκBα*	Forward Reverse	TGTGATCCTGAGCTCCGAGACTTT TTGTAGTTGGTGGCCTGCAGAATG	143	1.81
NM_2140055.1	*IL-1β1*	Forward Reverse	CAGCCAGTCTTCATTGTTCAGGTT AGATTTGCAGCTGGATGCTC	226	1.78
XM_003354714.2	*IL-1R1*	Forward Reverse	AATGCACTTCCTAGGCTTTCTG GGAACAGGATGTGGTGACAA	65	1.89
FJ914572.1	*β3*	Forward Reverse	AAGAAGGGGTGTGTGGAGTG TGGGACACTCTGGCTCTTCT	235	2.13
EF474019.1	*αV*	Forward Reverse	GATTGTTGTTACTGGCTGTTTTGG TGTTCCCTTTCCTGTTCTTCTTG	94	1.82
NM_213814.1	*SAL1*	Forward Reverse	GCTGACTCTAGCCTCTTCCCACAA CGTCTGAGGCCAAAAGAATGGAATA	110	1.94

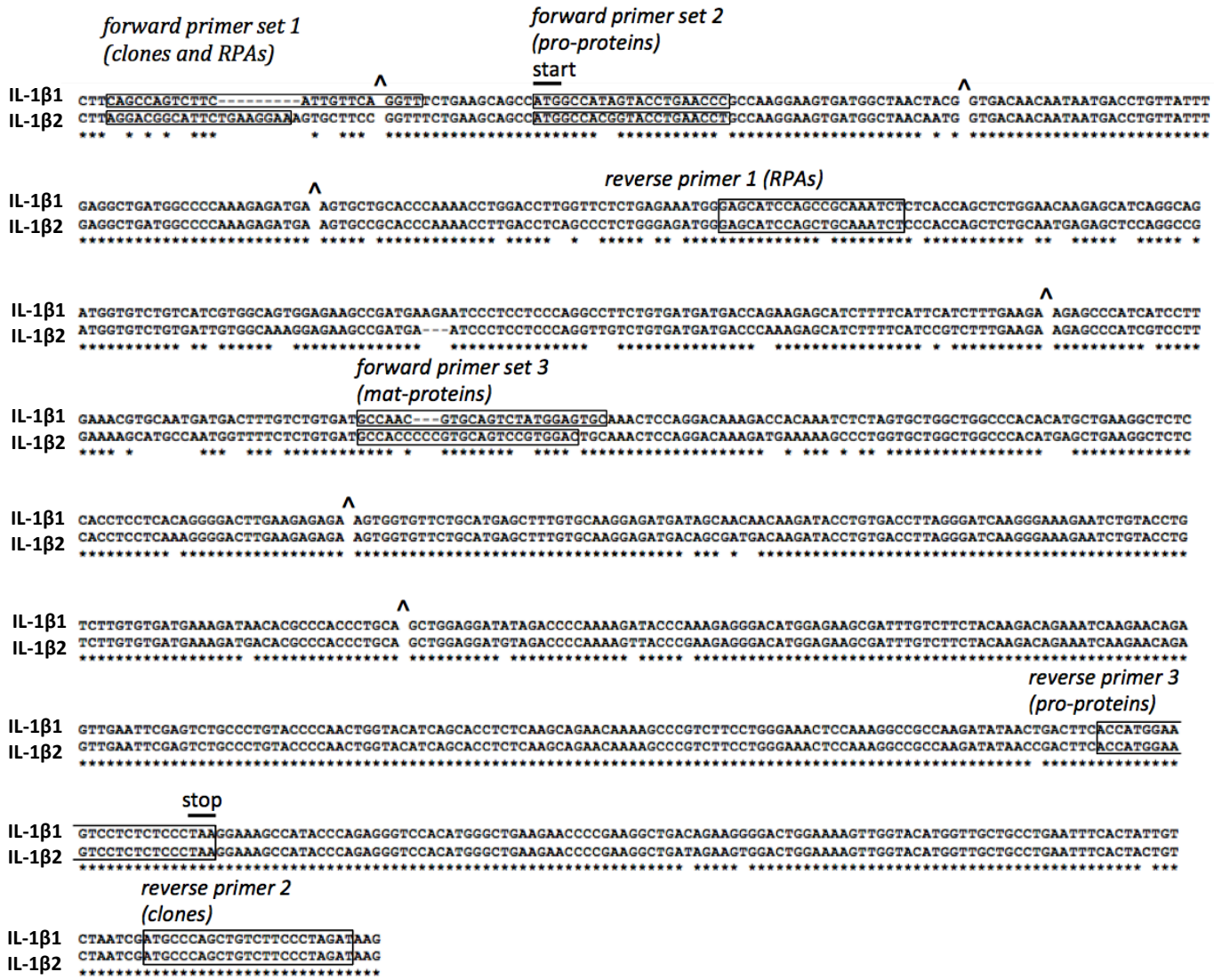
forward primer set 1
(clones and RPAs)
forward primer set 2
(pro-proteins)
start
IL-1β1
IL-1β2
reverse primer 1 (RPAs)
forward primer set 3
(mat-proteins)
reverse primer 3
(pro-proteins)
stop
reverse primer 2
(clones)

FIGURE 3.1 Alignment of full length *pro-IL-1β1* and *pro-IL-1β2* cDNA within CLUSTALW multiple sequence alignment program and location of forward and reverse primers used to amplify *IL-1β1* and *IL-1β2* sequences for gene cloning, ribonuclease protection assays (RPA) and protein expression studies. The *IL-1β1* and *IL-1β2* consist of seven exons and are 93% similar. Conjoined exons are designated by "^" and homologous base pairs (bp) between *IL-1β1* and *IL-1β2* have a star (*****) beneath the sequences. Translation start and stop codons within the sequences are designated by "start" and "stop", respectively.

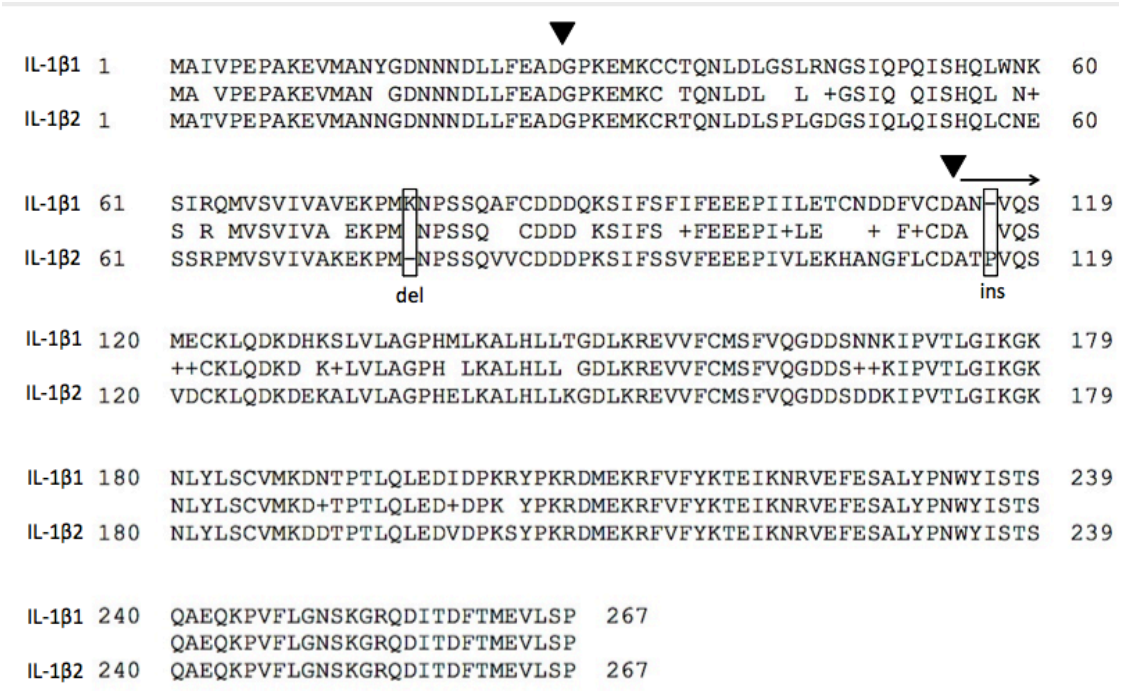

FIGURE 3.2 Alignment of full-length pig IL-1β1 and IL-1β2 amino acid sequences. Amino acids that are identical in IL-1β1 and IL-1β2 are displayed between the two sequences. The positive symbols (+) indicate conservative substitutions. The solid arrows above the sequences indicate locations of sequential caspase-1 (CASP1) protease cleavage sites during formation of the mature IL-1β1. The right arrow above the sequence signifies start of the mature region. Compared with IL-1β1, the IL-1β2 sequence has an inserted (ins) and deleted (del) amino acid upstream and downstream (mature region) of the second CASP1 cleavage site, respectively. IL-1β2 also has a glutamate residue substituted for a histidine and methionine at IL-1RI binding locations 129 and 139, respectively, compared to IL-1β1.

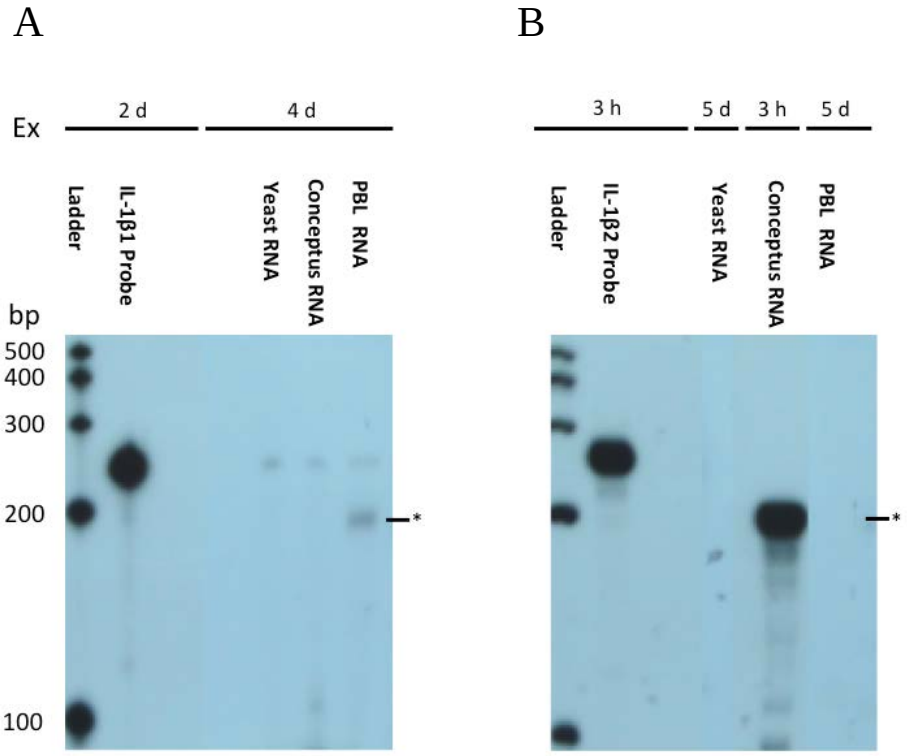

FIGURE 3.3 Autoradiograph of an RPA demonstrating hybridization of the *IL-1β1* (A) and *IL-1β2* (B) probes to pig peripheral blood leukocyte (PBL) and d 12 conceptus RNA, respectively. The IL-1β1 and IL-1β2 protected fragments are 196 and 205 base pairs (bp) in length, respectively. The star (*) indicates protected fragments and specific expression of unique IL-1β genes in adult pig PBL (*IL-1β1;* A) and d 12 pig conceptuses (*IL-1β2;* B). Negative controls consisted of Torulla yeast RNA. Ladder = 100 - 500 bp RNA century marker. Different exposure times (Ex) for the same RPA are shown side-by-side in the figure.

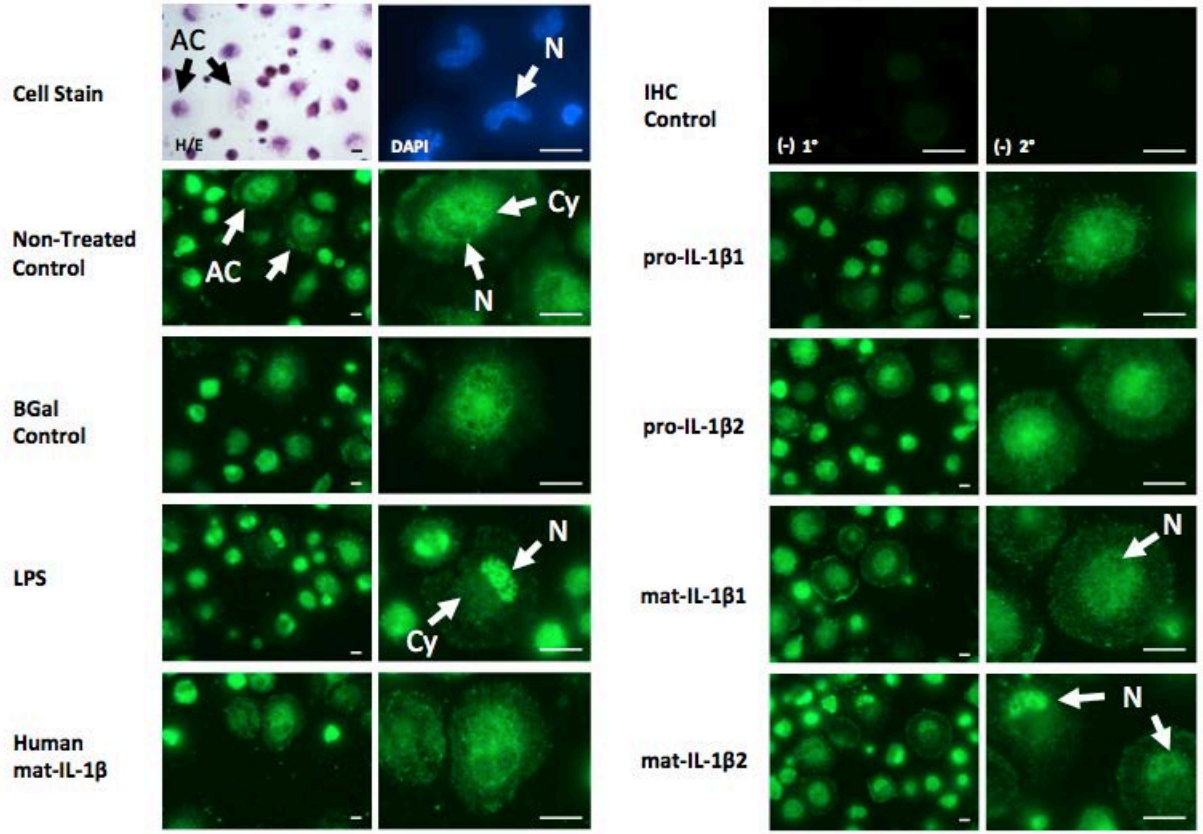

FIGURE 3.4 Images of NF-κB activation in alveolar cell (AC) nuclei (N) vs. cell cytoplasm (Cy) after cells were collected by lung lavage and left non-treated or treated with LPS or recombinant IL-1 cytokines for 4 h. Greater than 90% of AC in adult pigs are macrophages. Imunohistochemistry (IHC) control slides were made using pre-immune rabbit IgG in place of the primary antibody [(-) 1°] or in the absence of a secondary antibody [(-) 2°]. Images were taken with a Leica light microscope using a green fluorescent protein (GFP) filter. H/E, hemotoxylin and eosin cell stain; DAPI, 4',6-diamidino-2-phenylindole nuclear stain. Bar = 10 μm.

A

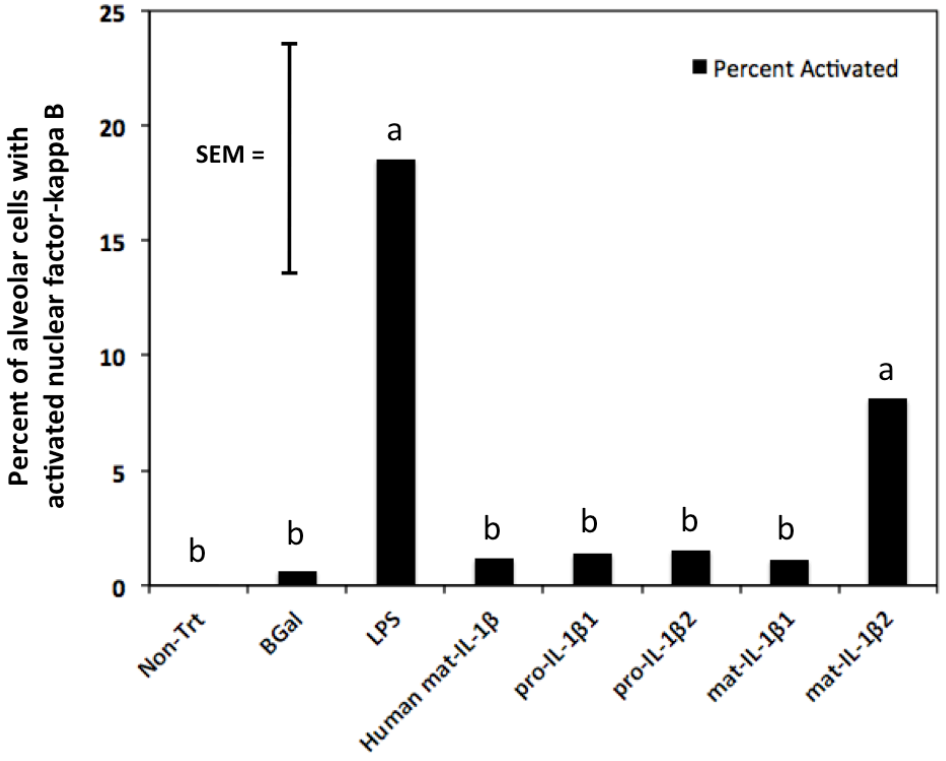
Percent of alveolar cells with activated nuclear factor-kappa B
25
20
15
10
5
0
Percent Activated
SEM =
a
b
b
b
b
b
b
b
a
Non-Trt
BGal
LPS
Human mat-IL-1β
pro-IL-1β1
pro-IL-1β2
mat-IL-1β1
mat-IL-1β2

B

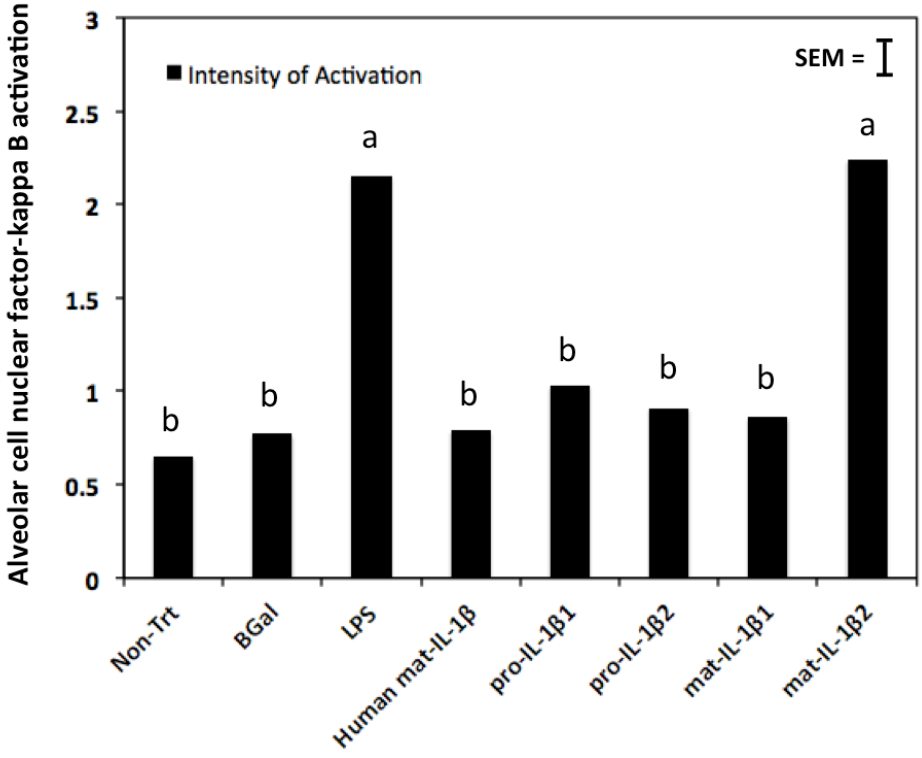
Alveolar cell nuclear factor-kappa B activation
3
2.5
2
1.5
1
0.5
0
Intensity of Activation
SEM =
b
b
a
b
b
b
b
a
Non-Trt
BGal
LPS
Human mat-IL-1β
pro-IL-1β1
pro-IL-1β2
mat-IL-1β1
mat-IL-1β2

FIGURE 3.5 Percent of alveolar cells (AC) with activated NF-κB (A) and intensity of NF-κB activation (IOA) in AC (B) after cells were collected by lung lavage and left non-treated or treated with LPS or recombinant IL-1 cytokines for 4 h. Data are presented as non-rank transformed LSM ± SEM (bar; SEM = 5.31 and 0.12 for percent of alveolar cells and IOA, respectively). Letters indicate a significance difference between treatments for transformed (A) and non-transformed (B) data. Significance was declared at $P < 0.05$.

A

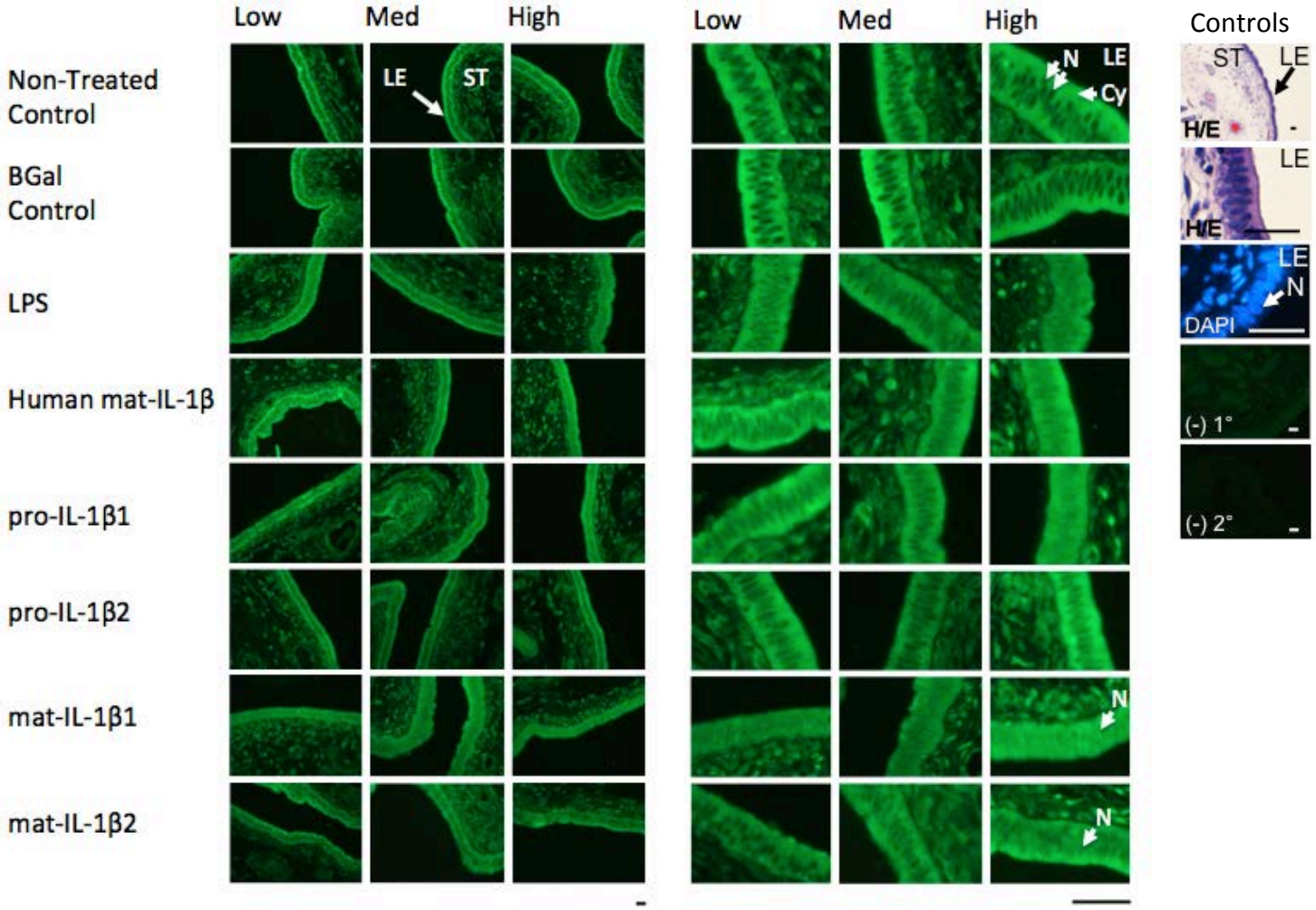
Low
Med
High
Low
Med
High
Controls
Non-Treated Control
BGal Control
LPS
Human mat-IL-1β
pro-IL-1β1
pro-IL-1β2
mat-IL-1β1
mat-IL-1β2
LE
ST
N
Cy
H/E
DAPI
(-) 1°
(-) 2°

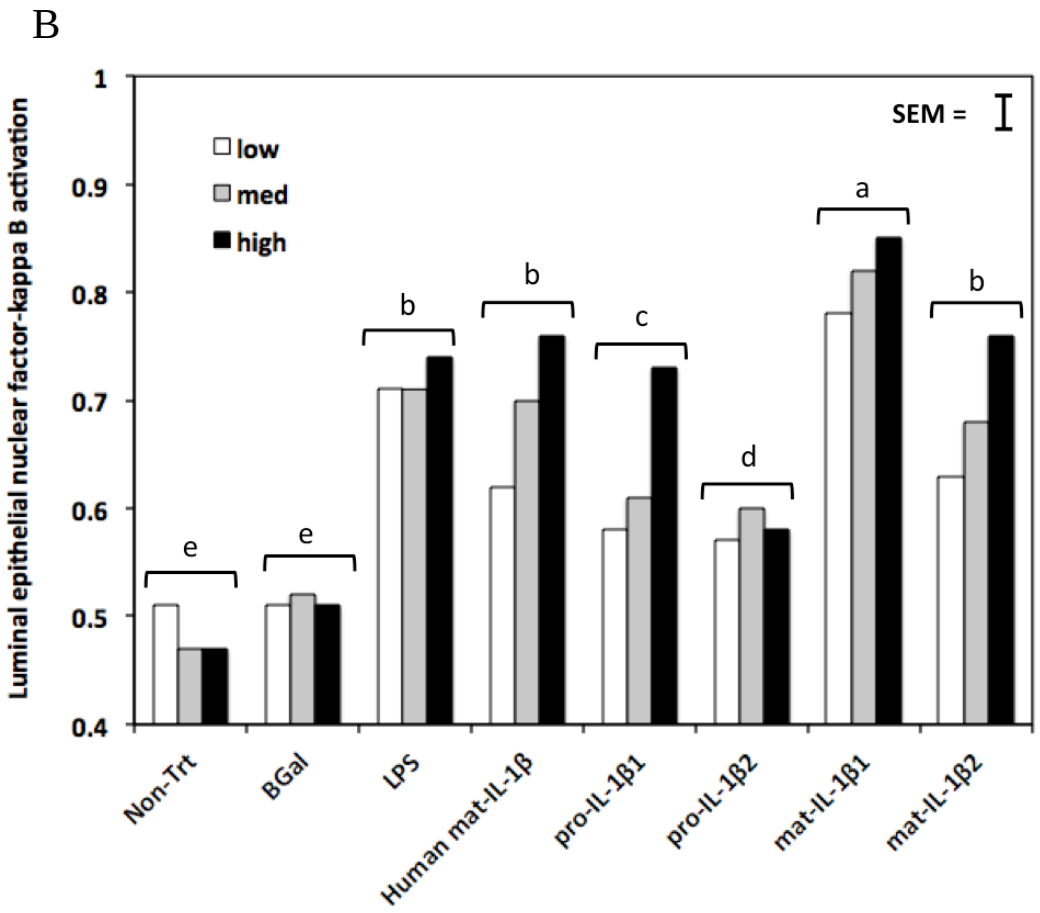

FIGURE 3.6 Images of NF-κB activation (A) and intensity of NF-κB activation (IOA) (B) in pig uterine luminal epithelium (LE) after endometrium was left non-treated or treated with low, medium or high concentrations of LPS (1, 10, or 100 μg/mL, respectively) or recombinant IL-1 cytokines (10, 100, or 1000 ng/mL, respectively) for 4 h. In A, immunohistochemistry (IHC) control slides were made using pre-immune rabbit IgG in place of the primary antibody [(-) 1°] or in the absence of a secondary antibody [(-) 2°]. Images were taken with a Leica light microscope using a green fluorescent protein (GFP) filter. In B, data are presented as LSM ± SEM (bar; SEM = 0.03). Different letters over bars indicated a significant difference between treatments ($P \leq 0.01$). H/E, hemotoxylin and eosin cell stain; DAPI, 4',6-diamidino-2-phenylindole nuclear stain; ST, stroma; N, nucleus; Cy, cytoplasm; Bar in A = 20 μm.

TABLE 3.2 Fold changes in gene expression (relative to internal medium control) of selected genes from total endometrium left non-treated or treated with LPS (1, 10 or 100 μg/mL) or recombinant IL-1 cytokines (10, 100 or 1000 ng/mL). Data were normalized to the geometric mean of total endometrial *RPL7* and *ACTβ* fold change in gene expression. Data are presented as LSM ± SEM.

	Treatment (T)								P<[f]		
Gene	Non-Trt	BGal	LPS	Hum IL-1β	pro-IL-1β1	pro-IL-1β2	mat-IL-1β1	mat-IL-1β2	T	C	TXC
SAL1	1.4 ± 0.2^{a,b}	1.3 ± 0.3^{b}	1.3 ± 0.3^{a,b}	1.9 ± 0.2^{a}	1.2 ± 0.2^{b}	1.3 ± 0.2^{b}	1.6 ± 0.2^{a,b}	1.8 ± 0.2^{a,b}	NS	NS	NS
IL-1RI	1.2 ± 0.2^{a}	1.3 ± 0.2^{a}	1.5 ± 0.2^{a}	1.5 ± 0.2^{a}	1.2 ± 0.2^{a}	1.1 ± 0.2^{a}	1.4 ± 0.2^{a}	1.3 ± 0.2^{a}	NS	NS	NS
IL-1β1[g]	0.2 ± 0.3^{b}	0.3 ± 0.3^{b}	4.3 ± 0.3^{a}	0.3 ± 0.3^{b}	0.4 ± 0.3^{b}	0.3 ± 0.3^{b}	0.7 ± 0.3^{b}	0.4 ± 0.3^{b}	0.001	0.001	NS
PTGS2[g]	0.9 ± 0.3^{b}	1.0 ± 0.3^{b}	2.2 ± 0.3^{a}	1.0 ± 0.3^{b}	1.0 ± 0.3^{b}	0.8 ± 0.2^{b}	1.9 ± 0.2^{a}	1.2 ± 0.3^{b}	0.001	NS	NS
IκBα	0.4 ± 0.1^{d,e}	0.5 ± 0.1^{d,e}	2.0 ± 0.1^{a}	0.9 ± 0.1^{b,c}	0.9 ± 0.1^{b,c}	0.4 ± 0.1^{e}	1.1 ± 0.1^{b}	0.7 ± 0.1^{c,d}	0.001	0.001	NS
αV	0.8 ± 0.1^{a}	0.7 ± 0.1^{a}	0.8 ± 0.1^{a}	0.8 ± 0.1^{a}	0.6 ± 0.1^{b}	0.6 ± 0.1^{b}	0.7 ± 0.1^{a}	0.8 ± 0.1^{a}	NS	NS	NS
β3	1.4 ± 0.3^{c}	1.8 ± 0.3^{b,c}	2.5 ± 0.4^{b}	2.5 ± 0.3^{b}	1.8 ± 0.3^{b,c}	1.5 ± 0.3^{c}	3.6 ± 0.3^{a}	1.6 ± 0.3^{c}	0.001	0.009	NS

[f] P value for treatment (T), concentration (C) and T by C (TXC). Not significant (NS) was declared as P > 0.10.
[g] The presented *IL-1β1* and *PTGS2* data are the untransformed means but the reported statistical tests are for log 10 transformed data; the log 10 transformation eliminated heterogeneous variance.
Letters to the right of data indicated significant differences between treatment LSM. Significance was declared as P < 0.05.

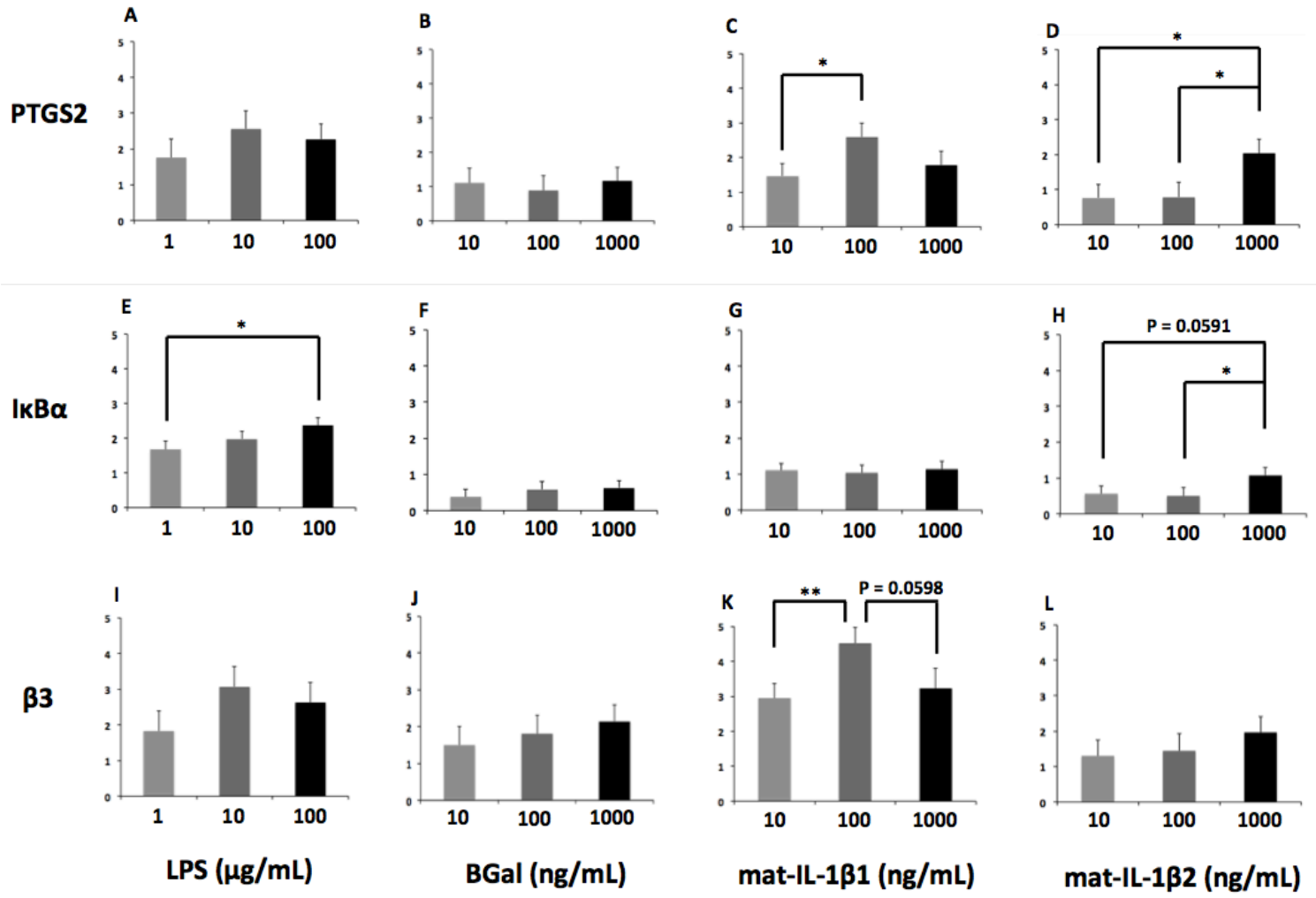
PTGS2
IκBα
β3
A
B
C
D
E
F
G
H
I
J
K
L
*
**
P = 0.0591
P = 0.0598
1
10
100
1000
LPS (µg/mL)
BGal (ng/mL)
mat-IL-1β1 (ng/mL)
mat-IL-1β2 (ng/mL)

FIGURE 3.7 Fold changes in gene expression (relative to internal medium control) of *PTGS2* (A-D), *IκBα* (E-H) and *β3* (I-L) from total endometrium treated with LPS (1, 10 or 100 μg/mL) or 10, 100 or 1000 ng/mL of recombinant BGal (protein expression control), mat-IL-1β1 and mat-IL-1β2. Data were normalized to the geometric mean of total endometrial *RPL7* and *ACTβ* fold change in gene expression. Data are presented as LSM ± SEM. Black stars (*) over bars indicate significant differences in gene expression between concentrations (* $P \leq 0.05$, ** $P \leq 0.01$ *** $P \leq 0.001$).

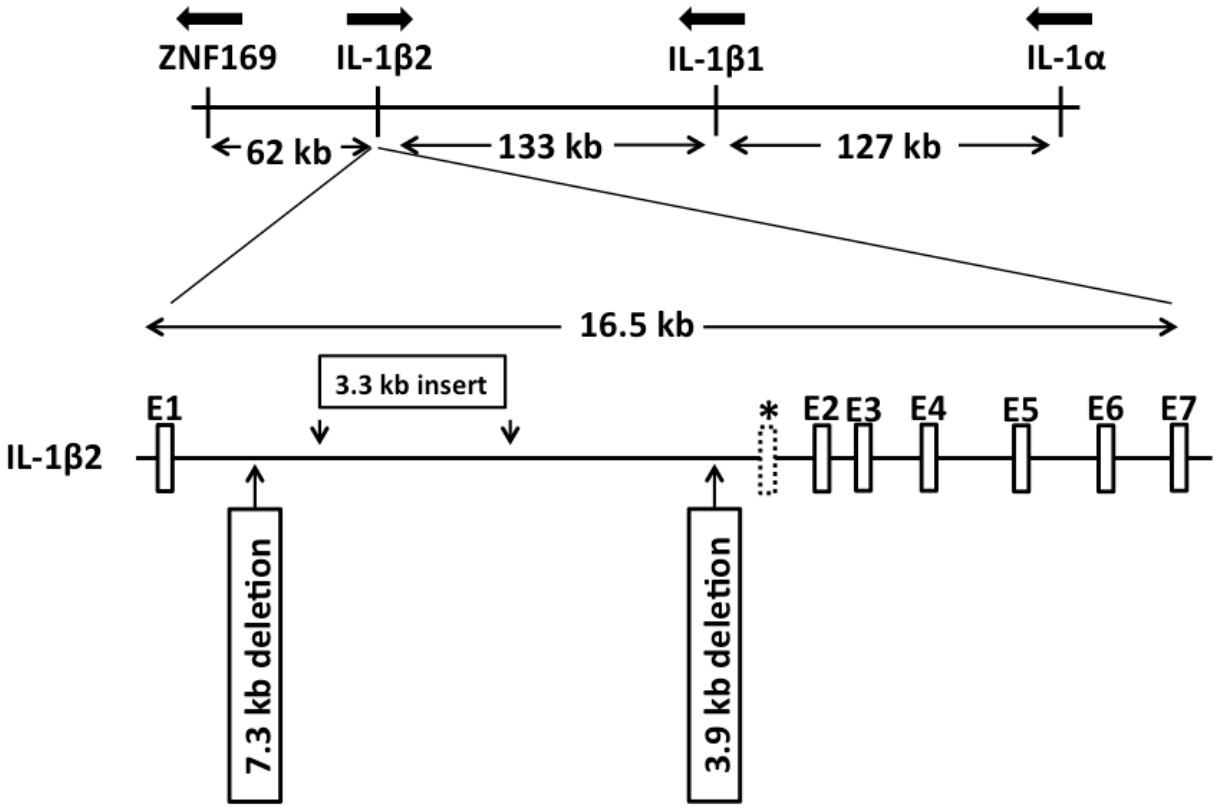

FIGURE 3.8 Diagram of pig genomic region of chromosome 3 containing *IL-1β2*. The genomic region covers >300 kb and contains genes *ZNF169*, *IL-1β2*, *IL-1β1*, and *IL-1α* (top of figure). The *IL-1β2* gene (bottom of figure) covers approximately 16.5 kb. Exon 1 (E1) of the *IL-1β2* gene is upstream from the location of exon 1 in *IL-1β1* (*, dashed box). The remaining *IL-1β2* exons (E2-E7) are arranged in a manner similar to *IL-1β1*. Sequence alignment of *IL-1β2* and *IL-1β1* suggests there are two deletions and an insertion of genomic sequence in the intron between E1 and E2 for *IL-1β2* compared with *IL-1β1*. Based on Sus scrofa genome build 10.2. NCBI reference sequence: NC_010445.3. Black arrows above gene name indicate direction of transcription.

CHAPTER FOUR

DEVELOPMENT OF A LENTIVIRAL MEDIATED RNAi SYSTEM FOR KNOCKDOWN OF INTERLEUKIN-1 BETA 2, A NOVEL INTERLEUKIN-1 EXPRESSED BY THE ELONGATING PIG CONCEPTUS

Abstract

Embryonic loss in the pig is greatest during rapid elongation, a process by which the trophoblast and endoderm undergo extensive remodeling resulting in formation of a filamentous conceptus. Rapid elongation of the pig conceptus occurs between days (d) 11 and 12 of development and is necessary to increase the size of the fetal placental unit. During this process, pig conceptuses increase gene expression of interleukin-1 beta 2 (*IL-1β2*), a novel IL-1 not found in other mammals. Conceptus expression of *IL-1β2* is transient. Expression of *IL-1β2* increases during the onset of rapid elongation, peaks at the height of this process and decreases 2000 fold thereafter. Interleukin-1 signaling factors, IL-1 receptor type 1 (*IL-1RI*) and IL-1 receptor accessory protein (*IL-1RAP*), also transiently increase in the conceptus. Therefore, it's hypothesized that IL-1β2 is

necessary for conceptus elongation. To test this hypothesis, we developed a lentiviral mediated RNAi (knockdown) system targeting *IL-1β2* in early pig conceptuses. Multiple knockdown (KdV) and scrambled control knockdown (SV) viruses were developed and microinjected under the zona pellucida of *in vitro* produced pig zygotes. Conceptuses were then allowed to develop in culture (d 6 or 8) or were transferred to the oviduct of recipient gilts on d 4 of the estrous cycle. Transferred conceptuses were flushed from the uterus on d 13 of development. In all, 1725 pig zygotes were produced, of which 1196 were microinjected with lentivirus. Ten embryo transfers were performed. Microinjections of pig zygotes with V (KdV and SV combined) reduced the number conceptuses that became blastocyst by d 6 compared with conceptus that were not microinjected (no virus controls; NV; $P < 0.001$). Expression of beta actin (*ACTB*), a developmental control gene, in individual pig blastocyst treated with SV tended to be less when compared with NV conceptuses ($P = 0.071$). Expression of *IL-1β2* was detected in individual d 6 pig blastocysts and although expression was numerically lower in KdV when compared with NV and SV treated conceptuses, the expression level was not significantly different. With respect to the embryo transfer experiments, NV conceptuses were elongated on d 13. Out of the three gilts that received KdV conceptuses, one gilt produced two elongated conceptuses (GFP positive) and two gilts produced abnormally small spherical conceptuses on d 13. Gilts (n=6) that received SV conceptuses produced fragments of conceptus tissue or no tissue. A lentiviral mediated RNAi system-targeting *IL-1β2*, therefore, could not be used to effectively test the function of this cytokine during elongation of the early pig conceptus. As an alternative, the CRISPR/Cas9 system could be used to produce *IL-1β2* knockout conceptuses, which could then be transferred to

recipient gilts. Expression of *IL-1β2* in the d 6-pig blastocyst suggests that this cytokine may play an important role in development of the pig conceptus prior to elongation.

INTRODUCTION

Conceptus elongation is the process by which the spherical blastocyst undergoes a morphological change that results in the formation of a filamentous or more elongated conceptus. In cattle and pigs, mammals with a less invasive placentation, elongation is thought to increase the placental surface area, maximizing contact between the fetal chorion and uterus for efficient nutrient and gas exchange with the mother (Vallet et al., 2009; Bazer and Johnson, 2014). Elongation may also maximize conceptus uptake of uterine gland secretions (Bazer and Johnson, 2014).

Throughout the 114-day pregnancy in pigs, embryonic mortality is greatest at the time of elongation (Bazer and Johnson, 2014). This is referred to as early embryonic loss and can account for 30% of the potential litter (Bazer and Johnson, 2014). Because some conceptuses may elongate later than others as a result of differences in the timing of ovulation and or fertilization of the ova, it's hypothesized that smaller conceptuses are out competed by more advanced conceptuses for uterine space resulting in embryonic mortality (Vallet et al., 2002; Bazer and Johnson, 2014). A better understanding of factors controlling elongation, therefore, could lead to development of applications that reduce early embryonic loss.

Compared with elongation of the bovine and ovine conceptus, elongation of the pig conceptus is considered to be more rapid and extensive. Before elongation, pig conceptuses are first spherical and expand at a rate of 0.25 mm/h until approximately 9 mm in diameter (Geisert et al., 1982; Bazer and Johnson, 2014). Between d 11 and 12 of gestation the pig conceptus quickly becomes ovoid, tubular and then filamentous in morphology, elongating through the uterine lumen at a rate of 30 to 45 mm/h (Geisert et al., 1982). During rapid elongation and within 2 h, the pig conceptus transforms from a 10 X 10 mm sphere into a 1 X 200 mm thread like structure (Geisert et al., 1982; Bazer and Johnson, 2014). The pig conceptus will continue to elongate but more slowly between d 12 and 18 of gestation, simultaneously expanding within the uterine lumen and attaching to the uterine surface. By d 16, the pig conceptus can be over a meter in length but will occupy only 20 cm of uterine space due to extensive folding of the lumen (Engelhardt et al., 2002; Bazer and Johnson, 2014).

It's hypothesized that *IL-1β2*, a newly discovered IL-1 expressed by the pig conceptus, is essential for rapid elongation. Expression of *IL-1β2* transiently increases during rapid elongation and is synchronous with the formation of the filamentous conceptus (Tuo et al., 1996; Smith et al., 2001; Ross et al., 2003a; Tuggle et al., 2003). Expression of *IL-1β2* peaks at the height of the elongation and mRNA for *IL-1β2* is one the most abundant transcripts in the conceptus at that time (Smith et al., 2001; Ross et al., 2003b). Once rapid elongation is complete (d 12 of development), expression of *IL-1β2* decreases 2000 fold and is nearly undetectable thereafter (Ross et al., 2003a; 2003b; Tuggle et al., 2003). Intra uterine concentrations of *IL-1β2* protein are greatest during elongation, decrease after d 15 and reach a nadir by d 18 (Ross et al., 2003a). IL-1

signaling factors, *IL-1RI* and *IL-1RAP*, are also up regulated in the conceptus during elongation (Ross et al., 2003a). Interleukin-1 beta 2 may increase trophoblast and endodermal cell motility during this process. IL-1 is well known to increase cell motility through modification of actin filaments (Ma et al., 2014; Ferreira et al., 2012).

The discovery of interfering RNA (RNAi) and recent advances in the areas lentiviral mediated transgenics has lead to the development lentiviral mediated RNAi systems. Using these systems, both non-dividing and actively dividing mammalian cells can be targeted for infection, stable integration of viral DNA and constitutive expression of viral short hairpin RNAs (shRNA) that reduce (knockdown) endogenous mRNA translation through the mammalian microRNA (miRNA) pathway (Manjunath et al., 2009). A lentiviral mediated RNAi system was successfully used to target mRNA of the elongation factor Proline-Rich 15 (*PRR15*) in sheep conceptuses (Purcell et al., 2009). In pigs, lentiviruses were used to infect zygotes, integrating a GFP gene into the conceptus genome. Subsequent embryo transfer experiments with these conceptuses resulted in birth of 46 piglets, 30 of which expressed GFP based on western blot analysis (Hofmann et al., 2003).

In this study and similar to experiments conducted by Hofmann et al. (2003) and Purcell et al. (2009), we attempt to elucidate the role of a possible elongation factor in pigs by developing a lentiviral mediated RNAi system targeting *IL-1β2*, a novel IL-1 expressed by the elongating pig conceptus. To achieve this, we *in vitro* produced pig zygotes, microinjected the zygotes with control and *IL-1β2* knockdown lentiviruses and transferred these conceptuses to the oviducts of recipient pigs. We then removed the

reproductive tract on d 13 (after rapid elongation) to observe development of the conceptus.

MATERIALS AND METHODS

General Culture Conditions for the Baby Hamster Kidney-21 Cell Line

Baby hamster kindney-21 (BHK-21) cells were cultured in T-75 flasks with 20 mL of growth medium [modified MEM containing 10% fetal bovine serum (FBS; Gibco, Life Technologes) and 1% of 1 X antibiotic-antimycotic (Gibco, Life Technologies)] and incubated with 5% CO_2 and balanced air at 37°C. On the day of cell passage, growth medium was removed and cells (approximately 90% confluent) were washed with 10 mL of 1 X DPBS (Gibco, Life Technologies) before the addition of 3 mL of trypsin containing 0.25% EDTA (Gibco, Life Technologies) for 5 min. The trypsin was neutralized with the addition of 12 mL of growth medium. To pass the cells, 1 mL of neutralized cell solution was added to 14 mL of growth medium in new T-75 flasks.

General Culture Conditions for the Human Embryonic Kidney 293FT Cell Line

During general culture and unless specified by the BLOCK-iT Lentiviral Pol II miR RNAi Expression System kit, 293FT cells (Invitrogen) were maintained in a complete growth medium consisting of high glucose (25 mM) DMEM (Gibco; Life Technologies) containing 10% FBS and 1% Penicillin-Streptomycin (Gibco, Life Technologies) supplemented with 0.1 mM MEM Non-Essential Amino Acids (NEAA; Gibco, Life Technologies), 2 mM L-glutamine (Gibco, Life Technologies) and 1 mM

sodium pyruvate (Gibco, Life Technologies) with the addition of 500 μg/mL of Geneticin (Life Technologies). During cells passage, growth medium was removed and cells (approximately 90% confluent) were washed twice with 10 mL of 1 X DPBS before 2 mL of trypsin containing 0.25% EDTA was added to the cells for 5 min. To pass the cells, trypsin was neutralized with 8 mL of complete growth medium and 3 mL of neutralized cells were added to a new T-75 flask containing 15 mL of new complete growth medium. Cells were maintained at 37°C in 5% CO_2 and balanced air.

Constructs for Small Interfering RNA (siRNA) Luciferase Reporter Assays

In development of an interleukin-1 beta 1 (*IL-1β1*) and *IL-1β2* siRNA reporter assay, full-length cDNAs for *IL-1β1* and *IL-1β2* (see Chapter Three) were inserted into the psi-CHECK1 expression vector containing a luciferase reporter (C8011; Promega; Madison, WI). To insert *IL-1β2* into the psi-CHECK1 vector, 4 μg of the pCR 2.1-TOPO plasmid containing the *IL-1β2* sequence was partially digested with EcoR1 for 50 min at 37°C. For *IL-1β1*, 300 μg of the pCR-2.1 plasmid containing the *IL-1β1* sequence was partially digested with EcoR1 for 25 min at 37°C. The enzymatic reactions were inactivated by incubating the solutions at 65°C for 20 min. Within the pCR-2.1 plasmid, EcoR1 sites flank the *IL-1β2* and *IL-1β1* sequences. The psi-CHECK1 vector also has an EcoR1 site within its multiple cloning region [basepair (bp); 1636-1680]. To linearize the psi-CHECK1 vector, 1 μg of plasmid was digested with EcoR1 for 3 h at 37°C following the manufacturers recommendations. The *IL-1β2* and psi-CHECK1 digested sequences were then electrophoresed for 1 h through a 0.8% low melt agarose gel in 0.04 M Tris-Acetate and 0.001 M EDTA buffer with 0.5 μg/mL ethidium bromide at 80V. The *IL-1β2*

and psi-CHECK1 sequences were gel purified and *IL-1β2*, ethanol precipitated, and the psi-CHECK1 vector, dephosphorylated and phenol-chloroform extracted using standard procedures. For *IL-1β1*, the digestion was first electrophoresed through a 1.0% low melt agarose gel at 80V before *IL-1β1* was electrophoresed into DE81 grade Whatman chromatography paper for 4 min at 120V. The DNA was then displaced from the Whatman and phenol-chloroform extracted using standard procedures. The concentration of *IL-1β2*, *IL-1β1* and the psi-CHECK1 vector DNA was later determined by gel electrophoresis (concentration gel) also using standard procedures. To ligate *IL-1β2* into the psi-CHECK1 plasmid, 40 ng of linear psi-CHECK1 and 34 ng of *IL-1β2* were incubated together with T4 ligase at 4°C. For the *IL-1β1* ligation, 200 ng linear psi-CHECK1 and 175 ng of *IL-1β1* were used. The ligations were verified by gel electrophoresis before TOP-10 *E. coli* cells were transformed with the psi-CHECK1 vectors containing *IL-1β1* and *IL-1β2* and plated onto LB agar plates containing ampicillin (100 μg/mL). The cells were incubated overnight at 37°C before single colonies were picked and grown overnight in 3 mL of LB containing ampicillin (100 μg/mL), while shaking at 35°C. The plasmid DNA was then phenol-chloroform extracted and DNA sequenced at the University of Missouri DNA Core to verify sequence and orientation.

Interleukin-1 Beta 2 siRNA Luciferase Reporter Assays

Using the siRNA Target Designer program (Promega) eight 19 basepair (bp) oligonucleotides complimentary to the *IL-1β2* sequence were identified (Fig. 4.1). Longer oligonucleotides, containing these sequences, were designed to form a shRNA and

annealed to their complimentary oligonucleotides before inserted into the pGeneClip U1 (C8750; Promega) expression vector following the manufactures recommendations. Sequences complimentary to *IL-1β2* should reduce (knockdown) *IL-1β2/luciferase* mRNA and, therefore, decrease luciferase activity. BHK-21 cells, in 24 well plates and approximately 95% confluent, were simultaneously transfected with 2.5 μg of psi-CHECK1 vector containing either *IL-1β1* or *IL-1β2* and one of eight shRNA vectors (2.5 μg) in MEM (non-modified; see above for BHK-21 culture conditions) with the addition of the Transfast transfection reagent (E2431; Promega) following the manufacture's recommendations for adherent cells. The cells were allowed to incubate for 48 h in 5% CO_2 at 37°C. After the incubation, cells were lysed and assayed for luciferase activity using the Renilla Luciferase Assay System (E2820; Promega) and the Synergy HT multidetection microplate reader (BioTek). As a positive luciferase control, cells were simultaneously transfected with the psi-CHECK1 vector containing either *IL-1β2* or *IL-1β1* and a control plasmid incapable of producing a shRNA (pCR 2.1-TOPO containing the *IL-1β1* sequence). As a negative control, cells were not transfected with plasmid DNA. As a negative knockdown control, cells were also transfected with the psi-CHECK1 vector containing either *IL-1β2* or *IL-1β1* and the pGeneClip U1 vector containing scrambled oligonucleotides of the original *IL-1β2* knockdown sequences. Each knockdown and scrambled siRNA oligonucleotide was tested for its effects on *IL-1β1* and *IL-1β2*. Treatments within a plate were replicated in quadruplicate and each plate contained a positive control. The knockdown was replicated at least twice (i.e., each knockdown oligonucleotide was tested in at least two different plates). The knockdown luciferase activity was expressed as a ratio to the positive control within the plate (Table

4.1). The ratio was then tested by using the PROC GLM of SAS (SAS Inst.) with a model that included treatment. Least squares means (LSM) were separated by using the PDIFF procedure of SAS. Significance was declared at $P < 0.05$ (Table 4.1). To verify cell viability, MTT [3-(4,5-dimethylthiazol-2-yl)-2,5 diphenyl tetrazolium bromide] assays were also performed in duplicate as described in Beagin and Merkel, (2002). The optical densities and absorbance readings were calculated using Synergy HT multidetection microplate reader.

Lentiviruses

Lentiviruses were used to infect and stably integrate viral DNA, with the capacity to express a shRNA, into the porcine zygote genome. Based on the siRNA luciferase reporter assays, the viral shRNA containing the knockdown sequences have the capacity to target *IL-1β2* but not *IL-1β1* mRNA through the miRNA pathway. Two different lentiviruses (based on the manufacturer and method of production) were used during the lentiviral experiments: 1) Invitrogen lentiviruses, developed using the BLOCK-iT Lentiviral Pol II miR RNAi Expression System following the manufactures recommendations (K4938-00; Invitrogen, Life Technologies) and 2) Applied StemCell lentiviruses, developed by Applied StemCell Inc. using the Clontech pLVX-shRNA2 expression vector (632179, Clontech).

Invitrogen Lentiviruses

Briefly, to develop the Invitrogen lentiviruses, 64 bp oligos containing a 21 bp knockdown (Kd7 or Kd9) or scrambled knockdown (S6 or S9) sequence, an internal 19

bp loop sequence and a 19 bp sequence complimentarily to the knockdown or scrambled sequence (two nucleotides were omitted to create an internal RNA loop sequence to enhance miRNA knockdown efficiency) were annealed to their complimentary oligos (Table 4.2). The Invitrogen lentiviral kit required the addition of two extra bp in the original knockdown sequences (see Fig. 4.1). The double stranded DNA was then ligated into the pcDNA 6.2-GW/± EmGFP-miR plasmid downstream of the emerald green fluorescent protein (EmGFP) sequence (bp 713-1432). Plasmids that contain the knockdown sequences have the capacity to produce a miRNA targeting *IL-1β2*. As an infection positive control, the Invitrogen kit supplied a double stranded DNA, that when ligated into the pcDNA 6.2-GW/± EmGFP-miR plasmid, has capacity to produce a miRNA against *lacZ*. Subsequent recombination reactions between the pcDNA 6.2-GW/± EmGFP-miR (containing knockdown or scrambled knockdown sequences), pDONR 221 (donor vector) and the pLenti6/V5-DEST plasmids, following the manufactures recommendations, resulted in the development of pLenti6/V5-GW/EmGFP-miR knockdown or scrambled knockdown expression plasmids. These final plasmids were used to produce the lentiviral RNA.

293FT cells were cotransfected with a ViraPower Packaging Mix and one of five Lenti6/V5-GW/±EmGFP-miR expression vectors following the manufacture's recommendations. The pLenti6/V5-GW/±EmGFP-miR plasmid has the capacity to express a single viral RNA containing a Pol II-cytomegalovirus (CMV) promoter (bp 1809-2392), the *EmGFP* sequence, a sequence capable of producing a shRNA containing the knockdown or scrambled knockdown sequence and a blastocide S deaminase sequence (*bsd*; blasticidin resistance gene; bp 4724-5122). In the 293FT cells, vectors

supplied by the ViraPower Packaging Mix have the capacity to express viral proteins [gag, pol, rev and vsv-g (env)] needed to package and release a non-replicating infectious lentivirus containing the viral RNA. During infection, viral DNA can be stably integrated into the host's genome where *EmGFP* and a miRNA targeting *IL-1β2* can be constitutively expressed. As a positive virus control, lentivirus was generated by transfecting 293FT cells with the ViraPower Packaging Mix and the pLenti6/V5-GW/±EmGFP-miR-lacZ plasmid capable of expressing *EmGFP* and miRNA targeting the *lacZ*. As a negative virus control, 293FT cells were not transfected with DNA.

The 293FT cell medium, containing viruses or no viruses (medium alone; no transfection; negative virus control), was collected 72 h after cotransfection with DNA and centrifuged at 3000 rpm for 5 min at 4°C. The supernatant was filtered through a 0.45 μM low protein binding filter and viruses were concentrated using the Lenti-X concentrator (631231; Clontech) following the manufactures recommendations.

Five Invitrogen lentiviruses were developed: 1) a lentivirus capable of transducing a 21 bp miRNA sequence targeting region seven of *IL-1β2* (Invitrogen knockdown lentivirus 7; KdV7; Fig. 4.1), 2) a lentivirus capable of targeting region nine of *IL-1β2* (Invitrogen knockdown lentivirus 9; KdV9), 3) a knockdown control lentivirus capable of transducing a scrambled region six miRNA (Invitrogen scrambled lentivirus 6; SV6), 4) a control lentivirus capable of transducing a scrambled region nine miRNA (Invitrogen scrambled lentivirus 9; SV9) and 5) a transduction positive control lentivirus capable of transducing a miRNA sequence (5′-AAATCGCTGATTTGTGTAGTC-3′) targeting *lacZ* (Invitrogen positive control lentivirus; PosV). Complications occurred while producing

the scrambled region seven lentiviruses, therefore, SV6 was used as a scrambled control lentivirus.

To detect lentiviral infection, 293FT cells were incubated with the lentiviruses and observed under a Leica light microscope for expression of GFP. To do this, a single T-75 flask of 293FT cells was washed twice with 1 X DPBS and trypsinized. Complete medium (without geneticin), containing approximately 5.4 X 10^5 cells, was added to 24 well plates with round 12 mm glass cover slips (Fisher) on the bottom. In duplicate, viruses were added to the wells (1:100 dilution) and allowed to incubate overnight under standard culture conditions. For the negative controls, two wells received cells only and two wells received medium collected from 293FT cells not transfected with DNA (no virus control; see above). Lentivirus stock and negative control solutions were stored in cryovials at -80°C in 10 μL aliquots. The next day, medium (containing lentiviruses) was removed from the wells and replaced with 1 mL of complete medium without geneticin. The next morning, cover slips (containing adhered cells) were placed facedown onto frosted white microscope slides and multiple pictures were taken of the cells with a leica microscope capable of detecting fluorescence (Fig. 4.2).

Invitrogen Lentiviral Titer

Viral infectious units (IFU) were measured using a blasticidin selection method following recommendations provided by the Invitrogen kit. The day before transduction, a single T-75 flask of 293FT cells were trypsinized, diluted in complete medium, plated into multiple 6 well plates and incubated overnight at 37°C in 5% CO_2 and balanced air (standard culture conditions). The next day, five 10-fold serial dilutions of each lentivirus

(10^{-3} to 10^{-7}) were prepared in complete medium, old medium was removed from the wells containing the 293FT cells (approximately 30 to 50% confluent) and medium containing diluted virus (i.e. one virus at five dilutions/plate) was added. The sixth well in the plate received medium alone. The 293FT cells incubated in the viral solutions overnight under standard culture conditions (see above). The next day, the medium was removed from the wells and replaced with 2 mL of fresh complete medium. Again, cells were cultured overnight in standard culture conditions. The next morning, old complete medium was removed and cells received new complete medium containing 10 μg/mL of Blasticidin (K4938-00; Invitrogen). The cells continued to grow under standard culture conditions for the next twelve days. New complete medium, containing 10 μg/mL blasticidin, was added to the cells every four days. After twelve days of selection, cells were washed twice with 1 X DPBS before 1 mL of crystal violet solution (F907-3; Baker Chem. Co.) was added for 10 min at room temperature. After removing the staining solution, the wells were washed repeatedly with 1 X DPBS and the cell colonies counted. The IFU was calculated based on the number of growing colonies within the wells as described by the Invitrogen Kit. The KdV7 and KdV9 titers were 31.5×10^4 IFU/mL and 28.5×10^4 IFU/mL, respectively. The SV6 and SV9 titers were 49.5×10^4 IFU/mL and 23.5×10^4 IFU/mL, respectively. The PosV titer was 2.5×10^5 IFU/mL.

Applied StemCell Lentiviruses

For the Applied StemCell lentiviruses, all viral constructs were developed, viruses packaged and viral infections units (IFU) calculated by Applied StemCell Inc. The Applied StemCell lentiviruses were packaged within 293FT cells and concentrated in 1 X

PBS supplement with FBS (10%) using a 2nd generation packaging system. In this system, cells were transfected with the pLVX-shRNA2 (632179; Clontech) expression and psPAX2 and pMD2.G packaging vectors, respectively (12260 and 12259, respectively; Addgene). In development of the expression plasmid, 65 bp oligos containing a 19 bp knockdown or scrambled sequence, a 10 bp loop sequence and 19 bp sequence complementary to the siRNA sequence (Table 4.3) were annealed together and inserted into the pLVX-shRNA2 plasmid multiple cloning site (bp 2440-2457). The pLVX-shRNA2 expression vector has the capacity to express a single viral RNA containing a Pol III-human U6 promoter (P_{U6}; bp 2187-2444), a sequence that can form a shRNA containing a 19 bp knockdown or scrambled knockdown sequence, a human CMV immediate early promoter sequence (bp 2462-3050) and an enhanced green fluorescent protein (GFP) sequence (*ZsGreen1*; bp 3074-3769) in the 293FT cells. Plasmids psPAX2 and pMD2.G have the capacity to express viral proteins [Gag, Pol, Rev and VSV-G (Env)] needed to package and release non-replicating infectious Applied StemCell lentiviruses from the 293FT cells. The lentiviral titer (IFU) was determined by Applied StemCell Inc. using the Lenti-X qRT-PCR titration kit (631235; Clontech). Four lentiviruses were provided by Applied StemCell: 1) a lentivirus capable of transducing a 19 bp miRNA sequence targeting region seven of *IL-1β2* (Applied StemCell knockdown lentivirus 7; KdV7), 2) a lentivirus capable of transducing a 19 bp sequence targeting region nine of *IL-1β2* (Applied StemCell knockdown lentivirus 9; KdV9), 3) a knockdown control lentivirus capable of transducing a scrambled *IL-1β2* region seven sequence (Applied StemCell scrambled lentivirus 7; SV7) and 4) a knockdown control lentivirus capable of transducing a scrambled *IL-1β2* region nine sequence (Applied

StemCell scrambled lentivirus 9; SV9). The KdV7 and KdV9 titers were 2.16 ± 0.29 x 10^9 IFU/mL and 3.52 ± 1.17 x 10^9 IFU/mL, respectively. The SV7 and SV9 titers were 1.39 ± 0.26 x 10^9 IFU/mL and 2.50 ± 0.52 x 10^9 IFU/mL, respectively. Over night and on dry ice, viruses were shipped from Applied StemCell Inc. to the lab in five 20 μL aliquots/virus. Once in the lab, viruses were removed from the dry ice and immediately placed in a -80°C freezer.

Production of Pig Zygotes for Lentiviral Infection

Oocytes were aspirated from follicles of pre-pubertal gilts and *in vitro* fertilized as described by Lee et al. (2013) and Hamm et al. (2014). Porcine ovaries were collected from an abattoir (Farmland Foods Inc., Milan, MO) and transported in plastic containers at room temperature to the University of Missouri Animal Sciences Research Center (ASRC). Medium-sized follicles (3-6 mm) were aspirated with an 18 g short bevel needles attached to a syringe. The follicular fluid was aliquoted into 50 mL conical tubes. After a pellet (containing oocytes) accumulated at the bottom of the tube the overlaying solution was drained and the pellet was washed three times with a polyvinyl alcohol-Tyrodes lactate (PVA-TL)-HEPES [4-(2-hydroxyethyl)-1-piperazineethanesulfonic acid] solution consisting of 114.01 mM NaCl, 2mM $NaHCO_3$, 340.06 μM NaH_2PO_4, 3.2 mM KCl, 1.868 mL sodium DL-lactate solution (60%), 2 mM $CaCl_2$, 426.77 μM HEPES, 1.07 μM PVA, 12 mM sorbitol, and 249.83 μM pyruvate. After the third wash, the pellet was re-suspended in 40 mL of PVA-TL-HEPES and the entire solution was transferred to multiple 100 X 15 mm petri dishes. Oocytes were then selected for maturation if they had an evenly distributed dark cytoplasm and were surrounded by multiple layers of cumulus

cells (cumulus oocyte complex; COC). The COCs were placed in 500 μL of maturation medium consisting of TCM 199 (Invitrogen) with 3.05 mM glucose, 0.91 mM sodium pyruvate, 0.57 mM cysteine, 10 ng/mL epidermal growth factor (EGF), 0.5 μg/mL luteinizing hormone (LH), 0.5 μg/mL follicle stimulating hormone (FSH), 10 ng/mL gentamicin and 0.1% polyvinyl alcohol for 42-44 hr at 38.5°C in 5% CO_2 and humidified air.

After maturation, the cumulus cells were removed from the oocytes by vortexing the COCs for 4 min at a medium speed in a 0.1% hyaluronidase solution. The oocytes were then placed in manipulation medium (TCM199 with 0.6 mM $NaHCO_3$, 2.9 mM HEPES, 30 mM NaCl, 10 ng/mL gentamicin, and 3 mg/mL of bovine serum albumen (BSA) and selected for fertilization. Oocytes with a polar body between the plasma membrane and perivitelline space (metaphase II; MII), an evenly distributed cytoplasm and round zona pellucida were selected. The 20-30 selected oocytes were placed in 50 μL of *in vitro* fertilization (IVF) medium [a modified tris buffer medium (MTBM) consisting of 113.1 mM NaCl, 3.0 mM KCl, 7.5 mM $CaCl_2$, 11 mM glucose, 20 mM tris, 5 mM sodium pyruvate, 0.05 mg/mL gentamicin, 0.664 mM caffeine and 2 mg/mL of BSA] and each group was covered in mineral oil. Frozen semen from a single boar was thawed, washed and finally, diluted in IVF medium (0.5×10^6 cell/mL) before 50 μL was added to each group of oocytes. Sperm and oocytes were incubated together for 4-5 h at 38.5°C in an atmosphere of 5% CO_2 in air. After fertilization, the IVF-derived pig embryos were cultured overnight in 4 well plates (50/well) containing University of Missouri-1 (MU-1; Bauer et al., 2011) medium at 38.5°C in 5% CO_2 in humidified air.

Conceptus Microinjection with Lentiviruses (Invitrogen and Applied StemCell)

The next morning, the lentiviral solutions in cryovials were removed from the -80°C freezer and placed on ice. In preparation for microinjections, viruses and pig zygotes (in four well plates) were transported (5 min walk) in separate Styrofoam containers (the viral container contained ice) to a BSL-2 laboratory at the University of Missouri, College of Veterinary Medicine. There, the zygotes were place in an incubator at 38.5°C in 5% CO_2 and balanced air until microinjection. The *IL-1β2* knockdown viral solutions were mixed [KdV7 and KdV9 for microinjections with Invitrogen or Applied StemCell lentiviruses (treatment Invitrogen KdV or Applied StemCell KdV)] and the combined solution centrifuged at 14,000 rpm for 1 min. All zygotes from one well (approximately 50) were placed in micromanipulation medium, covered in mineral oil and microinjected between the perivitelline space and plasma membrane using an immobilizing holding pipette and microinjection pipette (2-5 μm inner diameter) loaded with the mixed viral solution using an NK 2 micromanipulator (Eppendorf) and Eclipse TE-200 microscope (Nikon). Each zygote received approximately 100-200 pL of viral solution. The microinjected zygotes were transferred back to their wells (containing MU-1 medium) and placed back in the incubator. As a control, another group of zygotes (approximately 50) were microinjected with a mixed solution of scrambled knockdown sequence viruses [SV6 and SV9 for Invitrogen lentiviruses (treatment Invitrogen SV) and SV7 and SV9 for Applied StemCell lentiviruses (treatment Applied StemCell SV)]. As a non-injected control, another group of zygotes were never removed from the four well plate and were not microinjected (treatment no virus; NV). Groups of zygotes were microinjected one at a time and immediately transferred back to their original well in the

four well plate after each treatment. The process took on average 30 min/treatment. The remaining mixed viral solutions were aliquoted (5 μL) into 0.2 mL tubes and re-frozen at -80°C.

Conceptuses and Invitrogen lentiviruses

Invitrogen lentiviruses were used to infect pig zygotes. Five microinjection sessions (MS; 1-5; Table 4.4) and two embryo transfers (ET; 1-2) were performed using the Invitrogen lentiviruses. After microinjection, conceptuses remained in culture at the University of Missouri, College of Veterinary Medicine in an incubator at 38.5°C in 5% CO_2 and balanced air until d 4 of development (ET) or d 6 of development (*in vitro* culture). On the morning of transfer, conceptues were brought back to ASRC and visualized for GFP expression using the DIAPHOT 300 microscope (Nikon) capable of detecting fluorescence. If conceptuses were not transferred they were checked for GFP on d 4 of development at the College of Veterinary Medicine using the Eclipse TE-200 microscope (Nikon) capable of detecting fluorescence and on day 6 conceptuses were transferred back to ASRC. There, pictures of fluorescent conceptuses were taken at a 100 X magnification using the Eclipse Ti microscope (Nikon). The number of conceptuses that developed to blastocyst on d 6 in each treatment was recorded. When possible, blastocysts were collected and snap frozen for RNA extraction and detection of *EmGFP*, *IL-1β2*, and *ACTβ* using RT-PCR followed by gel electrophoresis (see below). After MS 1, ten blastocyst from the NV and ten blastocysts from the Invitrogen KdV treatments were pooled, snap frozen in 1.5 mL eppendorf tubes containing 100 μL of lysis buffer [supplied by the Dynabeads DIRECT kit (Invitrogen); see below] and stored at -80°C

until RNA extraction. After MS 2, five blastocyst from the NV and five blastocysts from the Invitrogen SV treatments were pooled and snap frozen in lysis buffer.

Conceptuses and Applied StemCell Lentiviruses

Applied StemCell Lentiviruses were also used to transduce pig zygotes. In total, eight MS (6-13; Tables 4.5 and 4.6) and eight ET (3-10) were performed. After microinjections, conceptuses were brought back to ASRC and incubated at 38.5°C in 5% O_2, 5% CO_2 and nitrogen balance in humidified air until d 4 of development (embryo transfer) or d 6 or d 8 of development (*in vitro* culture). On the morning of transfer, conceptuses were visualized for GFP using the DIAPHOT 300 microscope (Nikon) capable of detecting fluorescence. As a preliminary study, conceptuses were microinjected with lentiviruses and cultured *in vitro* until d 6 of development, after which the number of blastocysts in each treatment was recorded, the blastocysts were checked for GFP and pictures were taken (40 X and 100 X) of the conceptuses using the Eclipse Ti microscope (Nikon) (MS 6; Table 4.6). Individual GFP positive blastocysts were collected (three from each treatment; NV, Applied StemCell SV and Applied StemCell KdV), snap frozen in 1.5 mL eppindorf tubes containing 100 µL of lysis buffer (Invitrogen), and stored at -80°C until RNA extraction (see below). Using RT-PCR, conceptuses were measured for expression of *ZsGreen1GFP*, *ACTβ*, and *IL-1β2* (see below). For conceptuses cultured until d 8 of development (extended culture; MS 11-13; Table 4.6) on d 6 GFP was visually detected and the number of blastocysts in each treatment was recorded. FBS was then added to the culture medium (10%). The number

of hatched blastocysts were recorded on d 8 and when possible, individual conceptuses were collected, snap frozen and stored at -80°C.

Embryo Transfer

Embryo transfers were performed at the University of Missouri swine complex as previously described (Ross et al., 2012). At the complex, gilts were monitored for estrus daily. Gilts between d 3 and 5 of the estrous cycle were chosen for ET. Briefly, on the morning of transfer, a single oviduct was exposed by mid ventral laparotomy. Approximately 20 to 50 pig conceptuses (d 4 of development) were transferred through the infundibulum and released into the ampullary-isthmus junction using a transfer pipette. Gilts received conceptuses from a single treatment [i.e. one treatment per gilt; NV, KdV or SV (Invitrogen or Applied StemCell)].

Uterine Tissues

Embryos were flushed from the uterine horns as previously described by Mathew et al. (2011). Nine days after the embryo transfer (d 13 of development), the gilts were euthanized at the University of Missouri Veterinary Medicine Diagnostic Laboratory (VMDL) and the reproductive tract was removed and placed on ice. Within minutes of euthanasia, the reproductive tract was brought to the laboratory (5 min walk), the ovaries were removed and CL counted. The broad ligament was dissected away and the uterus was washed with ice-cold saline. Hemostats were used to clamp the uterine horns near the uterine body and both horns were removed. The oviducts were partially removed and each uterine horn, still clamped at the base, was infused with of 40 mL of ice cold 1 X

DPBS through the utero-tubule junction using a needle and syringe. To collect conceptuses, the DPBS was massaged through the uterine horn and released back out the utero-tubule junction into a 100 mL petri dish.

Uterine Flushings

Pictures were taken of flushings containing conceptuses or conceptus fragments that were then counted and measured (diameter) using a calibrated eyepiece micrometer. Conceptus tissues were mounted onto microscope slides using 1 X DPBS and pictures were taken at various magnifications using a Leica microscope capable of detecting expression of GFP. When possible, conceptus tissues were collected and snap frozen in liquid nitrogen and stored at -80°C. Some tissues were stained with DAPI and pictures of fluorescent nuclei were taken using the Leica microscope. Uterine flushings from both horns were centrifuged at 1,500 rpm for 10 min and the supernatant was collected and snap frozen before stored at -80°C.

Conceptus RNA Extraction, cDNA Production and real-time RT-PCR

RNA was extracted from elongated conceptuses (MS 5) and cDNA was reversed transcribed and RT-PCR were performed as described in Chapter Three. RNA was extracted from pooled blastocysts (MS 1-2) or individual blastocysts (MS 6) as described by Huffman et al. (2012). During extraction of blastocyst RNA, embryos in lysis buffer were removed from the -80°C freezer and thawed. To control for variation in RNA extraction between samples for single blastocyst, each sample was spiked with 1 μL of diluted (1 ng/mL) maize aquaporin mRNA (zea mays NIP3-1; *ZmNIP3-1*) mRNA. RNA

was then isolated from the blastocysts using the Invitrogen Dynabeads DIRECT kit following the manufacturer's recommendations. A negative control sample (Blank; lysis buffer only) was included with each extraction. Reverse transcription of mRNA to cDNA was achieved using the High-Capacity cDNA Reverse Transcription Kit following the manufacturer's recommendations (4368814; Applied Biosystems). For each mRNA sample (10 μL), a 20 μL reverse transcription (RT) reaction was prepared with the High Capacity cDNA RT kit master mix with the addition of an RNase inhibitor (RNaseOut; 10777-019; Invitrogen). The real-time RT-PCR were performed as in Chapter Three for elongated conceptuses and blastocysts (see standard procedures). Primer sets for *IL-1β2* and *ACTβ* were designed based on published porcine nucleotide sequences within GenBank (see Chapter Three, materials and methods section ribonuclease protection assays and Table 3.1, respectively). The average amplification efficiencies were 2.52 and 1.88 for *IL-1β2* and *ACTβ*, respectively. Primer sets for *EmGFP*, *ZsGreen1GFP* and *ZmNIP3-1* were designed based on sequences provided by Invitrogen, Clontech and published maize nucleotide sequences within GenBank, respectively. The forward and reverse primer sequences were 5′-ACGTAAACGGCCACAAGTTC-3′ and 5′-AAGTCGTGCTGCTTCATGTG-3′, respectively, for *EmGFP* and 5′-CCCCGTGATGAAGAAGATGA-3′ and 5′-GTCAGCTTGTGCTGGATGAA-3′, respectively, for *ZsGreen1GFP*. The forward and reverse primer sequences were 5′-TTCAACCTCCTCTTCGTCGT-3′ and 5′-CCAGCAGGTAGATCCAGAGC-3′, respectively, for *ZmNIP3-1*. The RT-PCR were prepared with 1 μL of cDNA sample and the products were DNA sequenced to verify amplification of the target sequence. For single blastocysts, fold changes in gene expression for all genes were normalized to fold

changes in control gene *ZmNIP3-1*. Amplification of desired sequences were verified by gel electrophoresis (4 μL of RT-PCR reaction; all samples) and sequencing of the amplicons at the University of Missouri DNA core (see Chapter Three, standard procedures).

Statistics

A Chi-square test was used to assess differences between treatments NV and V (KdV and SV combined) and KdV and SV for the percentage of blastocysts that developed on d 6 using the Proc Freq procedure of the Statistical Analysis System SAS (SAS institute Inc. Cary, NC, USA). This was done for both the Invitrogen (Table 4.4) and Applied StemCell lentivirus infected conceptuses (Tables 4.5 and 4.6 combined). The level of significance was set at $\alpha = 0.05$. Fold change over medium control for individual blastocyst (MS 6) gene expression was analyzed using the general linear models (GLM) procedure of SAS. The model statement included an effect treatment. Least squares means (LSM) and standard errors were generated using the LSMeans statement of SAS. All reported means are the adjusted LSM ± standard error of the least squares means (SEM) and the significance was declared when $P < 0.05$.

RESULTS

Invitrogen lentiviruses (MS 1-5 and ET 1-2)

Microinjection of early pig conceptuses with the Invitrogen lentiviruses (KdV and SV) resulted in a reduction in the number of blastocysts that developed *in vitro* when compared with NV control conceptuses (Chi-square test, $P < 0.001$; Table 4.4). There

was no difference in the number of blastocyst that developed in the KdV-treated conceptuses compared with the SV treated conceptuses. There was a reduction in the capacity to detect GFP by using fluorescent microscopy in the microinjected conceptuses over time (Table 4.4). Although the lentiviral solutions were filtered (see development of Invitrogen lentiviruses), formation of particulates in the viral solutions that clogged the microinjection pipette resulted in complications during the MS. Unsuccessfully, we attempted to centrifuge the viral solutions before microinjection (MS 2-5) and microinject early cleavage (2-4 cell) pig conceptuses (MS 4) to reduce clogging of the pipette and increase conceptus transduction, respectively. Invitrogen lentiviruses were not used for further experiments after MS 5.

Microinjection Session 1. Twelve and ten conceptuses developed into blastocysts out of fifty that did not receive virus (NV) and fifty that were microinjected with KdV, respectively (Table 4.4). None of the NV blastocysts and most (~ 90%) of the blastocysts in KdV treatment expressed GFP (Fig. 4.3A). Ten blastocysts from the NV treatment and all of the blastocyst from the KdV treatment were collected and measured for expression of *IL-1β2* and *ACTβ*. RT-PCR results indicated that KdV blastocysts had less *IL-1β2* and *ACTβ* compared with NV blastocysts (Fig. 4.3B and 4.3C).

Microinjection Session 2. Eight and five conceptuses developed into blastocyst out of 20 conceptuses that did not receive virus (NV) and 40 that were microinjected with the SV, respectively (Table 4.4). None of the conceptuses that received the KdV (n=20) developed into blastocysts. The SV blastocysts expressed GFP (Fig. 4.4A). Five

blastocysts from the NV treatment and all of the blastocyst from the SV treatment were collected and measured for expression *IL-1β2* and *ACTβ*. Expression of *IL-1β2* and *ACTB* was greater and less, respectively, in SV blastocysts when compared to NV blastocysts (Fig. 4.4B and 4.4C).

Microinjection Session 5 and Embryo Transfers 1-2. One hundred pig zygotes were microinjected with the SV and KdV in preparation for ET. Forty-two pig conceptuses (d 4 of development) from the SV and KdV treatments were transferred to the oviduct of two gilts. Nine days later (d 13 of development), the uterine horns were flushed. Only tissue fragments (≤ 2 mm in diameter) were flushed from the gilt that received the SV conceptuses, however, 2 elongated conceptuses were flushed from the KdV gilt (Table 4.4 and Fig. 4.5A). Expression of GFP could not be verified in the elongated conceptus tissues using fluorescent microscopy but was later verified for *GFP* by PCR and gel electrophoresis (Fig 4.5G). Compared with *in vivo* derived d 12 elongated pig conceptuses (see Chapter Three), expression of *IL-1β2* and *ACTβ* in the elongated KdV conceptuses was less (Fig. 4.5E and 4.5F).

Applied StemCell lentiviruses (MS 6-13 and ET 2-10)

Overall, similar to the Invitrogen lentiviruses, microinjections of early pig conceptuses with the Applied StemCell lentiviruses (KdV and SV) resulted in a reduction in the number of conceptuses that developed into blastocysts compared with NV controls conceptuses (Chi square test, $P < 0.001$; data from Table 4.5 and Table 4.6 combined). Again, there was no difference in the number of blastocyst that developed in the KdV

treated conceptuses compared with the SV treated conceptuses (data from Table 4.5 and Table 4.6 combined). Unlike the Invitrogen lentiviruses, there was not a reduction in GFP (Tables 4.5 and 4.6 combined).

Microinjection Session 6. Before the ET experiments, a preliminary study was conducted to determine the level of *IL-1β2* knockdown achieved in pig conceptuses microinjected with the Applied StemCell lentiviruses. During the study, zygotes were not treated (NV), treated with SV or treated with KdV (100, 47 and 49 zygotes, respectively). Twelve conceptuses in the NV treatment developed to blastocyst and three conceptuses in both the SV and KdV treatments developed to blastocyst. By microscope, GFP could be detected in all six blastocysts produced from the SV and KdV treated conceptus (Fig. 4.6). Three blastocysts from each treatment were individually measured for expression of *IL-1β2* and *ACTβ* using RT-PCR followed by gel electrophoresis. Interleukin-1 beta 2 was undetectable ($C_t > 39$) in all three KdV blastocysts and could be detected in two of three SV and NV blastocysts (Fig. 4.7A), however, there was not an effect of treatment on fold change in gene expression of *IL-1β2*. There was a tendency for an effect of treatment on expression of *ACTβ* ($P = 0.0712$). Expression of *ACTB* was less in SV blastocyst when compared to NV controls (Fig. 4.7B; $P < 0.05$).

Microinjection Sessions 7-10 and Embryo Transfers 3-10. During embryo transfer experiments with the Applied StemCell lentiviral treated conceptuses, three of eight gilts produced conceptuses on d 13 of pregnancy. One gilt received NV embryos and produced normal elongated conceptuses on d 13 (MS 9; Fig. 4.8). Two gilts received the KdV

embryos, both of which produced abnormal (spherical; ≤ 6 mm) conceptuses on d 13 (MS 7-8; Fig. 4.9). All gilts (n=5) that received SV embryos produced nothing at all or produced what appeared to be fragments of conceptus tissues by d 13, some of which appeared to express GFP and had a poly lobular appearance (MS 7-10; Fig. 4.10 and Fig. 4.11).

Because the concentration of infections units (10^9) within the Applied StemCell lentiviral solution could have a negative impact on conceptus development, during MS 10, conceptuses were microinjected with SV at two different dilutions in 1 X DPBS (10^8 and 10^7 infectious units, respectively; 50 conceptuses per dilution). On the day of transfer (d 4 of development), GFP could not be detected by microscope in the microinjected conceptuses, however, 30 conceptuses, microinjected with diluted SV (10^8), were transferred to a recipient gilt. Nine days later, fragments resembling conceptus tissues, some of which appeared to express GFP, were flushed from the uterine horns (Fig. 4.11D-F).

Microinjection Sessions 11-13

Failure of SV conceptuses to survive embryo transfers resulted in termination of *in vivo* experiments. Further experiments, using the Applied StemCell lentiviruses (MS 11-13), were conducted to monitor blastocyst development and hatch rate of NV and lentivirus treated (KdV and SV) conceptuses *in vitro*. Statistically, there was not a difference in the number of conceptuses that became blastocysts or hatched blastocyst between the KdV and SV treatments, however, SV conceptuses numerically produced fewer blastocysts and fewer hatch blastocysts on d 6 and d 8 of development,

respectively, when compared to KdV conceptuses (Table 4.6) and the study was concluded.

DISCUSSION

This study was designed to examine the role of *IL-1β2*, a novel IL-1, in elongation of the early pig conceptus. Elongation occurs near d 11 of development in the pig and is considered necessary for establishment of pregnancy (Geisert et al., 1982; Bazer and Johnson, 2014). It allows for efficient uptake of uterine gland secretions that aid in development of the conceptus and expands the surface area of the placental unit for nutrient and gas exchange along the fetal-maternal interface (Vallet et al., 2002; 2009; Bazer and Johnson, 2014). Complications during this process and elongation asynchrony between conceptuses are hypothesized to reduce litter sizes in pigs (Vallet et al., 2002). Factors controlling elongation, a process that does not occur ex utero, have not been identified (Vallet et al., 2009).

Rapid elongation of the pig conceptus is achieved through modifications of the endoderm and trophoblast. The cellular processes associated with elongation were characterized by Geisert et al. (1982) and reviewed by Bazer and Johnson (2014). During elongation, the blastocyst decreases proliferation by 40% and the trophoblast and the extra embryonic endodermal cells migrate, through the use of filapodia, toward the inner cell mass (ICM; embryo proper). There, the trophoblast and underlying endodermal cells on both sides of the ICM change shape and extend in opposite directions forming what is referred to as the “elongation zone”. Along the zone, the trophoblast cells condense and

become columnar in shape as a result of modifications made to cellular microfilaments and junctional complexes. The endodermal cells also condense along the elongation zone and have extensive surface microvilli. Continued extension of the zone drives elongation of the conceptus.

Conceptuses up regulate *IL-1β2* and IL-1 signaling components, *IL-1RI* and *IL-1RAP*, at the time of elongation, suggesting that *IL-1β2* plays a critical autocrine role in the process of elongation (Ross et al., 2003a). Interleukin-1 beta 2 signaling may promote actin filament modifications in the trophoblast, thereby enhancing trophoblast cell motility during formation of the elongation zone. Interleukin-1 has been shown to increase motility of brain cortical neurons, airway epithelial cells, neutrophils, tumor cells and microglia cells through modifications made to cell integrins and actin filaments (Ferreira et al., 2012; Ma et al., 2014)

Previously, lentiviruses were used to knockdown expression of an elongation factor in sheep conceptuses and in one study, to produce transgenic pigs (Hofmann et al., 2003; Purcell et al., 2009). Similar to the study by Purcell et al. (2009), we developed a lentiviral mediated RNAi system targeting *IL-1β2*, a possible elongation factor, in early pig conceptuses. We then microinjected pig zygotes with the viruses and transferred the conceptuses to the oviduct of recipient pigs. On d 13 of development, approximately two days after initiation of elongation, we removed the reproductive tract and flushed the uterine horns to observe development of the conceptuses.

After performing five embryo transfer experiments, which involved the transfer of 198-control virus (SV) infected conceptuses into the oviducts of recipient gilts; we were unable to collect normal elongated conceptuses on d 13 of development in this treatment.

Besides two Invitrogen KdV treated conceptuses (Table 4.4 and Fig. 4.5A) only *in vitro* produced conceptuses, not microinjected with the lentiviruses (no virus; NV), elongated while in utero. Abnormal spherical conceptuses were flushed from two gilts that received conceptuses microinjected with the Applied StemCell *IL-1β2* knockdown lentiviruses.

To the best of our knowledge, only one study has reported using sub zonal microinjections of lentivirus to infect pig conceptuses with subsequent transfer of conceptuses to the oviduct of recipient pigs. In this study, Hofmann et al. (2003) microinjected early pig conceptuses with the lentiviruses in an attempt to produce transgenic animals. After six embryo transfers, Hofmann et al. (2003) reported the birth of 46 piglets, 30 of which expressed the GFP transgene based on western blot analysis. They reported no significant differences between the number of pregnancies derived from transfers of virus-injected and control (buffer-injected) conceptuses (Hofmann et al., 2003).

Our study was carried out similarly to Hofmann et al. (2003) with a few exceptions. In the study by Hofmann et al. (2003), superovulated and inseminated gilts (6 months of age) were used to collect *in vivo* produced pig conceptuses for the microinjections rather than *in vitro* produced pig conceptuses. The gilts were slaughtered 36 hours after first insemination and conceptuses were flushed from the oviduct with pre-warmed (38°C) PBS supplemented with lamb serum (20%) and 50 mg gentamicin sulphate before they were used directly for sub-zonal injections with concentrated lentiviruses (10^{10}-10^{9}) (Hofmann et al., 2003). Further, in the study by Hofmann et al. (2003), they used pre pubertal, synchronized gilts, as recipients rather than naturally

cycling gilts and transferred conceptuses (30-40) to the oviduct by laparoscopy rather than laparotomy.

The differences between our experiments and those described by Hofmann et al. (2003) with respect to the production of conceptuses and embryo transfer procedures do not explain our inability to produce normal pregnancies from gilts receiving conceptuses treated with control viruses. In the one gilt that received non-injected or no virus (NV) *in vitro* produced conceptuses, she maintained a normal pregnancy and produced elongated conceptuses on d 13. However, Hofmann et al. (2003) used lentiviruses to promote transgenics alone and not RNAi. The observation that our lentivirus-infected conceptuses were less likely to become blastocysts (KdV and SV) and had a significant reduction in *ACTβ* expression (SV conceptuses) suggests that the type of lentiviruses used during our experiments had an overwhelming negative effect on development that could not be overcome by d 13 (MS 6; Fig. 4.7B). For instance, it's possible that our KdV and SV sequences may have targeted mRNAs of developmentally important proteins, other than *IL-1β2*, resulting in compromised embryonic development (Manjunath et al., 2009). Other groups have experienced similar complications when using lentiviral directed RNAi in sheep conceptuses (verbal communicated with Dr. Thomas Spencer; Washington State University).

Some conceptuses in the KdV and SV treatments may not have been successfully infected with the lentiviruses during the MS and should theoretically develop normally in utero along side developmentally abnormal conceptuses. It's possible that the lentivirus treatments had an overall negative effect on the uterus and therefor resulted in complete pregnancy failure. Out of nine embryo transfers that included transfer of 280 KdV or SV

conceptuses, only two conceptus of normal morphology (elongated) were recovered (MS 5; Table 4.4 and Fig. 4.5B). Pig uteri are extremely sensitive to inflammatory stimuli and its possible that viral factors, such as proteins or nucleic acids, transferred along with conceptuses or released from healthy or dying conceptuses while in utero resulted in an exacerbated inflammatory response within the endometrium and complete pregnancy failure. While flushing uteri of gilts that received KdV or SV conceptuses, we noted that some reproductive tracts had an abnormal coloration and texture that may have been associated with a strong inflammatory response.

As an alternative to lentiviral mediated RNAi, the CRISPR/Cas9 system in combination of somatic cell nuclear or *in vitro* produced pig zygotes could be used to efficiently produce pig conceptuses with bi allelic ablation (knockout) of *IL-1β2* (Whitworth et al., 2014; Sander and Joung; 2014). Implementation of embryo transfer and uterine flushing experiments with the *IL-1β2* knockout conceptuses could potentially reveal the function of *IL-1β2* during elongation without the risk of negative effects triggered by the RNAi pathway or lentiviruses.

Although we were unable to test the hypothesis that *IL-1β2* is involved in elongation of the early pig conceptus, RT-PCR analysis revealed that *IL-1β2* is expressed in d 6, *in vitro* produced, pig blastocyst, suggesting that this cytokine may control important developmental processes prior to elongation. Further, because *IL-1β2* is highly up regulated during trophoblast expansion and elongation of the conceptus and because porcine fibroblast cells with an induced trophoblast (iTR) phenotype express an *IL-1β*, expression of *IL-1β2* is thought to be trophoblast lineage specific (Ross et al., 2003a; Ezashi et al., 2011). Observation made during our experiments may further support this

theory as some, but not all, NV or SV blastocysts expressed *IL-1β2* on d 6 (Fig. 4.7C), a time closely associated with differentiation and formation of the trophoblast lineage.

SUMMARY AND CONCLUSION

Near d 11 of gestation, pig trophoblast cells rapidly migrate and change shape, resulting in extensive remodeling and elongation of the early pig conceptus. Elongation increases the uterine surface area occupied by the conceptus, enhancing fetal-maternal exchange. Interleukin-1 beta 2, a novel IL-1, is highly up regulated in the conceptus during elongation and is hypothesized to play a critical role in this process. To test this hypothesis, we developed a lentiviral mediated RNAi system to specifically target *IL-1β2* in early pig conceptuses. Microinjections of pig zygotes with knockdown (KdV) and control (SV) viruses resulted in a reduction of the number of conceptuses that developed into blastocysts *in vitro* and significantly reduced expression of *ACTβ* in the SV blastocyst compared to conceptuses that did not receive virus (NV). Transfer of control SV conceptuses into the oviduct of recipient gilts on d 4 resulted in complete reproductive failure in all gilts by d 13 of pregnancy. Therefore, using lentiviral mediated RNAi technology; we were unable to effectively test the hypothesis that *IL-1β2* is necessary for elongation of the pig conceptus. However, NV and SV conceptuses did express *IL-1β2* on d 6 of development suggesting that this cytokine may have an important function prior to elongation. As an alternative approach, utilization of the newly developed CRISPR/Cas9 system, in combination with somatic cell nuclear transfer or *in vitro* produced pig zygotes, could be used to efficiently produce pig conceptuses

with bi allelic ablation of *IL-1β2*. Subsequent transfer of these conceptuses to recipient gilts could reveal the true function of *IL-1β2* during elongation and establishment of pregnancy in the pig.

TABLE 4.1 Percentage of luciferase expression in BHK-21 cells relative to control for knockdown (Kd) and scrambled (S) sequence oligonucleotides (oligos). The oligos were designed to knockdown the *IL-1β2*. Specificity was achieved for Kd7 and Kd9. Relative to control: * P < 0.05; ** P < 0.01; *** P < 0.001. Kd2 was omitted because of complications during Kd2 oligo and pGeneClip U1 ligations.

Oligos	*IL-1β2*	*IL-1β1*
Control	100 ± 4.6	100.0 ± 5.4
Kd1	25.6 ± 4.5***	29.2 ± 1.5*
Kd3	74.6 ± 7.5	120.7 ± 12.1
Kd4	36.4 ± 3.7	159.8 ± 16.5
Kd5	19.1 ± 2.9***	75.5 ± 12.4
Kd6	13.1 ± 1.9**	26.5 ± 4.0**
Kd7	10.5 ± 0.6***	231.6 ± 19.6***
Kd8	22.4 ± 2.0***	18.3 ± 1.5***
Kd9	8.6 ± 1.0***	85.9 ± 8.0
S7	109.5 ± 19.5*	196.9 ± 20.3***
S8	120.7 ± 20.1***	219.5 ± 14.6***
S9	91.4 ± 14.0	212.9 ± 27.4**

TABLE 4.2 Oligos (top and bottom strands) containing Kd7 and Kd9 sequences (see Figure 4.1). The oligos were annealed and ligated into the pcDNA 6.2-GW/± EmGFP-miR plasmids. As controls, oligos containing scrambled sequences (S6 and S9) were also annealed and ligated into the plasmid. The *IL-1β2* antisense (mature miRNA) and sense sequences are underlined. The internal italicized sequences represent loop regions in production of short hairpin RNA (shRNA). Two bp were omitted in the sense sequence to produce a short internal RNA loop within the mature miRNA sequence to enhance knockdown efficiency.

miRNA	*Strand*	*Oligo sequence (5′-3′)*
Kd7	Top	TGCTGCTTTCCTTCAGAATGCCGTCC*GTTTTGGCCACTGACTGAC*GGACGGCACTGAAGGAAAG
	Bottom	CCTGCTTTCCTTCAGTGCCGTCC*GTCAGTCAGTGGCCAAAAC*GGACGGCATTCTGAAGGAAAGC
S6	Top	TGCTGCACTATTATGCGCTCTTCTCC*GTTTTGGCCACTGACTGAC*GGAGAAGAGCATAATAGTG
	Bottom	CCTGCACTATTATGCTCTTCTCC*GTCAGTCAGTGGCCAAAAC*GGAGAAGAGCGCATAATAGTGC
Kd9	Top	TGCTGCTTGTCATCGCTGTCATCTCC*GTTTTGGCCACTGACTGAC*GGAGATGAGCGATGACAAG
	Bottom	CCTGCTTGTCATCGCTCATCTCC*GTCAGTCAGTGGCCAAAAC*GGAGATGACAGCGATGACAAGC
S9	Top	TGCTGCTCATCGCTCGTTTTCGATCC*GTTTTGGCCACTGACTGAC*GGATCGAACGAGCGATGAG
	Bottom	CCTGCTCATCGCTCGTTCGATCC*GTCAGTCAGTGGCCAAAAC*GGATCGAAAACGAGCGATGAGC

TABLE 4.3 Oligos (top and bottom strands) containing Kd7 and Kd9 sequences (see Figure 4.1). The oligos were annealed and ligated into pLVX-shRNA2 plasmids at Applied StemCell Inc. As controls, oligos containing scrambled knockdown sequences (S7 and S9) were also annealed and ligated into the plasmids. The *IL-1β2* antisense (mature miRNA) and sense sequences are underlined. The internal italicized sequences represent loop regions in production of the short hairpin RNA (shRNA).

miRNA	*Strand*	*Oligo sequence (5′-3′)*
Kd7	Top	GATCCCGACGGCATTCTGAAGGAAA*TTGATATCCG*TTTCCTTCAGAATGCCGTCTTTTTTCCAAG
	Bottom	AATTCTTGGAAAAAAGACGGCATTCTGAAGGAAA*CGGATATCAA*TTTCCTTCAGAATGCCGTCGG
S7	Top	GATCCCGAAAGATTCGAGGCTCGAA*TTGATATCCG*TTCGAGCCTCGAATCTTTCTTTTTTCCAAG
	Bottom	AATTCTTGGAAAAAAGAAAGATTCGAGGCTCGAA*CGGATATCAA*TTCGAGCCTCGAATCTTTCGG
Kd9	Top	GATCCCGAGATGACAGCGATGACAA*TTGATATCCG*TTGTCATCGCTGTCATCTCTTTTTTCCAAG
	Bottom	AATTCTTGGAAAAAAGAGATGACAGCGATGACAA*CGGATATCAA*TTGTCATCGCTGTCATCTCGG
S9	Top	GATCCCGATCGAAAACGAGCGATGA*TTGATATCCG*TCATCGCTCGTTTTCGATCTTTTTTCCAAG
	Bottom	AATTCTTGGAAAAAAGATCGAAAACGAGCGATGA*CGGATATCAA*TCATCGCTCGTTTTCGATCGG

TABLE 4.4 Microinjection sessions 1-5 (MS 1-5), treatments (Trt), number of conceptuses treated, number and percent of conceptuses that became blastocyst during *in vitro* culture, detection of GFP in conceptuses, number of conceptuses transferred and morphology of conceptuses collected on d 13 after transfer for conceptuses either not treated (no virus; NV) or treated with Invitrogen *IL-1β2* knockdown (KdV; mixed Kd7 and Kd9) or scrambled knockdown (SV; mixed S6 and S9) lentiviruses. NA, Not Applicable. D, divided or early cleavage embryos.

MS	Trt	Conceptuses	Blast (%)	GFP	Transfer	Morphology
1	NV	50	12 (24.0%)	-	NA	NA
	KdV	50	10 (20.0%)	-/+	NA	NA
2	NV	20	8 (40.0%)	-	NA	NA
	SV	40	5 (12.5%)	-/+	NA	NA
	KdV	20	0 (0.0%)	NA	NA	NA
3	NV	45	10 (22.2%)	-	NA	NA
	SV	40	1 (2.5%)	-	NA	NA
	KdV	47	3 (6.4%)	-/+	NA	NA
4	NV	37 (D)	10 (27.0%)	-	NA	NA
	SV	25 (D)	3 (12.0%)	-	NA	NA
	NV	61	22 (36.1%)	-	NA	NA
	SV	60	13 (21.7%)	-	NA	NA
5	SV	100	NA	-/+	42	Fragments
	KdV	100	NA	-/+	42	2 Elongated

TABLE 4.5 Microinjection sessions 6-10 (MS 6-10), treatments (Trt), number of conceptuses treated, number and percent of conceptuses that became blastocyst during *in vitro* culture, detection of GFP in conceptuses, number of conceptuses transferred and morphology of conceptuses collected on d 13 after transfer for conceptuses either not treated (no virus; NV) or treated with Applied StemCell *IL-1β2* knockdown (KdV; mixed Kd7 and Kd9) or scrambled knockdown (SV; mixed S7 and S9) lentiviruses. NA, Not Applicable.

MS	Trt	Conceptuses	Blast (%)	GFP	Transfer	Morphology
6	NV	100	12 (12.0%)	-	NA	NA
	SV	47	3 (6.4%)	+	NA	NA
	KdV	49	3 (6.1%)	+	NA	NA
7	NV	18	6 (33.3%)	-	NA	NA
	SV	50	NA	-/+	20	None
	KdV	50	NA	-/+	20	Spherical (6, 2 and 1 mm)
8	NV	50	12 (24.0%)	-	NA	NA
	SV	50	NA	-/+	40	Fragments
	KdV	50	NA	-/+	40	Spherical (< 1mm)
9	NV	23	NA	-	23	Elongated
	SV	23	NA	-/+	23	Fragments
	SV	23	NA	-/+	23	Fragments
10	SV*	50	NA	-	30	Fragments
	SV**	50	NR	-	NA	NA

*viral solution diluted 10^8; ** viral solutions diluted 10^7.

TABLE 4.6 Microinjection sessions 11-13 (MS 11-13), treatments (Trt), number of conceptuses treated, number and percent of conceptuses that became blastocyst during *in vitro* culture, detection of GFP in conceptuses and number of conceptuses that hatched for conceptuses either not treated (no virus; NV) or treated with Applied StemCell *IL-1β2* knockdown (KdV; mixed Kd7 and Kd9) or scrambled knockdown (SV; mixed S7 and S9) lentiviruses. NA, Not Applicable

MS	Trt	Conceptuses	Blast (%)	GFP	Hatched
11	NV	37	9(24.3%)	-	3
	SV	55	0 (0.0%)	NA	NA
	KdV	53	7(13.2%)	-/+	0
12	NV	38	17 (46.0%)	-	10
	SV	45	10 (22.2%)	-/+	0
	KdV	37	6 (16.2%)	-/+	4
13	NV	50	14 (28.0%)	-	1
	SV	42	2 (4.8%)	-/+	1
	KdV	40	4 (10.0%)	-/+	0

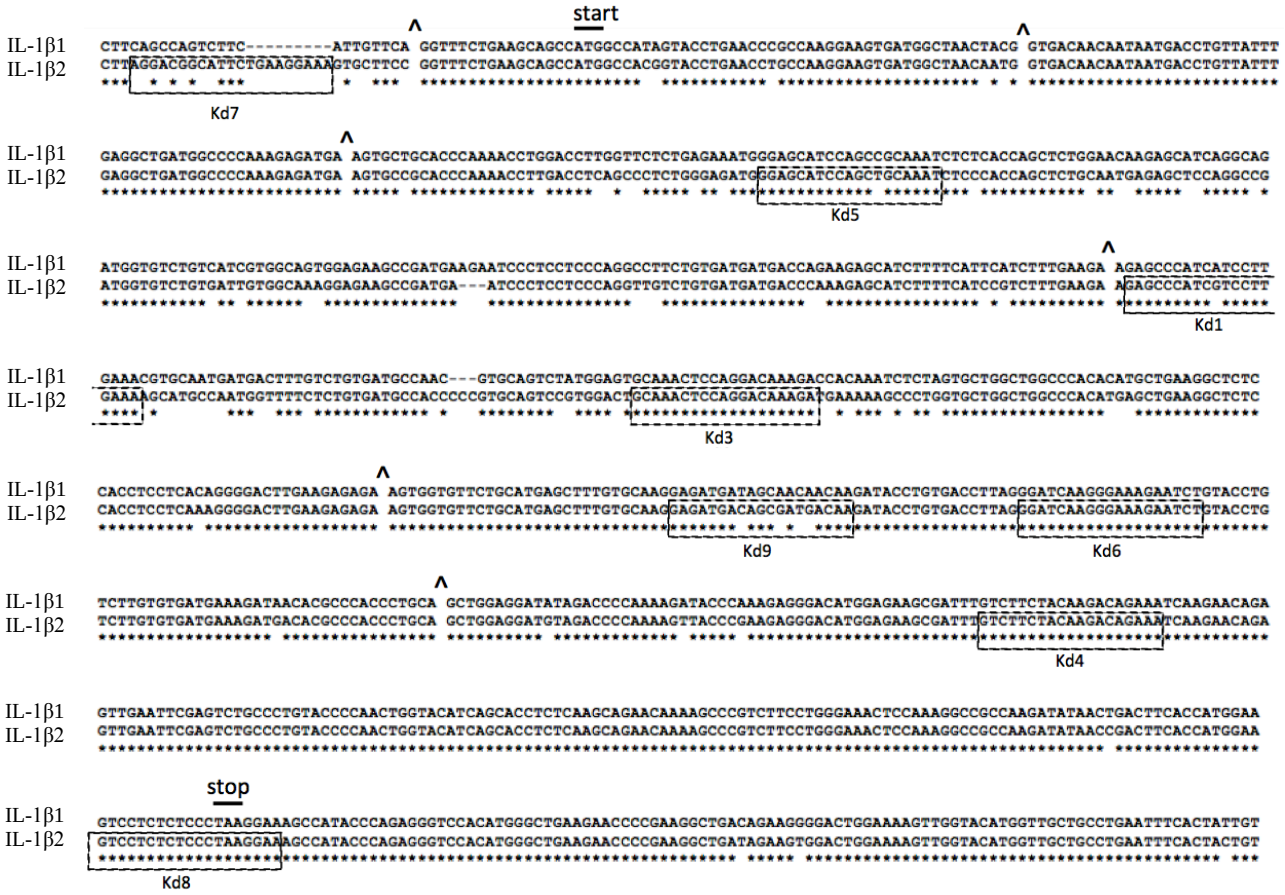
start
IL-1β1
IL-1β2
Kd7
Kd5
Kd1
Kd3
Kd9
Kd6
Kd4
stop
Kd8

FIGURE 4.1 Alignment of *IL-1β1* and *IL-1β2* cDNA sequences using CLUSTALW multiple sequence alignment program and locations where eight different knockdown (Kd) oligonucleotides (boxes) were designed to target *IL-1β2*. Stars (*****) indicate the location of bp homology between *IL-1β1* and *IL-1β2*. Dashes (-) indicate insertions or deletions. “Start” and “Stop” indicates of start and stop codons.

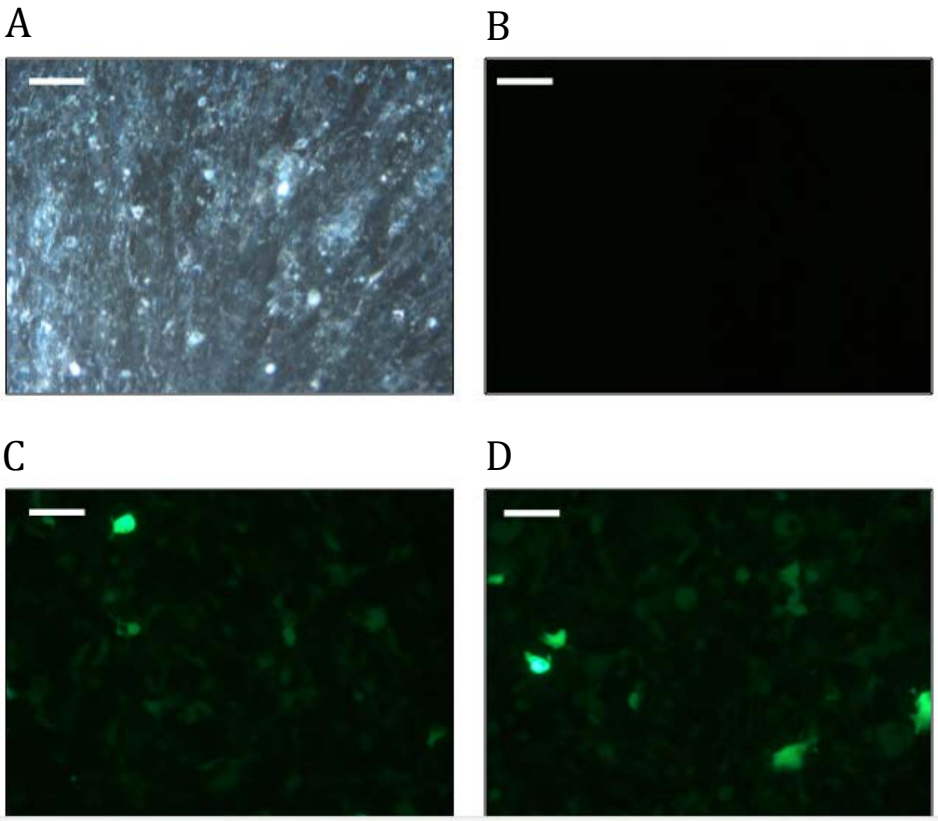

FIGURE 4.2 Infection of the 293FT cells with an Invitrogen *IL-1β2* knockdown lentivirus capable of transducing GFP. Interleukin-1 beta 2 knockdown lentiviruses were harvested from the 293FT mammal cell line using the BLOCK-iT Lentiviral Pol II miR RNAi Expression System (Invitrogen). (A) Dark field image and (B) GFP negative control image of 293FT cells treated with negative (no virus) control medium. (C) GFP image of 293FT cells treated with a positive control lentivirus (PosV). (D) GFP image of 293FT cells treated with Invitrogen *IL-1β2* knockdown lentivirus 9 (KdV9). Cells were visualized for GFP using a Leica Light microscope equipped with a GFP filter (B, C and D). Images were taken at a 400 X magnification. Bar = 50μm.

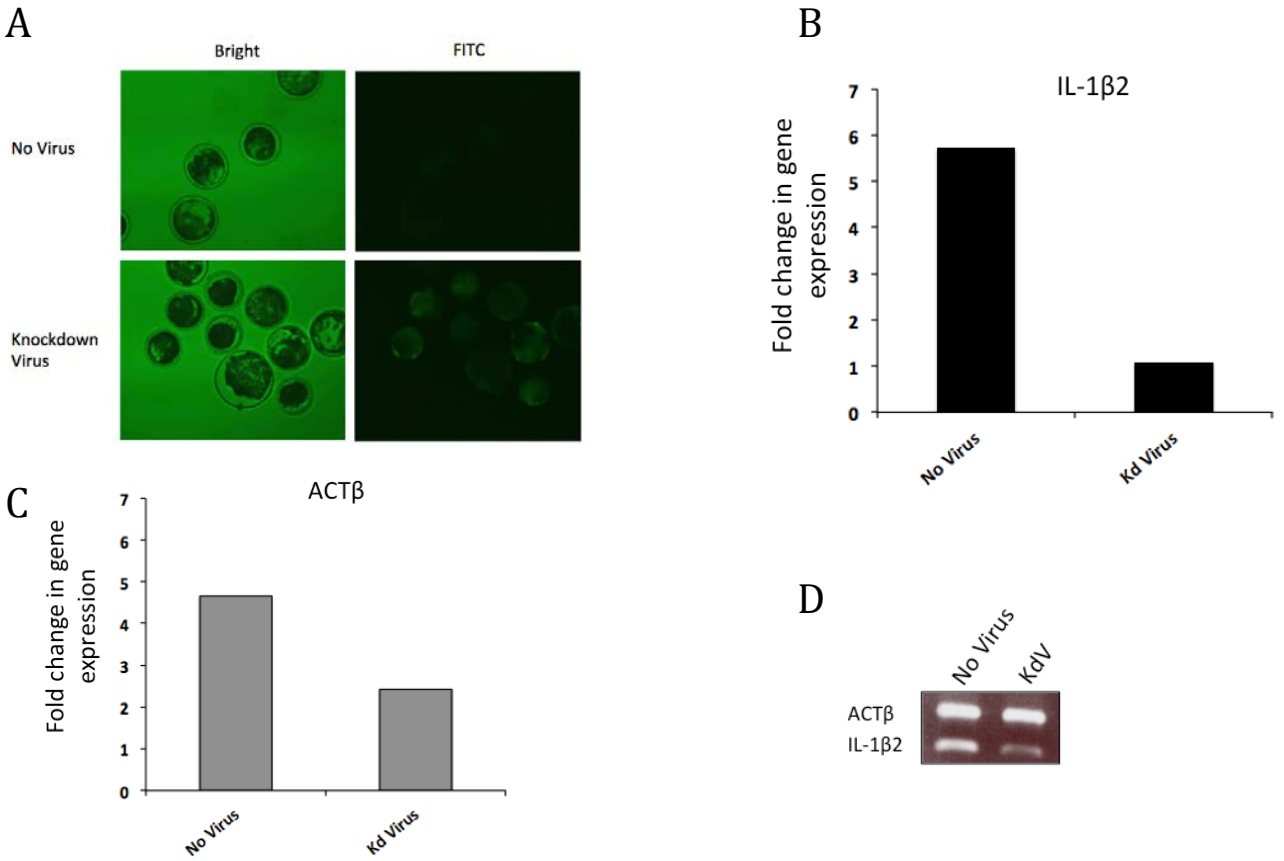

FIGURE 4.3 Expression of GFP (A), *IL-1β2* and *ACTβ* (B-D; relative expression) in pig conceptuses not treated (No Virus; NV) and treated with Invitrogen knockdown lentivirus (KdV; mixed Kd7V and Kd9V) during microinjection session 1 (MS 1). Pictures of fluorescent blastocysts on d 6 of development (A) were taken at 100 X magnifications using the Eclipse Ti microscope (Nikon). RNA was extracted from 10-pooled NV and KdV blastocysts for RT-PCR gene expression analysis of *IL-1β2* and *ACTβ* (B-D). Data are presented as least squares means (LSM). During gel electrophoresis experiments, 4 μL of the RT-PCR reactions were electrophoresed through a 0.8% gel (D).

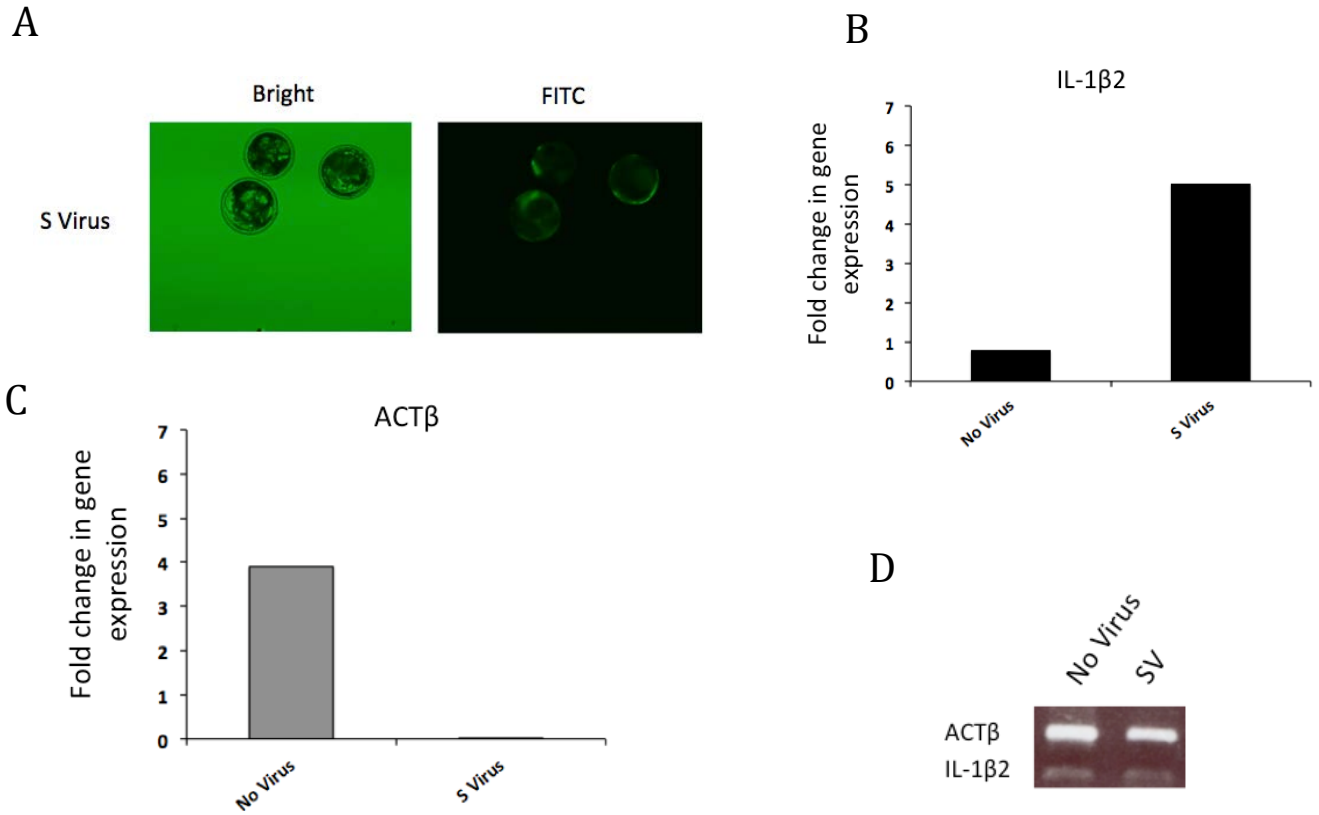

FIGURE 4.4 Expression of GFP (A), *IL-1β2* and *ACTβ* (B-D; relative expression) in pig conceptuses not treated (No Virus; NV) and treated with Invitrogen scrambled knockdown lentivirus (SV; mixed S6V and S9V) during microinjection session 2 (MS 2). Pictures of fluorescent blastocysts on d 6 of development (A) were taken at 100 X magnification using the Eclipse Ti microscope (Nikon). RNA was extracted from 5-pooled NV and KdV blastocysts for RT-PCR gene expression analysis of *IL-1β2* and *ACTβ* (B-D). Data are presented as least squares means (LSM) During gel electrophoresis experiments, 4 μL of the RT-PCR reactions were electrophoresed through a 0.8% gel (D).

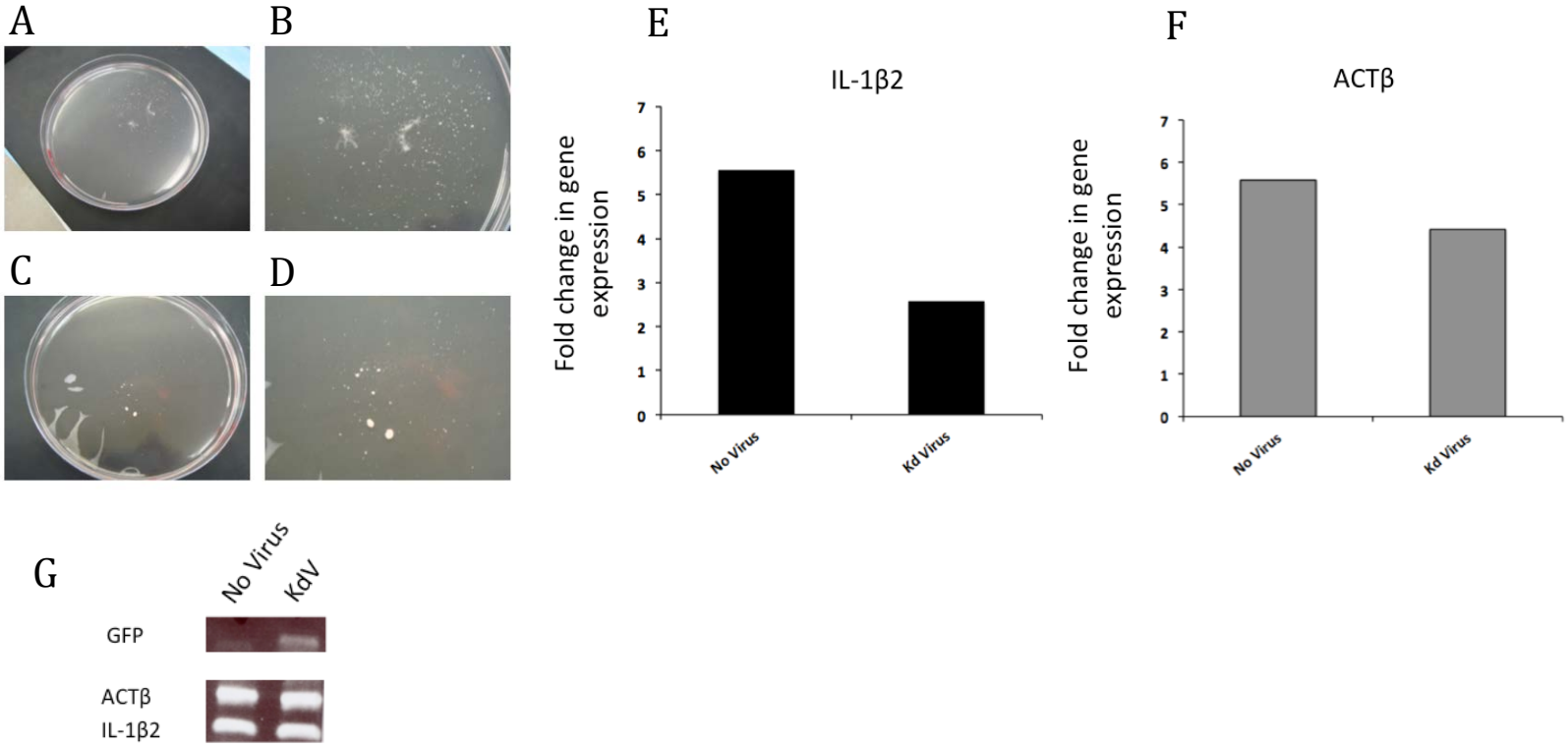

FIGURE 4.5 Elongated conceptuses and conceptus fragments flushed from a gilt that received Invitrogen KdV (A and B) and SV (C and D) treated conceptuses, respectively after microinjection 5 (MS 5). Expression of *IL-1β2* and *ACTβ* (E-G) and expression of GFP (G) in the elongated KdV conceptuses and elongated conceptuses produced from artificial insemination (AI; see Chapter II). *IL-1β2* and *ACTβ* fold change in gene expression are presented as least squares means (LSM). 4 μL of the PCR and RT-PCR reactions were electrophoresed through a 0.8% gel (D). GFP could not be detected by microscope in the KdV conceptus but expression was later verified by PCR (G).

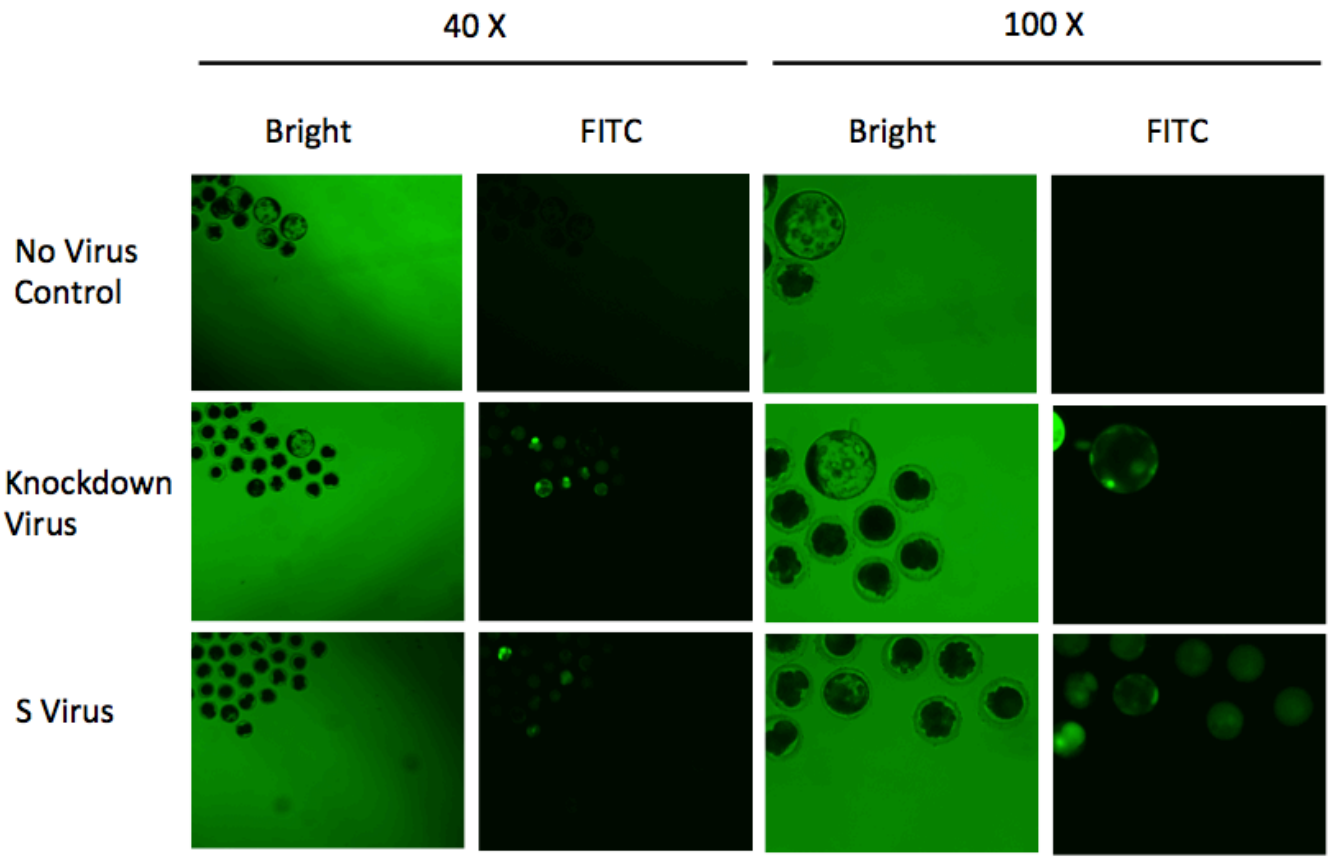

FIGURE 4.6 Expression of GFP in pig conceptuses treated with Applied StemCell knockdown (KdV; mixed KdV7 and KdV9) and scrambled knockdown (SV; mixed SV7 and SV9) lentiviruses after microinjection session 6 (MS 6). Expression of GFP was not detected in conceptuses that did not receive virus (No Virus controls) Pictures of fluorescent blastocysts (d 6 of development) were taken at 40 X and 100 X magnifications using the Eclipse Ti microscope (Nikon).

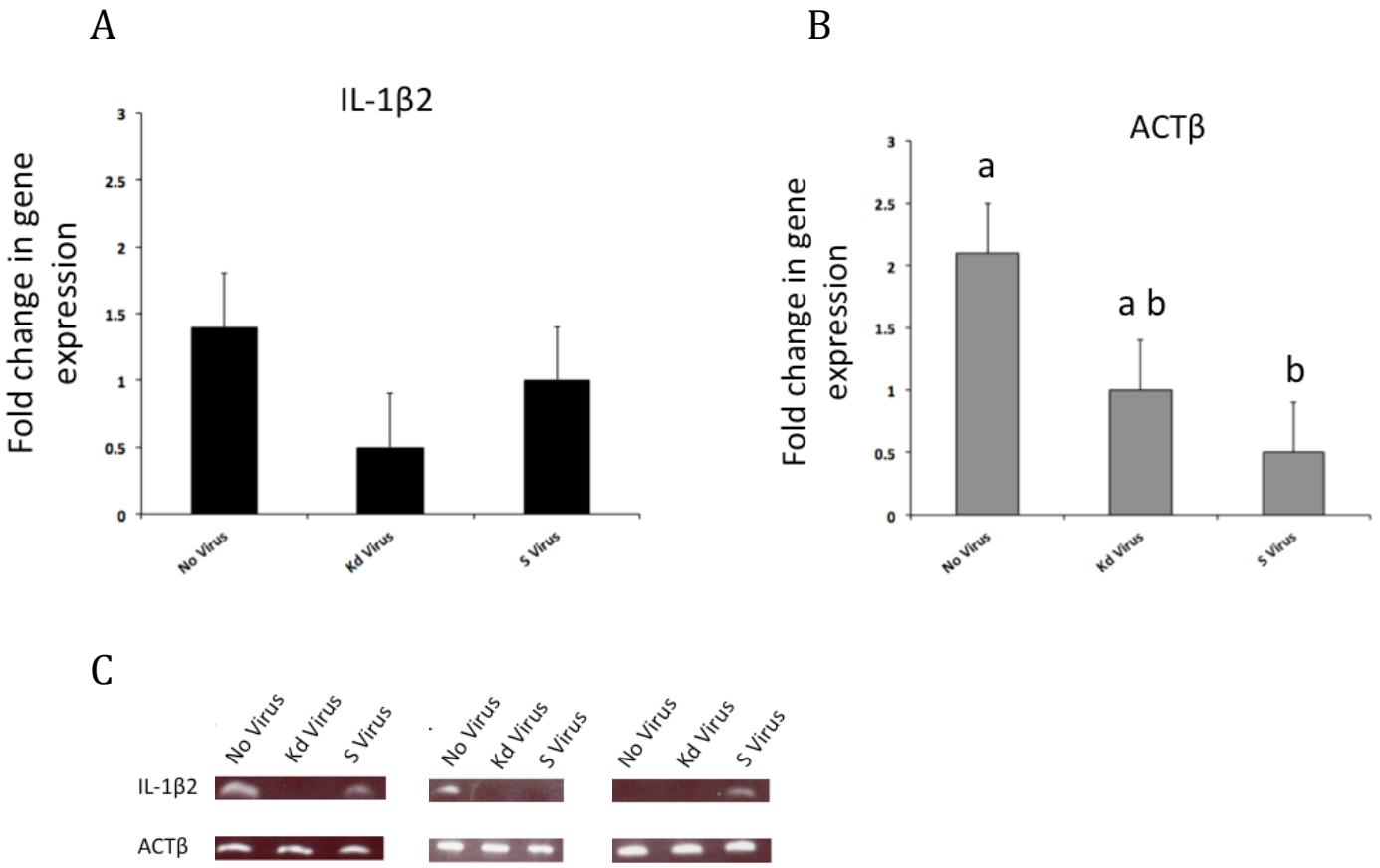

FIGURE 4.7 Relative RT-PCR fold change in gene expression for *IL-1β2* and *ACTβ* in individual NV, KdV and SV blastocyst from Fig. 4.6 (n=3 per treatment; A-C). Data are presented as least squares means (LSM) ± standard error of the least squares means (SEM). Different letters over bars represent significant differences between treatment means. During gel electrophoresis experiments, 4 μL of the RT-PCR reactions were electrophoresed through a 0.8% gel (C).

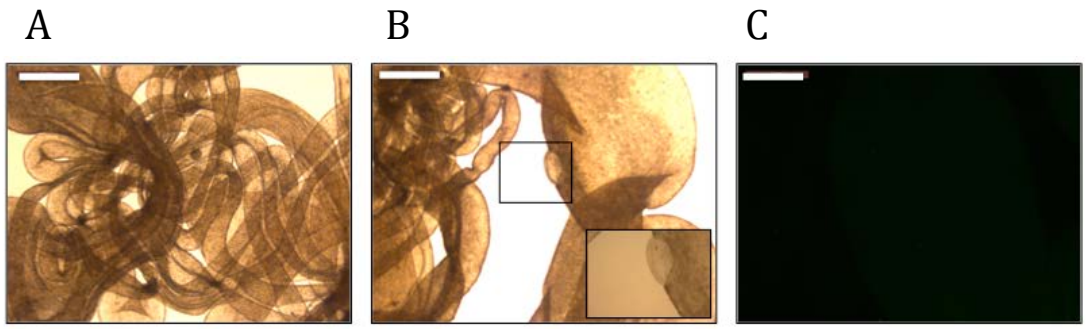

FIGURE 4.8 Bright field images (A and B) and a negative GFP image (C) of an elongated, no virus control (NV), pig conceptus flushed from the uterus after microinjection session 5 (MS 5) and nine days after embryo transfer (d 13 of development). A picture of the inner cell mass (ICM) was taken from the location of the black box in image B and presented as an inset image. Bar = 1 mm.

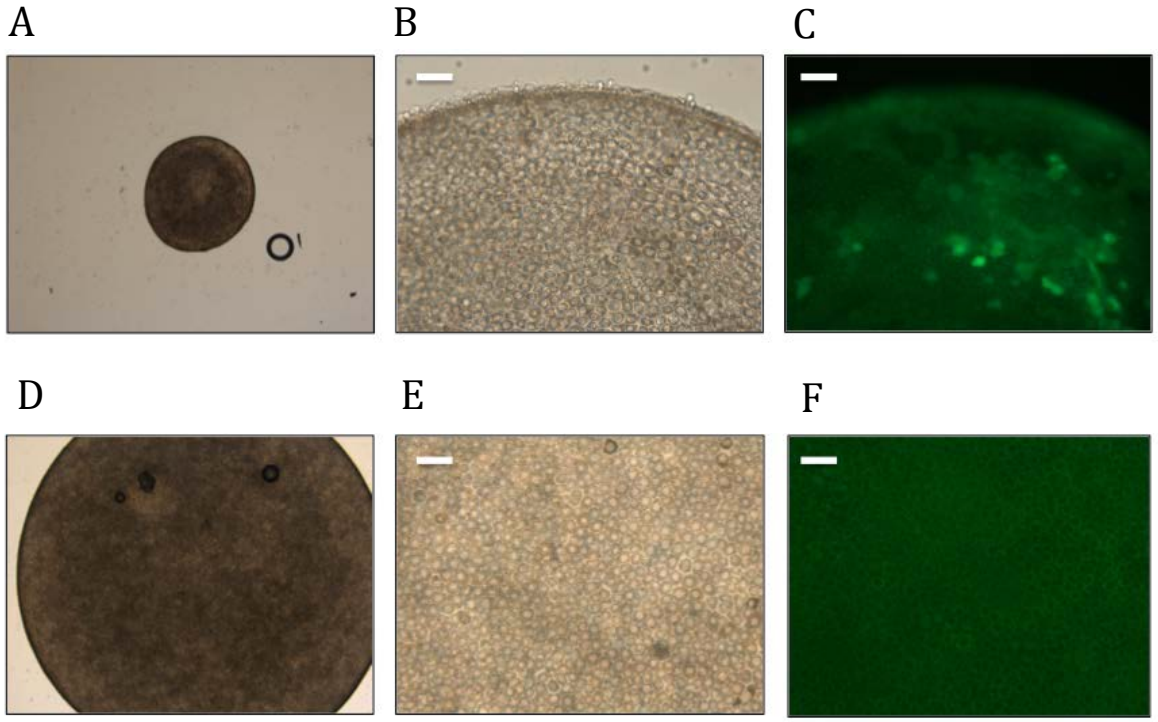

FIGURE 4.9 Bright field and GFP images of two Applied StemCell KdV conceptuses flushed from a single gilt on d 13 of pregnancy. Conceptuses were abnormal in morphology (not elongated) and 1 mm (A-C) and 2 mm (D-F) in diameter based on measurement with a calibrated eyepiece micrometer. Bar = 100 μm. Images A and D were taken at a 25 X magnification. Images B and C were taken at 400 X and images E and F were taken at 100 X plus zoom.

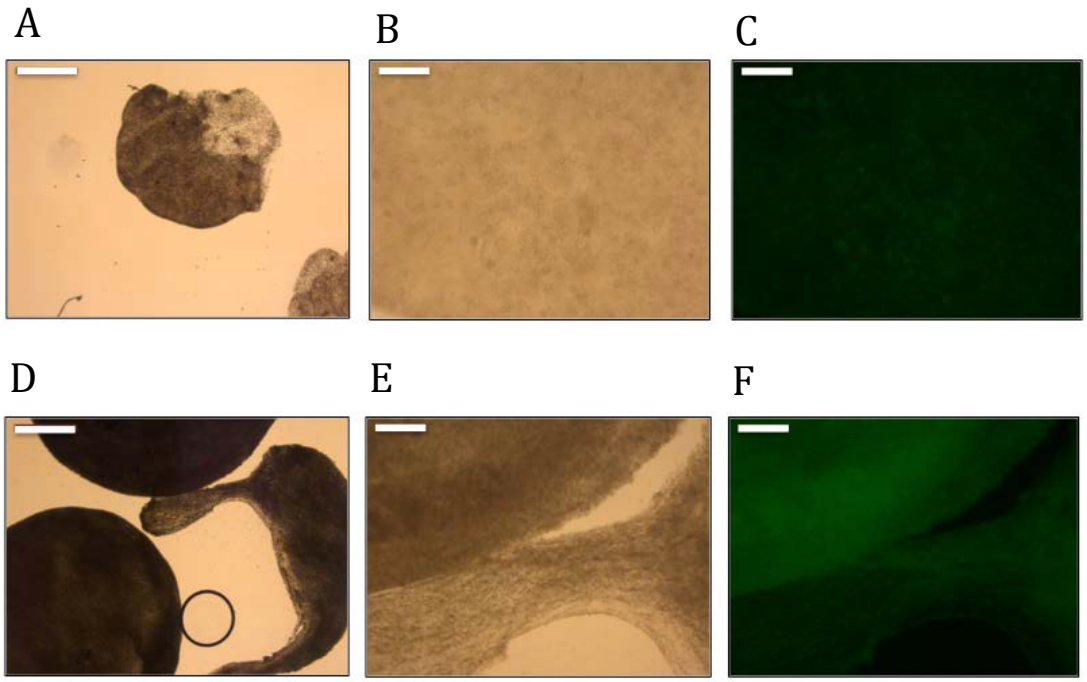

FIGURE 4.10 Bright field and GFP images of conceptus fragments flushed from two gilts (A-C and D-F) on d 13 of pregnancy. Fragments flushed from one gilt had an elongated appearance (D-F). Bar = 1 mm in images A and D. Bar = 100 μm in images B and C. Bar = 200 μm in images E and F.

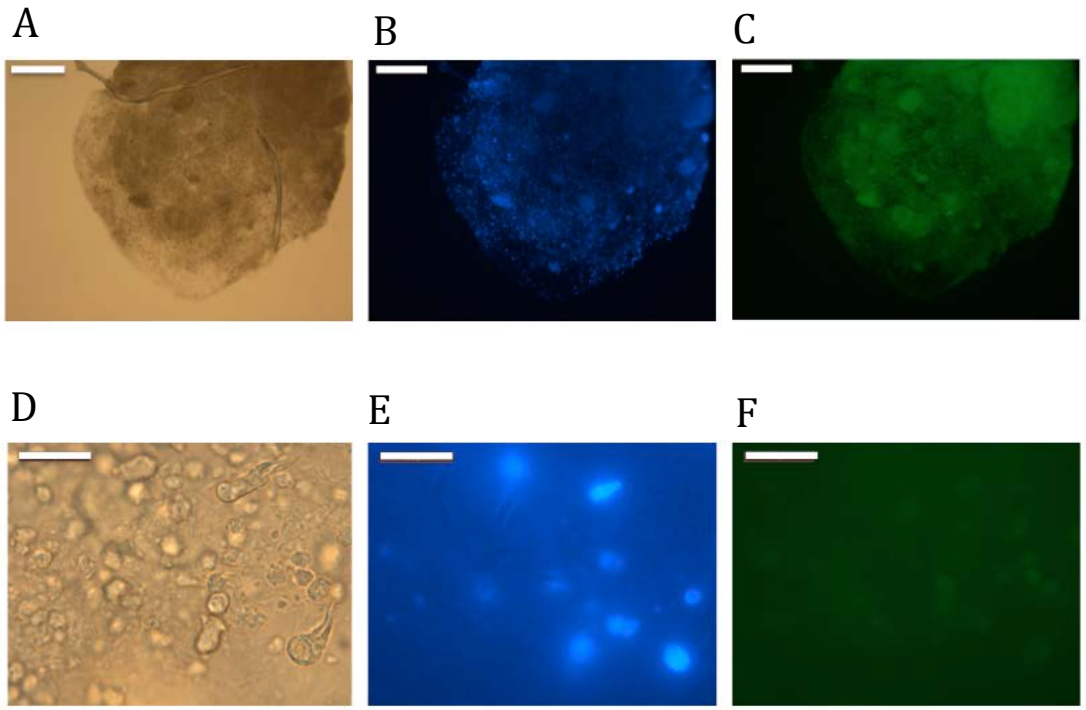

FIGURE 4.11 Bright field, DAPI and GFP images of a conceptus fragment flushed from a gilt (A-C) on d 13 of pregnancy. High magnification bright field, DAPI and GFP images of cells within the fragment (D-F). Bar = 200 μm in images A-C and 20 μm in images D-F. Images A-C and D-F were taken a 100 X and 1000 X magnifications, respectively.

CHAPTER FIVE

PREDICTED PROTEIN STRUCTURE, FUNCTION AND ALIGNMENT OF PIG INTERLEUKIN-1 BETA 1 (IL-1β1) AND INTERLEUKIN-1 BETA 2 (IL-1β2), THE LATTER A NOVEL IL-1 EXPRESSED BY THE EARLY PIG CONCEPTUS

Abstract

Interleukin-1 beta (IL-1β) is a master pro-inflammatory cytokine commonly released by leukocytes with functions in immunity and when mis-regulated, manifestation of disease. IL-1β also promotes implantation when released by the primate and rodent conceptus. In the pig, the gene encoding *IL-1β* has duplicated resulting in genes interleukin-1 beta 1 (*IL-1β1*) and interleukin-1 beta 2 (*IL-1β2*). Interleukin-1 beta 1 is expressed by blood leukocytes and *IL-1β2* is expressed by the early pig conceptus. An increase in IL-1 receptor type I (*IL-1RI*) expression in the pig uterine surface epithelium during early pregnancy suggests that IL-1β2 functions to promote implantation by binding this receptor. Compared with IL-1β1, recombinant IL-1β2 had a lesser capacity to activate nuclear factor-kappa B (NF-κB), a transcription factor commonly activated

during IL-1β-IL-1RI signaling, in the uterine surface epithelium indicating the IL-1β2 may have reduced activity. In order for IL-1β to bind the IL-1RI, the cysteine protease, caspase-1 (CASP1), must process pro-IL-1β into a mature functional cytokine. To investigate differences in protein structure between IL-1β1 and IL-1β2, we predicted and aligned the atomic structures of pro and mature IL-1β1 and IL-1β2 using DNASTAR's Novafold program. Alignment of predicted pro and mature proteins resulted in an RMSD of (3.47 Å) and (0.70 Å), respectively, indicating that IL-1β1 and IL-1β2 are highly similar in structure in absence of the pro-domains. Viewing the solvent accessible surface area of the pro-proteins suggested that there is a possible steric hindrance of the first CASP1 site in IL-1β2 compared with that of IL-1β1. For the mature proteins, Novafold predicted that IL-1β1 and IL-1β2 bind the IL-1RI with 35 and 32 binding sites, respectively. Thirty-two binding sites were shared between the two proteins. Of these binding sites, IL-1β2 had three non-conserved amino acid substitutions that resulted in a complete change of charge and solvent accessible surface areas compared with IL-1β1. Overall, differences in protein structure, the number of IL-1RI binding sites and amino acid side chain charges could affect the availability and activity of IL-1β2 compared with IL-1β1.

INTRODUCTION

Interleukin-1 beta is an important pro-inflammatory signaling factor released by leukocytes that can coordinate innate and adaptive immune responses (Dinarello, 2011; Garlanda et al., 2013). Human IL-1β is first translated into an inactive pro-protein with a

molecular weight of approximately 31 kilodalton (kDa) (Hailey et al., 2009). During cell stress, tissue injury or infection, activation of the inflammasome in the cell cytoplasm triggers processing of pro-IL-1β by caspase-1 (CASP1) proteases. Caspase-1 proteolytically cleaves pro-IL-1β in two sequential locations (CASP1 site-1 and site-2) (Hailey et al., 2009). Removal of the pro-domain allows folding of the C-terminus and formation of mature, functional IL-1β (mat-IL-1β) (Hailey et al., 2009). The tertiary structure of human mat-IL-1β resembles a β trefoil, consisting of twelve β strands that fold into a four sided tetrahedral like shape containing a hydrophobic barrel core motif common to other active members within the IL-1 superfamily including IL-1 alpha (IL-1α), IL-33 and the interleukin-1 receptor antagonist (IL-1RA) (Krumm et al., 2014).

Interleukin-1 beta signals by binding the IL-1RI located within the target cell membrane. The crystal structure of human IL-1β-IL-1RI complex has been solved (Vigers et al., 1997). The tertiary structure of IL-1RI resembles a question mark that grasps IL-1β like a hand (Krumm et al., 2014). Clinching the cytokine in a C-like shape, the IL-1RI immunoglobulin domains interact with residues located on mat-IL-1β's exterior, many of which are important for signal activation (Krumm et al., 2014). Formation of this complex attracts the IL-1 receptor accessory protein (IL-1RAP), also located within the membrane (Dunne and O'Neill, 2003; Sims and Smith, 2010; Krumm et al., 2014). Signaling is finally triggered after juxtapositioning of IL-1RI and IL-1RAP-toll IL-1R (TIR) domains within the cell cytoplasm ultimately activating the transcription factor nuclear factor-kappa B (NF-κB) (Dunne and O'Neill, 2003; Sims and Smith, 2010; Krumm et al., 2014).

Interleukin-1 beta can influence uterine receptivity for implantation in primates and rodents by increasing adhesion molecules along the uterine surface and matrix metalloproteinase (MMP) expression in the cytotrophoblast (Simón et al., 1998; Librach et al., 1994). The gene encoding *IL-1β* has duplicated in pigs resulting in two distinct genes, interleukin-1 beta 1 (*IL-1β1*) and interleukin-1 beta 2 (*IL-1β2*), that are tandem within pig chromosome three (Groenen et al., 2012). The *IL-1β1* is the prototypical cytokine expressed by leukocytes and *IL-1β2* is expressed by the early pig conceptus. The function of IL-1β2 during early pregnancy in the pig is not yet known. Conceptus expression of *IL-1β2* increases significantly during elongation, a morphological transformation of the conceptus that expands the placental unit, and prior to attachment (Tuo et al., 1996; Ross et al., 2003a; 2003b). Expression of *IL-1RI* and *IL-1RAP* increase in the conceptus and uterine surface epithelium at that time suggesting that IL-1β2 interacts with these signaling factors and has important roles in development and implantation (Ross et al., 2003a). However, interactions between mat-IL-1β2 and IL-1RI have not been verified. Data presented in Chapter Three suggests that mat-IL-1β2 can cause the translocation of NF-κB, transcription factor commonly activated during IL-1β-IL-1RI signaling, to the uterine epithelial and alveolar cell nucleus. Compared with recombinant IL-1β1, IL-1β2 had a lesser capacity to translocate NF-κB in the epithelium. Overall, these findings suggest the IL-1β2 interacts with the IL-1RI and that functional differences may exist between IL-1β1 and IL-1β2.

Katebi et al. (2010) used the I-TASSER platform to predict the tertiary structures of pro and mature IL-1β1 and IL-1β2 proteins. Based on their predictions, Katebi et al. (2010) suggested that amino acid residues up stream of CASP1 site-2 in pro-IL-1β2 could

reduce CASP1 activity and therefore, could result in less available mat-IL-1β2 for signaling. Further, Katebi et al. (2010) concluded that mat-IL-1β2 likely binds the IL-1RI but may have a different binding efficiency compared with mat-IL-1β1 based on residue substitutions in IL-1β2's binding motif. They also suggested that these substitutions could lead to interactions with other proteins.

To verify this and to specifically compare receptor-binding sites between the two pig IL-1β proteins, we predicted the atomic structure of both pro and mature IL-1β1 and IL-1β2 and aligned the structures against one another using DNASTARs, recently developed, Novafold program. Further, we aligned mat-IL-1β1 and mat-IL-1β2 structures to the predicted structure of human and mouse mat-IL-1β and to mat-IL-1β from a more closely related mammal, the minke whale (Yim et al., 2014).

MATERIALS AND METHODS

Based on full-length amino acid sequences and CASP1 proteolytic cleavage sites (Hailey et al., 2009; Fig. 5.1 and Fig. 5.2) tertiary structures for pro and mature IL-1β1 and IL-1β2 were predicted using DNASTAR's Novafold program (DNASTAR Inc.). Pro-IL-1β1 and pro-IL-1β2 protein sequences were 267 amino acids in length. Mat-IL-1β1 and mat-IL-1β2 protein sequences were 153 and 154 amino acids in length, respectively. Interleukin-1 beta-CASP1 sites are conserved across mammals (Hailey et al., 2009). Based on these sites, minke whale, human and mouse mat-IL-1β protein structures, consisting of 153, 153 and 152 amino acids, respectively, were also predicted (Fig. 5.1). Novafold utilizes I-TASSER (iterative threading assembly refinement)

algorithms that make protein tertiary structure predictions based on a combination of multiple-threading alignments [20 most similar sequences with solved tertiary structures in the protein data bank (PDB)] and iterative template fragment assembly simulations (Zhang and Skolnick, 2013).

For each sequence, the Novafold program provided the best five prediction models and a prediction confidence (C)-score for each. The I-TASSER C-score, typically ranging from -5 to 2, is an estimate of accuracy for a predicted protein model based on the quality of threading and structural assembly. A higher C-score is indicative of a better prediction (Zhang, 2008; Roy et al., 2010; 2012). For each structure, Novafold also predicted the protein's function and potential interactions with other proteins, such as during ligand-receptor binding. Amino acids involved in these activities were also predicted. We then performed a rigid body alignment of the predicted IL-1β1 and IL-1β2 protein structures within Novafold. For each alignment Novafold provides a root mean square deviation (RMSD) value. The RMSD is the average distance measured in angstroms (Å) between α carbon atoms of superimposed protein structures. The RMSD value can range can from 0 to approximately 30 with a lower value indicating greater structural similarity. As a positive prediction control, the human mat-IL-1β structure, predicted by Novafold, was aligned with the human mat-IL-1β structure predicted by X-ray diffraction in combination with solution nuclear magnetic resonance (NMR) imaging (PDB ID; 1IOB). This resulted in an RMSD value of 0.90 Å. As a negative control, the Novafold predicted human mat-IL-1β was aligned with the human IL-1 receptor antagonist (IL-1RA) protein structure predicted by solution NMR (PDB; 1IRP) resulting in an RMSD of 3.20 Å. Human mat-IL-1β and IL-1RA are 153 residues each and share

approximately 30% sequence identity. The Novafold human mat-IL-1β prediction was further aligned with the structure of human myoglobin determined by X-ray diffraction. Human myoglobin also consists of 153 residues and does not share sequence identity with human IL-1β (PDB; 3RGK). This alignment resulted in an RMSD of 4.66 Å.

RESULTS

Pro-IL-1β1 and IL-1β2

The best Novafold predictions of the atomic structure of pro-IL-1β1 and pro-IL-1β2, both of which consisted of 267 amino acids, received C-scores of -2.7 and -3.0, respectively, and took approximately 40 h to compute (Fig. 5.3). These C-scores are similar to those reported by Katebi et al. (2010) and as they suggested, indicate greater *ab initio* structure prediction within I-TASSER. Alignment of the best-predicted pro-structures resulted in an RMSD of 3.47 Å. Compared with pro-IL-1β2, the predicted tertiary structure of pro-IL-1β1 had a greater number of alpha helixes (2 and 7, respectively), five of which were located within the pro-region (Fig. 5.3). Pro-IL-1β2 alpha helixes were also located in the pro-region. Both predicted structures had 12 β strands located within the mature region. View of the solvent accessible surface area of pro-IL-1β1 and pro-IL-1β2 indicated that all CASP1 sites (site-1 and site-2) were near the protein surface (Fig. 5.4). However, a large molecular structure, resembling a Y, partially covered CASP1 site-1 in pro-IL-1β2 (Fig. 5.4). The opposite was true for CASP1 site-2 as this region was partially covered in pro-IL-1β1 but completely exposed in pro-IL-1β2.

Mature IL-1β1 and IL-1β2

Within pro-IL-1β1 and pro-IL-1β2, both CASP1 sites are conserved (CASP1 site-1, Asp^{27} and Gly^{28}; IL-1β1-CASP1 site-2, Asp^{114} and Ala^{115}; IL-1β2-CASP1 site-2 Asp^{113} and Ala^{114}). The best Novafold predictions of the atomic structure of mat-IL-1β1 and mat-IL-1β2 received C-scores of 1.9 and 1.8, respectively, and took approximately 13 h to compute (Fig. 5.5). Alignment of mature structures resulted in an RMSD of 0.70 Å, indicating that the predicted mat-IL-1β1 and mat-IL-1β2 structures were highly similar in the absence of the pro-domain (Fig. 5.5). The best Novafold predictions of the atomic structure of minke whale, human and mouse mat-IL-1β received C-scores of 1.9 (Fig. 5.6). Alignment of predicted mat-IL-1β1 with predicted minke whale, human and mouse mature-IL-1β protein structures resulted in RMSD's of 0.64, 0.67, and 0.63 Å, respectively, indicating slightly greater structural alignment compared to the mat-IL-1β1-mat-IL-1β2 structural alignment. Similarly, alignment of predicted mat-IL-1β2 with predicted minke whale, human and mouse mat-IL-1β protein structures resulted RMSDs of 0.62, 0.62 and 0.64 Å, respectively.

All the predicted tertiary structures retained the characteristic IL-1 superfamily β trefoil confirmation and, with the exception of minke whale mat-IL-1β, consisted of 12-β strands spanning at least four amino acids (Fig. 5.6). The minke whale mat-IL-1β was predicted to have ten β strands of at least four amino acids and four smaller strands. Mat-IL-1β1 and mat-IL-1β2 had three and two alpha helixes, respectively. Minke and human mat-IL-1β had two alpha helixes and mouse mat-IL-1β, one alpha helix. All helixes appeared to be near the protein surface.

Based on Novafold predictions, both mat-IL-1β1 and mat-IL-1β2 have immune modulatory activity and interact with IL-1RI (Gene Ontology (GO) score ≥ 0.98). Based

on interactions with the human IL-1RI, Novafold predicted 35 binding sites in mat-IL-1β1 (residues 1, 2, 4, 6, 11, 14, 15, 16, 25, 27, 30, 31, 32, 33, 34, 35, 38, 44, 45, 46, 48, 51, 53, 70, 92, 93, 94, 105, 108, 127, 128, 147, 149, 150 and 152) and 32 in mat-IL1β2 (residues 2, 3, 5, 7, 12, 15, 16, 26, 28, 31, 32, 33, 34, 35, 36, 39, 47, 49, 52, 54, 71, 92, 94, 95, 106, 109, 128, 129, 148, 150, 151 and 153) (Fig. 5.7). Sequence alignment of the mat-IL-1β1 with mat-IL-1β2 (blastp; NCBI) revealed the presence of an inserted proline and five non-conserved amino acid substitutions in the mat-IL-1β2 sequence. Five of these residues (including the proline) were suggested to be involved in receptor binding (mat-IL-1β2; residues 2, 3, 16, 26, 34) (Fig. 5.8-5.13). Of these five residues, three were substitutions that resulted in a different amino acid side chain charge (Fig. 5.8-5.13). There were three residues in the IL-1β1 sequence that were predicted to binding the IL-1R1 that were not predicted for IL-1β2. These residues, which were located on the inside of the solvent accessible surface area of IL-1β1, were located in amino acid positions 16, 44 and 45. Overall, there were noticeable differences in charge and solvent accessible surface area between mat-IL-1β1 and mat-IL-1β2 at predicted receptor-binding sites that could potentially affect the overall activity of mat-IL1β2 compared with mat-IL-1β1. (Fig. 5.13)

DISCUSSION

In this study, we used DNASTAR's Novafold program to predict the atomic structures of pig pro and mature IL-1β1 and IL-1β2. We then aligned the structures, and compared them based on CASP1 proteolytic sites-1 and 2 and surface amino acids predicted to interact with the IL-1RI. Major findings from this study are that 1) compared

with pro-IL-1β1, pro-IL-1β2 may have a less accessible CASP1 site-1 for processing into the mat-IL-1β2, 2) compared with mat-IL-1β1, mat-IL-1β2 has three non-conserved amino acid substitutions resulting in differently charged side chains in locations suggested to be involved in IL-1RI binding. Overall, these residue modifications could affect the availability and activity of mat-IL-1β2.

In the human, *IL-1β* is translated into a 269 amino acid pro-protein with a molecular weight of approximately 31 kDa. The pro-IL-1β can be proteolytically cleaved by CASP1 in two sequential locations (CASP1 site-1 and site-2) resulting in formation of mat-IL-1β of approximately 17 kDa (Hailey et al., 2009). Cleavage of CASP1 site-1 alone can result in formation of 28 kDa proteins with a partially remaining pro-domain (Hailey et al., 2009). Although pro-IL-1β is not active, mat-IL-1β may be bound by the IL-1RI and can initiate signaling (Krumm et al., 2014).

In the pig, pro-IL-1β1 and pro-IL-1β2 proteins are 267 amino acids in length and are approximately 30 kDa in molecular weight (see Chapter Three). Although there is an amino acid deletion (lysine; between amino acids Met^{76} and Asn^{77} in pro-IL-1β2) and an insertion (proline; amino acid Pro^{116} in pro-IL-1β2) within the full-length pro-IL-1β2 sequence compared with pro-IL-1β1, both CASP1 sites are conserved (Fig 5.2). Alignment of pro and mature IL-1β1 and IL-1β2 protein structures within Novafold suggested that the pro-molecules are less similar in tertiary structure (RMSD; 3.47 Å; Fig. 5.3) when compared to the mature molecules (RMSD; 0.70 Å; Fig. 5.5). These findings are similar to predictions reported by Ketabi et al. (2010) who recorded an RMSD of 3.06 Å for alignment of the pro-proteins. However, their predictions suggested that mat-IL-1β1 and mat-IL-1β2 may have been slightly more similar in structure

(RMSD; 0.48 Å). Advanced I-TASSER algorithms used by the Novafold program may account for these differences, however, amino acid sequences used to make these predictions in Ketabi et al., (2010) were not reported and differences in protein sequences used for that analysis could also be a factor. For instance, Ketabi et al. (2010) reported an 86% sequence identity between pro-IL-1β1 and pro-IL-1β2; however, we reported an 85% sequence identity.

The observation that the pro-proteins have a higher RMSD and are less similar in structure compared with the mature proteins is not surprising. The mat-IL-1β1 and mat-IL-1β2 protein sequences have greater sequence identity (92%) compared with the pro-proteins (85%) (see Chapter Three). Further, the N-terminal region of pro-IL-1β is cleaved away during processing into the mature form and is more prone to mutation. This region was the least similar in sequence (78%).

Compared with pro-IL-1β1, amino acids directly up-stream (N-terminus) and down stream of CASP1 site-1 are highly conserved in pro-IL-1β2. This was not true for CASP1 site-2 as there are a number of non-conserved amino acid substitutions in pro-IL-1β2 up and down stream of this location (Fig. 5.2). Further, in mat-IL-1β2, there is a non-conserved amino acid substitution next to an inserted proline down stream and directly adjacent to CASP1 site-2 (Fig. 5.2)

The pro-region of IL-1β does not allow folding of the C-terminus and blocks the formation of the mature molecule (Hailey et al., 2009). Interestingly, compared with pro-IL-1β1, the solvent accessible surface area of pro-IL-1β2 indicates that there is a large molecular structure, resembling a Y, covering CASP1 site-1 (Fig. 5.4). Amino acids methionine, lysine and cysteine (residue positions 32, 33 and 34, respectively) up-stream

of the CASP1 site are responsible for the structure. Also, there is an amino acid substitution near CASP1 site-2 that may to alter CASP1 activity (Fig. 5.2). CASP1 requires four amino acids up stream of a proteolytic site to function properly (Thornberry and Molineaux, 1994). The N-terminal sequence requires an asparagine directly adjacent to the CASP1 site and a valine is typically preferred as the third amino acid up-stream (Thornberry and Molineaux, 1994). Although the pro-IL-1β1 CASP1 site-2 retains a valine in this location, the pro-IL-1β2 sequence has substituted this residue for leucine, both of which have hydrophobic side chains (Fig. 5.2). When Katebi et al. (2010) conducted a similar protein structure analysis of IL-1β1 and IL-1β2 proteins, they concluded that this substitution could reduce CASP1 activity. However, minke whale and bovine pro-IL-1β protein sequences also have a leucine in this position (Fig. 5.1). Because this substitution is common among mammals that are phylogenetically similar, it may not have a significant effect on CASP1 processing of pro-IL-1β2. However, the solvent accessible surface area of this CASP1 site is considerably more exposed in pro-IL-1β2 compared with pro-IL-1β1 (Fig 5.4). Overall, the CASP1 site modifications in pro-IL-1β2, specifically, the molecular charge covering site-1 could potentially alter CASP1 processing of pro-IL-1β2 and therefore, availability of the mature, 17 kDa, form.

Interleukin-1 beta may be more susceptible to proteolysis by enzymes other than CASP1, such as proteinase K, when in its pro-form (Hailey et al., 2009). If the pro-form of IL-1β2 is more available it could provide a substrate for other proteases (Hailey et al., 2009). Interestingly, when Degrelle et al. (2009), conducted a proteomic analysis of elongating pig conceptuses, they detected the presence of multiple IL-1β proteins by 2D gel electrophoresis in combination with mass spectrometry. These proteins had molecular

weights ranging from ~36 to 14 kDa. Inspection of the mass spectrometry chromatograms revealed that three IL-1β proteins had molecular weights of approximately 36, 33 and 32 kDa. Four others may have had incomplete pro-domains, ranging in size from 28 to 22 kDa. One IL-1β protein was approximately 18 kDa and corresponded to the mature form. Two other smaller proteins, of approximately 14 kDa, were also detected. These proteins were referred to as IL-1β in this manuscript because IL-1β2 had not been discovered. Because we were unable to detect transcripts for IL-1β1 in pig conceptuses, these proteins are likely IL-1β2 (see Chapter Three). The detection of multiple IL-1β2 proteins with varying molecular weights could be the result of un-known protein modifications made by other enzymes and or altered CASP1 activity (Dinarello et al., 1996; Coeshott et al., 1999; Netea et al., 2010; Dinarello, 2011).

Processing of pro-IL-1β by CASP1 results in folding and activation of mature IL-1β. The structure of mat-IL-1β is described as a β trefoil or a tetrahedral barrel like structure with sides comprised of antiparallel beta strands, twelve in all (Priestle et al., 1988; Krumm et al., 2014). The trefoil structure and within, a hydrophobic core, is conserved among active members of the IL-1 superfamily of cytokines including IL-1A, IL-18, IL-33, and IL-1RA (Krumm et al., 2014). Mat-IL-1β1 and mat-IL-1β2 were predicted to have this conserved beta-trefoil structure (Fig. 5.6). Based on Novafold predictions, the mat-IL-1β1 structure has twelve β strands and three α helixes. The predicted mat-IL-1β2 structure also has twelve β strands but two α helixes. Alignment of the two structures resulted in a low RMSD (0.70 Å) indicating a high structural similarity between mat-IL-1β1 and mat-IL-1β2 (Fig. 5.5). However, structural alignments of mat-IL-1β1 or mat-IL-1β2 with other mammalian mat-IL-1β proteins, of which have less

sequence identity, have slightly lower RMSDs. For instance, alignment of mat-IL-1β2 with minke whale and mouse mat-IL-1β, which share a 78% and 67% sequence identity with mat-IL-1β2, resulted in RMSDs of 0.62 Å and 0.64 Å, respectively. This might suggest that despite a high degree of sequence similarity between mat-IL-1β1 and mat-IL-1β2 (92%), that a few amino acid substitutions have had a significant effect on the tertiary structure of these two proteins.

Based on interactions with the human IL-1RI, Novafold predicted 35 receptor-binding sites in mat-IL-1β1 and 32 in mat-IL-1β2 (Fig. 5.7). Interestingly, the three residues expected to interact with the IL-1RI in mat-IL1β1 but not the mat-IL1β2 are buried within the solvent accessible surface area of mat-IL1β1. However, binding studies between human mat-IL-1β and the human IL-1RI revealed that some residues in mat-IL-1β become available for binding after initial interactions with the receptor (Vigers et al., 1997). Sequence alignment of mat-IL-1β1 with mat-IL-1β2 revealed an inserted proline and five non-conserved amino acid substitutions in the mat-IL-1β2 sequence, 5 of these residues, including the proline, were suspected to be involved in receptor binding (Fig. 5.2; Fig. 5.8). Of these five residues, three substitutions resulted in a complete change of side change charge and structure in the mat-IL1β2 sequence (Fig. 5.10-5.12).

The first receptor binding substitution in mat-IL-1β2 includes a threonine (Thr^2) in place of an asparagine (Asn^2; mat-IL-1β1), both of which have polar uncharged side chains (Fig 5.9). This substitution comes directly adjacent to the inserted proline (Pro^3) within mat-IL-1β2, which is also predicted to be involved in receptor binding. Threonine commonly replaces other polar amino acids and is commonly found within functional areas (Betts and Russell, 2003). Proline is commonly found within tight turns and kinks

within alpha helixes and is the only amino acid where the side chain is connected to the protein backbone twice, forming a five-member ring (Betts and Russell, 2003). Because of this, proline is considered to be an imino rather than amino acid. Proline is rarely involved in receptor binding (Betts and Russell, 2003).

The second receptor binding substitution in mat-IL-1β2 includes the addition glutamic acid (glutamate; Glu^{16}) in place of a histidine (His^{15}; mat-IL1B1) with negative and positive charged side chains, respectively (Fig 5.10). Both histidine and glutamate have catalytic properties and are commonly involved in receptor binding, however, it is considered rare for a histidine to be replaced by any amino acid, practically one with an opposite charge (Betts and Russell, 2003). Residues in this location are considered to be important for receptor binding. Interestingly, human IL-1β has an uncharged glutamine in this location and its mutation to a glycine results in complete loss of receptor binding activity (Vigers et al., 1997).

The third and fourth receptor binding substitutions involve the exchange of a hydrophobic methionine (Met^{25}) and uncharged threonine (Thr^{33}) in mat-IL-1β1 for a negative charged glutamic acid (Glu^{26}) and positive charged lysine (Lys^{34}) in mat-IL-1β2, respectively (Fig. 5.11 and 5.12; respectively). Like glutamic acid, lysine is commonly found in protein binding sites (Betts and Russell, 2003).

Based on mutagenesis studies of human IL-1β, conserved amino acid mutations in many different receptor binding sites can result in a 30 to 50% reduction in binding activity (Vigers et al., 1997). Therefore, it can be hypothesized that alterations in the amino acid composition between mat-IL-1β1 and mat-IL-1β2, resulting in the loss of

receptor binding sites and the exchange of side chains with different charges, could have a significant effect on the activity of mat-IL-1β2 (Fig. 5.13).

SUMMARY AND CONCLUSION

In pigs, a duplication of the gene that encodes IL-1β has resulted in two distinct genes, IL-1β1 and IL-1β2. Expressed in blood leukocytes, IL-1β1 is the prototypical cytokine that controls innate and adaptive immune responses and IL-1β2 is a pregnancy specific cytokine expressed by the early pig conceptus. Both recombinant IL-1β1 and IL-1β2 activate NF-κB, a transcription factor commonly activated during IL-1β-IL-1RI signaling, in uterine surface epithelial cells. However, in regard to the epithelium, IL-1β2 appears to have less activity compared to IL-1β1. To investigate protein structural differences that may account for this, pro and mature IL-1β1 and IL-1β2 protein tertiary structures were predicted and aligned using DNASTAR's Novafold program. Compared with pro-IL-1β1, pro-IL-1β2 may have a less accessible CASP1 site-1 for processing into mature IL-1β2. Further, although both were predicted to bind the IL-1RI, compared with mat-IL1β1, mat-IL-1β2 is predicted to have less receptor binding sites and three non-conserved amino acid substitutions in receptor binding sites that affect the charge and structure of IL-1β2 in these locations. Overall, these modifications could potentially reduce the availably and activity of IL-1β2 compared with IL-1β1. To better understand role of IL-1β2 during early pregnancy in the pig investigations of IL-1β2's interactions with CASP1 and IL-1 signaling factors, IL-1R1 and IL-1RAP, are needed.

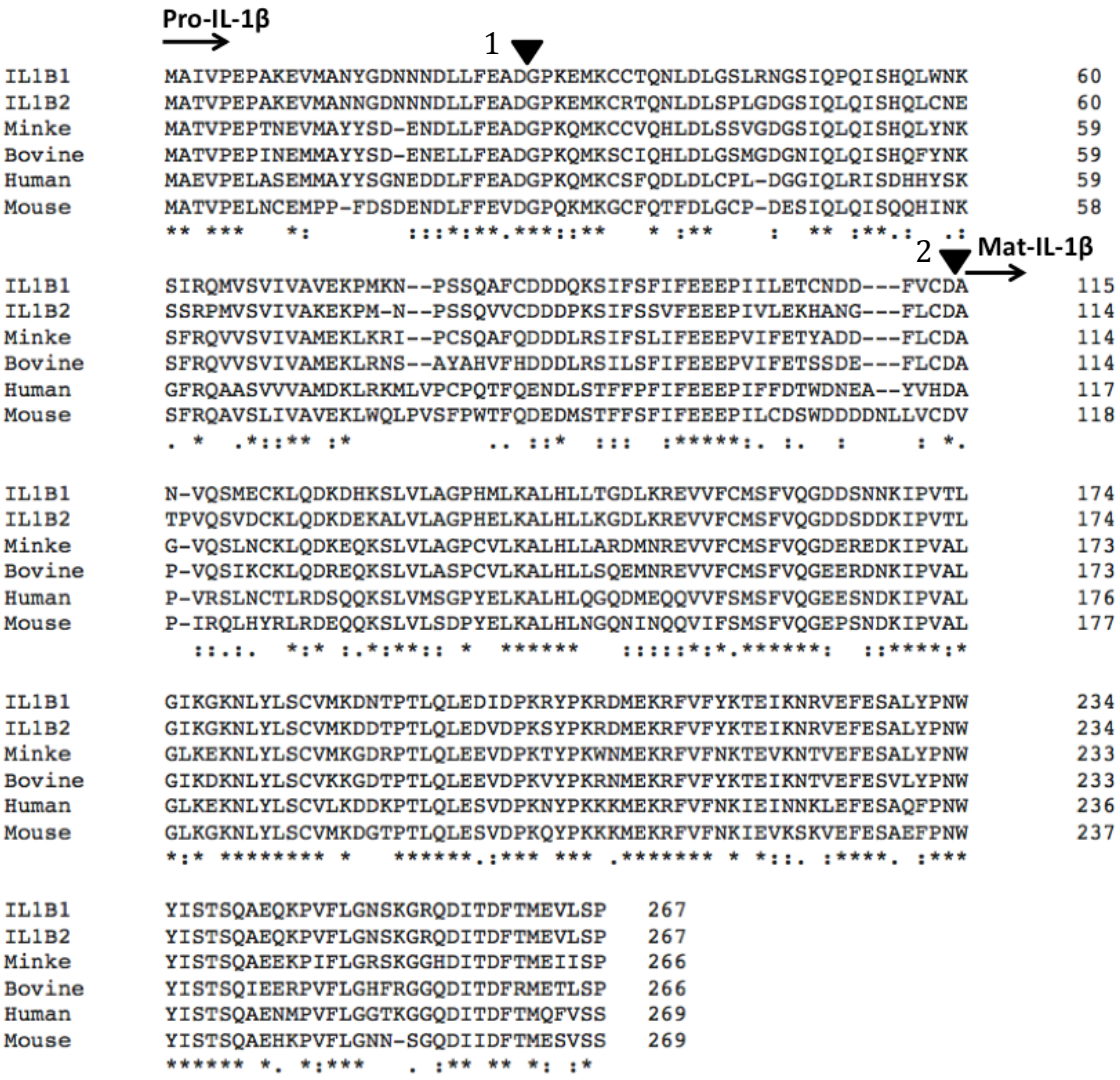

FIGURE 5.1 A multiple sequence alignment of full-length of pig (IL-1β1 and IL-1β2), minke whale, bovine, human and mouse IL-1β protein sequences using the Clustal Omega program. Dashes (-) in the sequences indicate amino acid deletions. Asterisks (*) below the sequences indicate fully conserved amino acids between the sequences. Colons (:) below the sequences indicate conservation of amino acids with strongly similar properties. Periods (.) below the sequences indicate conservation of amino acids with weakly similar properties. Solid arrows above the sequences indicate locations of sequential caspase-1 (CASP1) proteolytic sites (site-1 and site-2) during formation of the mature proteins. The right arrows above the sequences signify the start of the pro or mature protein regions. Using DNASTAR's Novafold program, tertiary structures were predicted for pig pro and mature IL-1β1 and IL-1β2 as well as minke whale, human and mouse mature IL-1β proteins. NCBI reference: IL-1β1, NP_999220.1; IL-1β2, NP_0010051949.1; Bovine, ABX72065.1; minke whale, XP_007197456.1; human, NP_000567.1; mouse, NP_032387.1.

FIGURE 5.2 Alignment of full-length IL-1β1 and IL-1β2 protein sequences in NCBI's blastp. Amino acids that are identical in IL-1β1 and IL-1β2 are displayed between the two sequences. Positive symbols (+) indicate conservative substitutions. The solid arrows above the sequences indicate locations of sequential caspase-1 (CASP1) protease cleavage sites (site-1 and site-2) during formation of the mature IL-1β1. The right arrows above the sequences signify the start of the pro or mature region. Periods (.) above and below the sequences indicted amino acids predicted to bind the IL-1RI in the mat-IL-1β1 and mat-IL-1β2 proteins, respectively. The numbers above and below the sequences indicate residues in the mat-IL-1β1 and mat-IL-1β2, respectively, that are not conserved between the two sequences and are predicted to bind the IL-1RI.

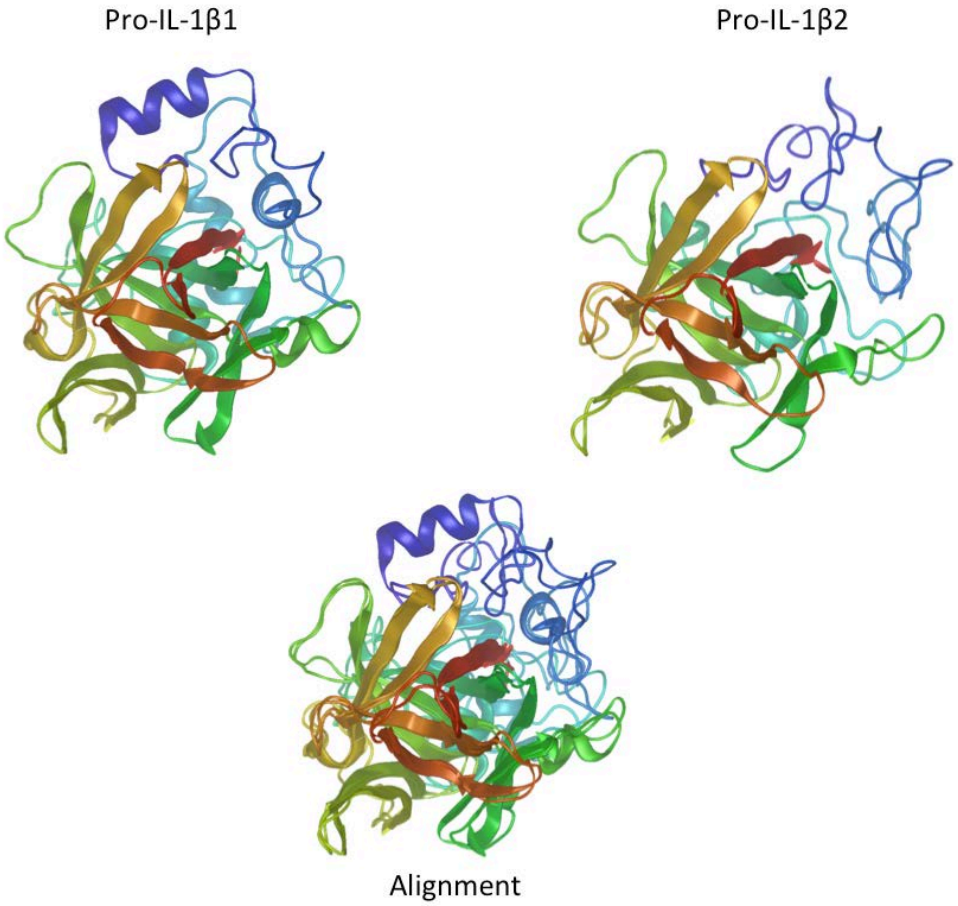

FIGURE 5.3 Ribbon model and ribbon model alignment of Novafold predicted tertiary structures of pro-IL-1β1 and pro-IL-1β2 proteins. The Novafold structure predictions of pro-IL-1β1 and pro-IL-1β2 received C-scores of -2.7 and -3.0, respectively. Alignment of the pro-structures resulted in an RMSD of 3.47 Å. Both predicted structures had 12 β strands that were located within the mature region. Compared with pro-IL-1β2, pro-IL-1β1 had a greater number of alpha helixes (2 and 7, respectively), five of which were located within the pro-region. Pro-IL-1β2 alpha helixes were also located in the pro-region.

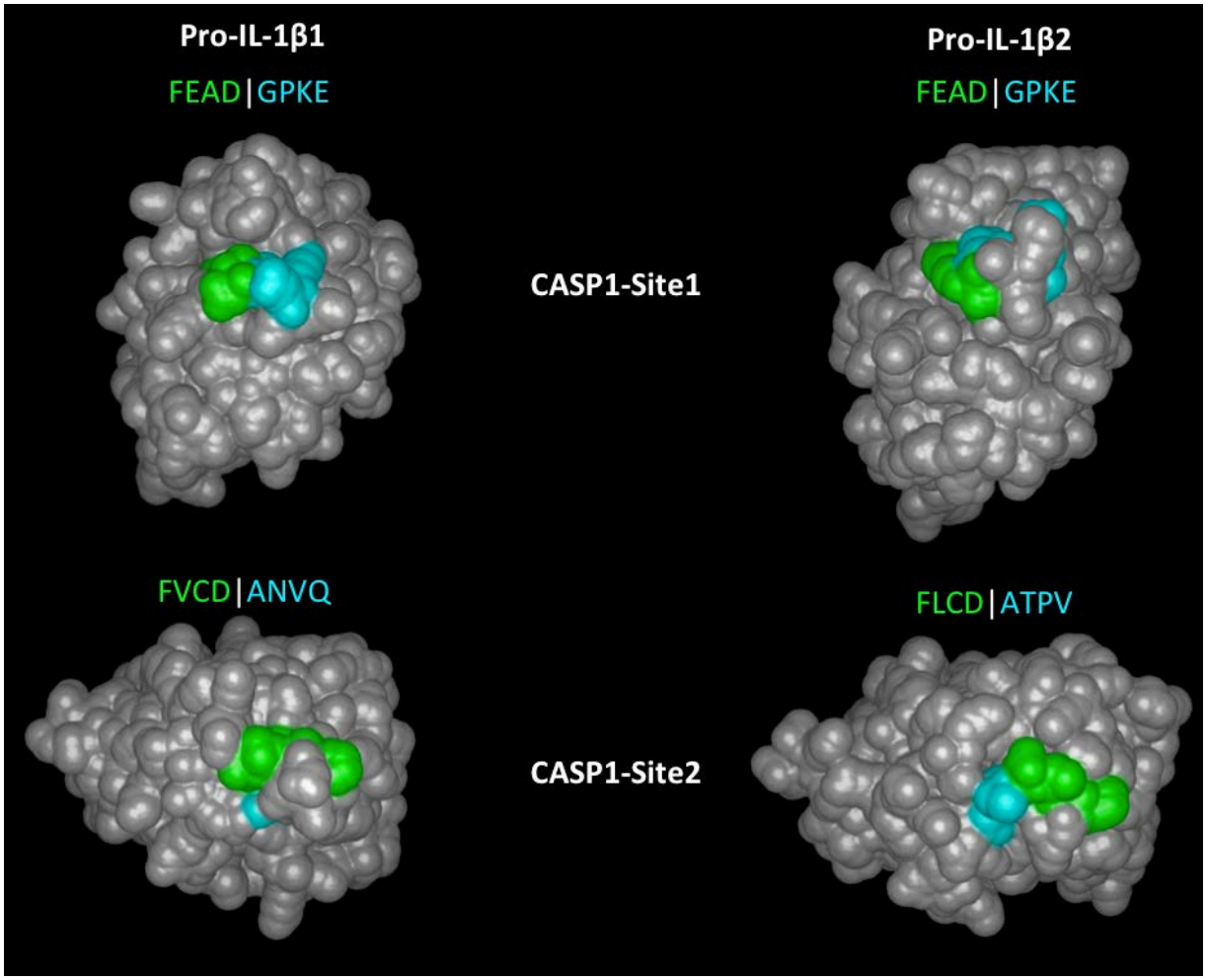

FIGURE 5.4 Solvent accessible surface areas of Novafold predicted pro-IL-1β1 (left) and pro-IL-1β2 (right) protein structures with caspase-1 (CASP1) site-1 (top structures) and site-2 (bottom structures) color filled (blue and green). Amino acids N-terminal and C-terminal to the CASP1 sites are color filled green and blue, respectively. Compared with pro-IL-1β1, pro-IL-1β2 has a large molecular structure, resembling a Y, covering CASP1 site-1. The opposite was true for CASP1 site-2. There, a large molecular structure covers CASP1 site-2 in pro-IL-1β1 but not pro-IL-1β2. The bottom structures are the top structures rotated 180° around a vertical axis and tilted to the right 90°.

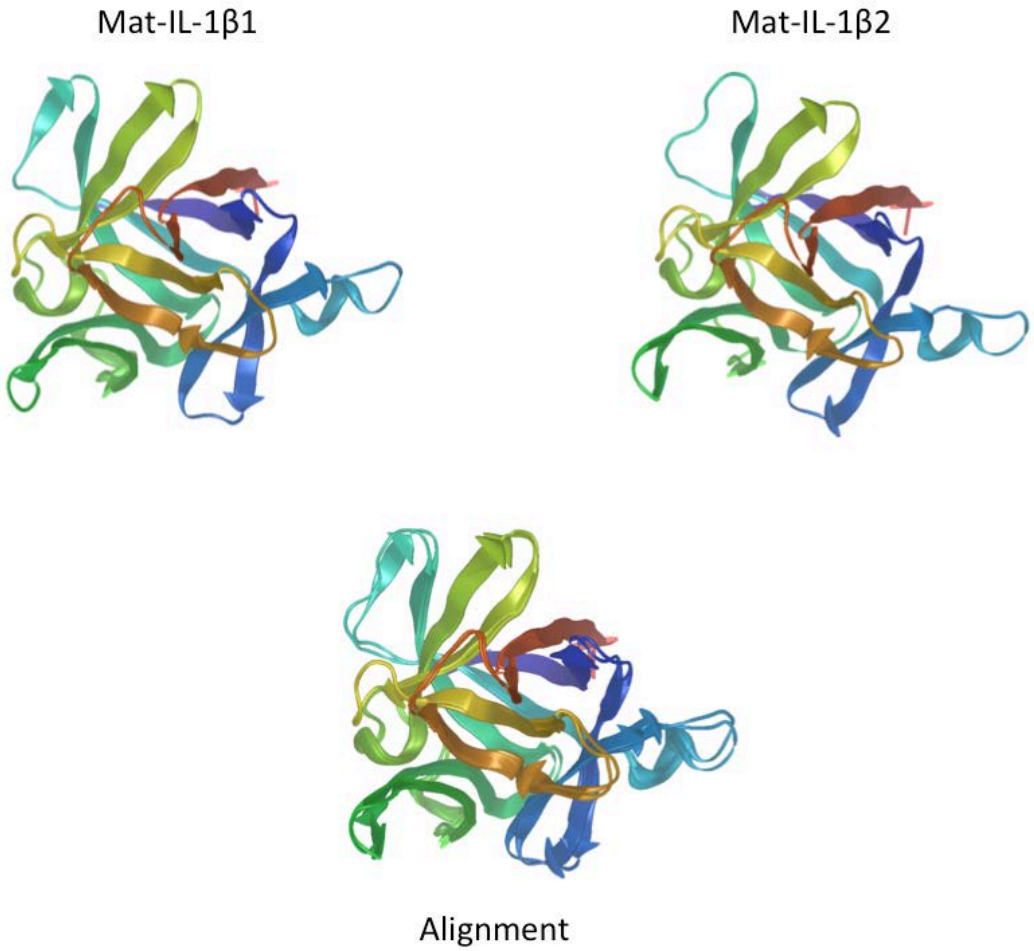

FIGURE 5.5 Ribbon model structures and ribbon model alignment of Novafold predicted pig mat-IL-1β1 and mat-IL-1β2. Novafold predictions of mat-IL-1β1 and mat-IL-1β2 received C-scores of 1.9 and 1.8, respectively. Alignment of mature structures resulted in an RMSD of 0.70 Å, indicating that the predicted structures were very similar in the absence of the pro-domain. Mat-IL-1β1 and mat-IL-1β2 consisted of 12-β strands and three and two alpha helixes, respectively.

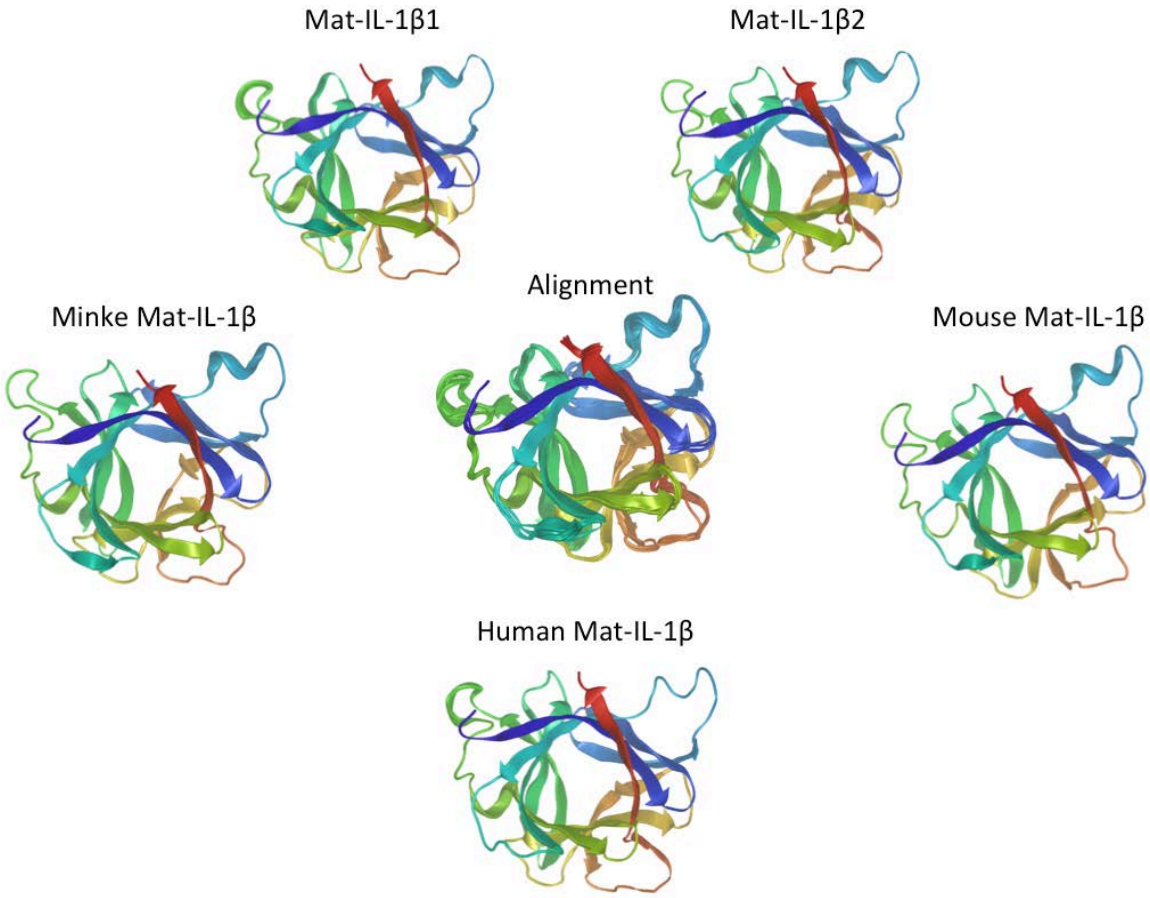

FIGURE 5.6 Ribbon model structures and ribbon model alignment of Novafold predicted pig mat-IL-1β1 and mat-IL-1β2 as well as minke whale, human and mouse mat-IL-1β proteins rotated to observe the characteristic IL-1 superfamily of cytokines β trefoil. Novafold structure predictions of all mature IL-1β proteins received C-scores of ≥ 1.8.

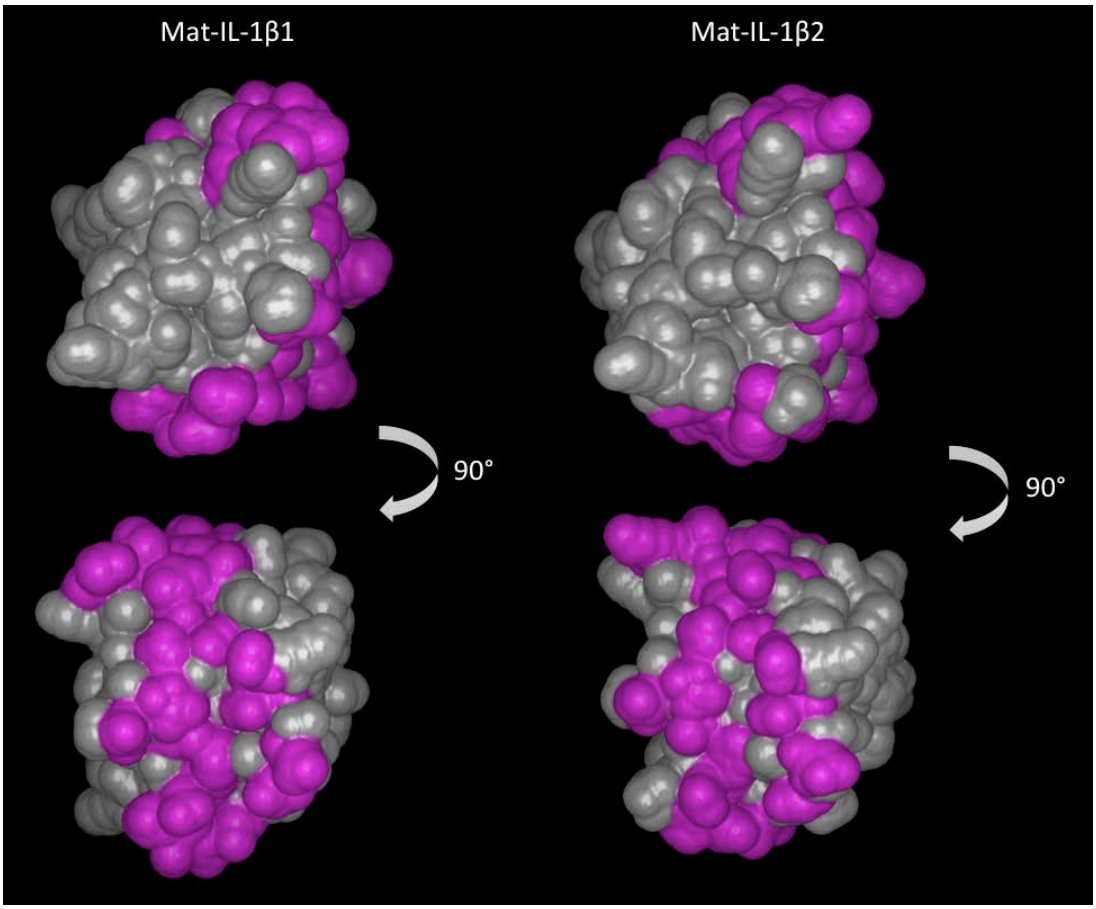

FIGURE 5.7 Solvent accessible surface area of mat-IL-1β1 (left) and mat-IL-1β2 (right) with residues predicted to be involved in receptor binding color filled (pink). The IL-1RI ecto-domain resembles a question mark in shape that wraps around IL-1β during binding, clenching the cytokine like a hand forming a C.

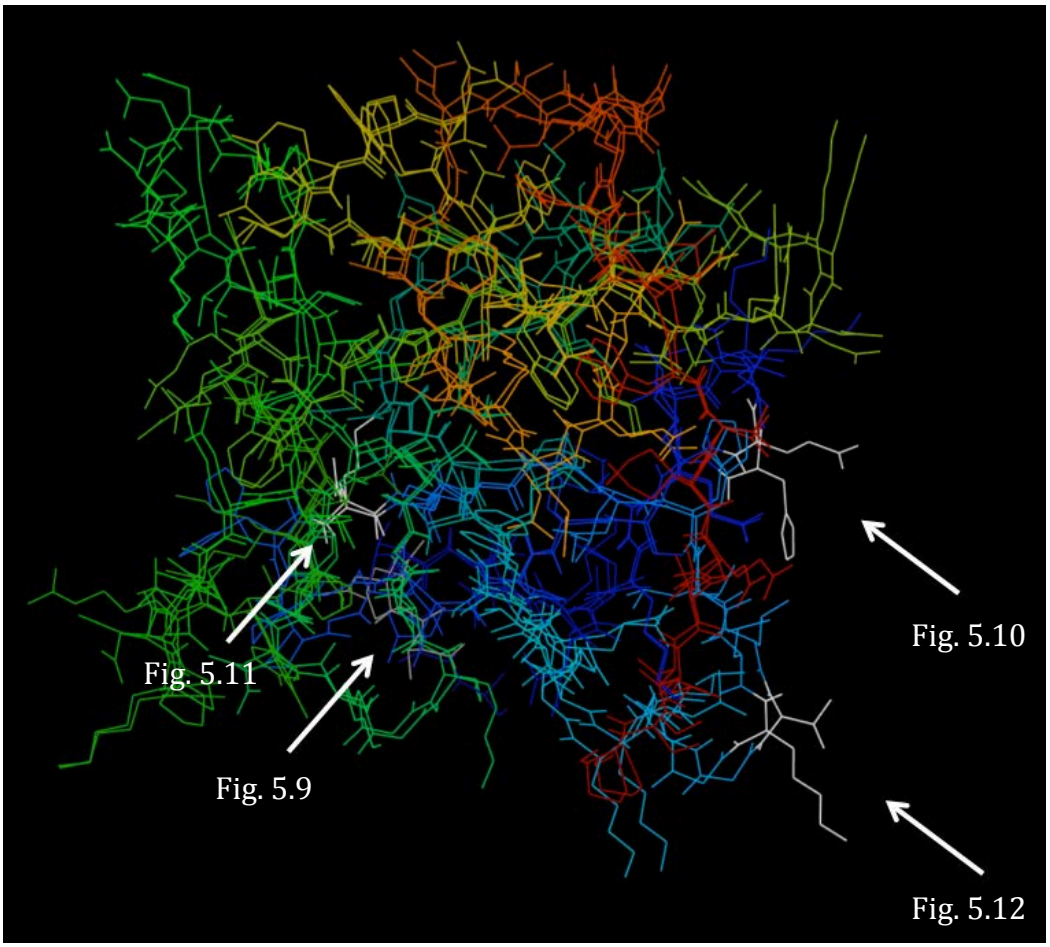

FIGURE 5.8 Wire frame models of Novafold predicted and aligned mat-IL-1β1 and mat-IL-1β2 proteins. The arrows indicate locations of non-conserved amino acid substitutions (white) between mat-IL-1β1 and mat-IL-1β2 predicted to be involved in receptor binding and depicted in Figures 5.9-5.12.

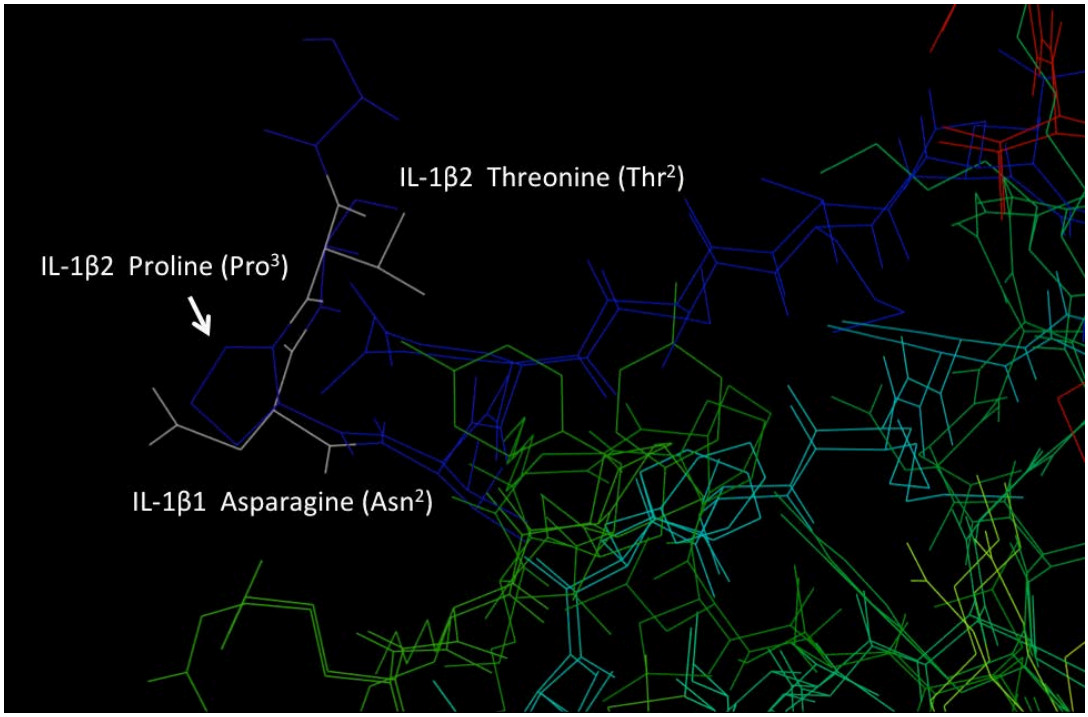

FIGURE 5.9 Receptor binding location of aligned mat-IL-1β1 and mat-IL-1β2 wire frame models where the first non-conserved amino acid substitution has occurred with the addition of an inserted proline (pro^3) in the mat-IL-1β2 sequence. At the second residue, the mat-IL-1β2 sequence has substituted a threonine (Thr^2) in place of an asparagine (mat-IL-1β1; Asn^2), both of which have polar uncharged side chains.

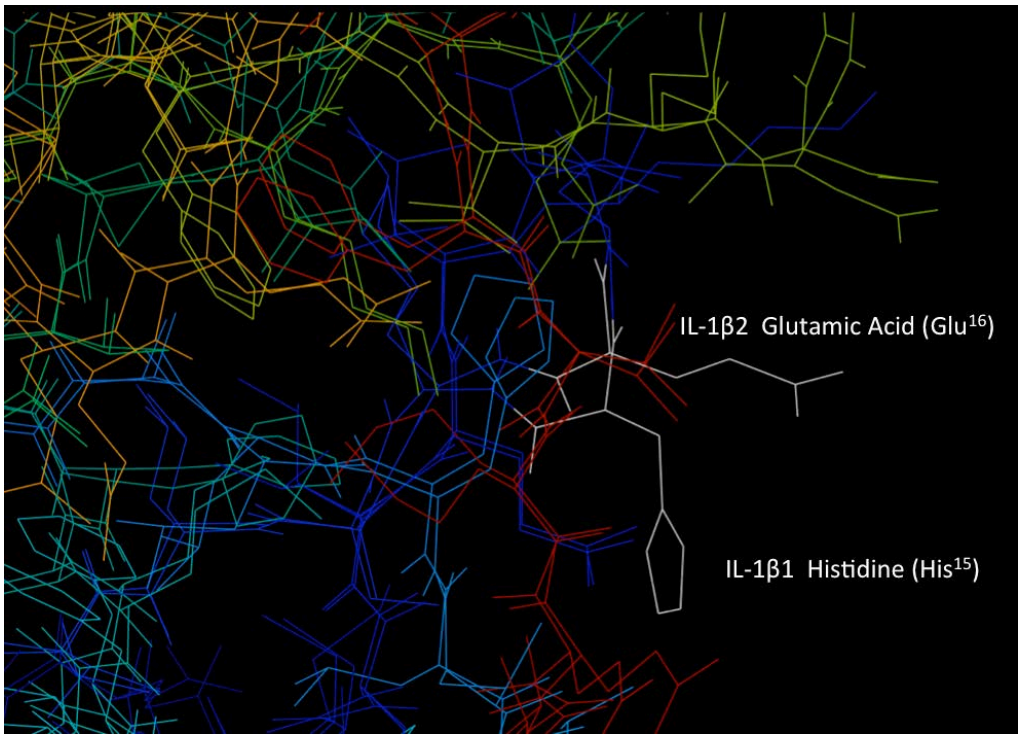

FIGURE 5.10 Receptor binding location of aligned mat-IL-1β1 and mat-IL-1β2 wire frame models where the second non-conserved amino acid substitution has occurred between mat-IL-1β1 and mat-IL-1β2. In this location, the mat-IL-1β2 sequence has a glutamic acid (glutamate; Glu^{16}) substituted for a histidine (mat-IL-1β1; His^{15}) with negative and positive charged side chains, respectively. Both histidine and glutamate have catalytic properties and are commonly involved in receptor binding. However, it is considered uncommon for a histidine to be substituted for another amino acid, specifically one with an opposite charged side chain (Betts and Russell, 2003). Mutations of this receptor-binding site in human IL-1β result in a complete loss of activity (Vigers et al., 1997).

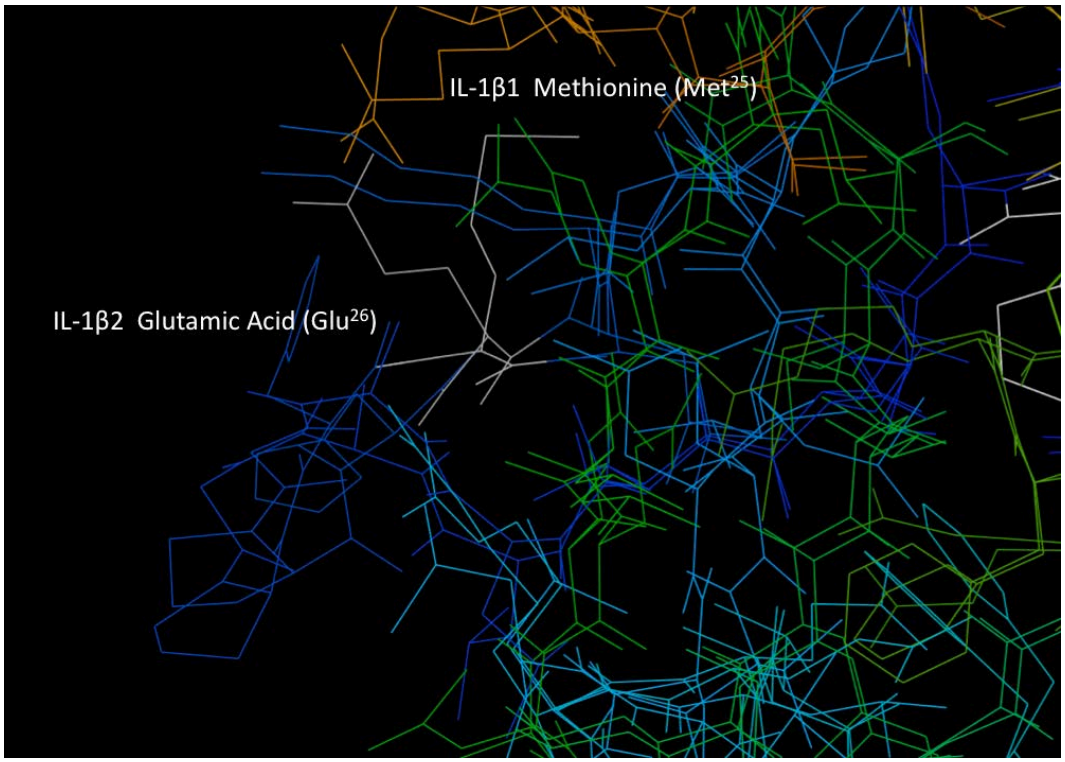

FIGURE 5.11 Receptor binding location of aligned mat-IL-1β1 and mat-IL-1β2 wire frame models where the third non-conserved amino acid substitution has occurred between the two sequences. In this location, the mat-IL-1β2 sequence has a glutamic acid (Glutamate; Glu^{26}) substituted for methionine (mat-IL-1β1; Met^{25}) with negative charged and hydrophobic side chains, respectively.

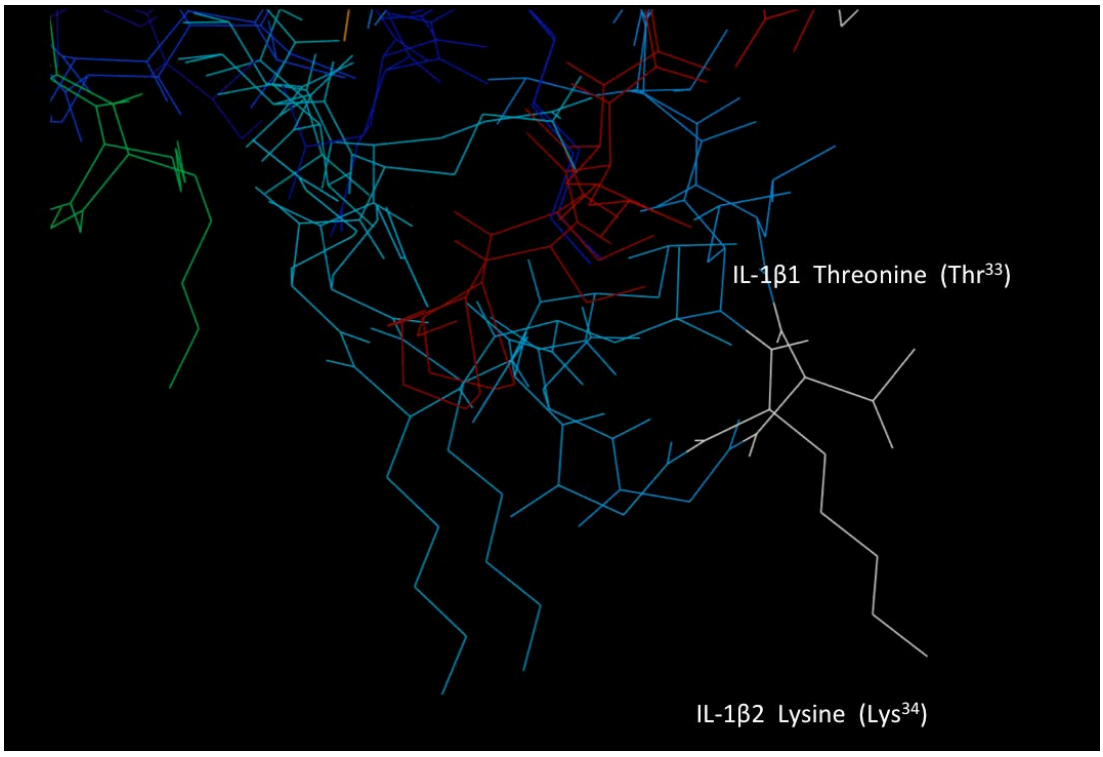

FIGURE 5.12 Receptor binding location of aligned mat-IL-1β1 and mat-IL-1β2 wire frame models where a fourth non-conserved amino acid substitution has occurred between the two sequences. In this location, the mat-IL-1β2 sequence has a lysine (lys^{34}) substituted for a threonine (Thr^{33}) with a positive charged and polar uncharged side chains, respectively.

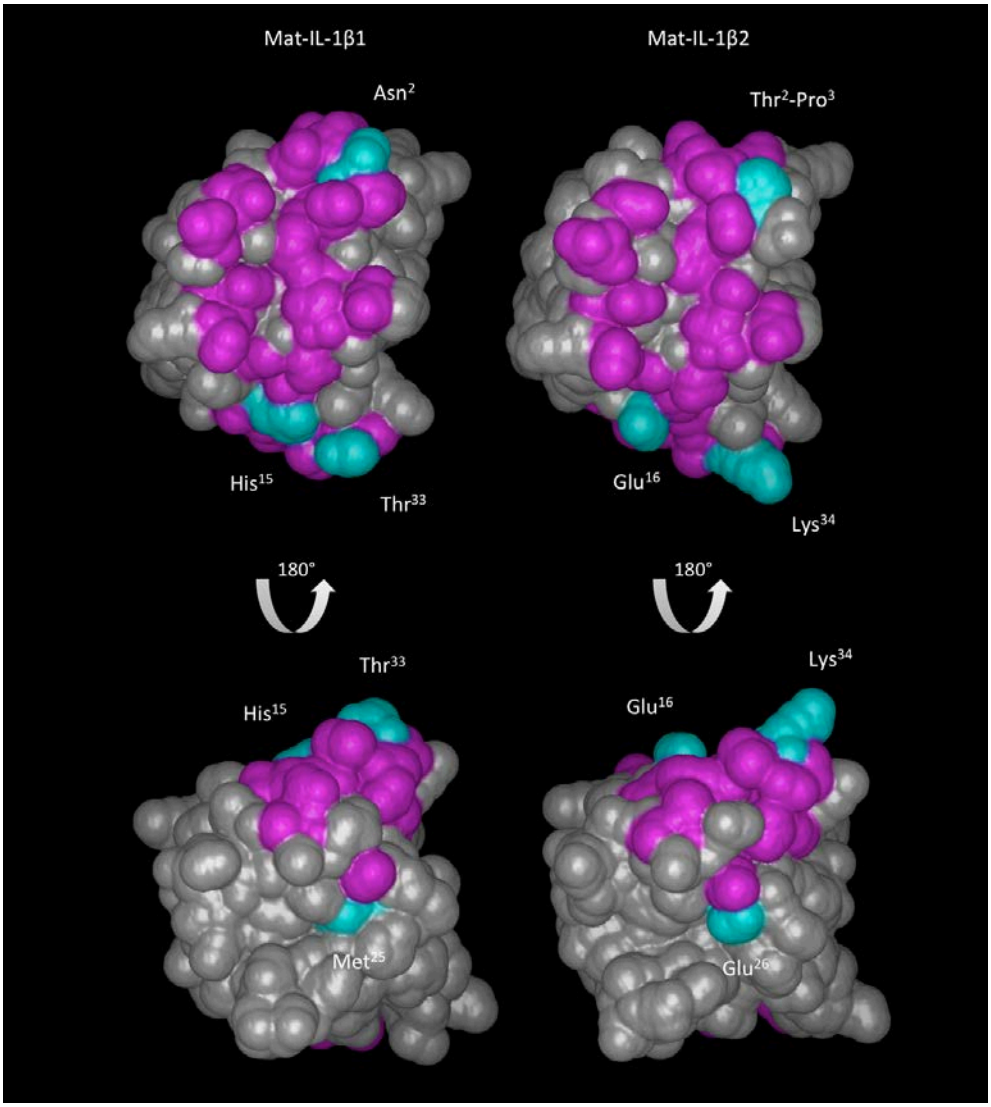

FIGURE 5.13 Solvent accessible surface areas of Novafold predicted mat-IL-1β1 (left) and mat-IL-1β2 (right) proteins with receptor binding sites (pink and blue) and non-conserved amino acid substitutions (with addition of inserted proline; mat-IL-1β2), depicted in Figures 5.9-5.12, in locations of receptor binding color filled blue. Considerable morphological differences in the solvent accessible surface areas were detected in these receptor-binding locations between mat-IL-1β1 and mat-IL-1β2, specifically between residues 33 and 34, respectively.

CHAPTER SIX

CONCLUSIONS AND FUTURE DIRECTIONS FOR RESEARCH

Embryo implantation in mammals requires apposition and attachment of the early embryo to the uterine surface for nutrient support during development in the mother. It is a phasic, non-reversible, process that includes intricate chemical communication and physical interactions between the foreign conceptus trophoblast cells and cells that make up the maternal endometrium. Although the mode of placentation can vary considerably between species the events that modulate early embryonic development, uterine receptivity and conceptus attachment appear to be more conserved. These events are no less complex, however, and are absolutely necessary for embryonic survival. Investigations of early pregnancy in primates, rodents and agricultural animals, including pigs, can help delineate essential, and yet, elusive factors that control these processes.

The study of early pregnancy in mammals has expanded drastically since Leo Loeb first reported, over 100 years ago, that endometrial trauma could promote decidualization in the guinea pig (Loeb, 1907; Dekel et al., 2010; Granot et al., 2012). We now know that pro-inflammatory cytokines are released by the mammalian conceptus and/or the endometrium and have essential functions during establishment of pregnancy.

As reviewed in Chapter One, observations made during recent human clinical studies, ironically similar to those described by Loeb during his studies with the guinea pig, support these conclusions (Dekel et al., 2010; Granot et al., 2012).

Interleukin-1 beta (IL-1β) is a pro-inflammatory cytokine that promotes early conceptus development, endometrial receptivity for attachment and trophoblast invasion during primate and rodent implantation (Simón et al., 1995; 2008). The IL-1β transcript is first translated into pro-IL-1β protein, which is then processed by the cysteine protease, caspase-1 (CASP1) into a mature functional cytokine (mat-IL-1β) (Hailey et al., 2009). The mat-IL-1β functions by binding the IL-1RI in the target cell membrane and activating NF-κB, a group of transcription factors that commonly modulate gene expression and cell biology during infection, injury and cell stress (Sims and Smith, 2010; Dinarello, 2011; Garlanda 2013). An IL-1β is also expressed by the pig conceptus prior to implantation (Tuo et al., 1996; Ross et al., 2003a). Expression of the IL-1β is temporally associated with elongation, a morphological change of the conceptus near d 12 of pregnancy that greatly expands the placental surface area before attachment (Tuo et al., 1996; Ross et al., 2003a). The IL-1RI and IL-1RAP are temporally expressed within the conceptus and uterine surface epithelium at that time, suggesting that the IL-1β promotes conceptus elongation and uterine receptivity for implantation (Ross et al., 2003a). Further, NF-κB is strongly activated within uterine surface epithelial cells directly adjacent to elongating pig conceptuses (Mathew et al., 2011). Interleukin-1 beta and NF-κB likely create a pro-inflammatory environment in the endometrium that enhances adhesion molecule expression, blood vessel permeability and cell motility for trophoblast migration and endometrial remodeling.

In pigs, the gene encoding IL-1β has duplicated resulting in two genes, IL-1β1 and IL-1β2, which are tandem within the pig genome (Groenen et al., 2012). Based on experiments conducted in Chapter Three, IL-1β1 is the prototypical cytokine and is expressed by blood leukocytes and other adult tissues. The IL-1β2, a novel IL-1, is abundantly and probably exclusively expressed by the elongating pig conceptus. Aside from its pattern of expression during elongation, little is known about *IL-1β2* or its product as IL-1β2 was recently discovered and functional studies have not been conducted. A protein modeling study did suggest that IL-1β2 might have a different binding efficiency for the IL-1RI compared with IL-1β1 (Katebi et al., 2010).

In Chapter Three, we verified expression of IL-1β2 in the elongating pig conceptus and expressed pro and mature IL-1β1 and IL-1β2 proteins *in vitro*; testing their activity with respect to activation of NF-κB and NF-κB-regulated gene expression within the endometrium. In Chapter Four, we developed a lentiviral mediated RNAi system to knockdown translation of IL-1β2 in early pig conceptuses so that we could test IL-1β2's influence on elongation *in vivo*. In Chapter Five, we used DNASTAR's Novafold program to predict and align the atomic structures of pro and mature IL-1β1 and IL-1β2. We then used this program to predict mat-IL-1β2's ligand-receptor interactions and compared these predicted binding sites to that of mat-IL-1β1.

Observations made during experiments in Chapter Three suggest that IL-1β2 is exclusively expressed by the elongating pig conceptus and that recombinant mat-IL-1β2 has the capacity to activate the p65 subunit of NF-κB within the uterine surface epithelium. However, within the endometrium, mat-IL-1β2 had a lesser capacity to activate NF-κB and up regulate NF-κB-responsive genes compared with mat-IL-1β1.

Interestingly, this was not true for alveolar macrophages in which there was greater NF-κB nuclear trans-location in response to mat-IL-1β2 compared with mat-IL-1β1. Based on Novafold predicted protein structures (Chapter Five), mature IL-1β2 has three less IL-1RI binding sites and three non-conserved amino acid substitutions in locations of shared binding sites that result in a different side chain charge and solvent accessible surface area compared with mat-IL-1β1. These modifications could have a significant effect on mat-IL-1β2's interaction with the IL-1RI compared to mat-IL-1β1 and may account for differences in activity observed within the endometrium. Further, the tertiary structure of pro-IL-1β2 is predicted to be different than that of pro-IL-1β1 (RMSD; 3.47 Å) which could affect processing of the pro-protein and folding of mat-IL-1β2 compared with IL-1β1. Interestingly, pro-IL-1β2 did have a large molecular configuration covering the CASP1 site-1 compared with pro-IL-1β1. These differences in protein structure could affect the activity as well as the availability of mat-IL-1β2.

If IL-1β2 does have reduced activity, this cytokine could provide a less intense inflammatory-like response within the endometrium that, if too strong, could be detrimental to pregnancy. Further, because pig conceptuses compete within the endometrium for uterine space, release of an IL-1β with a reduced activity could enhance each individual conceptus's development and inflammatory-like microenvironment without promoting development and implantation of near by conceptuses.

Interleukin-1 beta 2's interaction with other trans-membrane receptors could explain the differences in NF-κB activation observed within the alveolar macrophages compared with the uterine surface epithelium. No other receptors, however, were predicted by Novafold to interact with IL-1β2 besides the IL-1RI. If IL-1β2 does interact

with signaling factors other than IL-1RI, this could greatly expand the influence this cytokine has on establishment of pregnancy in the pig. Further, because this response was observed in macrophages and because the pig endometrium contains various types of leukocytes, including macrophages, this could mean that conceptuses release IL-1β2 to specifically modulate immune cell activity within the endometrium. Further experiments are needed to validate these findings.

In Chapter Four, we were unable to test the function of IL-1β2 on elongation of the conceptus using lentiviral mediated RNAi. This technique had an overwhelming negative effect on development of the conceptus and pregnancy by Day 13. Expression of IL-1β2 was detected in the Day 6 pig blastocyst suggesting that IL-1β2 may have functions in embryonic development much earlier than suspected and prior to elongation (Fig 6.1). Further research is needed to determine if the Day 6 pig blastocyst has IL-1RI protein.

As a final conclusion, we hypothesize that pig conceptuses release IL-1β2 at the fetal-maternal interface to act in a paracrine fashion, creating a balanced pro-inflammatory environment within the local endometrium by activating NF-κB in the adjacent uterine surface epithelium and glandular epithelium. There, we hypothesized that NF-κB up regulates genes that are essential for conceptus development and uterine receptivity for implantation (Fig. 6.2). These genes might include PTGS2, β3 integrin, LIF, and IL-6. Crosstalk between NF-κB, IP3K and MAPK signaling pathways are common and activation of the latter two pathways could further enhance implantation (Fig. 6.2). The uterine surface epithelium expresses the estrogen receptor (ESR1) meaning that conceptus estrogens, released during maternal recognition of pregnancy,

could further influence these events. Lastly, because the d 6 pig conceptus expresses IL-1β2 of which increases greatly during elongation (near d 12 of pregnancy), this cytokine could have an autocrine effect on the conceptus that persists for over a week as it continues to develop, un-attached, in the uterine lumen (Fig. 6.1). These effects may culminate near d 12 of gestation as the conceptus transitions from its spherical to filamentous form (Fig. 6.1).

Further research is needed to fully extrapolate the effects of IL-1β2 on establishment of pregnancy in the pig. These experiments should be geared toward elucidating the hypothesized autocrine effect of IL-1β2 on development and elongation of the conceptus. We were unsuccessful in using Lentiviral mediated RNAi, however, the new CRISPR/Cas9 system may prove to be an effective method for developing conceptuses with complete ablation of IL-1β2. Other experiments might include the study of CASP1-pro-IL-1β2 protease activity and uterine infusion of IL-1β2 followed by endometrial RNAseq analysis. The latter experiment could include the addition of estrogens and NF-κB inhibitors to better understand the combined effects of these factors during implantation in the pig.

Considering IL-1 has important functions during implantation in primates, rodents and pigs, a time when most embryonic mortality occurs in these species, further research of the IL-1 signaling system and activation of downstream factors, including NF-κB, could greatly benefit our understanding of establishment of pregnancy.

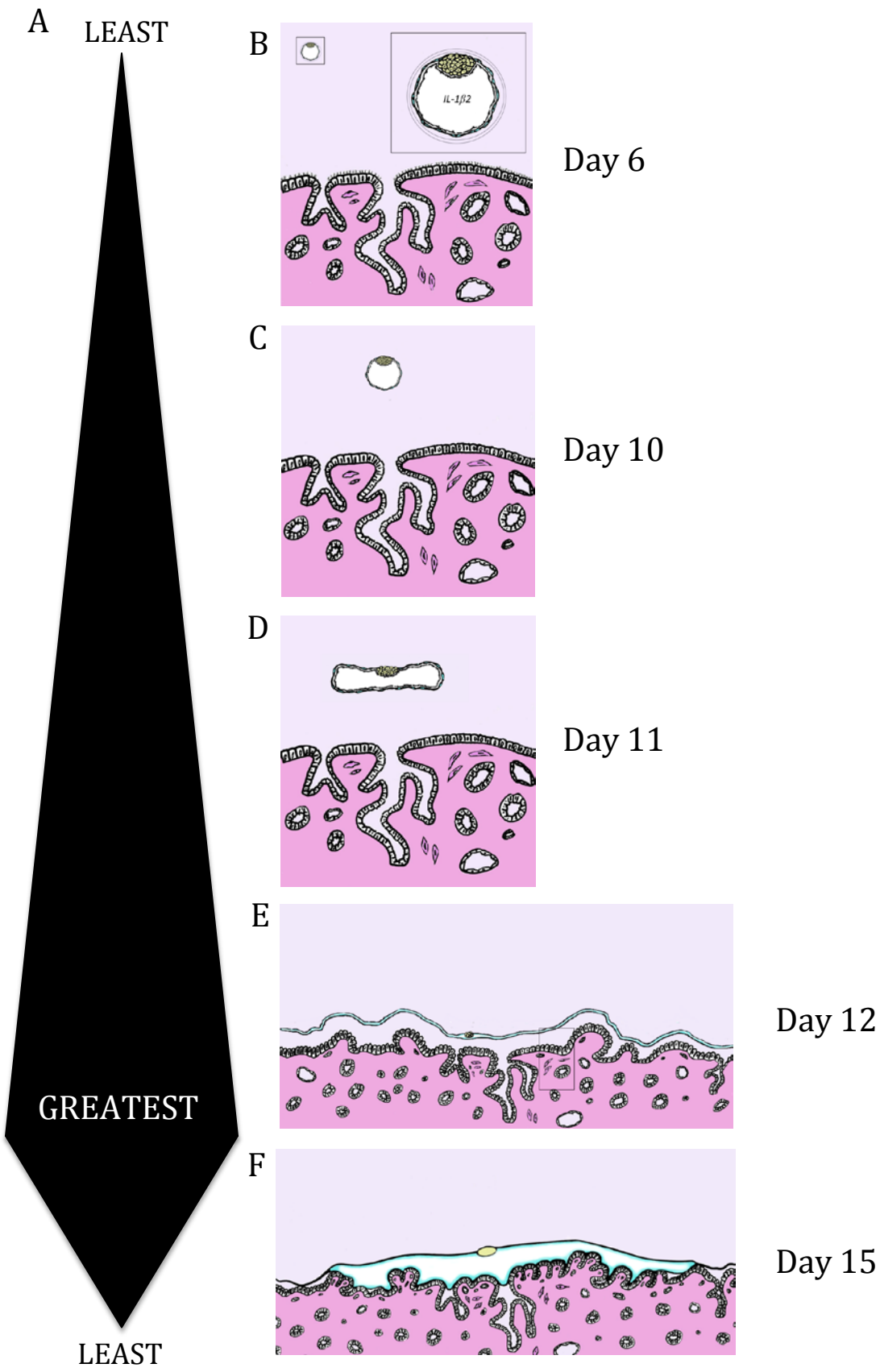
A
LEAST
GREATEST
LEAST
B
IL-1β2
Day 6
C
Day 10
D
Day 11
E
Day 12
F
Day 15

FIGURE 6.1 A working model representing the hypothesized pattern of expression of interleukin-1 beta 2 (IL-1β2) in the early pig conceptus. (A) Still within the zona pellucida, the day (d) 6 pig blastocyst (B; LEAST) expresses IL-1β2 of which increases over time (B-D) becoming maximum during conceptus elongation on d 12 of development (E; GREATEST). After elongation (d 12), expression of IL-1β2 decreases 2000 fold and is undetectable in the d 15 implanting conceptus (F; LEAST). IL-1β2 protein can be detected within the uterine lumen on d 15 but concentrations are nadir by d 18 of gestation.

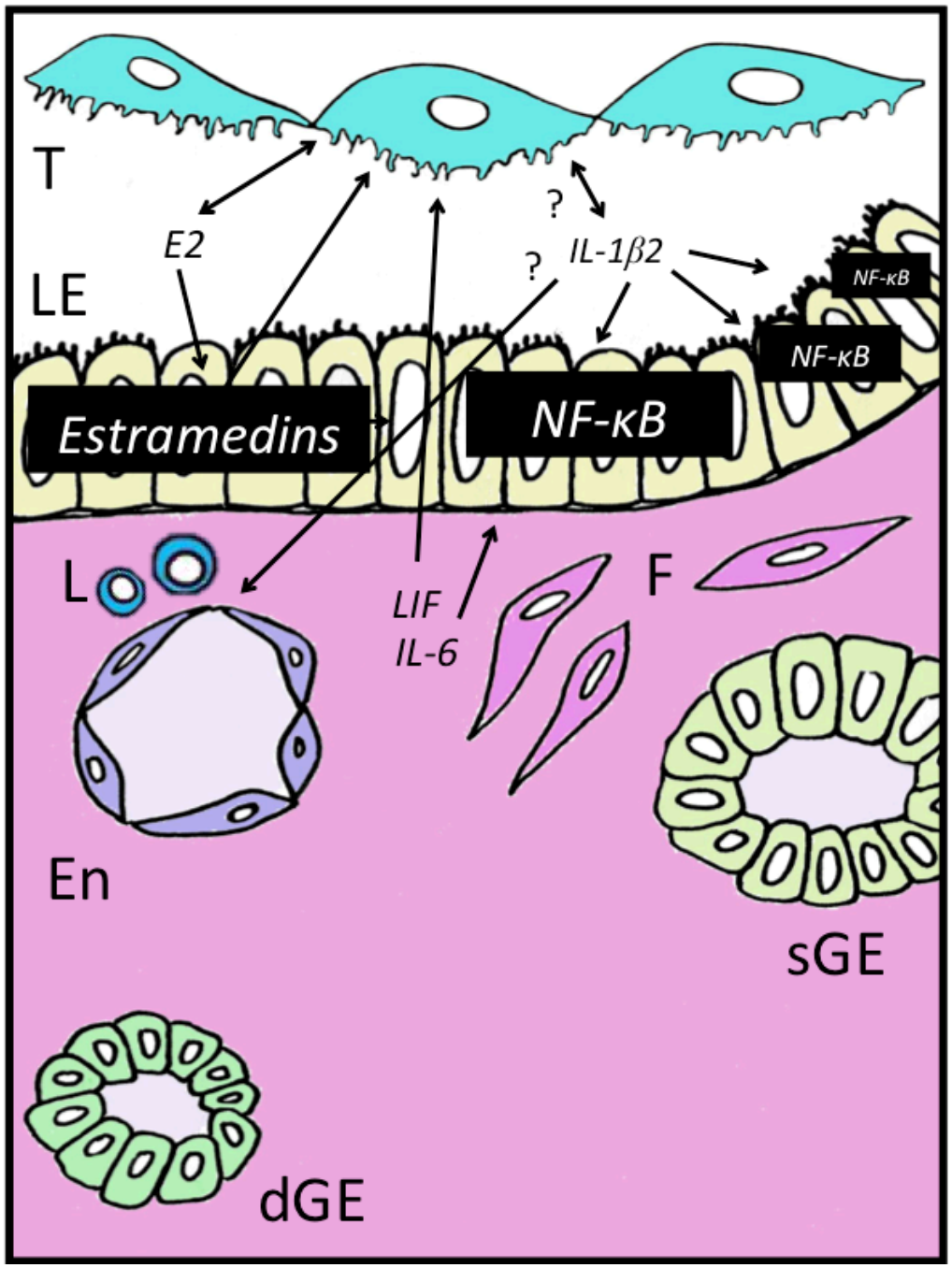
T
LE
E2
?
?
IL-1β2
NF-κB
NF-κB
Estramedins
NF-κB
L
LIF
IL-6
F
En
sGE
dGE

FIGURE 6.2 A working model of hypothesized autocrine and paracrine functions of interleukin-1 beta 2 (IL-1β2) and estradiol (E2) during elongation of the pig conceptus on d 12 of development (see Fig. 6.2E inset box). As described in Chapter Two Figure 2.2, auto-down regulation of progesterone receptors (PGRs) by progesterone in the uterine luminal (LE) and surface glandular epithelium (sGE) decreases expression of mucin-1 (MUC-1), a large glycoprotein, along the uterine surface. This enhances uterine receptivity and allows for conceptus attachment after d 13. During elongation, conceptus trophoblast (T) cells release E2 and other estrogens as the maternal recognition of pregnancy signal. Within the LE, estrogen receptors are hypothesized to increase expression of estramedins such as fibroblast growth factor 7 or secreted phosphoprotein 1. These factors are believed to enhance conceptus development, LE-T adhesion and implantation. Elongating pig conceptuses abundantly release IL-1β2, a novel IL-1, which likely acts on the conceptus and the adjacent LE and sGE through the interleukin-1 receptor type I. Compared with the prototypical IL-1β (IL-1β1 in the pig) IL-1β2 may have less activity within the endometrium but can activate the transcription factor nuclear factor-kappa B (NF-κB; p65 subunit). Crosstalk between NF-κB, mitogen-activated protein kinase (MAPK) and inositol 1, 4,5-triphosphate 3-kinase (IP3K) signaling pathways may enhance uterine receptivity for implantation. Activated NF-κB likely increases transcription of NF-κB-responsive genes such prostaglandin-endoperoxide synthase 2 for production of prostaglandins as well as leukemia inhibitory factor (LIF) or interleukin-6 (IL-6) within the adjacent endometrium. These factors likely bind receptors within the conceptus and LE, further promoting implantation. By stimulating the release of factors from LE or by passing through the LE barrier into the underling stroma, it's hypothesized that IL-1β2 influences endometrial leukocytes (L) and endothelial (En) cells, altering immune cell function/motility and increasing blood vessel permeability, respectively. Overall, IL-1β2 is hypothesized to create a balanced pro-inflammatory microenvironment at the fetal maternal interface that enhances conceptus development, uterine receptivity and implantation. dGE, deep glandular epithelium; F, stroma fibroblast.

BIBLIOGRAPHY

Abbas AK, Lichtman AH, Pillai S. Cellular and molecular immunology. Philadelphia: Saunders Elsevier; 2007.

Abbondanzo SJ, Cullinan EB, McIntyre K, Labow M, Stewart C. Reproduction in mice lacking a functional type 1 IL-1 receptor. Endocrinology 1996; 137:3598-3601.

Allen R. Non-classical immunology. Genome Biology 2001; 2:reports4001.1-4004.4

Ashkar AA, Di Santo JP, Croy BA. Interferon gamma contributes to initiation of uterine vascular modification, decidual integrity and uterine natural killer cell maturation during normal murine pregnancy. J Exp Med 2000; 192: 259-270.

Ashworth MD, Ross JW, Hu J, White FJ, Stein DR, Desilva U, Johnson GA, Spencer TE, Geisert RD. Expression of porcine endometrial prostaglandin synthase during the estrous cycle and early pregnancy, and following endocrine disruption of pregnancy. Biol Reprod 2006; 74:1007-1015.

Ashworth MD, Ross JW, Stein DR, White FJ, DeSilva UW, Geisert RD. Endometrial caspase 1 and interleukin-18 expression during the estrous cycle and peri-implantation period of porcine pregnancy and response to early exogenous estrogen administration. Reprod Biol Endocrinol 2010; 8:33.

Bamberger A, Erdmann I, Bamberger CM, Jenatschke SS, Schulte HM. Transcriptional regulation of the human 'leukemia inhibitory factor' gene: modulation by glucocorticoids and estradiol. Mol Cell Endocrinol 1997; 127:71-79.

Barañao RI, Piazza A, Rumi LS, Polak de Fried E. Interleukin-1β levels in human embryo culture supernatants and their predictive value for pregnancy. Early Hum Dev 1997; 48:71-80.

Basha SM, Bazer FW, Roberts RM. Effect of the conceptus on quantitative and qualitative aspects of uterine secretion in pigs. J Reprod Fertil 1980; 60:41-48.

Bauer BK, Spate LD, Murphy CN, Prather RS. Arginine supplementation in vitro increases porcine embryo development and affects mRNA transcript expression. Reprod Fertil Dev 2011; 23:107.

Bazer FW. Pregnancy recognition signaling mechanisms in ruminants and pigs. J Anim Sci Biotechnol 2013; 4:23

Bazer FW, Geisert RD, Thatcher WW, Roberts RM. The establishment and maintenance of pregnancy. In: Cole DJA and Foxcroft GR. (eds), Control of Pig Reproduction. London: Butterworth Scientific; 1982:227-252.

Bazer FW, Johnson GA. Pig-blastocyst-uterine interactions. Differentiation 2014; 87:52-65.

Bazer FW, Song G, Kim J, Dunlap KA, Satterfield MC, Johnson GA, Burghardt RC, Wu G. Uterine biology in pigs and sheep. J Anim Sci Biotechnol 2012; 3:23

Bazer FW, Spencer TE, Johnson GA, Burghardt RC, Wu G. Comparative aspects of implantation. Reproduction 2009; 138:195-209.

Bazer FW, Spencer TE, Ott TL. Interferon tau: a novel pregnancy recognition signal. Am J Reprod Immunol 1997; 37:412-20.

Bazer FW, Thatcher WW. Theory of maternal recognition of pregnancy in swine based on estrogen controlled endocrine versus exocrine secretion of prostaglandin F2alpha by the uterine endometrium. Prostaglandins 1977; 14:397-401.

Bazer FW, Wu G, Johnson GA, Kim J, Song G. Uterine histotroph and conceptus development: Select nutrients and secreted phosphoprotein 1 affect MTOR cell signaling in ewes. Biol Reprod 2011; 85:1094-1107

Bazer FW, Wu G, Spencer TE, Johnson GA, Burghardt RC, Bayless K. Novel pathways for implantation and establishment and maintenance of pregnancy in mammals. Mol Hum Reprod 2010; 16:135-152.

Beagin EE, Merkel BJ. Cleavage of MTT [3-(4,5-dimethylthiazol-2-yl)-2,5-diphenyl tetrazolium bromide] by HT2 and CTLL-2 cells. Bios 2002; 73:80-85.

Bellehumeur C, Blanchet J, Fontaine J, Bourcier N, Akoum A. Interleukin 1 regulates its own receptors in human endometrial cells via distinct mechanisms. Hum Reprod 2009; 24:2193-2204.

Betts M, Russell R. Amino acid properties and consequences of substitutions. In: Barnes M, and Gray I (eds.), Bioinformatics and Geneticists. England: John Wiley and Sons, Ltd. 2003; 289-316.

Bian C, Wu Y, Chen P. Telmisartan increases the permeability of endothelial cells through zonula occludens-1. Biol Pharm Bull 2009; 32:416-420.

Bird S, Zou J, Wang T, Munday B, Cunningham C, Secombes CJ. Evolution of interleukin-1 beta. Cytokine Growth Factors Rev 2002; 13:483-502.

Blitek A, Morawska E, Ziecik A. Regulation of expression and role of leukemia inhibitory factor and interleukin-6 in the uterus of early pregnant pigs. Theriogenology 2012; 78:951-964.

Blitek A, Waclawik A, Kaczmarek M, Stadejek T, Pejsak Z, Ziecik A. Expression of cyclooxygenase-1 and -2 in the porcine endometrium during the estrous cycle and early pregnancy. Reprod Dom Anim 2006; 41:251-257.

Blomberg L, Hashizume K, Viebahn C. Blastocyst elongation, trophoblast differentiation, and embryonic pattern formation. Reproduction 2008; 135:181-195.

Blumberg RS, van de Wal Y, Claypool S, Corazza N, Dickinson B, Nieuwenhuis E, Pitman R, Spiekermann G, Zhu X, Colgan S, Lencer WI. The multiple roles of major histocompatibility complex class I-like molecules in mucosal immune function. Acta Odontol Scand 2001; 59:139-144.

Boron WR, Boulpaep EL. Medical Physiology: A cellular and molecular approach. Philadelphia: Saunders-Elsevier; 2009:1246-1248.

Bowen J, Bazer F, Burghardt R. Spatial and temporal analyses of integrin and Muc-1 expression in porcine uterine epithelium and trophectoderm in vivo. Biol Reprod 1996; 55:1098-1106.

Caamaño J, Hunter CA. NF-κB Family of Transcription Factors: Central Regulators of Innate and Adaptive Immune Functions. Clin Microbiol Rev 2002; 15:414-429.

Caárdenas H, Pope W. Control of ovulation rate in swine. J Anim Sci 2002; 80:E36-E46.

Cakmak H, Taylor H. Implantation failure: molecular mechanisms and clinical treatment. Hum Reprod Update 2011; 17:242-253.

Cencič A, Guillomot M, Koren S, La Bonnardière C. Trophoblastic interferons: Do they modulate uterine cellular markers at the time of conceptus attachment in the pig? Placenta 2003; 24:862-869.

Cencič A, La Bonnardière C. Trophoblast interferon-gamma: current knowledge and possible role(s) in early pig pregnancy. Vet Res 2002; 33:139-157.

Cha J, Sun X, Dey S. Mechanisms of implantation: strategies for successful pregnancy. Nat Med 2012; 18:1754-1767.

Chardon P, Rogel-Gaillard C, Cattolico L, Duprat S, Valman M, Renard C. Sequence of the swine major histocompatibility complex region containing all non-classical class I genes. Tissue Antigens 2001; 57:55-65.

Chen JR, Cheng Jr-Gang, Shatzer T, Sewell L, Hernandez L, Stewart CL. Leukemia inhibitory factor can substitute for nidatory estrogen and is essential to inducing a receptive uterus for implantation but is not essential for subsequent embryogenesis. Endocrinology 2000; 141:4365-4372.

Chen S, Liu Y, Sytwu H. Immunologic regulation in pregnancy: from mechanism to therapeutic strategy for immunomodulation. Clin Develop Immuno 2012; doi:101155/2012/258391.

Choi Y, Johnson GA, Burghardt RC, Berghman LR, Joyce MM, Taylor KM, Stewart MD, Bazer FW, Spencer TE. Interferon regulatory factor-two restricts expression of interferon-stimulated genes to the endometrial stroma and glandular epithelium of the ovine uterus. Biol Reprod 2001; 65: 1038-1049.

Choi Y, Johnson GA, Spencer TE, Bazer FW. Pregnancy and interferon tau regulate MHC class I and beta-2-microglobulin expression in the ovine uterus. Biol Reprod 2003; 68:1703-1710.

Choi Y, Seo H, Shim J, Kim M, Ka H. Regulation of S100G expression in the uterine endometrium during early pregnancy in pigs. Asian Australas J Anim Sci 2012; 25:44-51.

Choudhuri R, Wood G. Production of interleukin-1, interleukin-6 and tumor necrosis factor alpha in the uterus of pseudopregnant mice. Biol Reprod 1993; 49:596-603.

Coeshott C, Ohnemus C, Pilyavskaya A, Ross S, Wieczorek M, Kroona H, Leimer AH, Cheronis J. Converting enzyme-independent release of tumor necrosis factor alpha and IL-1beta from a stimulated human monocytic cell line in the presence of activated neutrophils or purified proteinase 3. Proc Natl Acad Sci U S A. 1999; 96:6261-6266.

Cornetta K, Tessanne K, Long C, Yao J, Satterfield C, Westhusin M. Transgenic sheep generated by lentiviral vectors: safety and integration analysis of surrogates and their offspring. Transgenic Res 2013; 22:737-745.

Cross JC, Roberts RM. Porcine conceptuses secrete an interferon during the preattachment period of early pregnancy. Biol Reprod 1989; 40:1109-1118.

D'Andréa S, Chousterman S, Flechon JE, La Bonnardière C. Paracrine activities of porcine trophoblastic interferons. J Reprod Fertil 1994; 102:185-194.

D'Andréa S, La Bonnardière C. Cloning of the porcine interferon-gamma receptor and its foeto-endometrial expression in early pregnancy. Mol Reprod Dev 1998; 51:225-34.

Dantzer V. Electron microscopy of the initial stages of placentation in the pig. Anat Embryol 1985; 172:281-293.

Dawson H, Loveland J, Pascal G, Gilbert J, Uenishi H, Mann KM, Sang Y, Zhang J, Carvalho-Silva D, Hunt T, Hardy M, Hu Z. Structural and functional annotation of the porcine immunome. BMC Genomics 2013; 14:332.

Degrelle SA, Blomberg LA, Garrett WM, Li RW, Talbot NC. Comparative proteomic and regulatory analysis of the elongating pig conceptus. Proteomics 2009; 9:2678-2694.

Dekel N, Gnainsky Y, Granot I, Mor G. Inflammation and Implantation. Am J Reprod Immunol 2010; 63:17-21.

Dekel N, Gnainsky Y, Granot I, Racicot K, Mor G. The role of inflammation for a successful implantation. Am J Reprod Immunol 2014; 72:141-147.

Dinarello C. Interleukin-1 and interleukin-1 antagonism. Blood 1991; 77:1627-1652.

Dinarello C. Biologic Basis for Interleukin-1 in Disease. Amer J Hematol 1996; 87:2095-2147.

Dinarello C. Blocking IL-1 in systemic inflammation. J Exp Med 2005; 201:1355-1359.

Dinarello C. Immunological and inflammatory functions of the interleukin-1 family. Annu Rev Immunol 2009; 27:519-50.

Dinarello C. Interleukin-1 in the pathogenesis and treatment of inflammatory diseases. Blood 2011; 117:3720-32.

Dinarello C, Simon A, van der Meer J. Treating inflammation by blocking interleukin-1 in a broad spectrum of diseases. Nat Rev Drug Discov 2012; 11:633-652.

Dunne A, O'Neill LA. The interleukin-1 receptor/Toll-like receptor superfamily: signal transduction during inflammation and host defense. Sci STKE 2003; 171:re3.

Dushay M, Asling B, Hultmark D. Origins of immunity: Relish, a compound Rel-like gene in the antibacterial defense of Drosophila. Proc Natl Acad Sci 1996; 93:10343-10347.

Dziuk PJ. Effects of migration distribution and spacing of pig embryos on pregnancy and fetal survival. J Reprod Fertil Suppl 1985; 33:57-63.

Engelhardt H, Croy BA, King GJ. Conceptus influences the distribution of uterine leukocytes during early pregnancy. Biol Reprod 2002; 66:1875-1880.

Evans MJ, Eckert A, Lai K, Adelman SJ, Harnish, DC. Reciprical antagonism between estrogen receptor and NF-kappaB activity in vivo. Circ Res 2001; 89:823-830.

Ezashi T, Matsuyama H, Telugu B, Roberts MR. Generation of colonies of induced trophoblast cells during standard reprogramming of porcine fibroblast to induced pluripotent stem cells. Biol Reprod 2011; 85:779-787.

Foxcroft GR, Dixon WT, Novak S, Putman CT, Town SC, Vinsky MDA. The biological basis for prenatal programming of postnatal performance in pigs. J Anim Sci 2006; 84:E105-E112.

Franczak A, Zmijewska A, Kurowicka B, Wojciechowicz B, Kotwica G. Interleukin 1β-induced synthesis and secretion of prostaglandin E_2 in the porcine uterus during various periods of pregnancy and the estrous cycle. J Physiol Pharmacol 2010; 61:733-742.

Galien R, Garcia T. Estrogen receptor impairs interleukin-6 expression by preventing protein binding on the NF-kappaB site. Nucleic Acids Res 1997; 25: 2424-2429.

Garlanda C, Dinarello C, Mantovani A. The interleukin-1 Family: Back to the Future. Immunity 2013; 39:1003-1018.

Geisert RD, Brenner RM, Moffatt RJ, Harney JP, Yellin T, Bazer FW. Changes in oestrogen receptor protein, mRNA expression and localization in the endometrium of cyclic and pregnant gilts. Reprod Fertil Dev 1993; 5:247-260.

Geisert RD, Fazleabas A, Lucy MC, Mathew DJ. Interaction of the conceptus and the endometrium to establish pregnancy in mammals: Role of Interleukin 1 Beta. Cell Tissue Res 2012; 349:825-838.

Geisert RD, Brookbank JW, Roberts RM, Bazer FW. Establishment of pregnancy in the pig: II. Cellular remodeling of the porcine blastocyst during elongation of day 12 of pregnancy. Biol Reprod 1982; 27:941-955.

Geisert RD, Schmitt RAM. Early embryonic survival in the pig: can it be improved? J Anim Sci 2002; 80:E54-E65.

Gomez-Lopez N, Guilbert L, Olson D. Invasion of the leukocytes into the fetal-maternal interface during pregnancy. J Leuk Biol 2010; 88:625-633.

González-Navajas JM, Lee J, David M, Raz E. Immunomodulatory functions of type I interferons. Nature Rev Immuno 2012; 12:125-135.

Granot I, Gnainsky Y, Dekel N. Endometrial inflammation and effect on implantation improvement and pregnancy outcome. Reproduction 2012; 144:661-668.

Green ML, Chung TE, Reed KL, Modric T, Badinga L, Yang J, Simmen FA, Simmen RC. Paracrine inducers of uterine endometrial spermidine/spermine N^1 – acetyltransferase gene expression during early pregnancy in the pig. Biol Reprod 1998; 59:1251-1258.

Groenen M, Archibald A, Uenishi H, Tuggle C, Takeuchi Y, Rothschild MF, Rogel-Gaillard C, Park C, Milan D, Megens HJ, Li S, Larkin DM. Analysis of pig genomes provide insight into porcine demography and evolution. Nature 2012; 491:393-398.

Hailey K, Li S, Andersen M, Roy M, Woods V, Jennings P. Pro-interleukin (IL)-β shares a core region of stability as compared with mature IL-1β while maintaining a distinctly different configurational landscape; A comparative hydrogen/deuterium exchange mass spectrometry study. J Biol Chem 2009; 284:26137-26148.

Hamm J, Tessanne K, Clifton M, Prather R. Transcriptional regulators TRIM28, SETDB1, and TP53 are aberrantly expressed in porcine embryos produced by in vitro fertilization in comparision to in vivo- and somatic-cell nuclear transfer derived embryos. Mol Reprod Dev 2014; 81:552-566.

Hayden M, Ghosh S. NF-κB, the first quarter-century: remarkable progress and outstanding questions. Genes Dev 2012; 26:203-234.

Hicks BA, Etter SJ, Carnahan KG, Joyce MM, Assiri AA, Carling SJ, Kodali K, Johnson GA, Hansen TR, Mirando MA, Woods GL, Vanderwall DK. Expression of the uterine Mx protein in cyclic and pregnant cows, gilts, and mares. J Anim Sci 2003; 81:1552-1561.

Hiscott J, Marois J, Garoufalis J, D'Addario M, Roulston A, Kwan I, Pepin N, Lacoste J, Nguyen H, Bensi G. Characterization of a functional NF-kappa B site in the human interleukin 1 beta promoter: evidence for a positive autoregulatory loop. Mol Cell Biol 1993; 13:6231-6240.

Hofmann A, Kessler B, Ewerling S, Weppert M, Vogg B, Ludwig H, Stojkovic M, Boelhauve M, Brem G, Wolf E, Pfeifer A. Efficient transgenesis in farm animals by lentiviral vectors. EMBO reports 2003; 4:1054-1060.

Horai R, Asano M, Sudo K, Kanuka H, Suzuki M, Nishihara M, Takahashi M, Iwakura Y. Production of mice deficient in genes for interleukin (IL)-1α, IL-1β, IL-1α/β, and IL-1 receptor antagonist shows that IL-1β is crucial in turpentine-induced fever development and glucocorticoid secretion. J Exp Med 1998; 187:1463-1475.

Hu J, Ludwig TE, Salli U, Stormshak F, Mirando MA. Autocrine/Paracrine action of oxytocin in pig endometrium. Biol Reprod 2001; 64:1682-1688.

Huddleston H, Schust DJ. Immune reactions at the maternal-fetal interface: a focus on antigen presentation. American J Reprod 2004; 51:283-289.

Huffman S, Almamun M, Rivera R. Isolation of RNA and DNA from single preimplantation embryos and a small number of mammalian oocytes for imprinting studies. In Engel N (eds), Genomic Imprinting: Methods in Molecular Biology, Vol 925, New York: Humana Press; 2012:201-210.

Ivashkiv LB, Donlin LT. Regulation of type I interferon responses. Nat Rev Immunol 2014; 14:36-49.

Jantra S, Bigliardi E, Brizzi R, Letta F, Bechi N, Paulesu L. Interleukin 1 in oviductal tissues of viviparous, oviparous and ovuliparous species of amphibians. Biol Reprod 2007; 76:1009-1015.

Johnson GA, Bazer FW, Burghardt RC, Spencer TE, Wu G, Bayless KJ. Conceptus-uterus interactions in pigs: Endometrial gene expression in response to estrogens and interferons from conceptuses. In: Rodriguez-Martinez H, Vallet JL, Ziecik AJ (eds), Control of Pig Reproduction VIII. Nottingham University Press 2009:321-332.

Joyce MM, Burghardt JR, Burghardt RC, Hooper RN, Bazer FW, Johnson GA. Uterine major histocompatibility class I molecules and beta 2 microglobulin are regulated by progesterone and conceptus interferons during pig pregnancy. J Immunol 2008; 181:2494-2505.

Joyce MM, Burghardt JR, Burghardt RC, Hooper RN, Jaeger LA, Spencer TE, Bazer FW, Johnson GA. Pig conceptuses increase uterine interferon regulatory factor-1 (IRF-1), but restrict expression to stroma through estrogen-induced IRF-2 in luminal epithelium. Biol Reprod 2007b; 77:292-302.

Joyce MM, Burghardt RC, Geisert RD, Burghardt JR, Hooper RN. Pig conceptuses secrete estrogen and interferons to differentially regulate uterine STAT 1 in a temporal and cell type specific manner. Endocrinology 2007a; 148:4420-4431.

Ka H, Seo H, Kim M, Choi Y, Lee CK. Identification of differentially expressed genes in the uterine endometrium on Day 12 of the estrous cycle and pregnancy in pigs. Mol Reprod Dev 2009; 76:75-84.

Katebi AR, Gniewek P, Zimmermann M, Saraswathi S, Gong Z, Tuggle CK, Kloczkowski A, Jernigan R. Immunological implications of a structural analysis of two different porcine IL1β proteins expressed by macrophages and embryos. In: BCB ’10 Proceedings of the First ACM International Conference on Bioinformatics and Computational Biology. 2010:653-655.

Kennedy TG, Gillio-Meina C, Phang SH. Prostaglandins and the initiation of blastocyst implantation and decidualization. Reprod 2007; 134:635-43.

Keys JL, King GJ. Morphological evidence for increased uterine vascular permeability at the time of embryonic attachment in the pig. Biol Reprod 1988; 39:473-487.

Keys JL, King GJ. Microscopic Examination of Porcine Conceptus-Maternal Interface Between Days 10 and 19 of Pregnancy. Am J Anat 1990; 188:221-238.

Kim M, Seo H, Choi Y, Shim J, Bazer FW, Ka H. Swine leukocyte antigen-DQ expression and it's regulation by interferon-gamma at the maternal-fetal interface in pigs. Biol Reprod 2012; 86:1-11.

King A, Collins F, Klonisch T, Sallenave J, Critchley H, Saunders P. An additive interaction between the NFκB and estrogen receptor signaling pathways in human endometrial epithelial cells. Hum Reprod 2010; 25:510-8.

King GJ. Reduction in uterine intra-epithelial lymphocytes during early gestation in the pig. J Reprod Immunol 1988; 14:41-46.

Kol S, Kehat I, Adashi EY. Ovarian interleukin-1-induced gene expression: privileged genes threshold theory. Med Hyphothesis 2002; 58:6-8.

Kraeling RR, Rampacek GB, Fiorello NA. Inhibition of pregnancy with indomethacin in mature gilts and prepubertal gilts induced to ovulate. Biol Reprod 1985; 32:105-110.

Krumm B, Xiang Y, Deng J. Structural biology of the IL-1 superfamily: key cytokines in the regulation of immune and inflammatory responses. Prot Sci 2014; 23:526-538.

Krüssel J, Simón C, Rubio M, Pape A, Wen Y, Huang HY, Bielfeld P, Polan ML. Expression of interleukin-1 system mRNA in single blastomeres from human preimplantation embryos. Hum Reprod 1998; 13:2206-2211.

Krüssel JS, Haung H, Wen Y, Kloodt AR, Bielfeld P, Polan ML. Different pattern of interleukin-1β-(IL-1β), interleukin-1 receptor antagonist-(IL-1ra) and interleukin-1 receptor type 1-(IL-1R tI) mRNA-expression in single preimplantation mouse embryos at various developmental stages. J Reprod Immunol 1997; 34:103-120.

La Bonnardière C, Martinat-Botte F, Terqui M, Lefèvre F, Zouari K, Martal J, Bazer FW. Production of two species of interferon by large white and meishan pig conceptuses during the peri-attachment period. J Reprod Fert 1991; 91:469-478.

Laforest JP, King GJ. Structural and functional aspects of porcine endometrial capillaries on days 13 and 15 after oestrus or mating. J Repro Fert 1992; 94:269-277.

Laird SM, Tuckerman EM, Cork BA, Li TC. Expression of nuclear factor kappa B in human endometrium; role in the control of interleukin 6 and leukaemia inhibitory factor production. Mol Hum Reprod 2000; 6:34-40.

Le Bouteiller P, Fons P, Herault JP, Bono F, Chabot S. Soluble HLA-G and control of angiogenesis. J Reprod Immunol 2007; 76:17-22.

Lee K, Redel B, Spate L, Teson J, Brown A, Park K, Walters E, Samuel M, Murphy C, Prather R. Piglets produced from cloned blastocysts cultured in vitro with GM-CSF. Mol Reprod Dev 2013; 80:145-154.

Lefèvre F, Boulay V. A novel and atypical type 1 interferon gene expressed by trophoblast during early pregnancy. J Biol Chem 1993; 268:19760-19768.

Lefèvre F, Martinat-Botte F, Guillomot M, Zouari K, Charley B, La Bonnardière C. Interferon-gamma gene and protein are spontaneously expressed by the porcine trophectoderm early in gestation. Eur J Immunol 1990; 20:2485-2490.

Lefèvre F, Martinat-Botte F, Locatelli A, Niu PD, Terqui M, La Bonnardière C. Intrauterine infusion of high doses of pig trophoblast interferons has no antiluteolytic effect in cyclic gilts. Biol Reprod 1998; 58:1026-1031.

Librach CL, Feigenbaum SL, Bass KE, Cui T, Verastas N, Sadovsky Y, Quigley JP, French DL, Fisher SJ. Interleukin-1β regulates human cytotrophoblast metalloproteinase activity and invasion in Vitro. J Biol Chem 1994; 269:17125-17131.

Lim H, Paria B, Das S, Dinchuk J, Langenbach R, Trzaskos JM Dey SK. Multiple female reproductive failures in cyclooxygenase 2-deficient mice. Cell 1997; 91:197-208.

Lin H, Wang X, Liu G, Fu J, Wang A. Expression of alpha V and beta 3 integrin subunits during implantation in pig. Mol Reprod Dev 2007; 74:1379-1385.

Liu C, Wang L, Li W, Zhang X, Tian Y, Zhang N, He S, Chen T, Huang J, Liu M. Highly efficient generation of transgenic sheep by lentivirus accompanying the alteration of methylation. PLOS 2013; 8:1-9.

Loeb L. Ueber die experimentelle Erzeugung von Knoten von Deciduagewebe in dem Uterus des Meerschweinchens nach stattgefundener. Copulation Zentralbl Allg Pathol Pathol Anat 1907; 18:563-565.

Ludwig TE, Sun BC, Carnahan KG, Uzumcu M, Yelich JV, Geisert RD, Mirando MA. Endometrial responsiveness to oxytocin during diestrus and early pregnancy in pigs is not controlled solely by changes in oxytocin receptor population density. Biol Reprod 1998; 58:769-777.

Ma L, Li X, Zhang S, Yang F, Zhu G, Yuan X, Jiang W. Interleukin-1 beta guides the migration of cortical neurons. J Neuroinflammation 2014; 11:114.

Macklon NS, Geraedts JP, Fauser BC. Conception to ongoing pregnancy: the "black box" of early pregnancy loss. Hum Repro Update 2002; 8:333-343.

Manjunath N, Haoquan W, Sandesh S, Premlata S. Lentiviral delivery of short hairpin RNA's. Adv Drug Deliv Rev 2009; 61:32-745.

Marions L, Danielsson K. Expression of cyclo-oxygenase in human endometrium during the implantation period. Mol Hum Reprod 1999; 5:961-965.

Martin S, Maruta K, Burkart V, Gillis S, Kolb H. IL-1 and IFN-gamma increase vascular permeability. Immunology 1988; 64(2):301-305.

Mathew DJ, Newsom EM, Geisert RD, Green JA, Tuggle CK, Lucy MC. Characterization of nucleotide and predicted amino acid sequence of a porcine Interleukin-1 beta (IL1B) variant expressed in elongated porcine embryos. ADSA-ASAS Midwest Annual Meeting. March 14 – March 16, 2011, Des Moines, IA, USA, J Anim Sci Vol. 89 E-suppl.2; 2011b

Mathew DJ, Sellner EM, Green JC, Okamura CS, Anderson LL, Lucy MC, Geisert RD. Uterine progesterone receptor expression, conceptus development, and ovarian function in pigs treated with RU 486 during early pregnancy. Biol Reprod 2011a; 84:130-139.

McCracken JA, Custer EE, Lamsa JC. Luteolysis: a neuroendocrine-mediated event. Physiol Rev 1999; 79:263-323.

Mirando MA, Harney JP, Beers S, Pontzer CH, Torres BA, Johnson HM, Bazer FW. Onset of secretion of proteins with antiviral activity by pig conceptuses. J Reprod Fert 1990; 88:197-203.

Modrić T, Kowalski A, Green M, Simmen R, Simmen F. Pregnancy-dependent expression of leukaemia inhibitory factor (LIF), LIF receptor-β and interleukin-6 (IL-6) messenger ribonucleic acids in the porcine female reproductive tract. Placent 2000; 21:345-353.

Mor G, Cardenas I, Abrahams V, Guller S. Inflammation and pregnancy: the role of the immune system at the implantation site. N Y Acad of Sci 2011; 1221:80-87.

Mori N, Prager D. Transactivation of the interleukin-1alpha promoter by human T-cell leukemia virus type 1 and type II Tax proteins. Blood 1996; 87:3410-3417.

Nakamura H, Kimura T, Ogita K, Nakamura T, Takemura M, Shimoya K, Koyama S, Tsujie T, Koyama M, Murata Y. NF-κB activation at implantation window of the mouse uterus. Am J Reprod Immunol 2004; 51:16-21.

Nester JE. Interleukin-1 stimulates the aromatase activity of human placental cytotrophoblasts. Endocrinology 1993; 132:566-70.

Netea MG, Simon A, van de Veerdonk F, Kullberg B-J, Van der Meer JWM, Joosten LAB. IL-1B processing in host defense: beyond the inflammasomes. PLoS Pathog 2010; 6:e1000661.

Ni H, Sun T, Ding N, Ma X, Yang Z. Differential expression of microsomal prostaglandin E synthase at implantation sites and in decidual cells of the mouse uterus. Biol Reprod 2002; 67:351-358.

Oeckinghaus A, Hayden MS, Ghosh S. Crosstalk in NF-kB signaling pathways. Nat immuno 2011; 12:695-708.

Østrup E, Bauersachs S, Blum H, Wolf E, Hyttel P. Differential endometrial gene expression in pregnant and non-pregnant sows. Biol Reprod 2010; 83:277-285.

Page M, Tuckerman EM, Li TC, Laird SM. Expression of nuclear factor kappa B components in human endometrium. J Reprod Immunol 2002; 54:1-13.

Paulesu L, Romagnoli R, Bigliardi E. Materno-fetal immunotolerance: is Interleukin-1 a fundamental mediator in placental viviparity?. Dev Comp Immunol 2005; 29:409-415.

Platanias LC. Mechanisms of type-I and type-II-interferon-mediated signaling. Nature Rev Immunol 2005; 5:375-386.

Polge C. Fertilization in the horse and pig. J Reprod Fert 1978; 54:461-470.

Pollard JW, Hunt SJ, Wiktor-Jedrzejczak W, Stanley ER. A pregnancy defect in the osteopetrotic (op/op) mouse demonstrates the requirement for CSF-1 in female fertility. Dev Biol 1991; 148:273-83.

Prather RS, Shen M, Dai Y. Genetically modified pigs for medicine and agriculture. Biotechnol genet eng rev 2008; 25:245-266.

Priestle J, Schär H, Grütter M. Crystal structure of the cytokine interleukin-1 β. EMBO 1988; 7:339-343.

Puhlmann M, Weinreich D, Farma JM, Carrol NM, Turner EM, Alexander HR. Interleuukin-1B induced vascular permeability is dependent on induction of endothelial tissue factor (TF) activity. J Trans Medic 2005; 3:37

Purcell S, Cantlon J, Wright C, Henkes L, Seidel G, Anthony R. The involvement of proline-rich 15 in early conceptus development in sheep. Biol Reprod 2009; 81:1112-1121.

Quaedackers ME, van den Brink CE, van der Saag PT, Tertoolen LG. Direct interaction between estrogen receptor alpha and NF-kappaB in the nucleus of living cells. Mol Cell Endocrinol 2007; 273:42-50.

Ramsoondar JJ, Christopherson RJ, Guillbert LJ, Dixon WT, Ghahary A, Ellis S, Wegmann TG, Piedrahita JA. Lack of class I major histocompatibility antigens on trophoblast of peri-implantation blastocysts and term placenta in the pig. Biol Reprod 1999; 60:387-397.

Roberts RM, Ealy AD, Alexenko AP, Han CS, Ezashi T. Trophoblast interferons. Placenta 1999; 20:259-264.

Roberts RM. Interferon-tau, a type 1 interferon involved in maternal recognition of pregnancy. Cytokine Growth Factor Rev 2007; 18:403-408.

Ross JW, Ashworth M, Mathew D, Reagan P, Ritchey J, Hayashi K, Spencer TE, Lucy M Geisert RD. Activation of the transcription factor, nuclear factor kappa-B, during the estrous cycle and early pregnancy. Reprod Biol Endocrinol 2010; 8:39

Ross JW, Ashworth MD, Hurst AG, Malayer JR, Geisert RD. Analysis and characterization of differential gene expression during rapid trophoblastic elongation in the pig using subtractive suppression hybridization. Reprod Biol Endocrinol 2003b; 1:23.

Ross JW, Fernandez de Castro JP, Zhao J, Samuel M, Walters E, Rios C, Bray-Ward P, Jones BW, Marc RE, Wang W, Zhou L, Noel J et al. Generation of an inbred miniature pig model of retinitis pigmentosa. Invest Ophthalmol Vis Sci 2012; 53:501-507.

Ross JW, Malayer JR, Ritchey JW, Geisert RD. Characterization of the interleukin-1β system during porcine trophoblastic elongation and early placental attachment. Biol Reprod 2003a; 69:1251-1259.

Roy A, Kucukural A, Zhang Y. I-TASSER: a unified platform for automated protein structure and function prediction. Nature Protocols 2010; 5:725-738.

Roy A, Yang J, Zhang Y. COFACTOR: an accurate comparative algorithm for structure based protein function annotation. Nucleic Acids Research 2012; 40:W471-W477.

Sander JD, Joung JK. CRISPR-Cas systems for editing, regulating and targeting genomes. Nat Biotechnol 2014; 32:347-355.

Schroder K, Hertzog P, Ravasi T, Hume D. Interferon-gamma: an overview of signals, mechanisms and functions. J Leukoc Biol 2004; 75:163-189.

Sen R, Baltimore D. Multiple nuclear factors interact with the immunoglobulin enhancer sequences. Cell 1986; 46:705-716.

Seo H, Choi Y, Shim J, Choi Y, Ka H. Regulatory mechanism for expression of IL1B receptors in the uterine endometrium and effects of IL1B on prostaglandin synthetic enzymes during the implantation period in pigs. Biol Reprod 2012; 87:1-11.

Seo H, Kim M, Choi Y, Ka H. Salivary lipocalin is uniquely expressed in the uterine endometrial glands at the time of conceptus implantation and induced by interleukin 1beta in pigs. Biol Reprod 2011; 84:279-287.

Short RV. Implantation and the maternal recognition of pregnancy. In: Wolstenholme GEW, O'Connor M (eds), Cida Foundation Symposium on Foetal Automony London: Churchill; 1969:2-26

Simmons DL, Botting RM, Hla T Cyclooxygenase isozymes: The biology of prostaglandin synthesis and inhibition. Pharmacol Rev 2004; 56:387-437.

Simón C, Frances A, Piquette G, Hendrickson M, Milki A, Polan ML. Interleukin-1 system in the maternal trophoblast unit in human implantation: Immunohistochemical evidence for autocrine/paracrine function. J Clin Endocrinol Metab 1994a; 8:847-854.

Simón C, Frances A, Piquette GN, el Danasouri I, Zurawski G, et al. (1994b) Embryonic implantation in mice is blocked by interleukin-1 receptor antagonist. Endocrinology 134: 521-528.

Simón C, Gimeno MJ, Mercader A, O'Connor JE, Remohi J, Polan ML, Pellicer A. Embyronic regulation of integrins beta 3, alpha 4 and alpha 1 in human endometrial epithelial cells in vitro. J Clin Endocrinol Metab 1997b; 82:2607-2616.

Simón C, Mercader A, Gimeno MJ, Pellicer A. The interleukin 1 system and human implantation. Am J Reprod immunol 1997a; 37:64-72.

Simón C, Pellicer A, Polan M. Interleukin-1 system crosstalk between embryo and endometrium in implantation. Hum Reprod Suppl 1995; 2:43-54.

Simón C, Piquette GN, Frances A, Polan ML. Localization of Interleukin-1 type 1 receptor and Interleukin-1 Beta in human endometrium throughout the menstrual cycle. J Clin Endocrinol Metab 1993; 77:549-555.

Simón C, Valbuena D, Krüssel J, Bernal A, Murphy C, Shaw T, Pellicer A, Polan ML. Interleukin-1 receptor antagonist prevents embryonic implantation by a direct effect on the endometrium epithelium. Fertil Steril 1998; 70:896-906.

Sims JE, Smith DE. The IL-1 family: regulators of immunity. Nat Rev Immuno 2010; 10:89-102.

Smith MF Jr, Eidlen D, Arend WP, Gutierrez-Hartmann A. LPS-induced expression of the human IL-1 receptor antagonist gene is controlled by multiple interacting promoter elements. J Immunol 1994; 153:3584-3593.

Smith T, Fahrenkrug S, Rohrer G, Simmen F, Rexroad C, Keele J. Mapping of expressed sequence tags from a porcine early embryonic cDNA library. Anim Genet 2001; 32:66-72.

Sparacio SM, Zhang Y, Vilcek J, Benveniste EN. Cytokine regulation of interleukin-6 gene expression in astrocytes involves activation of an NF-kappa B-like nuclear protein. J Neuroimmunol 1992; 39:231-242.

Spencer TE, Burghardt, RC, Johnson GA, Bazer FW. Conceptus signals for the establishment of pregnancy. Anim Reprod Sci 2004; 83:537-550.

Spencer TE, Johnson GA, Bazer FW, Burghardt RC, Palmarini M. Pregnancy recognition and conceptus implantation in domestic ruminants: roles of progesterone, interferons and endogenous retroviruses. Reprod Fertil Dev 2007; 19:65-78.

Spencer TE, Sandra O, Wolf E. Genes involved in conceptus-endometrial interactions in ruminants: insights from reductionism and thoughts on holistic approaches. Reproduction 2008; 135:165-179.

St-Louis I, Singh M, Brasseur K, Leblanc V, Parent S, Asselin E. Expression of COX-1 and COX-2 in the endometrium of cyclic, pregnant and in a model of pseudopregnant rats and their regulation by sex steroids. Reprod Biol Endocrin 2010; 8:103.

Steele GL, Currie WD, Leung EH, Yuen BH, Leung PC. Rapid stimulation of human chorionic gonadotropin secretion by interleukin-1beta from perifused first trimester trophoblast. J Clin Endocrinol Metab 1992; 75:783-788.

Stewart MD, Choi Y, Johnson GA, Yu-Lee LY, Bazer FW, Spencer TE. Roles of Stat1, Stat2 and interferon regulatory factor-9 (IRF-9) in interferon tau regulation of IRF-1. Biol Reprod 2003; 66:393-400.

Stewert C, Kaspar P, Brunet L, Bhatt H, Gadi I, Köntgen F, Abbondanzo SJ. Blastocyst implantation depends on maternal expression of leukaemia inhibitory factor. Nature 1992; 359:76-9.

Takacs P, Kauma S. The expression of interleukin-1 alpha, interleukin-1 beta and interleukin-1 receptor type I mRNA during preimplanation mouse development. J Reprod Immunol 1996; 32:27-35.

Tanaka-Matsuda M, Ando A, Rogel-Gaillard C, Chardon P, Uenishi H. Difference in the number of loci of swine leukocyte antigen classical class I genes among haplotypes. Genomics 2009; 93:261-273.

Thornberry A, Molineaux S. Interleukin-1β converting enzyme: A novel cysteine protease required for IL-1β production and implicated in programmed cell death. Protein Sci 1995; 4:3-12.

Tuggle C, Gong Z, Huang T, Ross J. Duplication and divergence of expression and function of the IL1B gene in the pig genome. Symposium of the functional genomics of early development in livestock. July 24 – July 24, Banff, Alberta, Canada. 2012.

Tuggle CK, Green JA, Fitzsimmons C, Woods R, Prather RS, Malchenko S, Soares BM, Kucaba T, Crouch K, Smith C, Tack D, Robinson N, O'Leary B, Scheetz T, Casavant T, Pomp D, Edeal BJ, Zhang Y, Rothschild MF, Garwood K, Beavis W. EST-based gene discovery in pig: virtual expression patterns and comparative mapping to human. Mamm Genome 2003; 14:565-79.

Tuo W, Harney JP, Bazer FW. Developmentally regulated expression of interleukin-1β by peri-implantation conceptuses in swine. J Reprod Immunol 1996; 31:185-198.

Vallet J, Leymaster K, Christenson R. The influence of uterine function on embryonic and fetal survival. J Anim Sci 2002; 80:E115-E125.

Vallet J, Miles R, Freking B. Development of the pig placenta. Soc Reprod Fertil Suppl 2009; 66:265-79.

van Boxel-Dezaire AHH, Rani MRS, Stark GR. Complex modulation of cell type-specific signaling in response to type 1 interferons. Immunity 2006; 25:361-372.

van Mourik M, Macklon N, Heijnen C. Embryonic implantation: cytokines, adhesion molecules, and immune cells in establishing an implantation environment. J Leukoc Biol 2009; 85:4-19.

Vandenbroeck K, Fiten P, Beuken E, Martens E, Janssen A, Van Damme J, Opdenakker G, Billiau A. Gene sequence, cDNA construction, expression in Eschericia coli

and genetically approached purification of porcine interleukin-1B. Eur J Biochem 1993; 217:45-52.

Veerapandian B. Structure and function of interleukin-1, based on crystallographic and modeling studies. Biophysical Journal 1992; 62:112-115.

Vigers G, Anderson L, Caffes P, Brandhuber B. Crystal structure of the type-1 interleukin-1 receptor complexed with interleukin-1β. Nature 1997; 386:190-194.

Waclawik A. Novel insights into the mechanisms of pregnancy establishment: regulation of prostaglandin synthesis and signaling in the pig. Reproduction 2011; 142:389-99.

Waclawik A, Blitek A, Kaczmarek M, Kiewisz J, Ziecik AJ. Antiluteolytic mechanisms and the establishement of pregnancy in the pig. Soc Reprod Fertil Suppl 2009; 66:307-320.

White FJ, Kimbell EM, Wyman G, Stein DR, Ross JW, Ashworth MD, Geisert RD. Estrogen and interleukin-1B regulation of trophinin, osteopontin, cyclooxygenase-1, cyclooxygenase-2, and interleukin-1B system in the porcine uterus. In: Control of pig reproduction VIII. Rodriguez-Martinez H, Vallet JL, Ziecik AJ. (eds), Nottingham University Press 2009; 203-204.

White FJ, Ross JW, Joyce MM, Geisert RD, Burghardt RC, Johnson GA. Steroid regulation of cell specific secreted phophoprotein 1 (Osteopontin) expression in the pregnant porcine uterus. Biol Reprod 2005; 73:1294-1301.

Whitworth K, Lee K, Benne J, Beaton B, Spate L, Murphy S, Samuel M, Mao J, O'Gorman C, Walters E, Murphy C, Driver J, Mileham A, McLaren D, Wells K, Prather R. Use of the CRISPR/Cas9 system to produce genetically engineered pigs from in vitro-derived oocytes and embryos. Biol Reprod 2014; 91:78.

Wilmut I, Sales D, Ashworth C. Maternal and embryonic factors associated with prenatal loss in mammals. J Reprod Fert 1986; 76:851-864.

Yelich JV, Pomp D, Geisert RD. Ontogeny of elongation and gene expression in the early developing porcine conceptus. Biol Reprod 1997; 57:1256-1265.

Yim H, Cho Y, Guang X, Kang S, Jeong J, Cha S, Oh H, Lee J, Yang E, Kwon K, Kim Y, Kim T. Minke whale genome and aquatic adaptation in cetaceans. Nature genetics 2014; 46:88-94.

Youakim A, Ahdieh M. Interferon-gamma decreases barrier function in T84 cells by reducing ZO-1 levels and disrupting apical actin. Am J Physiol 1999; 276: G1279-G1288.

Zeidler RB, Kim HD. Phagocytosis, Chemiluminescence, and cell volume of alveolar macrophages from neonatal and adult pigs. J Leukoc Biol 1985; 37:29-43.

Zhang Y, Skolnick J. Segment assembly, structure alignment and iterative simulation in protein structure prediction. BMC Biol 2013; 11:44

Zhang Y. I-TASSER server for protein 3D structure prediction. BMC Bioinformatics 2008; 9:40

APPENDIX A

RECRUITMENT OF ENDOMETRIAL LEUKOCYTES TO THE UTERINE SURFACE BY PIG INTERLEUKIN-1 BETA 1 AND INTERLEUKIN-1 BETA 2

Endometrial leukocytes are important for host defense against intra uterine pathogens, initiation of menstruation and parturition, endometrial blood vessel remodeling, regulation of trophoblast invasion and immune tolerance of the fetal semi-allograft (Gomez-Lopez et al., 2010). Pro-inflammatory cytokines, such as IL-1β, modulate endometrial leukocyte activity (Gomez-Lopez et al., 2010). Interleukin-1 beta (IL-1β) can increasing endothelial cell adhesion molecule expression and blood vessel permeability resulting in recruitment of blood leukocytes into infected tissues, a process referred to as leukocyte extravasation (Dinarello, 1996; 2005; Dunne, 2003). Further, IL-1β can increase cell migration by modifying membrane integrins and cytoskeletal actin filaments in target cells including neurons, tumor cells and neutrophils (Ferreira et al., 2012; Ma et al., 2014).

In pigs, the early conceptus abundantly releases interleukin-1 beta 2 (IL-1β2), a newly discovered IL-1, at the fetal-maternal interface. The IL-1β2 may modulate

leukocyte activity during early pregnancy. Initial histological evaluation of LPS and recombinant IL-1 treated pig endometrium (see Chapter Three) suggested an increase in the number of intraepithelial leukocytes. To investigate this, we further stained the endometrial sections and recorded the phenotype and number of intraepithelial and sub-epithelial leukocytes.

MATERIALS AND METHODS

Endometrial Leukocytes

Frosted white microscope slides with tissue sections of endometrium (see Chapter Three) treated with 10 μg/mL of LPS or 100 ng/mL of BGal (protein expression control), pig mat-IL-1β1 or mat-IL-1β2 were rehydrated and stained with hematoxylin (Fisher HC) and eosin-Y (Richard-Allan Scientific) (H/E) before dehydrated through a graded series of alcohol solutions and xylene. Cover slips were then mounted to the slides using Permount (Fisher Scientific) and the identities of the sections were blinded from the investigator before pictures were taken of the tissue at 200 X and 400 X magnification using a Leica light microscope. Some tissue sections were stained with DAPI prior to H/E to observed LE and intraepithelial cell nuclei. Two non-epithelial cell phenotypes, resembling leukocytes, were observed within the uterine LE layer 1): large cytoplasmic cells with nuclei that stained lightly with hematoxylin and 2) small round cells with darkly stained nuclei. A third leukocyte phenotype, which stained well with eosin, was easily observed within the stroma nearest to the uterine surface. Later, the images were used to count the number cells for each phenotype within a computer generated rectangle,

corresponding to 300 X 150 μm of endometrium, using the NIH Image J computer program.

STATISTICS

A Mixed procedure within SAS was used to analyze the endometrial leukocyte data. For leukocyte data, the model statement included an effect of treatment on the number of cells. All data are presented as least squares means (LSM) ± standard error of the least square means (SEM). A significant difference was declared at $P < 0.05$.

RESULTS

Recruitment of endometrial leukocytes in response recombinant IL-1 cytokines

Treating cyclic endometrium with LPS and recombinant IL-1 cytokines recruited endometrial cells, resembling leukocytes, to the uterine surface (Table A.1 and Fig. A.1). For large intraepithelial cells, there tended to be an effect of treatment ($P = 0.060$; Table A.1 and Fig. A.1). Treating endometrium with pig mat-IL-1β1 increased the number of these cells within the uterine LE when compared with endometrium treated with the control protein, BGal ($P < 0.01$). In regards to the small intraepithelial cells, there was an effect of treatment ($P < 0.05$; Table A.1 and Fig. A.1). Endometrium treated with LPS and mat-IL-1β2 had a greater number of small cells within the uterine LE when compared with endometrium treated with pig mat-IL-1β1 ($P < 0.01$ and $P = 0.010$; respectively). There was also an effect of treatment on eosin stained cells within the stroma ($P < 0.001$; Table A.1 and Fig. A.1). Treating endometrium with LPS increased the number of these

cells within the stroma nearest to the uterine surface when compared to endometrium treated with BGal, pig mat-IL1β1 and mat-IL1β2 ($P < 0.01$).

DISCUSSION

Histological examination of endometrial explant tissue treated with LPS, mat-IL-1β1 or mat-IL-1β2 revealed an increase in the number of intraepithelial and sub-epithelial cells, resembling leukocytes, within 4 h of treatment (Fig. A.1 and A.2). The major leukocyte populations within the pig endometrium are lymphocytes, macrophages, neutrophils and dendritic-like cells with T cell and/or uterine natural killer (uNK) lymphocytes the most abundant during pregnancy (Engelhardt et al., 2002). There is an increase in the number of intraepithelial lymphocytes between d 10 and 19 of the estrous cycle; however, these cells decrease during early pregnancy possibly in response to unknown factors released by the conceptus (King et al., 1988). Interesting, Engelhardt et al. (2002) detected a 3-fold increase in the number of stromal leukocytes directly adjacent to the d 15-conceptus attachment vs. non-attachment sites. These cells had phenotypes similar to T, B and/or uNK cells. The number of intraepithelial leukocytes was independent of conceptus location on d 15 and remained low (Engelhardt et al., 2002).

During this study, two intraepithelial cell phenotypes were commonly found; 1) a population of what appeared to be large cells, possibly macrophages or NK cells, with lightly stained nuclei and extensive cytoplasm that increased in response to mat-IL-1β1 and 2) small cells, having darkly stained round nuclei, possibly B, T or small NK cells, that increased in endometrium treated with LPS and mat-IL-1β2 compared to tissue treated with mat-IL-1β1. A third cell phenotype, resembling eosinophils, accumulated

within the sub-epithelial stroma in response to LPS. Because the in vitro study utilized explant tissue, the LPS and recombinant IL-1 cytokines must have recruited these cells from the uterine stroma.

During pig uterine infusion studies, an increase in the number of stromal leukocytes near the uterine epithelial layer in response recombinant pig IL-1β1 was observed, suggesting that in pigs, this cytokine has to capacity to modulate endometrial leukocyte activity (Geisert, Roberts and White; data not published). During our study, we did not detect significant changes in leukocyte activity between control and mat-IL-1β2 treated endometrium and were unable to verity an immune modulatory role for this cytokine during establishment of pregnancy. However, based on observations made during our alveolar cell experiments (Chapter Three), it's possible that IL-1β2 has the capacity to modulate activity of some leukocyte populations within the endometrium during implantation of the pig conceptus.

TABLE A.1 Number of large intraepithelial (IE) cells, small IE cells and eosin stained stromal (S) cells counted within endometrium treated with 10 μg/mL of LPS or 100ng/mL of BGal (negative control) mat-IL-1β1 or mat-IL-1β2 after 4 h of treatment. Data are presented as LSM ± SEM.

	Treatment (T)				P<[c]
Endometrial Cell	BGal	LPS	mat-IL-1β1	mat-IL-1β2	T
Large IE	1.6 ± 0.5^{b}	$2.3 \pm 0.5^{a,b}$	$2.9 \pm 0.5^{a,b}$	2.3 ± 0.4^{a}	0.060
Small IE	$2.1 \pm 0.4^{a,b}$	2.7 ± 0.4^{a}	1.4 ± 0.5^{b}	2.6 ± 0.4^{a}	0.029
Eosin S	1.0 ± 0.3^{b}	2.0 ± 0.3^{a}	0.6 ± 0.3^{b}	0.7 ± 0.3^{b}	0.001

[c] P value for treatment (T); Significance was declared at $P < 0.05$.
Letters indicated significant differences between treatment LSM.

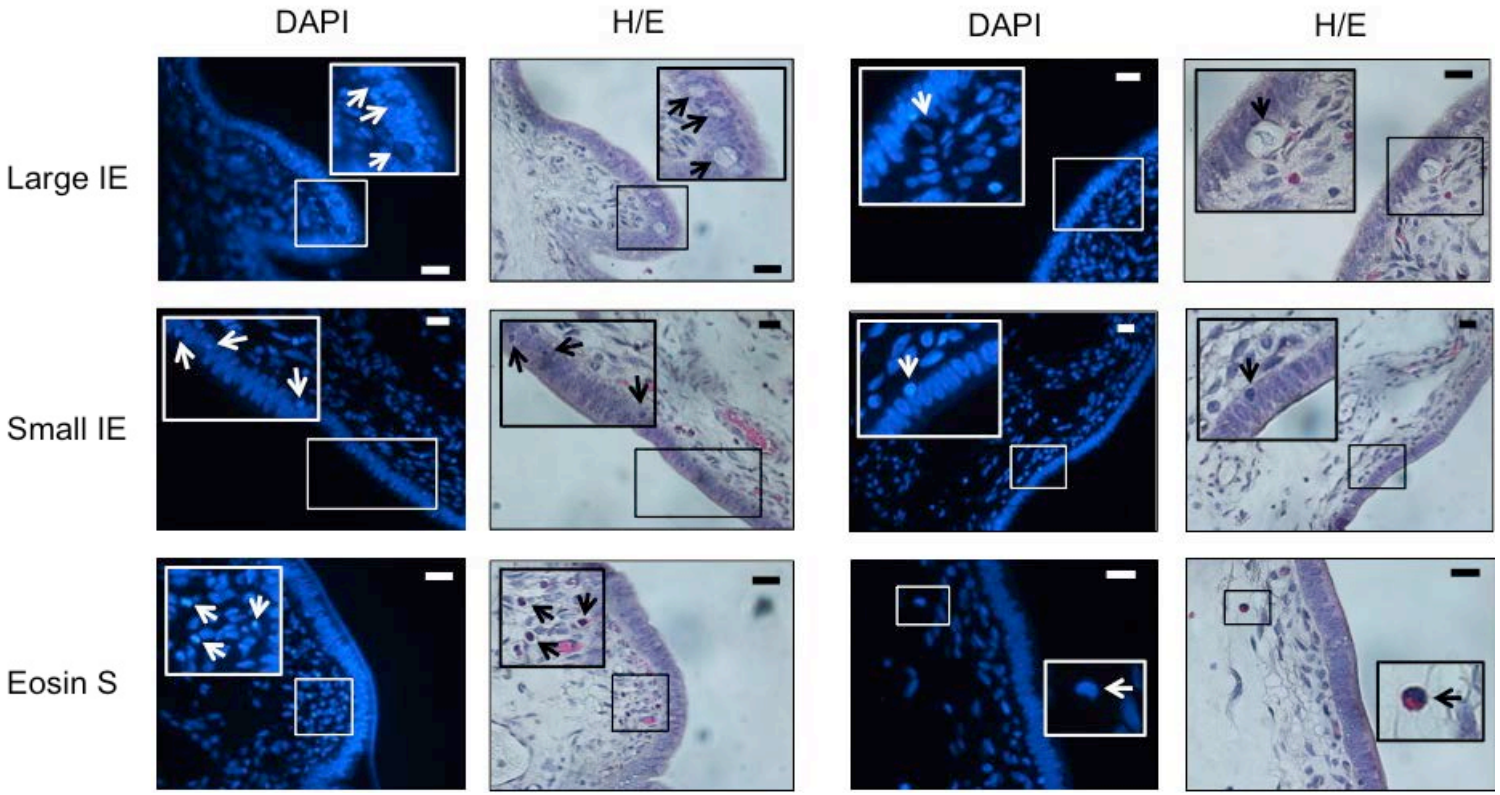

FIGURE A.1 Images of cyclic pig endometrium, first stained with DAPI and then H/E, containing large intraepithelial (IE) cells, small IE cells and eosin stained stromal (S) cells, resembling leukocytes, after treatment with LPS or recombinant IL-1 cytokines for 4 h. Pictures were taken with a Leica light microscope at a 400 X magnification. Black and white boxes represent locations of inset zoomed image. Black and white arrows represent locations of stained cells. Bar = 20 μM.

VITA

Daniel Joseph Mathew was born June 20, 1983 and grew up on the family swine farm managed by his father, Alan, uncle Brian and grandfather, Marvin, in Wolcott, Indiana. There, Daniel's interests in animal agriculture and nature began. Alan, a farmer and scientist, later moved his family to East Tennessee after accepting a faculty position at the University of Tennessee Department of Animal Sciences. Daniel's experiences in East Tennessee further propelled his love for animal agriculture and so he began to pursue a Bachelor's degree in Animal Sciences at the University of Tennessee. After attending the course Advanced Reproduction, Daniel was fascinated by the processes of early embryonic development and early pregnancy. He then pursued a M.S. and Ph.D. degree at the University of Missouri under the guidance of Drs. Matthew Lucy and Rodney Geisert in the area of Reproductive Physiology, focusing on conceptus-maternal interactions during early pregnancy in pigs. Daniel will receive his Ph.D. from the University of Missouri in December 2014 and has accepted a Post-Doctoral research position at the University College Dublin in Ireland, investigating early embryonic mortality. His adventures in Ireland will begin in January of 2015.